Total Synthesis of Biselide A and Studies Towards the Synthesis of a Chimeric Glycopeptide to Probe Peptide-Carbohydrate Mimicry

by

Venugopal Rao Challa

B.Sc. (Chemistry), Osmania University, Hyderabad, India, 2003

M.Sc. (Chemistry), Osmania University, Hyderabad, India, 2005

Thesis Submitted in Partial Fulfillment of the

Requirements for the Degree of

Doctor of Philosophy

in the

Department of Chemistry

Faculty of Science

SIMON FRASER UNIVERSITY

Fall 2019

Approval

Name:	**Venugopal Rao Challa**
Degree:	**Doctor of Philosophy (Chemistry)**
Title:	**Total Synthesis of Biselide A and Studies Towards the Synthesis of a Chimeric Glycopeptide to Probe Peptide-Carbohydrate Mimicry**
Examining Committee:	**Chair: Krzysztof Starosta** Associate Professor
	Robert A. Britton Senior Supervisor Professor
	B. Mario Pinto Supervisor Professor
	Tim Storr Supervisor Associate Professor
	Peter D. Wilson Internal Examiner Associate Professor
	David Leitch External Examiner Assistant Professor Department of Chemistry University of Victoria
Date Defended/Approved:	December 11, 2019

Abstract

The primary focus of the research described in this thesis deals with the studies geared towards the total synthesis of biselide A and phormidolide A, two tetrahydrofuran containing natural products with potentially useful biological activities. Additionally, efforts towards the synthesis of a chimeric glycopeptide is described.

Biselide A, is a chlorinated macrocyclic polyketide isolated from the Okinawan ascidian *Didemnidae sp*., possessing potent cytotoxicity against a variety of human cancer cell lines. The core molecular structure contains a densely substituted tetrahydrofuran ring and 5 stereogenic centres as a part of 14-membered macrolactone. To access this potentially useful marine macrolide we have utilized an asymmetric aldol reaction with enantiomerically-enriched chlorohydrins that affords a rapid and stereocontrolled access to the tetrahydrofuran core. The macrocycle was constructed through a series of transformations that include a cross metathesis, regioselective enzymatic acetylation, and Reformatsky macrocyclization. In this thesis we highlight a flexible and stereoselective total synthesis of biselide A.

Phormidolide A is a complex macrocyclic polyketide isolated from the cyanobacteria *Leptolyngbya sp.* It possess a highly oxygenated side chain and a macrocyclic core with an embedded substituted tetrahydrofuran. We exploit our previously developed α-chlorination/aldol reaction strategy to access the tetrahydrofuran motif. Synthesis of three model acetonide tetrahydrofuran derivatives allowed for the NMR comparison with the same previously reported triacetonide derivative of phormidolide A. NMR spectroscopic analysis supports a reassignment of seven of the eleven stereogenic centres initially reported for phormidolide A.

The second part of this thesis describes the progress made towards the synthesis of a chimeric glycopeptide. Two haptens, a pentasaccharide and a mimetic octapeptide bind with moderate affinity to a monoclonal antibody SYA/J6, specific for the O-polysaccharide of the *S.flexneri* Y bacterium. Based on the X-ray crystallography data and molecular docking studies, two chimeric glycopeptides (α-glycopeptide and β-glycopeptide) were designed in an attempt to improve the binding affinity to SYA/J6 antibody. Our group has previously synthesized α-glycopeptide and showed no inhibition of SYA/J6 antibody to the O-polysaccharide. Preliminary docking studies indicated that the β-glycopeptide might provide a better fit within the antibody combining site. The molecule consists of a rhamnose trisaccharide linked through a β-glycosidic linkage to an MDW moiety of a mimetic octapeptide. Our strategy involved linking three fragments, synthesized using solution and/or solid phase methodology. The key step in the synthesis was the formation of the thermodynamically less favoured β-linkage between the sugar and peptide. This was achieved following an ulosyl bromide approach. We herein describe our efforts towards the synthesis of a β-glycopeptide.

Keywords: Natural products; Total synthesis; Biselide A; Phormidolide A; Antibody; Glycopeptide

To my wonderful family,

with love and gratitude

for all their support and encouragement.

Acknowledgements

This dissertation would not have been possible without the help and support of many people. First and foremost, I would like to offer my deepest gratitude to my research supervisor Dr. Robert Britton, for his excellent guidance, supervision and encouragement throughout my Ph.D. program. I would also like to sincerely express my heartfelt gratitude to my first supervisor Dr. B. Mario Pinto for providing me an opportunity to work in his laboratory. I am truly grateful for his guidance and valuable advices throught these years. It has been a remarkable experience working with both the supervisors.

I would like to thank Dr. Tim Storr for serving on my supervisory committee and appreciate his helpful suggestions and feedback throughout my graduate studies. I would also like to extend my gratitude to Dr. Peter Wilson for serving as my internal examiner amidst his busy schedule, Dr. Krzysztof Starosta for chairing my thesis procedure and Dr. David Leitch for serving as my external examiner.

I would also like to thank Dr. Andrew Lewis, Dr. Eric Ye and Mr. Colin Zhang for their assistance to set up complex NMR experiments. Also, Ms. Nathalie Fournier for her administrative prowess. I would like to extend my thanks to library theses assistants Ms. Catherine Louie and Ms. Anise Ladha, who were always willing to help whenever I have questions or needed help with thesis formatting and writing.

I have had the opportunity to work with many wonderful people over the last few years. I would like to begin by thanking past and current members of the Britton group: Dr. Matt Nodwell for proofreading my second chapter, Michael Meanwell for being a great friend throughout my tenure in the Britton lab. It had always been enjoyable to work with and share fume hood space with Garrett Muir and thank you for your contribution in completing the project. I'd like to thank Dr. Michael Holmes, Dr. Milan Bergeron-Brlek, Dr. Vimal Varghese, Dr. Johannes Lehmann, Dr. Weiwu Ren, Dr. Santosh Kumar, Dr. Yang Wang, Dr. Zheliang Yuan, Abhi Bagai, Daniel Kwon, Chris Adamson, Anthony Fers - Lidou, Anissa Kaghad, Gaelen Fehr, Matthew Sutherland, Josiah Newton, Victoria Rose, Dimitri Panagopolos and Darryl Wilson for making the lab a convivial place to work and wish them much success in the future. Additionally, I'd like to thank past members of the Pinto group. I will always remember Dr. Sankar Mohan, Dr. John Pal Adabala and Dr. Ravinder Kongara both in lab and at residence tennis court playing cricket. Without

their encouragement, support and friendship, I am sure I could not have accomplished this huge task. I am grateful to Dr. Mohan for his suggestions in writing and proofreading the fourth chapter of my thesis. I'd also like to thank Dr. Silvia Borrelli, Kyle Greenway, and Dr. Yun Shi, for making my stay memorable in the Pinto lab. I'd also like to thank memebers from other groups, particularly Dr. Sundeep, Dr. Sachin and Dr. Srinivas for their friendship and expertise in chemistry.

I would like to acknowledge the help and support I have got from my friends who went through hard times together, cheered me on, and celebrated each accomplishment. Some of my friends whom I would like to thank are Ramana Murthy, Priyadarshini Balaraman, Govardhan Reddy and his family. Special thanks must go to Govardhan who was always willing to drive me to and from Burnaby Mountain on late nights and weekends, which reduced my commute time.

I would like to gratefully acknowledge the people who meant a lot to me, my parents, Mrs. Subba Lakshmi and Mr. Chinnaih Challa for their unconditional support, love, and for always believing in me and encouraging me towards my goals. My heartfelt thanks to my dear sister and her family, Mrs. Hemasree, Mr. Kiran Kumar and my nephew Snehith Simha, for their selfless love, care and encouragement despite the long distance between us. I am greatly indebted to my Uncle Dr. M. Srinivas Rao, Cousin Mr. Mallikarjun Rao and sister for their unwavering support and encouragement and for also taking care of my parents when needed, which allowed me to complete my studies with unfetterd attention. Most importantly, I would like to thank my mother for all the sacrifices she made for providing me with better education and life.

Finally, I would like to thank the most important person in my life, my wife, Dhana Laxmi, for her continued and unfailing love, support and dedication throughout the entire process. She has always stood by me through my travails and guided me in positive direction, when I thought it was impossible to continue. I greatly value her contribution and deeply appreciate her belief in me. I consider myself to be very fortunate, to have her in my life. I acknowledge my children Divyesh and Nehal Nidesh for being a great source of love and providing motivation to complete my studies with expediency.

Table of Contents

List of Tables

List of Figures

List of Schemes

List of Acronyms

μwave	Microwave
$[\alpha]_D$	Specific rotation at the sodium D line (589 nm)
°C	Degrees Celsius
Ac	Acetate
Aq	Aqueous
Bn	Benzyl
Bu	Butyl
Bz	Benzoyl
CAN	Ammonium cerium (IV) nitrate
COSY	Correlation Spectroscopy
CSA	10-Camphorsulfonic acid
DBU	1,8-Diazabicyclo[5.4.0]undec-7-ene
DDQ	2,3-Dichloro-5,6-dicyano-1,4-benzoquinone
DIBAL	Diisobutylaluminium hydride
DIC	Diisopropylcarbodimide
DIPA	Diisopropylamine
DIPEA	*N*-*N*-Diisopropylethyl amine
DMAP	*N,N*-dimethyl-4-aminopyridine
DMF	*N,N*-Dimethylformamide
DMP	Dess-Martin periodinane
DMSO	Dimethylsulfoxide
dr	diastereomeric ratio
DTBMP	2,6-Di-*tert*-butyl-4-methylpyridine
E	*Entgegen* (alkene geometry)
ECD	Electronic circular dichromism
ee	Enatiomeric excess
Equiv	Equivalent(s)
Et	Ethyl
Et_2O	Diethyl ether
EtOAc	Ethyl acetate
EtOH	Ethanol
HBTU	*O*-Benzotriazole-*N,N,N',N'*-tetramethyl-uronium-hexafluoro-phosphate

HMBC	Heteronuclear multiple bond correlation
HOBt	*N*-Hydroxybenzotriazole
HPLC	High performance liquid chromatography
HRMS	High resolution mass spectrometry
HSQC	Heteronuclear single quantum coherence
Hz	Hertz
IC_{50}	Half maximal inhibitory concentration
*i*Pr	*iso*-Propyl
LC/MS	Liquid chromatography/Mass Spectrometry
LDA	Lithium diisopropylamide
M	Molar (mol/L)
MALDI	Matrix Assisted Laser Desorption Ionization
Me	Methyl
MeCN	Acetonitrile
mmol	Millimole(s)
mol	Mole(s)
MS	Molecular sieves
MTPA	α-Methoxy-α-trifluoromethylphenylacetic acid
NBS	*N*-bromosuccinimide
NCS	*N*-chlorosuccinimide
NHK	Nozaki-Hiyama-Kishi
NIS	*N*-iodosuccinimde
NMO	*N*-methylmorpholine-*N*-oxide
NMR	Nuclear magnetic resonance
nOe	Nuclear Overhauser effect
NOESY	Nuclear Overhauser effect spectroscopy
Nuc	Nucleophile
PG	Protecting group
Ph	Phenyl
PMB	*para*-Methoxybenzyl
PMP	*para*-Methoxyphenyl
PPTS	Pyridinium *para*-toluenesulfonate
Pr	Propyl
PTSA	*para*-Toluenesulfonic acid monohydrate

R	Substituent
R	*Rectus* (chiral designation)
rt	Room temperature
S	*Sinister* (chiral designation)
SAR	Structure-activity-relationship
SCUBA	Self-contained underwater breathing apparatus
S_N2	Bimolecular nucleophilic substitution
SOMO	Singly occupied molecular orbital
TBAB	Tetrabutylammonium bromide
TBAF	Tetrabutylammonium fluoride
TBDPS	*tert*-Butyldiphenylsilyl
TBS	*tert-B*utyldimethylsilyl
*t*Bu	*tert-B*utyl
Tf	Triflurometahnesulfonyl
TFA	Trifluoroacetate
TFAA	Trifluoroaceticanhydride
THF	Tetrahydrofuran
TLC	Thin Layer Chromatography
TMS	Trimethylsilyl
TOF	Time of Flight
Ts	Tosyl
TS	Transition state
WHO	World Health Organization
Z	*Zusammen* (alkene geometry)

Chapter 1.

Introduction

1.1. Introduction to Natural Products

Natural products can be defined as chemical compounds that are created by living organisms and these compounds often play an important role in their survival or development. Natural products can be produced as either primary or secondary metabolites. Primary metabolites are those natural products that are vital for the basic metabolism and reproduction of an organism. Metabolites that are not essential for the growth or development are described as secondary metabolites.[1] These secondary metabolites are often considered to be biosynthesized by the microorganisms as a protection against predators, for use in communication or in response to extreme environmental conditions of the surroundings.[2,3] For instance, the roots of leguminous plants produce the flavonoids[4,5] (secondary metabolites) that can attract rhizobia (bacteria) to fix nitrogen gas from the atmosphere for plant uptake. Jellyfish produce toxins to prevent predation from higher organisms.[6] In order to protect their biological niche, some strains of bacteria produce antimicrobial agents such as streptomycin[7] to engage in chemical warfare against intruding strains, while some insects and ants produce highly volatile hydrocarbons that serve as chemical messengers for communication and mating.[8] Unlike primary metabolites, secondary metabolites exhibit a wide range of biological activity and cytotoxicity[9]. For millennia, mankind has relied heavily on natural products and their applications now reach widely into various aspects of human life ranging from cosmetics, dyes, perfumes, flavor, pesticides to pharmaceuticals.[10-12,]

1.1.1. Natural Products as Drug Leads: A Historical Perspective

Natural products have been used for therapeutic purposes by almost every society for centuries. Some of the earliest records of natural products date back to 2600 BC. and were written on clay tablets in cuneiform in Mesopotamia documenting approximately 1000 plant based ‘drugs’ used at that time. The ‘*Ebers Papyrus*’, an ancient Egyptian pharmaceutical record dating from 1500 BC, also documented more than 700 drugs

mainly of plant origin.[13] Other contemporary civilizations also recorded the medicinal value of herbs. For example, in the '*Chakra Samhita'* in India (~1000 BC, 900 drugs) and the '*Pen- Ts'ao Ching'* in China (~1100 BC).[14] The ancient Greeks are well known for their interest in medicine and the Greek physician Dioscorides (100 AD) kept an extensive collection and record of medicinal herbs in the '*De Materia Medica'*. Even today, many of the plant based remedies documented in these ancient texts are still in use to treat inflammation, parasitic infections, cold, and cough, which illustrates human dependence on natural products for medicine.[15] According to World Health Organisation (WHO), the global market for herbal medicines is one of the fastest growing pharmaceutical markets and is estimated to be worth approximately US $43 billion a year.[16]

The early 19th century witnessed unprecedented progress in rational drug discovery following German pharmacist Friedrich Wilhelm Sertürner's first isolation of the natural product morphine (**1**) from opium poppy in 1803, which was later marketed by E. Merck in 1826 as a pain killer and used for many decades.[17,18] Quinine (**2**), extracted from *Cinchona officialis* bark, exhibited anti-inflammatory, antipyretic and analgesic properties and was the first and only drug to treat malaria for a long time.[19] Bayer, in 1899, introduced the first semi synthetic drug aspirin®, based on natural product salicin (**3**) isolated from *Salix alba.*[20,21] Aspirin (**4**) is today the most widely used drug globally. By the end of 19th century, progress made in the isolation of pure bioactive metabolites from complex mixtures of compounds in plant extracts led to the isolation of early drugs such as digitoxin (**5**), codeine (**6**), pilocarpine (**7**), colchicine (**8**) and atropine (**9**).[13,17] The serendipitous discovery of the antibacterial activity of penicillin (**10**) from *Penicillium notatum* by Fleming in 1928, often described as a miracle drug, marked the 'golden era of antibiotics'.[22] The success of penicillin stemmed from the large-scale examination of fungi and other microorganisms as potential source of drugs. These efforts led to many further breakthroughs in the isolation and characterization of antibiotics such as streptomycin, erythromycin, cephalosporin, chlorotetracyclines and vancomycin.[23-27] While more than 70% of the earth's surface is covered by oceans, the natural products isolated to date have overwhelmingly been derived from terrestrial organisms (such as plants, insects, fungi and microorganisms).

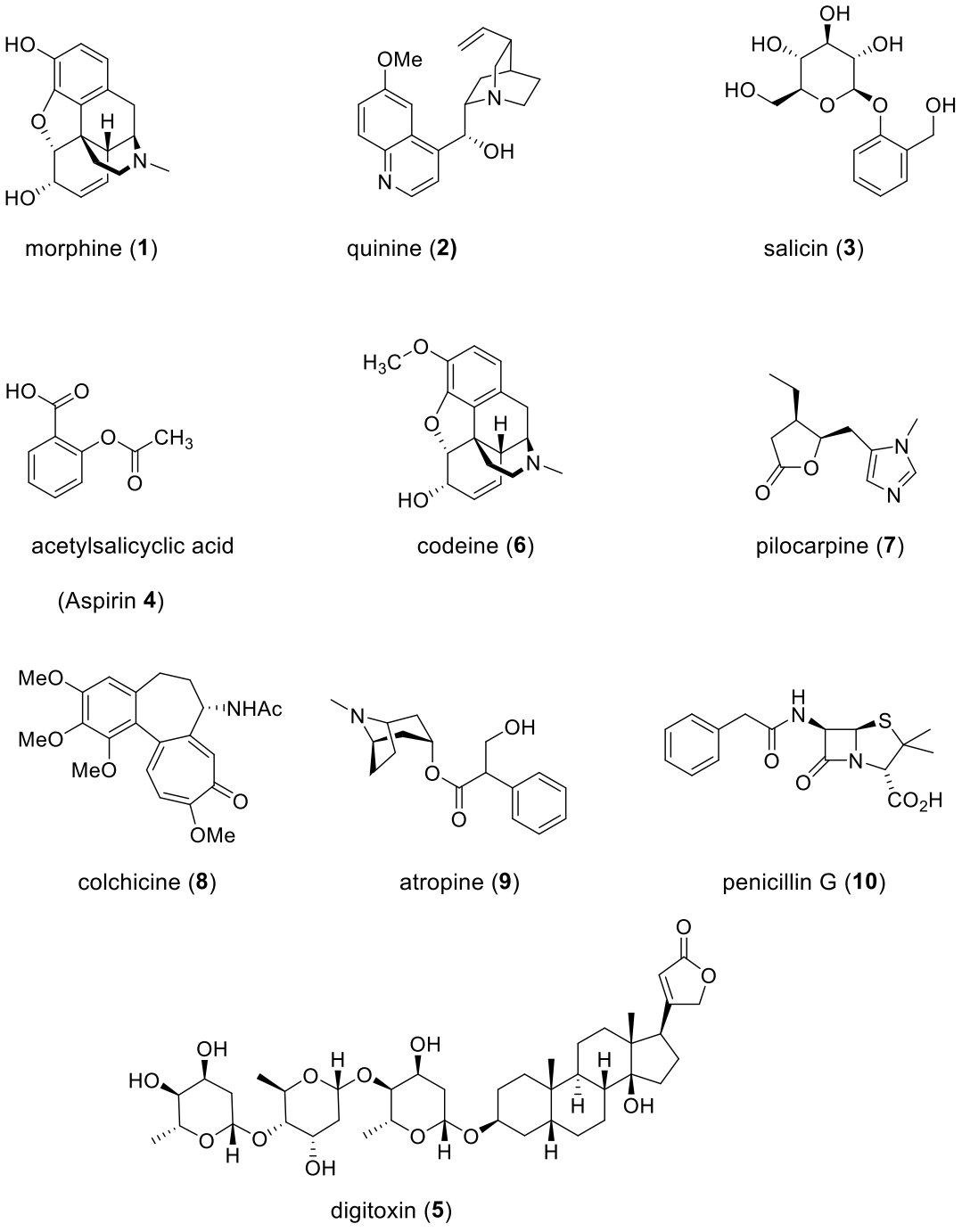

Figure 1-1 Representative examples of bioactive natural products.

With the advent of SCUBA (1950s) and further technological advancements researchers began to explore the depths of oceans, leading to the discovery of new marine organisms which have proven to be a rich source of bioactive natural products. Since 1970, approximately 30,000 natural products with novel molecular scaffolds and an array

of biological activities have been discovered from marine organisms.[28] To date, there are currently three Food and Drug Administration (FDA) approved drugs and one European Union (EU) administered drug derived from marine natural products. For example, Ziconotide (**11**) (Prilat®, Elan corporation) [29] a peptide isolated from marine cone snail, was the first marine natural product to be approved by FDA for the treatment of chronic pain. Another example, trabectedin (**12**) also known as ecteinascidin 743 (ET-743; Yondelis™)[30] was isolated from a sea squirt and became the first marine anticancer drug to be approved in the EU in 2007.

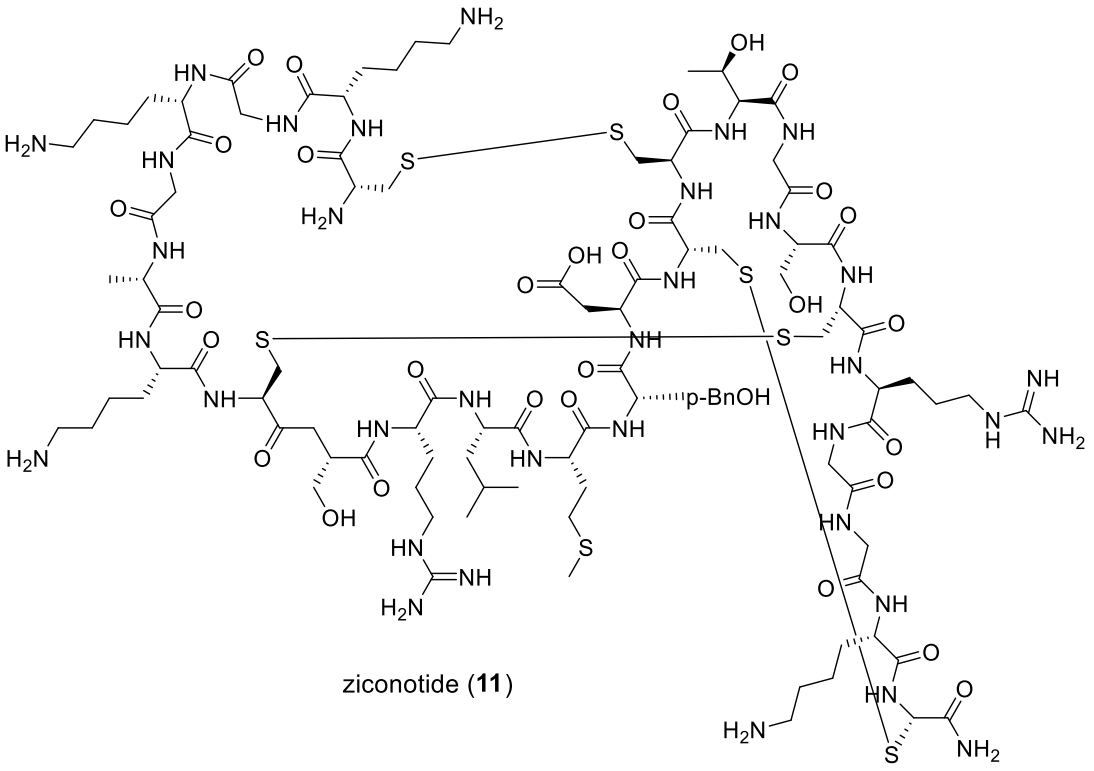

ziconotide (**11**)

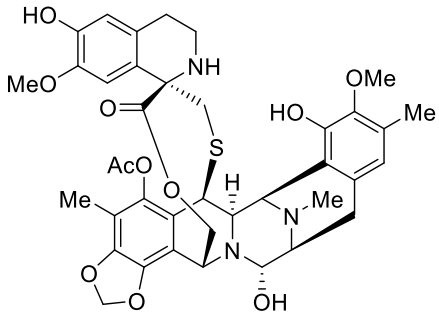

Et-743 (**12**)

Figure 1-2 Structures of ziconotide (11) and trabectedin (12).

While the importance of natural products to the drug discovery process is unquestionable, there are many challenges associated with the development of natural products from a drug lead to a pharmaceutical. These relate mainly to identification of the active natural product, issues of supply and limited possibility for structural modification. Most natural products are produced on a very small scale by their host organisms and isolation of pure active metabolites requires considerable resources and large quantities (multi kilogram) of biomass, which represents an environmental concern. Although the isolated amounts may suffice to support the initial structure elucidation, further studies into their biological activity tend to be hampered by the limited supply of the pure bioactive compound. Total synthesis of the natural product provides a practical solution to support biological testing and to allow modifications for structure activity relationship (SAR) studies (requires gram quantities). A remarkable and ingenious example of a scalable total synthesis that overcame the issue of supply is that of (+)-discodermolide (**13**). This polyketide natural product was first isolated by Gunasekar *et al*. in 1990 from a marine deep-sea sponge.[31] Given its promising *in vitro* and *in vivo* activity, discodermolide garnered considerable interest from the pharmaceutical industry. However, further clinical evaluation was impeded by lack of material available from its natural host, since discodermolide (**13**) accounts for only 0.002% of dried *D. dissoluta.*[32] This has inspired several total syntheses from the Schreiber,[33] Smith[34] and Paterson[35] groups. Building on this seminal work, a team of scientists at Novartis Pharma were able to prepare 60 g of discodermolide in 39 steps (26 steps for the longest linear sequence) with 1.1% overall yield (Scheme 1-1).[36] Another recent example includes an extraordinarily efficient synthesis of (+)-artemisinin (**14**), the most effective drug against malaria. Zhu and Cook[37] accomplished the total synthesis of artemisinin (**14**) in six steps with 3 column chromatography purifications. Given the economic and concise nature of Cook's synthesis, this process may well lead to an improvement in the economy of production of this important drug.

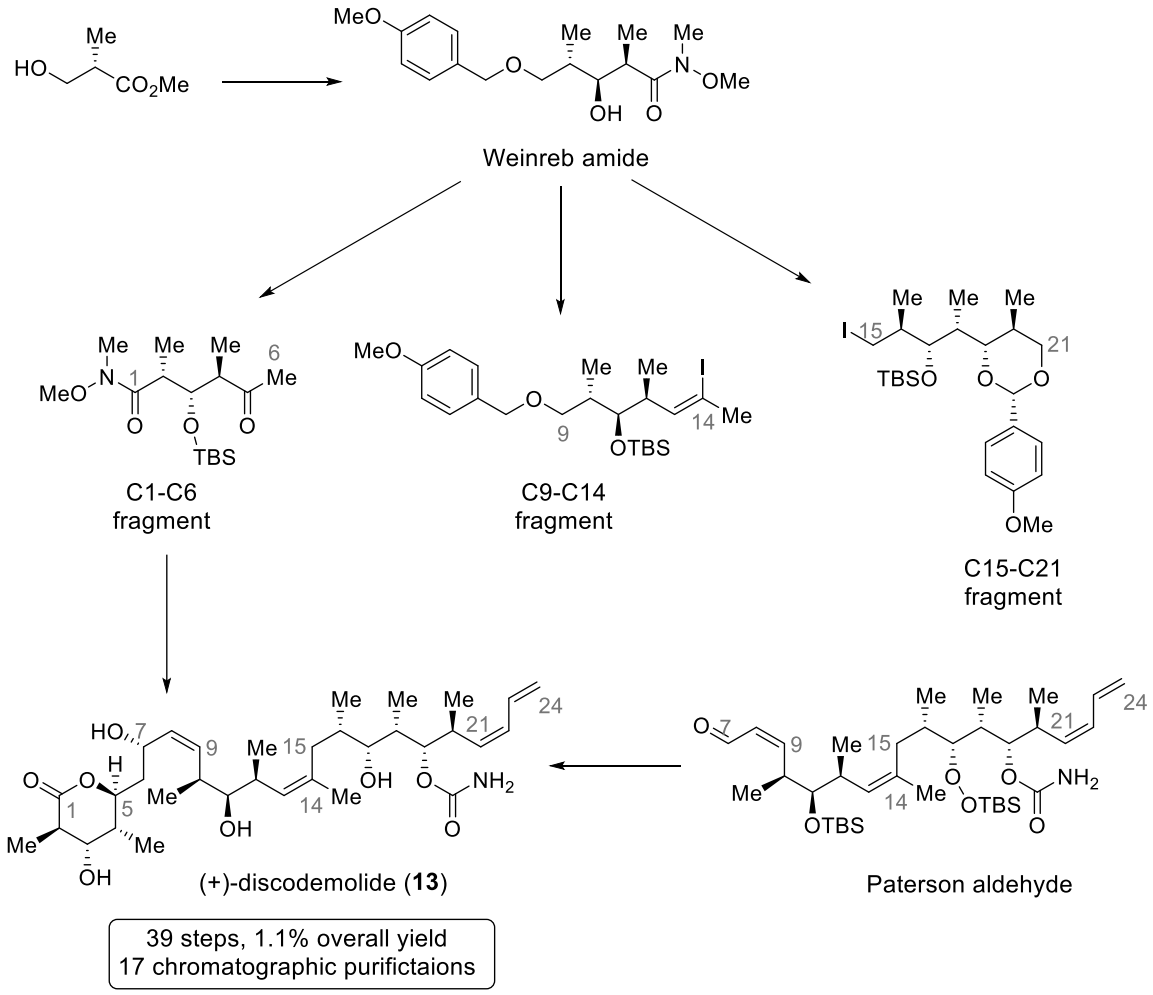

Scheme 1-1 Summary of Novartis Pharma gram-scale synthesis of (+)-discodermolide[32] (13)

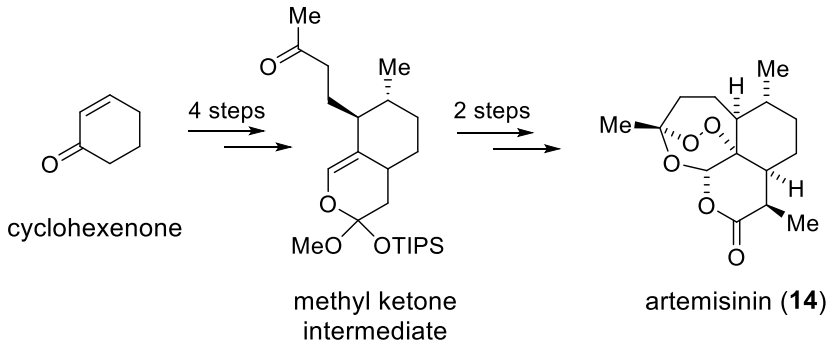

Scheme 1-2 Summary of Cook's synthesis of (+)-artemisinin (14)

Despite tremendous advances in modern spectroscopy, it is not always possible to assign the complete stereochemistry of a natural product based on spectroscopic methods. In such cases, total synthesis also offers an opportunity to determine the absolute and relative configuration of a natural product. Prominent examples include diazonomide A isolated from the colonial asicidian *Diazona angulata* by Fenical[38] and co-workers in 1991. This compound showed potent cytotoxicity against several tumor cell lines and was assigned the structure **15**. A decade later, Harran *et al.*[39] completed the synthesis of **15** and proved that the spectral data did not match with the natural product and instead proposed the structure **16** for diazonomide A. The revised structure included an additional ring H and a nitrogen atom instead of oxygen in ring F. Later, total synthesis of compound **16** by K.C Nicolaou and co-workers[40] proved that the structure **16** was indeed diazonomide A, whose spectral data was in excellent agreement with the isolated natural product. Mandelalide A was originally assigned as structure **17**, containing a 24 membered α,β-unsaturated macrolactone that included a trisubstituted tetrahydrofuran (THF) moiety and a trisubstituted tetrahydropyran (THP) moiety. However, synthesis of this compound by Lei *et al*.[41] revealed that the relative stereochemistry of the THF motif was misassigned and further spectral analysis followed by synthesis indicated that the correct structure of mandelalide A (**18**) had a THF motif with inverted stereochemistry compared to the initial proposed structure **17** (Scheme 1-3). These examples highlight the continued value total synthesis has in validating natural product structures.

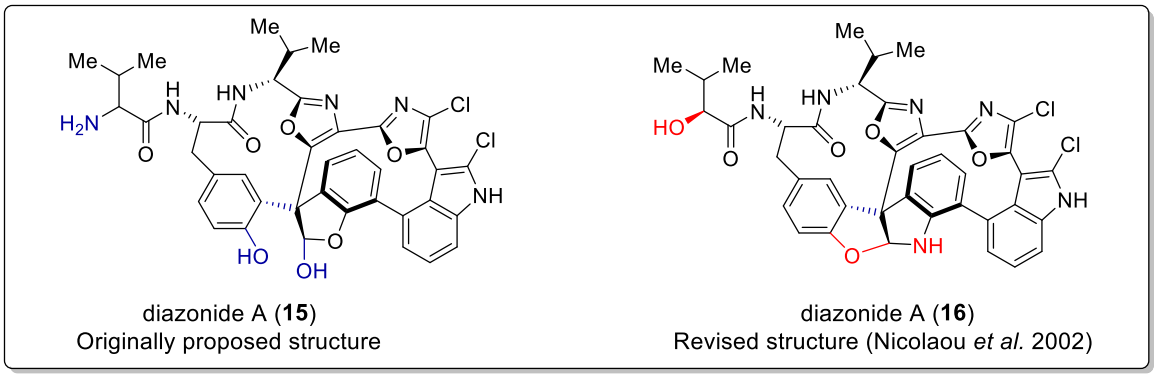

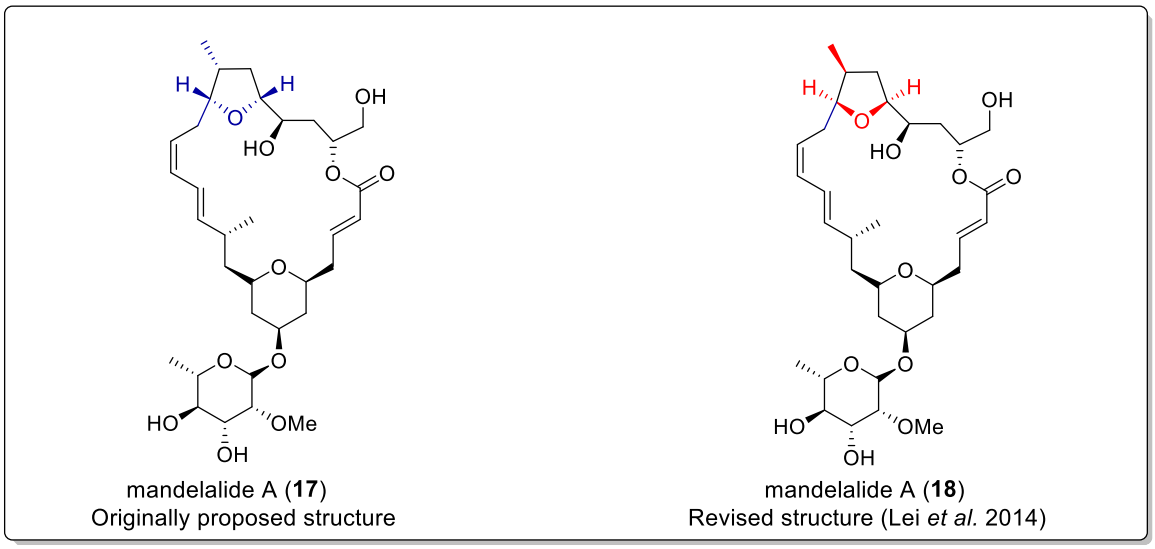

Scheme 1-3 Structural reassignment of natural products based on total synthesis

While combinatorial chemistry and high throughput screening technologies have played a significant role in exploring SAR studies of a lead molecule and generating a large library of new molecules, there has been only one *de novo* combinatorial compound that was approved as a drug in the past 25 years. Recently, Newman and Cragg[42] reported a survey of all drugs approved by the FDA during the period 1981 to 2014. These survey results indicate that ~50% (Figure 1-3) of the 1562 drugs that were approved were either unaltered natural product (5%), derived from a natural product (21%), synthetic drugs that contain a natural product pharmacophore (14%), or synthetic drugs that mimic biological activity of a natural product (11%). These results further demonstrate that natural products are undeniably valuable sources for drug discovery and development. Moreover, the structural complexity often encountered in natural products continues to inspire the

development of new synthetic methods and challenge chemists to synthesize these fascinating scaffolds in an efficient and scalable manner.

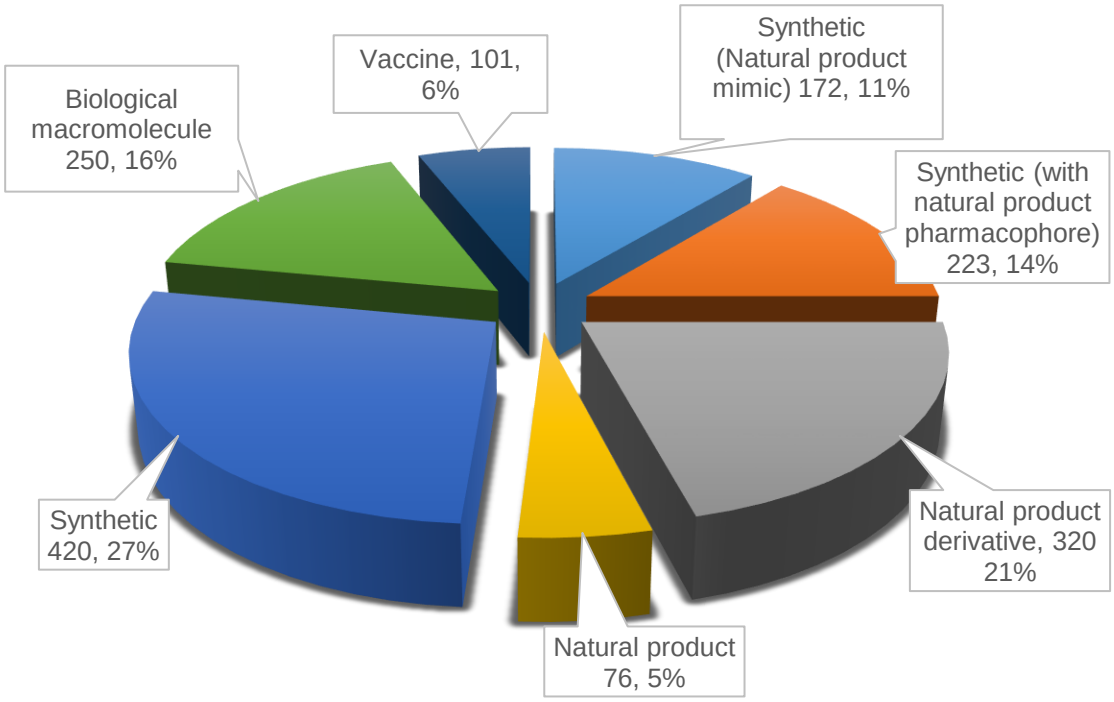

Figure 1-3 Source of all new approved drugs from 1981-2014.[42]

1.2. Tetrahydrofuran Containing Natural Products

Tetrahydrofuran (THF) is an oxygen-containing five membered heterocycle found in myriad natural products and other biologically active molecules. Typical classes of compounds that contain the THF motifs in their core structures include lignans,[43] polyether ionophores,[44] macrolides[45] and acetogenins.[46] These THF containing natural products exhibit a diverse array of biological properties ranging from anti-microbial, antitumor, antihelmic and antiprotozoal effects. Some representative examples of natural products containing a THF core are shown in Figure 1-4. Biselide A (**19**) is a marine macrolide that contains a 2,5-disubstituted THF ring and was isolated from an Okinawan ascidian in 2004 and found to be cytotoxic against a variety of cancer cell lines.[47] Uvaricin (**20**), isolated from the roots of the *Uvaria acuminate* in 1982, is another example of a THF-containing natural product and the first annonaceous acetogenin reported. Structurally, uvaricin consists of two adjacent 2,5-disubstitited THF motifs flanked by secondary carbinols. Importantly, this natural product also showed potent antitumor activity against P-388

lymphocytic leukemia cells.[48] Amphidinolide T3 (**21**) is a member of the amphidinolide class of polyketides and was isolated from a marine dinoflagellate of the genus *Amphidinium Sp*.[49] This compound is a 19-membered macrolactone possessing seven stereogenic centres and a trisubstituted THF ring. Interest in amphidinolide T3 (**21**) stems primarily from its cytotoxic activities against L1210 murine lymphoma cells and KB human epidermoid carcinoma cells.[50] Eribluin mesylate (**23**) (Halaven™) (Figure 1-5) is a THF-containing anticancer drug used in the treatment of late stage metastatic breast cancer.[51] Eribulin is a synthetic analogue of the marine natural product halichondrin B (**22**), a highly complex polyether macrolide which features multiple substituted THF rings.[52]

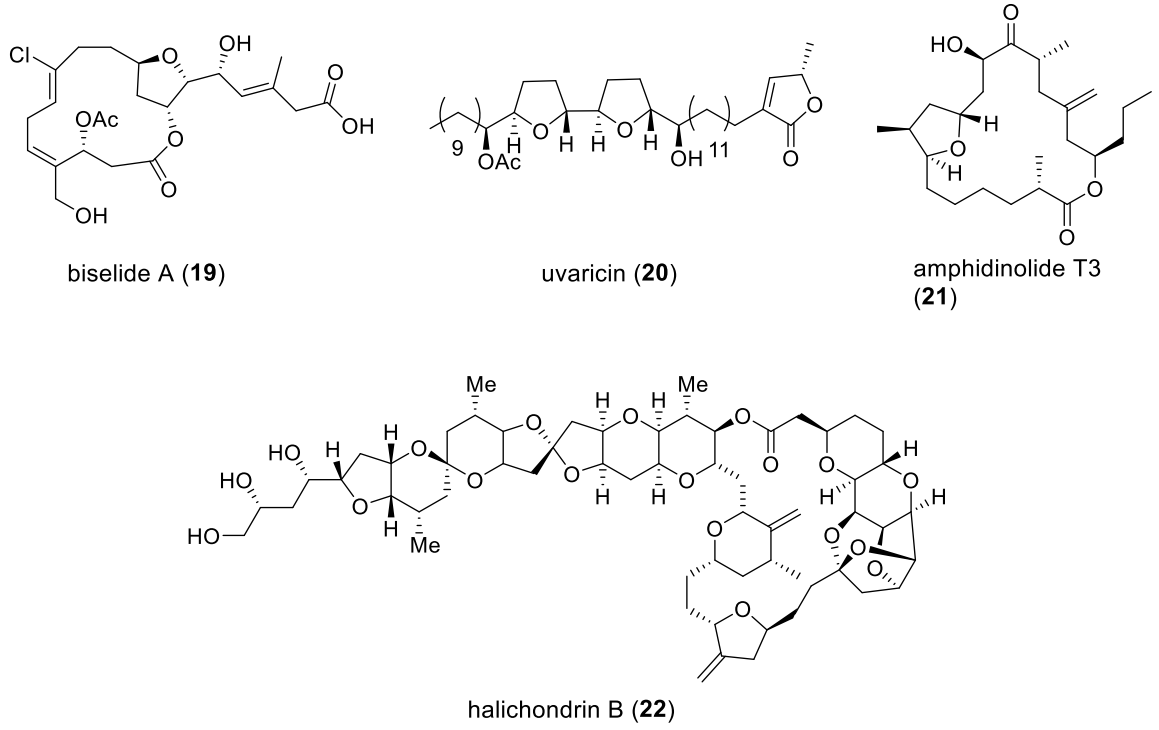

Figure 1-4 Representative examples of THF containing natural products.

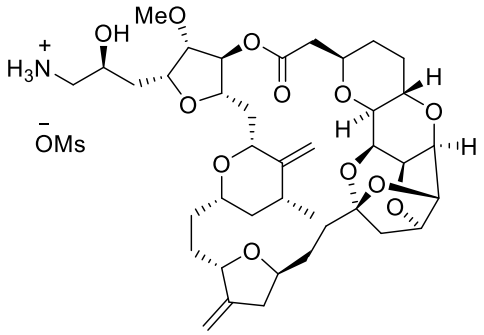

Eribulin mesylate (Halaven) (**23**)

Figure 1-5 Structure of Eribulin mesylate a THF containing anticancer drug.

1.2.1. Strategies Towards the Synthesis of Tetrahydrofuran Scaffolds

Due to the structural complexity and therapeutic potential of THF containing natural products, significant efforts have been expended towards the development of versatile methods for their stereoselective synthesis. As a result, there exists an abundance of literature detailing unique ways to access THF scaffolds,[53] and an exhaustive review of these studies would be impractical. Instead the present discussion will focus on some of the key strategies explored to access the substituted THF core in natural product synthesis (Figure 1-6)

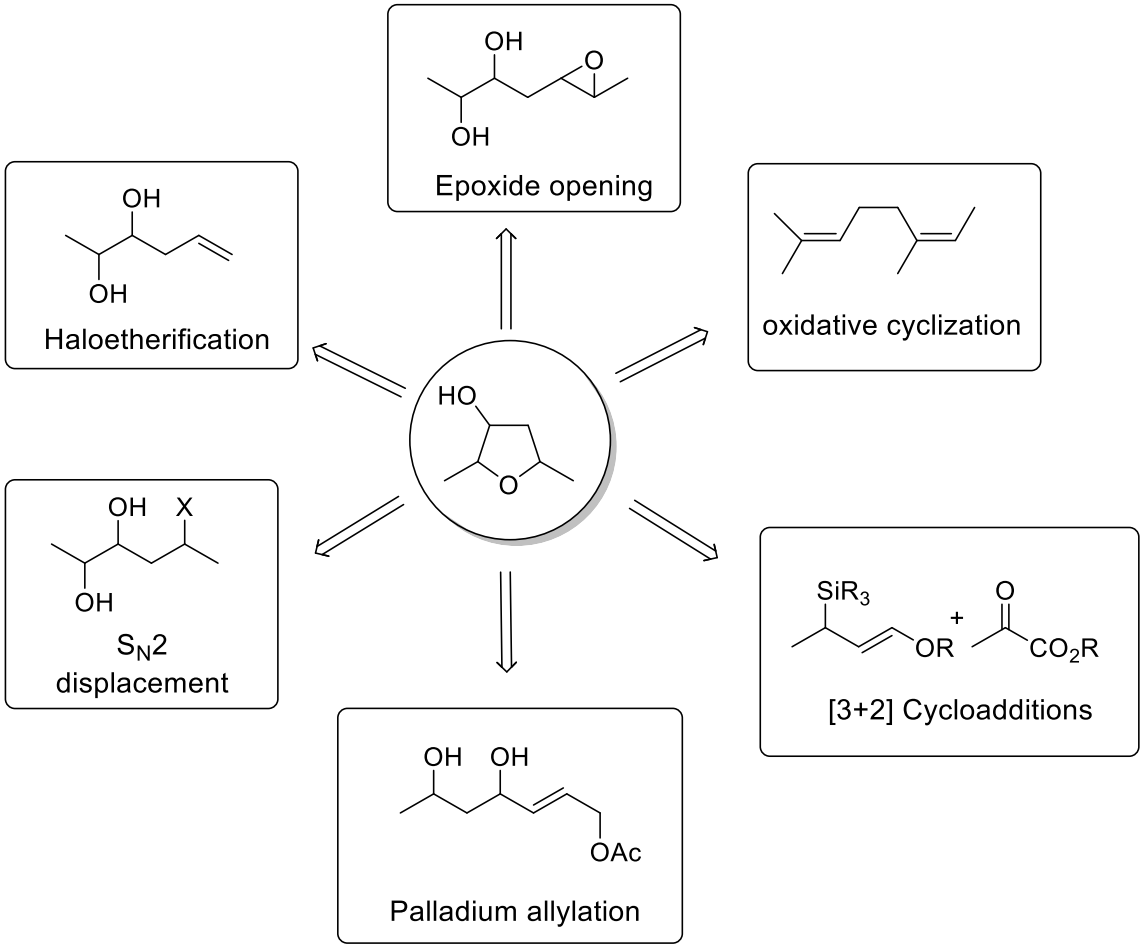

Figure 1-6 Selected methodolgies to access tetrahydrofuran scaffolds

Oxidative Cyclization of Alkenes: The first reported synthesis of tetrahydrofuran dates back to 1924[54,55] and involves the oxidative cyclization of 1,5 diene **24** to generate hydroxylated THF derivative **25** (Scheme 1-4). The need for stoichiometric amounts of oxidants such as OsO_4 and $KMnO_4$ limits the use of this reaction in natural product synthesis. However, considerable efforts have been expended to develop catalytic versions of this transformation. Donohoe *et al*.[56] applied Os-catalyzed oxidative cyclization for the synthesis of compound **27** as a single stereoisomer from compound **26** in single step. Another example[57] demonstrates the use of RuO_4-catalyzed oxidation of squalene (**28**) to afford pentatetrahydrofuran **29** in 50% yield. Notably, this transformation led to the generation of 10 stereogenic centres and 12 bonds in the formation of. compound **29**.

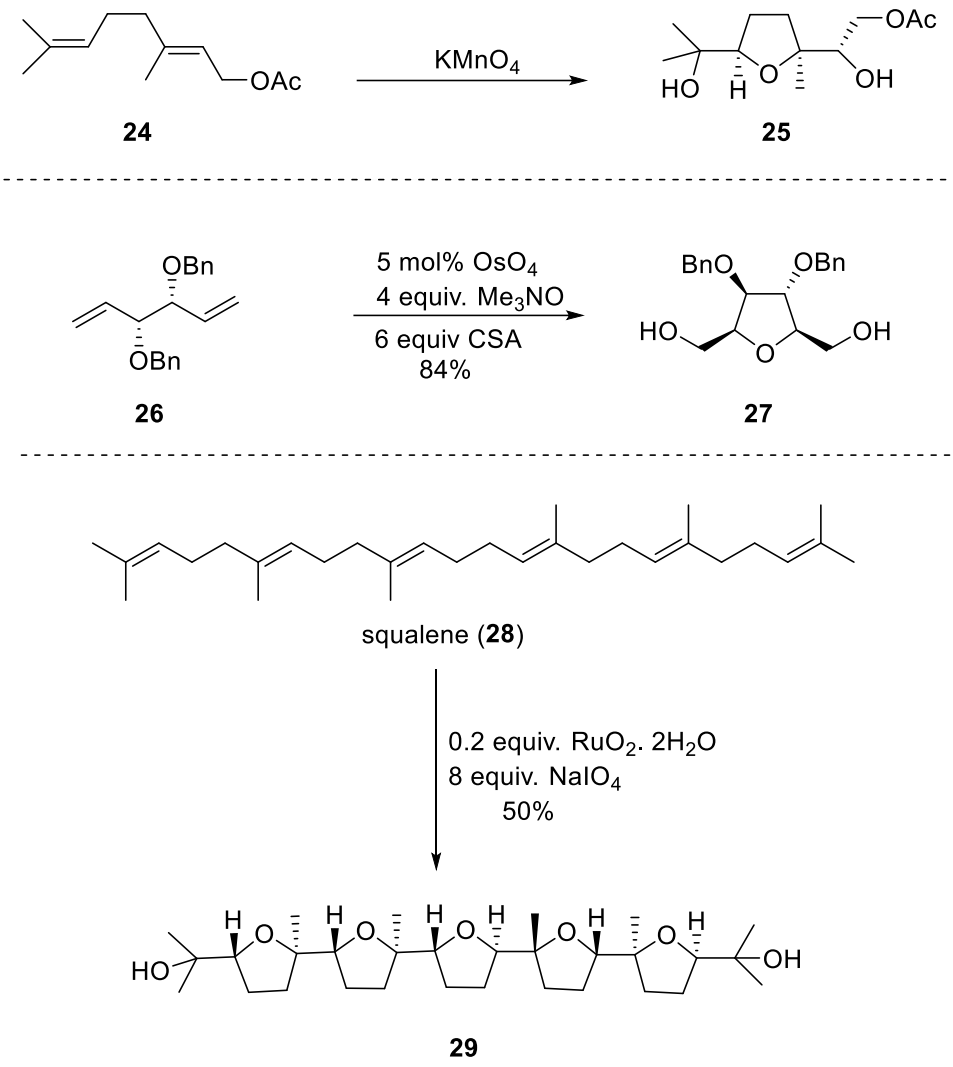

Scheme 1-4 Oxidative cyclizations of alkenes to generate THF derivatives

Intramolecular Epoxide Opening: In general, the opening of an epoxide by intramolecular attack of a nucleophilic oxygen has been widely used in the synthesis of saturated *O*-heterocycles[58] such as tetrahydrofurans. This approach achieved popularity because the epoxide can be synthesized stereoselectively employing Sharpless[59], Katsuki,[60] or Jacobsen[61] methods and in most cases the epoxide opening occurs with complete inversion of stereochemistry *via* an S_N2 type reaction. For instance, in Hoye's[62] synthesis of *hexepi*-uvaricin (**33**), the diol **30** was subjected to Sharpless asymmetric epoxidation to install the required stereogenic centres. Subsequently, monotosylation followed by acid-catalyzed acetonide cleavage with simultaneous double cyclization *via* epoxide opening provides access to the *trans*-bis-tetrahydrofuran **32** as a single

diastereomer in good yield. A further sequence of reactions yielded *hexepi*-uvaricin (**33**) in 20 steps (Scheme 1-5).

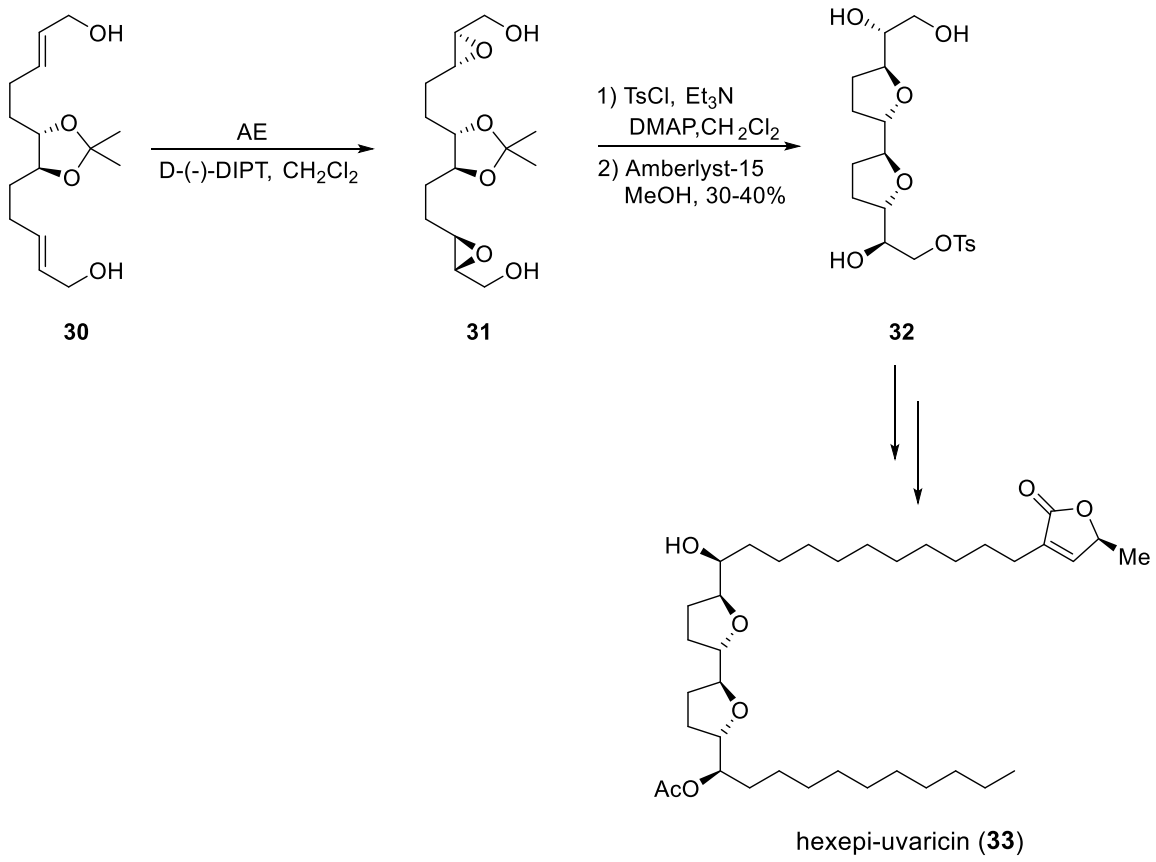

Scheme 1-5 Hoye's synthesis of bis-tetrahydrofuran via intramolecular epoxide opening route

Substitution Reactions: A classical approach towards the THF synthesis employs an intramolecular S_N2 substitution reaction between a hydroxyl group and a tethered leaving group (halides, sulfonates). Despite the success of this strategy to stereoselectively access THF rings in natural products synthesis, most of the precursors are prepared with all product stereocentres in place which can be challenging and require multiple steps[53f]. Marshal *et al*.[63] applied this strategy to construct two THF subunits in the synthesis of (+)-asimicin (**40**) (Scheme 1-6). Addition of γ-alkoxy allylic stannane **35** to the dialdehyde **34** in the presence of $InCl_3$ gave **36** as a single isomer. Tosylation of the newly formed secondary hydroxyl group, followed by silyl deprotection with concomitant S_N2 displacement of the tosylate generated the bis-THF derivative **37**. This was further elaborated to (+)-asimicin (**40**) in 4 steps.

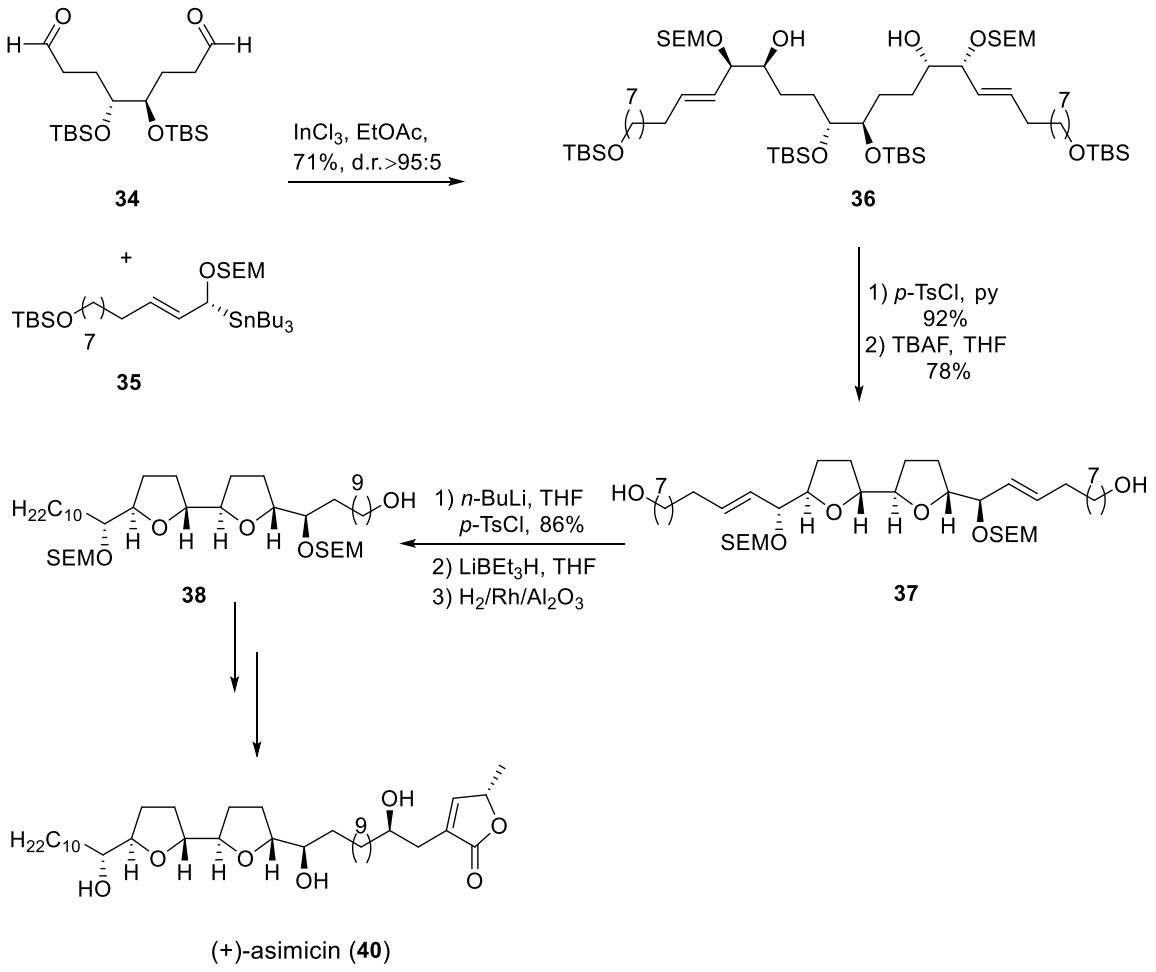

Scheme 1-6 Synthesis of (+)-asimicin (40) by tosylate displacement strategy

Haloetherifictaion: Another popular route to substituted tetrahydrofurans involves haloetherification, although the stereochemistry of the reaction outcome is mostly substrate dependent.[50f] The general reaction mechanism is outlined in Scheme 1-7 and favours a 5-*exo*-tet-cyclization. This strategy is best exemplified in Fujioka and Kita's synthesis of rubrenolide,[64] a THF-containing natural product originally isolated from the trunk wood of the Amazonia tree *Nectandra rubra* that exhibits a potent insecticidal property. Here, the authors demonstrated the application of a double intramolecular iodoetherification of acetal **44** to generate the key bi cyclic THF motif **45** *en route* to the total synthesis of rubrenolide (**46**) (Scheme 1-8).

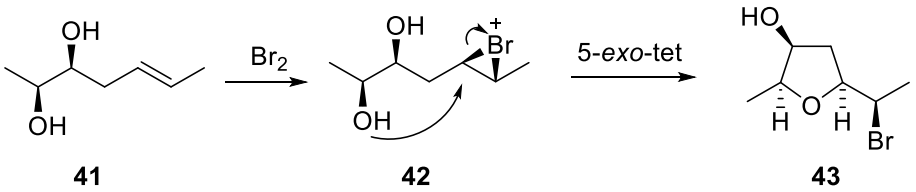

41 42 43

Scheme 1-7 Haloetherification reaction mechanism.

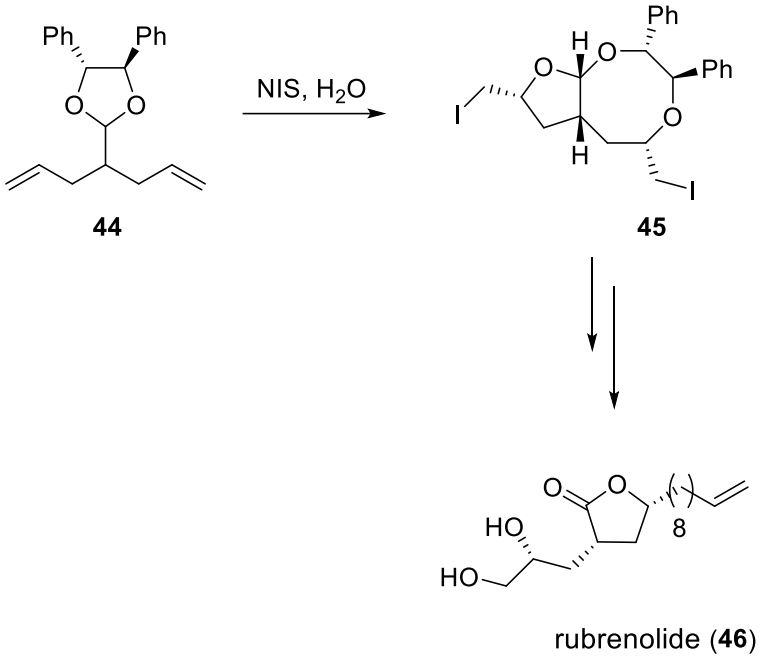

44 45

rubrenolide (**46**)

Scheme 1-8 Fujioka and Kita's synthesis of rubrenolide (46)

[3+2] Annulation / Cycloaddition: [3+2] annulation is a valuable method to generate THFs from two components and set two or three stereocentres in one step. An excellent example of the use of this methodology in Johnson and co-worker's[65] synthesis of a wide range of 2,5-*cis*-tetrahydrofurans (Scheme 1-9). These authors have also demonstrated the application of this approach in the total synthesis of (+)-virgatusin (**52**).[66] The [3+2] cycloaddition reaction between enantiomerically pure *trans*-cyclopropane **49** and piperonal (**50**) in the presence of a Lewis acid led to the formation of *cis*-THF derivative **51**, which was further elaborated to (+)-virgatusin (**52**) in 4 steps. Another striking example of this approach was employed by Roush *et al.*[67] in the total synthesis of amphidinolide E (**56**). Here, the [3+2] annulation reaction between aldehyde **54** and allyl silane **53** gave the THF derivative **55** with required stereochemistry in one step (Scheme 1-10).[67a] Further elaboration of compound **55** afforded amphidinolide E (**56**) with a step count of 19 steps

in its longest linear sequence. Although this method provides the desired THF motif in excellent yield and diastereoselctivity, this process is limited to a certain class of activated substrates.[53f]

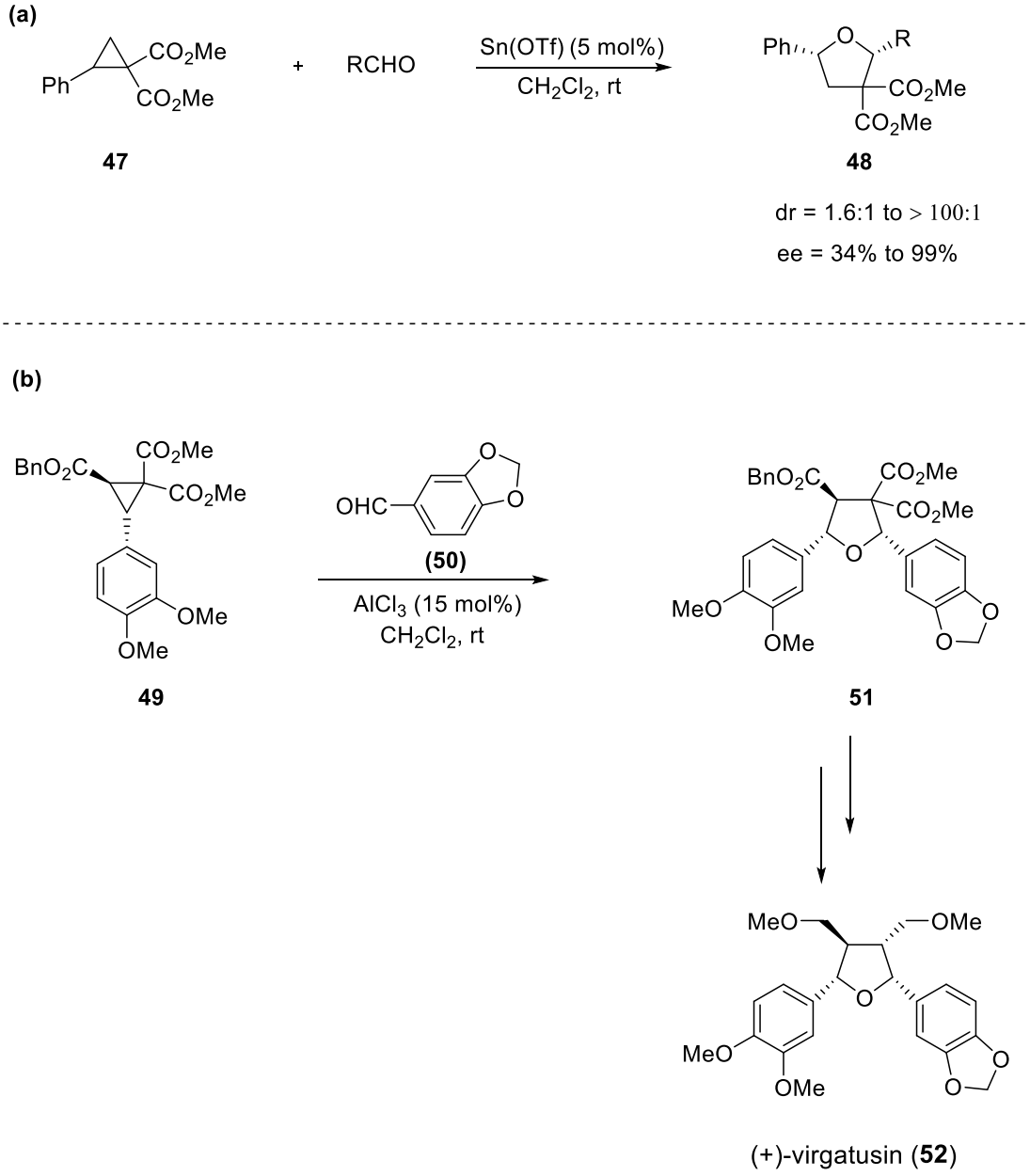

Scheme 1-9 Use of [3+2] cycloaddition to construct THF motif (a) Johnson *et al*, method to access THF ring (b) Application of methodolgy in the synthesis of virgatusin (52)

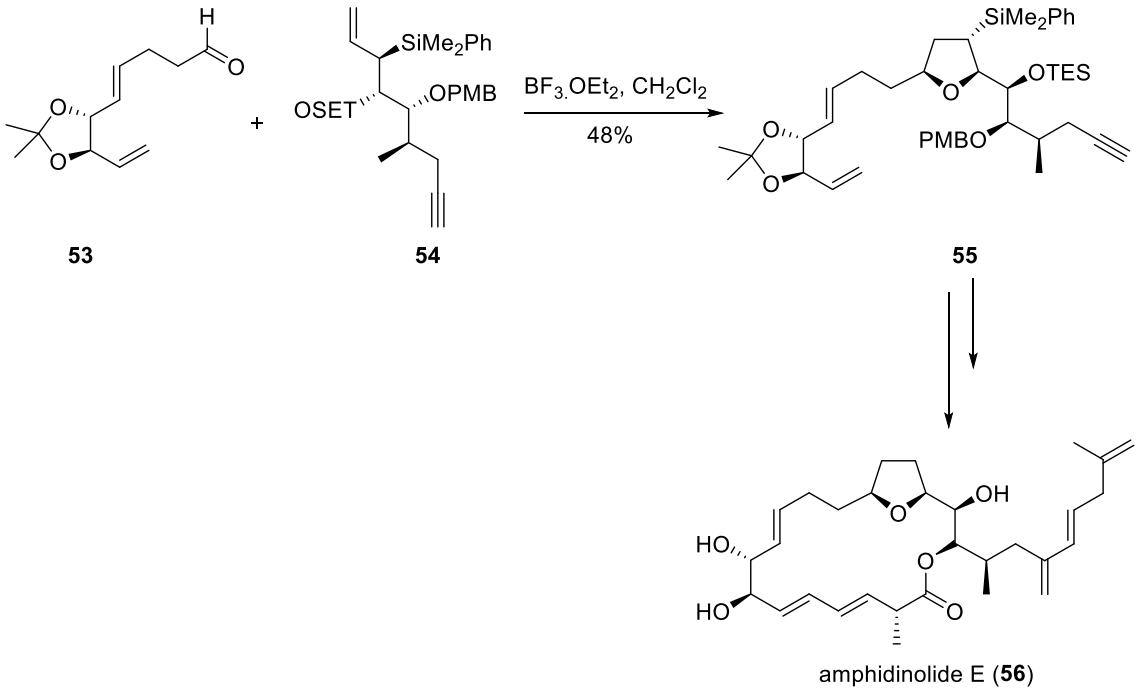

Scheme 1-10 Roush's synthesis of amphidinolide E (56) *via* [3+2] annulation

Palladium-Catalyzed π-allyl Additions: In recent years, the use of transition metal catalyzed reactions to synthesize *O*-heterocycles has gained popularity.[53f] This method proceeds *via* trapping of π-allyl palladium complex with an oxygen nucleophile to access the THF motifs with good diastereoselctivity. Enantioselective variants of this reaction have also been developed through the use of chiral catalysts (Scheme 1-11).[68] For instance, Koskinen *et al.*[69] have employed this approach in the total synthesis of a cytotoxic natural product pachastrissamine. From *Z*-allyl acetate **60** they were able to generate THF **61** as the major product in 59% yield. THF **61** was subsequently transformed into pachastrissamine (**62**).

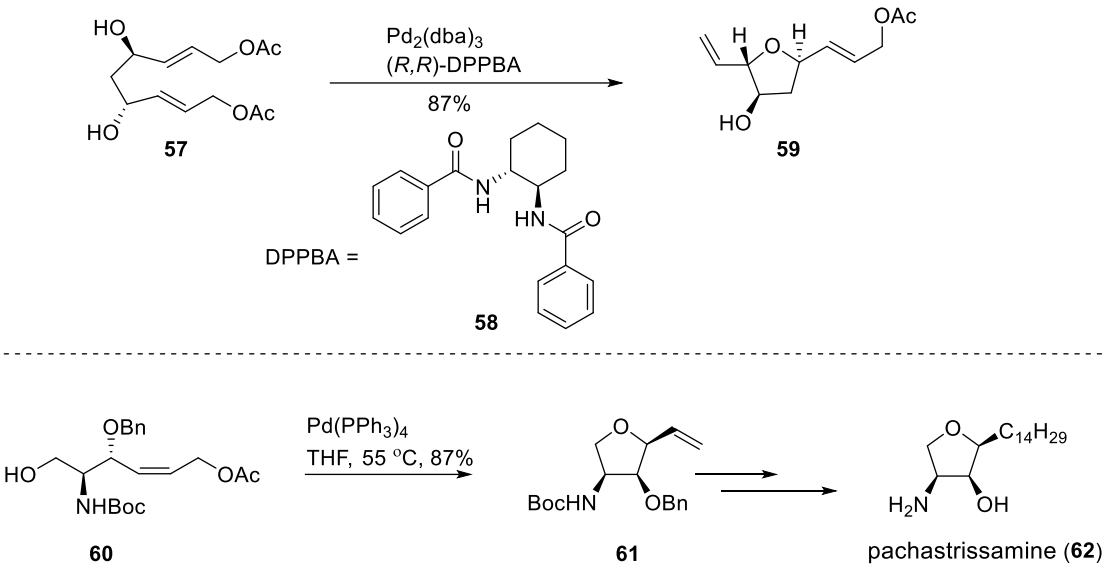

Scheme 1-11 Palladium catalyzed cyclizations to access THF derivatives

Despite a multitude of synthetic methods available to access biologically active THF-containing natural products, there are significant challenges to construct these molecular scaffolds stereoselectively and in an efficient manner. As shown from the previous studies, the processes required to synthesize substituted THF-containing natural products rely mainly on chiral building blocks and require several protecting groups or functional group transformations, which significantly impacts overall efficiency. Therefore, it is important to develop novel strategies that include atom, step and redox economy.[70] In line with these synthetic challenges, a major part of this thesis aims to establish a viable and efficient synthetic route to two THF-containing marine natural products through the use of α-chloroaldehydes.

1.2.2. Britton Group Approach to Stereoselective Synthesis of Substituted Tetrahydrofurans

In view of the potential significance of THF scaffolds present in numerous natural products and biologically active compounds, over the past few years the Britton group have expended significant efforts in the development of efficient and stereoselective methods to access THF ring systems.[71] Here, chlorohydrins are used as key building blocks, which are easily accessible in 2-3 steps from inexpensive and commercially available starting materials. Our approach initiates with the synthesis of enantiomerically enriched α-chloroaldehydes, which can be synthesized by employing the Jorgensen

procedure[72] or MacMillan's[73] method using L-prolinamide or imidazolidine as the organocatalyst, respectively. Christmann[74] recently reported a simplified procedure combining the MacMillan catalyst and the inexpensive, bench stable NCS as chlorinating agent (Scheme 1-12 a). Subsequently, an aldol reaction between the enantiomerically enriched α-chloroaldehyde and a lithium enolate affords *anti*-configured β-ketochlorohydrin in excellent diastereoselctivity and good yield (Scheme 1-12 b).

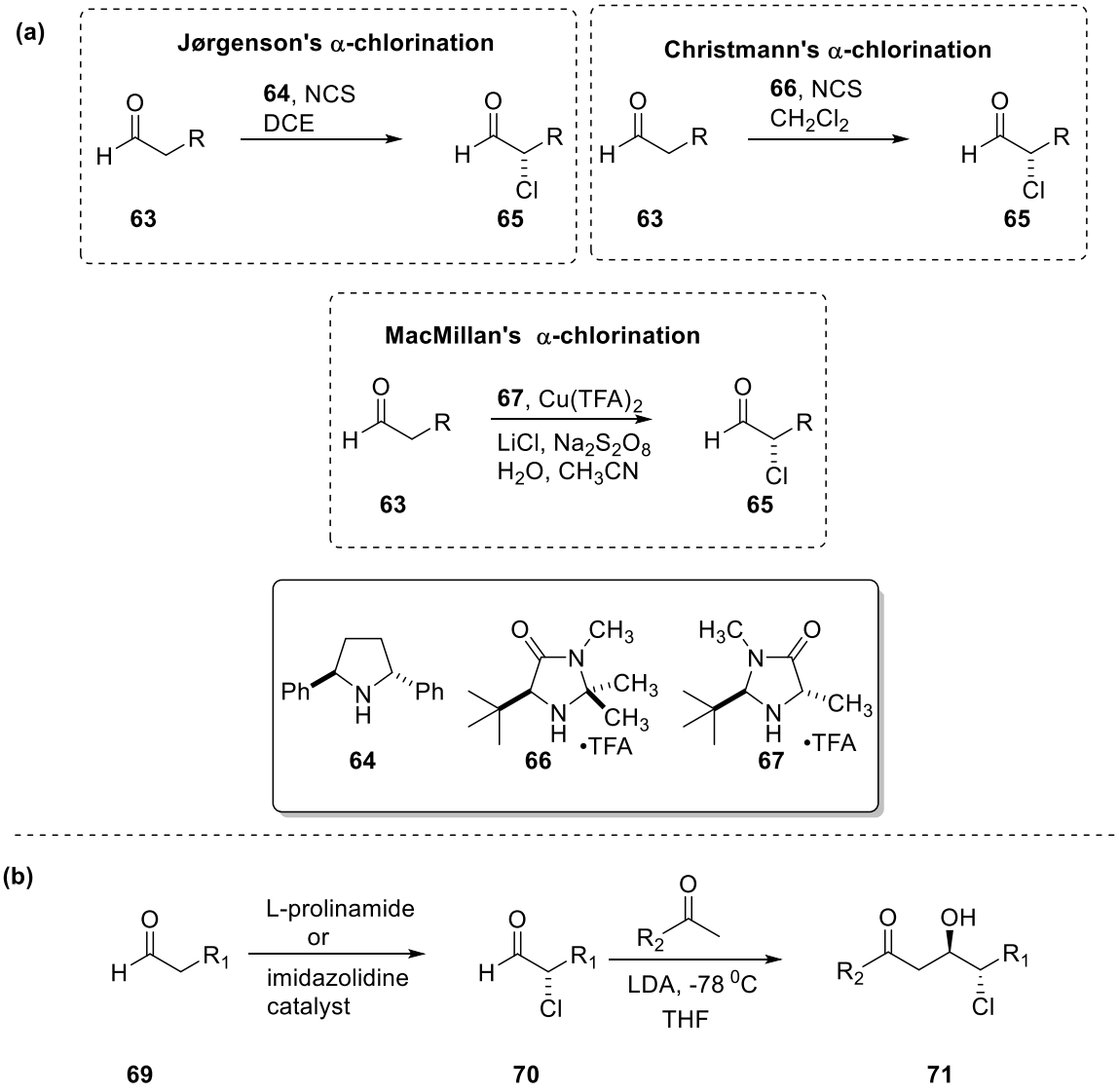

Scheme 1-12 (a) Synthesis of α-chloroaldehydes form Jorgensen's, MacMillan's or Christmann's method. (b) Synthesis of *anti*-configured β-ketochlorohydrins from a lithium aldol reaction

The diastereoselctivity of the aldol reaction can be rationalized using the well established Evans-Conforth[75,76] model for acyclic stereocontrol (Scheme 1-13) that

predicts the carbon-chlorine bond and the adjacent C-O bond of the carbonyl group will be aligned in opposite directions to mimimize the overall dipole moment of the molecule in the lowest energy transition state. Next, the nucleophile approaches the carbonyl function preferentially from the least sterically hindered face of the aldehyde, leading to the formation of 1,2-*anti*-aldol adducts as the major product of the reaction (*anti*-relationship between adjacent chloromethine and hydroxymethine stereogenic centres).

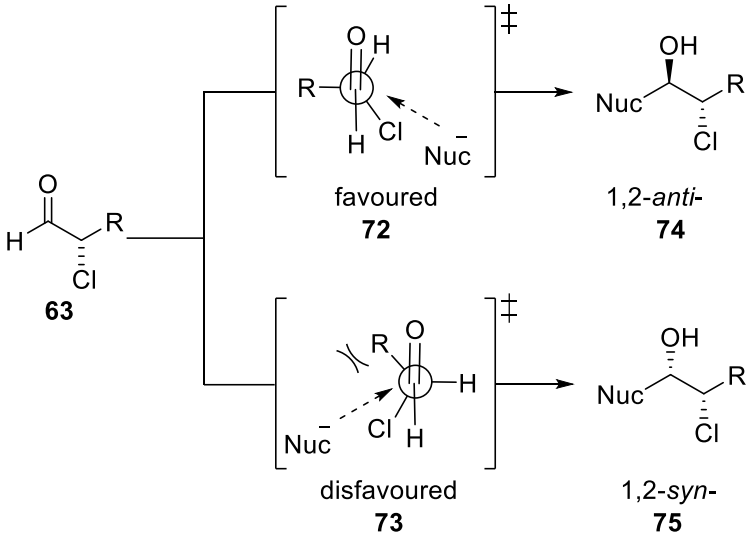

Scheme 1-13 Evans-Conforth model for rationalizing the stereochemical outcome of nucleophilic addition to α-chloroaldehyde.

Stereoselective reduction of the resulting β-ketochlorohydrin **71** in either a 1,3-*anti* or 1,3-*syn* fashion affords the diastereomeric alcohols **76** and **77** respectively.[77-79] The alcohols **76** and **77** can be cyclized *via* S_N2 displacement of the Cl atom by the hydroxyl group at C5 in the presence of stoichiometric amounts of silver (I) oxide (Ag_2O) and silver (I) trifluromethanesulfonate (AgOTf) to afford 2,3-*syn* tetrahydrofurans **78** and **80**. or by heating in H_2O or MeOH. On the other hand, 2,3-*anti* tetrahydrofurans **79** and **81** can be accessed by epoxidation of chlorodiols **76** and **77** under basic conditions followed by Lewis acid-promoted rearrangement, leading to double inversion.[80] It is noteworthy that this approach allows rapid access to all the potential 2,5-disubstituted 3-hydroxy tetrahydrofuran diastereomers from a single β-ketochlorohydrin in 2 to 3 steps. (Scheme 1-14).

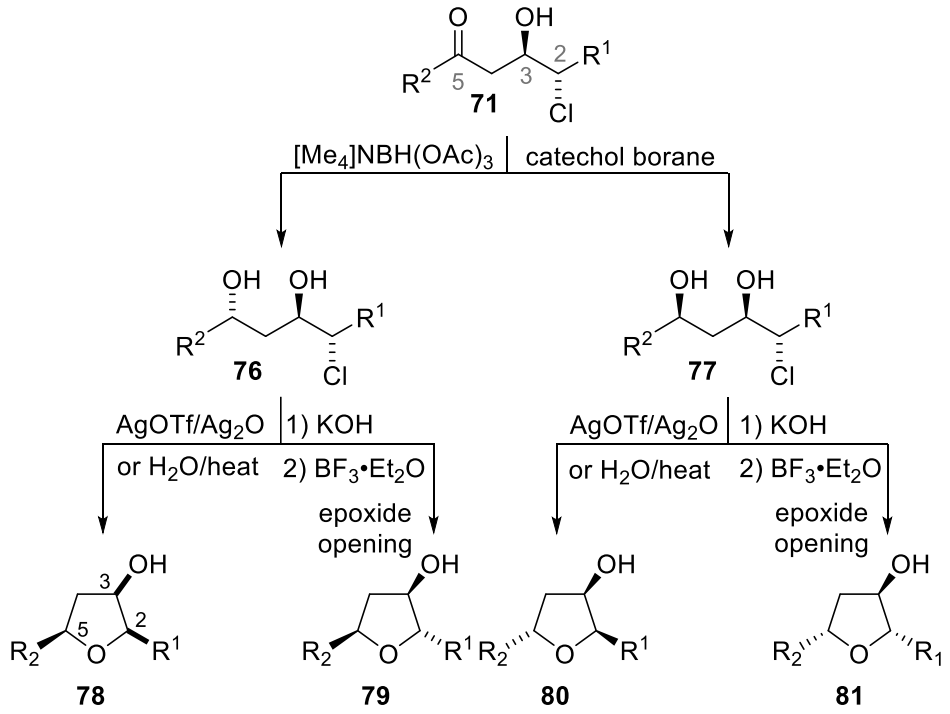

Scheme 1-14 Britton group's approach to access all configurational isomers of 2,5-disubstituted 3-hydroxy tetrahydrofuran scaffolds.

The efficiency of this methodology has been demonstrated by successful total syntheses of several THF-containing natural products. (selected examples are shown in Figure 1-7).[80-84]

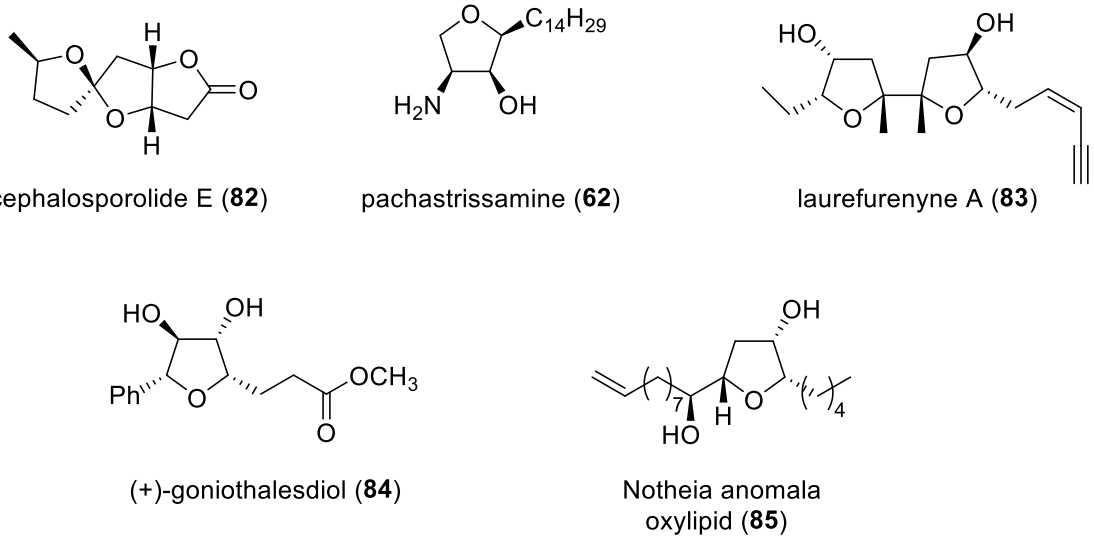

Figure 1-7 Examples of natural products synthesized in the Britton group using a chlorohydrin-based startegy.

To illustrate these methods, the total synthesis of (+)-goniothalesdiol (**84**) was achieved in 4 steps with excellent yield,[80] whereas the previously reported syntheses[85] were completed in 10 to 16 linear steps. Here, the synthesis began with the lithiation of vinyl iodide **86** followed by nucleophilic addition to the α-chloroaldehyde **87**, which afforded the 1,2-*anti* chlorohydrin **88** in excellent yield and good diastereoselctivity (d.r 13:1). The chlorohydrin **88** was subjected to hydroxyl directed dihydroxylation to give the triol **89**, followed by thermal cyclization (microwave heating) to afford (+)-goniothalesdiol in 4 steps and in 49% overall yield.

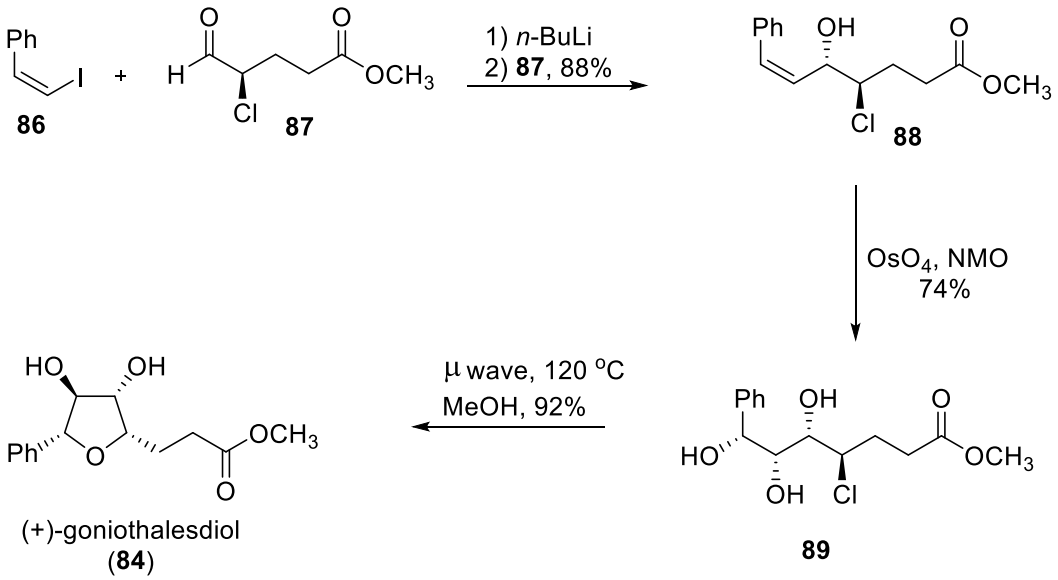

Scheme 1-15 Synthesis of (+)-goniothalesdiol (84) via a chlorohydrin-based strategy

1.3. Thesis Overview

This thesis is presented in journal article style, with *Chapter 1* as a general introduction, followed by *Chapter 2* as a research work prepared for submission, *Chapter 3* as a journal article and *Chapter 4* as unpublished research work.

Chapter 1 introduces the background information about the role of natural products as therapeutics in drug discovery and development, followed by a brief review of methods to access tetrahydrofuran scaffolds in natural product synthesis.

Chapter 2 delineates a successfully completed total synthesis of a potent cytotoxic natural product biselide A, isolated from a marine Okinawan ascidian. This work involved the application of the chlorohydrin-based strategy to construct the key tetrahydrofuran core of the molecule, which was rapidly elaborated into the desired natural product. A critical aspect of this work involves in depth optimization of a cross metathesis reaction and a Reformatsky macrocyclization. Notably, this flexible and efficient synthetic approach can be readily applied to the synthesis of other members of the biselide family.

Chapter 3 contains the manuscript "A counterintuitive stereochemical outcome from a chelation-controlled vinylmetal aldehyde addition leads to the configurational reassignment of phormidolide A" (Lam, N. Y. S.; Muir. G.; Challa, V. R.; Britton, R.; Paterson, I. *Chem. Commun*., **2019**, *55*, 9717-9720). It describes the studies towards the synthesis of phormidolide A, a macrocyclic polyketide isolated from the cyanobacteria *Leptolyngbya sp*. This was a collaborative project with Paterson group at the University of Cambridge. We exploit our previously established chlorohydrin-based strategy to access the tetrahydrofuran motif in high enantiomeric purity. The synthesis of three model acetonide derivatives and its NMR spectroscopic comparison with the reported triacetonide derivative of phormidolide A supports a reassignment of seven of the eleven stereogenic centres in phormidolide A.

In *Chapter 4,* the efforts towards the synthesis of the chimeric glycopeptide corresponding to *Shigella flexneri* Y O-polysaccharide and its peptide mimic MDWNMHAA is presented. Two haptens, a pentasaccharide and a mimetic octapeptide bind with moderate affinity to a monoclonal antibody SYA/J6 specific for the O-polysaccharide of the *S.flexneri* Y bacterium. Based on X-ray crystallography data and molecular modelling studies, two chimeric glycopeptides (α-glycopeptide and β-glycopeptide) were designed to improve the binding affinity to SYA/J6. The Pinto group had previously synthesized α-glycopeptide which did not inhibit the binding of SYA/J6 to *S.flexneri* Y lipopolysaccharide. Next, we turned our attention towards the synthesis of the β-glycopeptide, as docking studies indicated a potentially better fit within the antibody binding site. Progress towards the synthesis of the β-glycopeptide is described.

Chapter 5 summarizes the thesis work and provides suggestions for future work.

References

(1) Gurnani, N.; Mehta, D.; Gupta, M.; Mehta, B. K. *Afr. J. Basic Appl. Sci.* **2014**, *6*, 171–186.

(2) Dewick, P. M. *Medicinal Natural Products: A Biosynthetic Approach*, 2nd ed.; John Wiley and Sons, Ltd: UK, **2002**; pp 8-15.

(3) Dias, D. A.; Urban, S.; Roessner, U. *Metabolites* **2012**, *2*, 303–336.

(4) Abdel-Lateif, K.; Bogusz, D.; Hocher, V. *Plant Signal Behav*. **2012,** *7*, 636-641.

(5) Liu, C. W.; Murray, J. D. *Plants*. **2016**, *5,* 33.

(6) Tibballs, J.; Yanagihara, A. A.; Turner, H. C.; Winkel, K. *Inflamm. Allergy Drug Targets* **2011**, *10*, 438–446.

(7) Schatz, A.; Bugle, E.; Waksman, S. *Proc. Soc. Exp. Biol. Med.* **1944**, *55*, 66–69.

(8) Gries, R.; Britton, R.; Holmes, M.; Zhai, H.; Draper, J.; Gries, G. *Angew. Chem., Int. Ed.* **2015**, *54*, 1135–1138.

(9) Demain, A. L. *Appl. Microbiol. Biotechnol*. **1999**, *52,* 455–463.

(10) Lahlou, M. *Flavour Fragr J.* **2004**, *19*, 159–165.

(11) Croteau, R.; Kutchan, T. M.; Lewis, N.G. In *Biochemistry and Molecular Biology of Plants*; Wiley Interscience, 2000; pp. 1250–1318.

(12) Butterworth, J. H.; Morgan, E. D. *Chem. Commun.* **1968**, 23-24.

(13) Newman, D. J.; Cragg, G. M.; Snader, K. M. *Nat. Prod. Rep.* **2000**, *17*, 215–234.

(14) Hou, J. P. The Development of Chinese Herbal Medicine and the Pen-Ts'ao. *Comp. Med. East West* **1977**, *5*, 117–122.

(15) Cragg, G. M.; Newman, D. J. *Pure Appl. Chem*. **2005**, *77*, 7–24.

(16) Aschwanden, C. *Bull. World Health Organ.* **2001**, *79*, 691–692.

(17) Kinghorn, A. D. *J. Pharm. Pharmacol.* **2001**, *53*, 135–148.

(18) Huxtable, R. J.; Schwarz, S. K. The Isolation of Morphine-First Principles in Science and Ethics. *Mol. Interv.* **2001**, *1*, 189–191.

(19) Corson, T. W.; Crews, C. M. *Cell* **2007**, *130*, 769–774.

(20) Atanasov, A. G.; Waltenberger, B.; Pferschy-Wenzig, E.-M.; Linder, T.; Wawrosch, C.; Uhrin, P.; Temml, V.; Wang, L.; Schwaiger, S.; Heiss, E. H.; Rollinger, J. M.; Schuster, D.; Breuss, J. M., Bochkov, V.; Mihovilovic, D. M.; Kopp, B.; Bauer, R; Dirsch, V. M.; Syuppner, H. *Biotechnol. Adv.* **2015**, *33*, 1582–1614.

(21) Jeffreys, D. *Aspirin: The Remarkable Story of a Wonder Drug*; Bloomsbury: USA **2004**, pp 1-300.

(22) Beutler, J. A. *Curr. Protoc. Pharmacol*. **2009**, *46*, 911-921.

(23) Schatz, A.; Bugle, E.; Waksman, S. A. *Proc.Soc. Exp. Biol. And Med,* **1944**, *55,* 66-69.

(24) (a) McGurie, J. M.; Powell, H. M.; Smith, J. W. *Antibiotics and Chemotherapy,* **1952**, *2*, 281 (b) Wiley, P. F.; Gale, R.; Pettinga, C. W.; Gerzon, K. C. *J. Am. Chem. Soc.* **1957**, *79*, 6074–6077.

(25) Abraham, E. P. *Drugs* **1987**, *34*, 1–14.

(26) (a) Burton, H. S.; Abraham, E. P. *Biochem. J.* **1951**, *50*, 168–174. (b) Newton G. C. F.; Abraham, E. P. *Biochem. J.* **1951**, *58*, 103-111 (c) Wick, W. E. *Appl Microbiol.* **1967**, *15*, 765-769.

(27) Donald, P. L. *Clin. Infect. Dis.* **2006**, *42,* 5-12.

(28) (a) Radjasa, O. K.; Vaske, Y. M.; Navarro, G.; Vervoort, H. C.; Tenney, K.; Linington, R. G.; Crews, P. *Bioorganic Med. Chem.* **2011**, *19*, 6658–6674. (b) Leal, M. C.; Puga, J.; Serôdio, J.; Gomes, N. C. M.; Calado, R. *PLoS ONE,* **2012**, *7*, e30580

(29) Miljanich, G. *Curr. Med. Chem.* **2004**, *11*, 3029–3040.

(30) D'Incalci, M.; Galmarini, C. M. *Mol. Cancer Ther.* **2010**, *9*, 2157–2163.

(31) Gunasekera, S. P.; Gunasekera, M.; Longley, R. E.; Schulte, G. K. *J. Org. Chem.* **1990**, *55*, 4912–4915.

(32) Hong, J. *Chem. Eur. J.* **2014**, *20*, 10204–10212.

(33) Nerenberg, J. B.; Hung, D. T.; Somers, P. K.; Schreiber, S. L. *J. Am. Chem. Soc.***1993**, *115*, 12621–12622; (b) Hung, D. T.;Nerenberg, J. B.; Schreiber, S. L. *Chem. Biol.***1994**, *1*, 67–71; (c) Hung, D. T.; Nerenberg, J. B.; Schreiber, S. L. *J. Am.Chem. Soc*. **1996**, *118*, 11054–11080.

(34) Smith, A. B.; Freeze, B. S. *Tetrahedron* **2008**, *64*, 261–298.

(35) Florence, G. J.; Gardner, N. M.; Paterson, I. *Nat. Prod. Rep.* **2008**, *25*, 342-375.

(36) (a) Mickel, S. J.; Sedelmeier, G. H.; Niederer, D.; Daeffler, R.; Osmani, A.; Schreiner, K.; Seeger-Weibel, M.; Bérod, B.; Schaer, K.; Gamboni, R. *Org. Process Res. Dev.* **2004**, *8* , 92–100.; (b) Mickel, S. J.; Sedelmeier, G. H.; Niederer, D.; Schuerch, F.; Grimler, D.; Koch, G.; Daeffler, R.; Osmani, A.; Hirni, A.; Schaer, K.; Gamboni, R. *Org. Process Res. Dev.* **2004**, *8*, 101–106.; (c) Mickel, S. J.; Sedelmeier, G. H.; Niederer, D.; Schuerch, F.; Koch, G.; Kuesters, E.; Daeffler, R.; Osmani, A.; Seeger-Weibel, M.; Schmid, E.; Hirni, A.; Schaer, K.' Gamboni, R. *Org. Process Res. Dev.* **2004**, *8*, 107–112.; (d) Mickel, S. J.; Sedelmeier, G. H.; Niederer, D.; Schuerch, F.; Seger, M.; Schreiner, K.; Daeffler, R.; Osmani, A.; Bixel, D.; Loiseleur, O.; Cercus, J.; Stettler, H.; Schaer, K.; Gamboni, R. *Org. Process Res. Dev.* **2004**, *8* , 113–121.; (e) Mickel, S. J.; Niederer, D.; Daeffler, R.; Osmani, A.; Kuesters, E.; Schmid, E.; Schaer, K.; Gamboni, R. *Org. Process Res. Dev.* **2004**, *8*, 122–130.

(37) (a) Zhu, C.; Cook, S. P. *J. Am. Chem. Soc*. **2012**, *134,* 13577-13579; (b) Cook, S. P. *Future Med. Chem*. **2013**, *5*, 233-236

(38) Lindquist, N.; Fenical. *J. Am. Chem. Soc*. **1991**, *113*, 2303-2304

(39) (a) Li, J.; Jeong, S.; Esser, L.; Harran, P. G. *Angew. Chem* **2001**, *113*, 4901–4906.; (b) Li, J.; Burgett, A. W. G.; Esser, L.; Amezcua, C.; Harran, P. G. Total Synthesis of Nominal Diazonamides - Part 2: On the True Structure and Origin of Natural Isolates. *Angew. Chem., Int. Ed.* **2001**, *40*, 4770–4773.

(40) (a) Nicolaou, K. C.; Bella, M.; Chen, D. Y.-K.; Huang, X.; Ling, T.; Snyder, S. A. *Angew. Chem., Int. Ed.* **2002**, *41*, 3495–3499.; (b) Nicolaou, K. C.; Bheema Rao, P.; Hao, J.; Reddy, M. V.; Rassias, G.; Huang, X.; Chen, D. Y. K.; Snyder, S. A. *Angew. Chem., Int. Ed.* **2003**, *42*, 1753–1758.

(41) Lei, H.; Yan, J.; Yu, J.; Liu, Y.; Wang, Z.; Xu, Z.; Ye, T. *Angew. Chem., Int. Ed.* **2014**, *53*, 6533–6537.

(42) Newman, D. J.; Cragg, G. M. *J. Nat. Prod.* **2016,** *79***,** 629-661.

(43) Saleem, M.; Hyoung, J. K.; Ali, M. S.; Yong, S. L. *Nat. Prod. Rep*. **2005**, *22*, 696–716.

(44) Faul, M. M.; Huff, B. E. *Chem. Rev.* **2000**, *100*, 2407–2473.

(45) Lorente, A.; Lamariano-Merketegi, J.; Albericio, F.; Álvarez, M. *Chem. Rev.* **2013**, *113*, 4567–4610.

(46) Bermejo, A.; Figadère, B.; Zafra-Polo, M. C.; Barrachina, I.; Estornell, E.; Cortes, D. *Nat. Prod. Rep*. **2005**, *22*, 269-303.

(47) (a) Teruya, T., Shimogawa, H., Suenaga, K., & Kigoshi, H. *Chemistry Letters*, **2004**. *33*, 1184-1185; (b) Teruya, T.; Suenaga, K.; Maruyama, S.; Kurotaki, M.; Kigoshi, H. *Tetrahedron* **2005**, *61*, 6561–6567. (c) Kigoshi, H.; Hayakawa, I. *Chem. Rec.* **2007**, *7*, 254–264.

(48) Jolad, S. D.; Hoffmann, J. J.; Schiam, K. H.; Cole, J. R.; Tempesta, M. S.; Kriek, G. R.; Bates, R. B. *J. Org. Chem.* **1982**, *47*, 3151–3153.

(49) (a) Aïssa, C.; Riveiros, R.; Ragot, J.; Fürstner, A. *J. Am. Chem. Soc.* **2003**, *125*, 15512–15520.; (b) Deng, L. S.; Huang, X. P.; Zhao, G. *J. Org. Chem.* **2006**, *71*, 4625–4635.

(50) (a) Kobayashi, J.; Kubota, T.; Endo, T.; Tsuda, M. *J. Org. Chem.* **2001**, *66*, 134-142. See also: (b) Tsuda, M.; Endo, T.; Kobayashi, J. *J. Org. Chem.* **2000**, *65*, 1349-1352.; (c) Kubota, T.; Endo, T.; Tsuda, M.; Shiro, M.; Kobayashi, J. *Tetrahedron* **2001**, *57*, 6175-6179.

(51) (a) Aicher, T. D.; Buszek, K. R.; Fang, F. G.; Forsyth, C. J.; Jung, S. H.; Kishi, Y.; Matelich, M. C.; Scola, P. M.; Spero, D. M.; Yoon, S. K. *J. Am. Chem. Soc.* **1992**, *114*, 3162–3164; (b) Chase, C. E.; Fang, F. G.; Lewis, B. M.; Wilkie, G. D.; Schnaderbeck, M. J.; Zhu, X. *Synlett* **2013**, *24* , 323–326.(c) Austad, B. C.; Benayoud, F.; Calkins, T. L.; Campagna, S.; Chase, C. E.; Choi, H. W.; Christ, W.; Costanzo, R.; Cutter, J.; Endo, A.; et al. *Synlett* **2013**, *24*, 327–332.; (b) Austad, B. C.; Benayoud, F.; Calkins, T. L.; Campagna, S.; Chase, C. E.; Choi, H. W.; Christ, W.; Costanzo, R.; Cutter, J.; Endo, A.; Fang, F. G.; Hu, Y.; Lewis, B. M.; Lewis , D. M.; Mckenna, S.; Noland, T. A.; Orr, J. D.; Peasnt, Marc.; Schnaderbeck, M. J.; Wilkie, G. D.; Abe, T.; Asai, N.; Kayano, Y.; Kimoto, Y.; Komatsu, Y.; Kubota, M.; Kuroda, H.; Mizuno, M.; Nakamura, T.; Omae, T.; Ozeki, N.; Suzuki, T.; Takigawa, T.; Watanabr, T.; Yoshizawa, K. . *Synlett* **2013**, *24* (3), 327–332.

(52) Hirata, Y.; Uemura, D. *Pure Appl. Chem*. **1986**, *58*, 701– 710.

(53) For selected reviews on synthetic approaches to tetrahydrofurans, see: (a) Boivin, T. L. B. *Tetrahedron* **1987**, *43*, 3309–3362; (b) Cardillo, G.; Orena, M. *Tetrahedron* **1990**, *46*, 3321–3408; (c) Harmange, J.-C.; Figadere, B. *Tetrahedron: Asymmetry* **1993**, *4*, 1711–1754; (d) Koert, U. Synthesis 1995, 115–132; (e) Miura, K.; Hosomi, A. *Synlett* **2003**, 143–155; (f) Wolfe, J. P.; Hay, M. B. Tetrahedron, **2007**, *63*, 261-290.

(54) Kotz, A.; Steche, T. *J. Pract. Chem.* **1924,***107,* 193-195.

(55) Klein, E.; Rojahn, W. *Tetrahedron* **1965**, *21,* 2353-2358.

(56) Donohoe, T. J.; Butterworth, S. *Angew. Chem., Int. Ed*. **2003**, *42*, 948-951.

(57) Caserta, T.; Piccialli, V.; Gomez-Paloma, L.; Bifulco, G. *Tetrahedron* **2005**, *61*, 927–939.

(58) (a) Li, K.; Vig, S.; Uckun, F. M. *Tetrahedron Lett.* **1998,** *39,* 2063-2066; (b) Maguire, R. J.; Thomas, E. J. *J. Chem. Soc., Perkin Trans. 1* **1995,** 2487–2495

(59) (a) Sharpless, K. B.; Akashi, K. *J. Am. Chem. Soc.* **1976**, *98*, 1986–1987; (b) Hentges, S. G.; Sharpless, K. B. *J. Am. Chem. Soc.* **1980**, *102*, 4263–4265.

(60) Irie, R.; Noda, K.; Ito, Y.; Matsumoto, N.; Katsuki, T. *Tetrahedron Lett.* **1990**, *31*, 7345–7348.

(61) Zhang, W.; Loebach, J. L.; Wilson, S. R.; Jacobsen, E. N. *J. Am. Chem. Soc.* **1990**, *112*, 2801–2803.

(62) Hoye, T. R.; Hanson, P. R.; Kovelesky, A. C.; Ocain, T. D.; Zhuang, Z. *J. Am. Chem. Soc.* **1991**, *113*, 9369–9371.

(63) Marshall, J. A.; Hinkle, K. W. *J. Org. Chem.* **1997**, *62*, 5989–5995.

(64) Fujioka, H.; Ohba, Y.; Hirose, H.; Murai, K.; Kita, Y. *Angew. Chem. Int. Ed.* **2005**, *44,* 734-737.

(65) (a) Pohlhaus, P. D.; Johnson, J. S. *J. org. Chem.* **2005**, *70,* 1057-1059; (b) Smith, A. G.; Slade, M. C.; Johnson, J. S. *Org. Lett.* **2011**, *13*, 1996–1999.

(66) Sanders, S. D.; Ruiz-Olalla, A.; Johnson, J. S. *Chem. Commun.* **2009**, *34*, 5135–5137.

(67) (a) Va, P.; Roush, W. R. *J. Am. Chem. Soc.* **2006**, *128*, 15960–15961; (b) Micalizio, G. C.; Roush, W. R. *Org. Lett.* **2000**, *2*, 461–464.

(68) Jiang, L.; Burke, S. D. *Org. Lett.* **2002**, *4*, 3411–3414.

(69) Passiniemi, M.; Koskinen, A. M. P. *Org Biomol Chem* **2011**, *9*, 1774–1783.

(70) Kuttruff, C. A.; Eastgate, M. D.; Baran, P. S. *Nat. Prod. Rep.* **2014**, *31*, 419–432.

(71) Kang, B.; Mowat, J.; Pinter, T.; Britton, R. *Org. Lett.* **2009**, *11*, 1717–1720.

(72) Halland, N.; Braunton, A.; Bachmann, S.; Marigo, M.; Jørgensen, K. A. *J. Am.Chem. Soc.* **2004**, *126*, 4790–4791.

(73) Amatore, M.; Beeson, T. D.; Brown, S. P.; MacMillan, D. W. C. *Angew. Chem. Int.Ed.* **2009**, *48*, 5121–5124.

(74) Winter, P.; Swatschek, J.; Willot, M.; Radtke, L.; Olbrisch, T.; Schäfer, A.; Christmann, M. *Chem. Commun.* **2011**, *47*, 12200–12202.

(75) Cornforth, J. W.; Cornforth, R. H.; Mathew, K. K. *J. Chem. Soc.* 1959, 112–127.

(76) Evans, D. A.; Siska, S. J.; Cee, V. J. *Angew. Chemie Int. Ed.* 2003, *42*, 1761–1765.

(77) Narasaka, K.; Pai, H. C. *Chem. Lett.* **1980**, 1415–1418.

(78) Chen, K. M.; Hardtmann, G. E.; Prasad, K.; Repi, O.; Shapiro, M. J. *TetrahedronLett.* **1987**, *28*, 155–158.

(79) Evans, D. A.; Chapman, K. T.; Carreira, E. M. *J. Am. Chem. Soc.* **1988**, *110*, 3560–3578.

(80) Kang, B.; Chang, S.; Decker, S.; Britton, R. *Org. Lett.* **2010**, *12*, 1716–1719.

(81) Chang, S.; Britton, R. *Org. Lett.* **2012**, *14*, 5844–5847.

(82) Dhand, V.; Chang, S.; Britton, R. *J. Org. Chem.* **2013**, *78*, 8208–8213.

(83) Holmes, M. T.; Britton, R. *Chem. Eur. J.* **2013**, *19*, 12649–12652.

(84) Mowat, J.; Kang, B.; Fonovic, B.; Dudding, T.; Britton, R. *Org. Lett.* **2009**, *11*, 2057–2060.

(85) (a) Babjak, M.; Kapitan, P.; Gracza, T. *Tetrahedron* **2005**, *61*, 2471–2479; (b) Carreno, M. C.; Herna´ndez-Torres, G.; Urbano, A.; Colobert, F. *Org. Lett.* **2005**, *7*, 5517–5520; (c) Prasad, K. R.; Gholap, S. L. *J. Org. Chem.* **2006**, *71*, 3643–3645; (d) Ghosh, S.; Rao, C. N.; Dutta, S. K. *Synlett* **2007**, *9*, 1464–1466; (e) Yoda, H.; Nakaseko, Y.; Takabe, K. *Synlett* **2002**, *9*, 15321534; (f) Yadav, J. S.; Raju, A. R.; Rao, P. P.; Rajaiah, G. *Tetrahedron: Asymm*. **2005**, *16*, 3283–3290; (g) Babjak, M.; Kapita´n, P.; Gracza, T. *Tetrahedron Lett*. **2002**, *43*, 6983–6985; (h) Murga, J.; Ruiz, P.; Falomir, E.; Carda, M.; Peris, G.; Marco, J.-A. *J. Org. Chem*. **2004**, *69*, 1987–1990.

Chapter 2.

Concise Total Synthesis of Biselide A: A Cross Metathesis Approach

2.1. Haterumalide and Biselide Family of Tetrahydrofuran Containing Marine Macrolides

2.1.1. Isolation and Structure of the Haterumalides and Biselides

The haterumalides are a family of marine macrocyclic polyketides isolated from various organisms. In 1999, the first member of the haterumalide family, haterumalide B (**6**), was isolated from an Okinawan ascidian *Lissoclinium sp*. by Ueda and Hu[1] and the structure was determined with partial stereochemical assignment by NMR spectroscopy. At the same time, an additional group of haterumalides termed NA (**1**), NB (**2**), NC (**3**), ND (**4**) and NE (**5**) were isolated by Takeda *et al.* from the Okinawan sea sponge *Ircinia* sp. collected off the coast of Japan.[2] Interestingly, haterumalide NA (**1**) was also isolated from a bacterium *Serratia marcencens*[3] found growing as an epiphyte on an aquatic plant in Venezuela. Subsequently in 2001, Lavenfors[4] and coworkers reported the isolation of haterumalide X, along with haterumalides NA, B and NE from a soil bacterium *Serratia plymuthica*, in Sweden. Haterumalide X was found to be the *Z* isomer at the C16 olefin of haterumalide NA. It is intriguing that a natural product of such complexity is present in unrelated organisms around the globe. One possible explanation is that these compounds are metabolites of bacterium living synergistically within the sea sponge/ascidian. This was further corroborated with the evidence that haterumalide NA showed a potent activity towards phytopathogenic oomycetes [4,5] (i.e., water moulds). It is worth noting that even though the NMR spectral data of haterumalide NA (**1**) isolated from the sea sponge and bacterial species are identical, there are marked differences in their reported specific rotations, which are also of the opposite sign,[6] raising questions regarding the relationship between their absolute stereochemistry.

Structurally, members of the haterumalide family display many unique features that include a 14 membered macrocyclic lactone, a 2,5-*trans* trisubstituted tetrahydrofuran ring, a *Z*-vinylchloride functionality, a skipped diene, and five stereogenic centres. While

all members of the haterumalide family have a similar core structure, haterumalides NA (**1**), ND (**4**) and NE (**5**) have a free carboxylic acid, while NB (**2**), NC (**3**) and B (**6**) have various esters at C19 (Figure 2-1). Furthermore, only haterumalide NE lacks an acetate group at C3 while haterumalide NC and ND possess additional oxidation at C9.

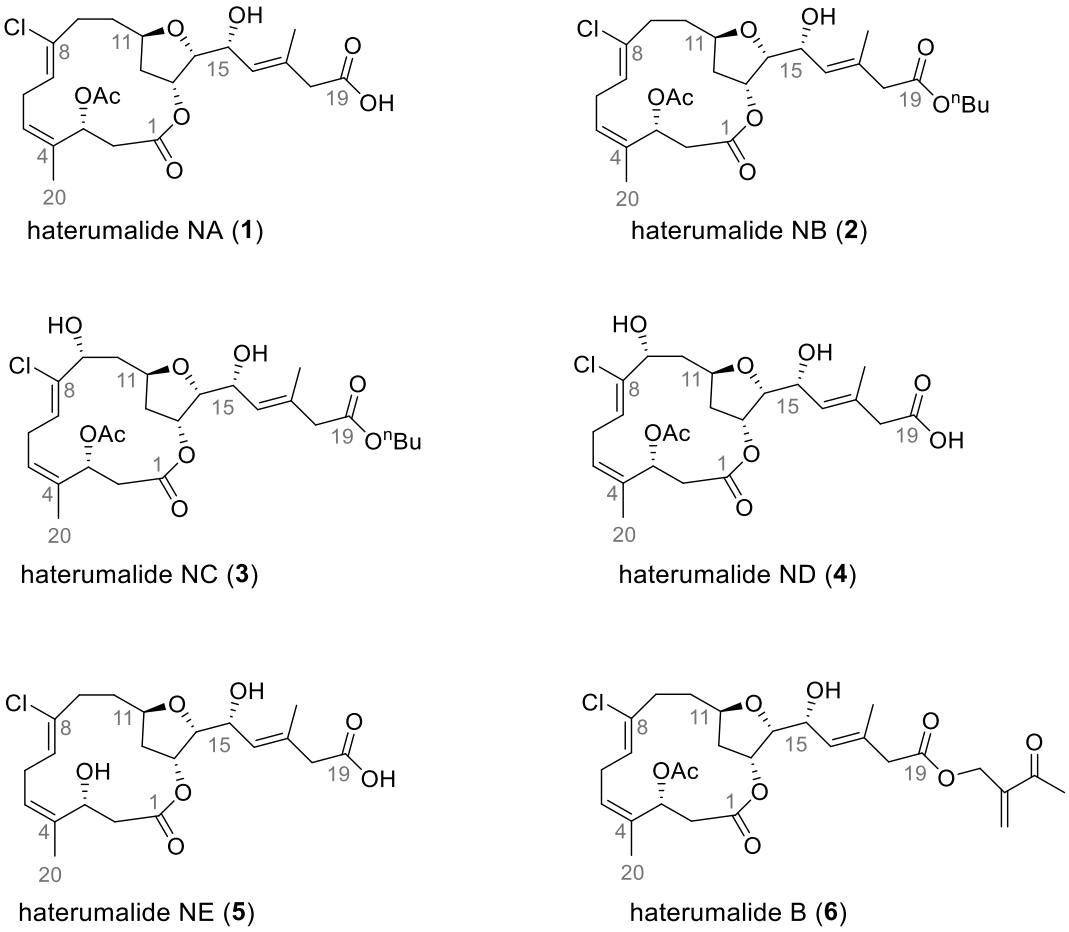

Figure 2-1 Structures of the memebrs of the haterumalide natural product family.

The initial relative and absolute stereochemical assignments of haterumalide NA were proposed by Takeda *et al.*[2] to be 3*S*, 11*S*, 13*S*, and 14*S*. Later, in 2003, Kigoshi[7] reported a revised absolute stereochemistry following completion of the total synthesis of *ent*-haterumalide NA methyl ester and confirming that each stereogenic centre has an *R* configuration as shown in Figure 2-2

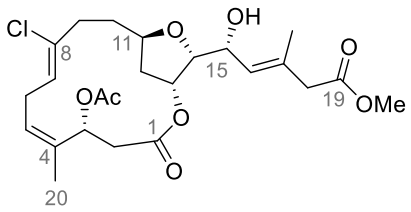

haterumalide NA methyl ester (**7**)
(corrected structure)

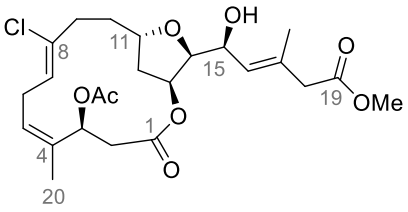

ent -haterumalide NA methyl ester (**7a**)
(first synthesis by Kigoshi *et al*. in 2003)

Figure 2-2 Structures of haterumalide NA methyl ester and its enantiomer.

In 2004, Kigoshi's group isolated two congeners of haterumalide family, biselides A (**8**) and B (**9**) from the marine Okinawan ascidian *Didemnidae sp*.[8] A year later, they reported the isolation of three additional analogues of the biselide family:[9] biselides C (**10**), D (**11**) and E (**12**) from the same organism. Much like the haterumalides, the biselides are 14-membered macrolides though they incorporate additional oxygenation at C20. Moreover, biselide D incorporates an amide linkage at C19 and lacks the acetate group at C20. Unique among all members of biselides and haterumalides, biselide E (**12**) possess a distinct linear carbon framework without a macrocyclic core (Figure 2-3).

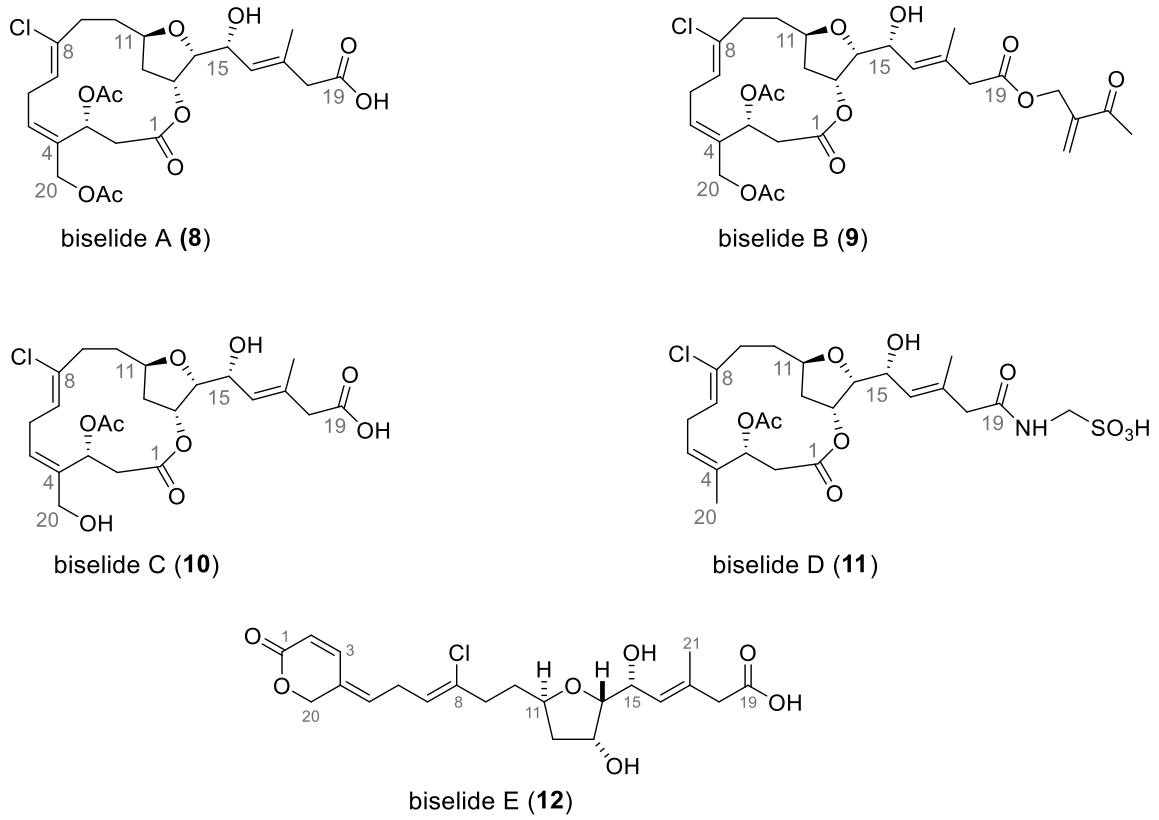

Figure 2-3 Structures of the members of the biselide natural product.

2.1.2. Biological Activity of the Members of the Haterumalide and Biselide Family

In addition to their intriguing structures, the haterumalides and biselides have demonstrated potent cytotoxic, fungistatic and anti-hyperlipidemiant activity[10-13] . The first biological testing of these compounds was reported by Ueda and Yu,[1] who reported that haterumalide B (**6**) inhibits the division of fertilized sea urchin egg cells at a concentration of 0.01 µg/ml. Preliminary studies revealed that haterumalide NA exhibited cytotoxic effects against P388 leukemia cells (IC_{50} of 0.32 µg/ml), BT-20 breast cancer cells (IC_{50} of 0.2 µg/ml), and MCF-7 breast cancer cells (IC_{50} of 0.42 µg/ml).[2,3] However, haterumalide NA was also found to be toxic towards normal mammary cell lines (IC_{50} of 0.6 µg/ml) and moderately toxic towards mice (LD_{99} = 0.24 g/kg).[3] These results suggest that despite its anti cancer activity, inherent toxicity and lack of cancer specificity preclude the further pharmaceutical development of this compound.

In 2005, Kigoshi[9] and coworkers compared the cytotoxicity of biselides A (**8**), C (**10**) and haterumalide NA methyl ester (**7**) with commercially available chemotherapeutic drugs (Table 1). Unfortunately, they were unable to test biselides B (**9**), D (**11**) and E (**12**) due to limited quantities of these compounds being available from the producing organisms. Haterumalide NA methyl ester (**7**) and biselide A (**8**) displayed potent cytotoxicity against PC-3 prostate cancer cell line (IC_{50} of 0.539 µM for (**7**) and 2.07 µM for (**8**)), DLD-1 colon cancer cell line (IC_{50} of 0.141 µM for (**7**) and 0.513 µM for (**8**)) and renal cancer cell line (IC_{50} of 0.335 for (**7**) and 1.79 µM for (**8**)), while biselide C (**10**) was the least toxic. In fact, these inhibitory activities were comparable to those of cisplatin and doxorubicin, two common chemotherapy drugs (Table 2-1). Despite the higher mean cytotoxicity exhibited by haterumalide NA methyl ester (**7**), it showed strong toxicity against brine shrimp, with an LD_{50} of 0.6 µg/ml indicating inherent cytotoxicity. Interestingly, biselides A (**8**) and C (**10**) displayed no toxicity towards brine shrimp at concentrations as high as 50 µg/ml. These results suggest the biselides and potentially unnatural analogues of these compounds could serve as lead compounds in the development of novel anticancer drugs. Unfortunately, the further biological evaluation of these compounds has been prevented by the insufficient quantities obtained from natural product isolation. The unique structural features, biological activity and the need for larger amounts of material have highlighted the biselides as attractive targets for total synthesis and inspired several groups to develop concise and a flexible synthetic routes to access these compounds.

Table 2-1 Cytotoxicity of biselide A (8), C (10) and haterumalide NA methyl ester with IC_{50} values (μM) compared to Cisplatin and Doxorubicin.[9]

Cell Line	Biselide A (8)	Biselide C (10)	Haterumalide NA methyl ester (7)	Cisplatin	Doxorubicin
MDA-MB-231 (breast)	3.72	25.5	0.406	4.83	0.186
HOP18 (lung)	9.35	82.7	0.739	4.08	0.159
NCI-H460 (lung)	3.53	18.0	0.135	0.600	0.00823
A498 (renal)	1.79	16.3	0.335	4.01	0.166
PC-3 (prostate)	2.07	18.2	0.539	4.01	0.357
DLD-1 (colon)	0.513	17.1	0.141	2.11	0.190
HCT116 (colon)	3.01	18.0	0.292	2.23	0.0629
P388 (leukemia)	3.72	21.2	0.408	0.0754	0.0252
P388/ADR (leukemia)	7.78	34.6	0.621	0.271	5.79
Mean	3.94	27.9	0.402	2.47	0.772

2.2. Previous Synthesis of Haterumalide and Biselide Family

2.2.1. Kigoshi's Synthesis of *ent*-Haterumalide NA Methyl Ester

In 2003, Kigoshi *et al*. reported the first total synthesis of a member of the haterumalide family, completing an enantioselective synthesis of the methyl ester of *ent*-haterumalide NA (**7a**).[7] This work resulted in the reassignment of the absolute stereochemistry of haterumalide NA (**7**). Here, they utilized an intramolecular Reformatsky type reaction as a key step in the synthesis of the macrocycle. The synthesis of tetrahydrofuran ring began with commercially available (+)-2,3-*O*-isopropylidene-L-

threitol,[14] which was converted into the sulphoxide **14** in 4 steps. A subsequent two-step deprotection[15] afforded the hemiacetal **15**, which upon Wittig reaction followed by Michael addition and cyclization provided the tetrahydrofuran **17** in a 5:3.1 diastereomeric mixture. This mixture was separated after silyl protection to give the desired *trans* tetrahydrofuran **17**, thus establishing the stereochemistry at C11, C13 and C14. Next the desired tetrahydrofuran **17** was converted to the alkyl bromide **18** in three steps. (Scheme 2-1)

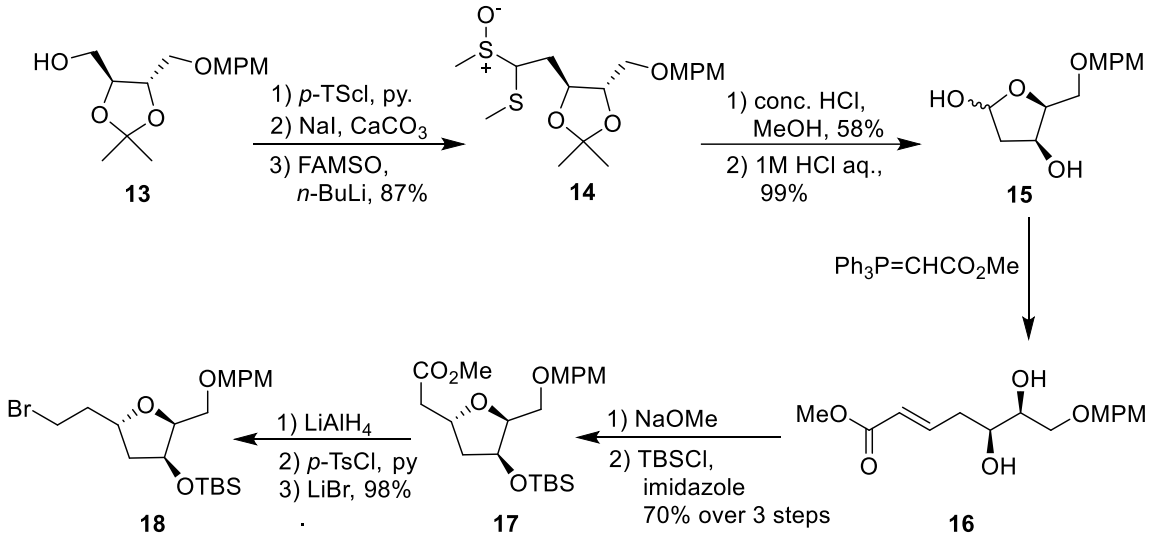

Scheme 2-1 Kigoshi's synthesis of tetrahydrofuran (18) of *ent*-haterumalide NA

The bromide **18** was then coupled to vinyl bromide **19** to give olefin **20**, which upon treatment with *N*-chlorosuccinimide (NCS) using a modified Tamao[16] procedure underwent a stereoselective halogenation reaction to yield vinyl chloride **21**. After acidic hydrolysis and oxidation of the resulting alcohol, a Still-Gennari modified Horner-Wadsworth-Emmons reaction[17] was employed to generate the *Z*-conjugated ester **22**. DIBAL reduction of compound **22** and temporary trityl protection followed by a 2-step sequence involving removal of the silyl protecting group and acylation gave the bromo ester **23**. Deprotection of the monomethoxytrityl (MMTr) group and oxidation afforded the desired conjugated aldehyde **24** a key precursor of the intramolecular Reformatsky-type reaction. Macrocyclization under Honda's[18] conditions generated the reactive β-lactone intermediate, which was effectively trapped by the addition of acetic anhydride to give the requisite macrocycle **25**, albeit in low yield (9%). Deprotection of the MPM group and oxidation of the alcohol gave the aldehyde **27**. Subsequently the aldehyde was subjected to Nozaki-Hiyama-Kishi[19,20] coupling with vinyl iodide **28** to complete the first synthesis of

ent-haterumalide NA methyl ester (**7a**) (11:1 dr) (Scheme 2-2). The major isomer displayed identical spectral properties as that of the natural product except for the opposite sign in the CD spectrum. The overall synthesis was completed in 26 steps (0.2% overall yield).

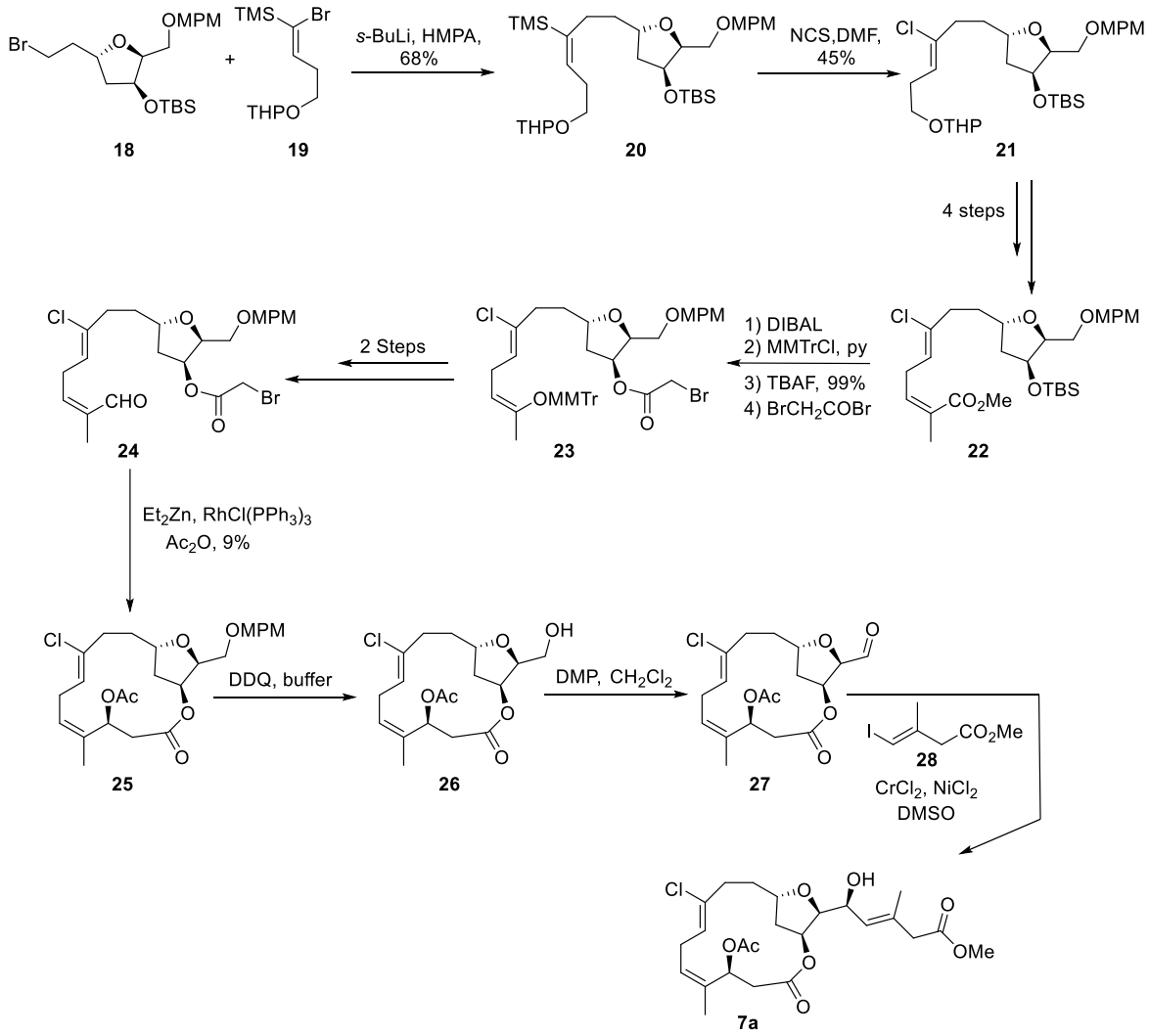

Scheme 2-2 Completion of the syntheis of *ent*- Haterumalide NA methyl ester

2.2.2. Snider's Synthesis of *ent*-Haterumalide NA Methyl Ester

A few months after Kigoshi *et al*.[7] reported the total synthesis of *ent*-haterumalide NA methyl ester, a second total synthesis of the same compound was accomplished by Snider and coworkers.[21] Their strategy involved a key Stille coupling reaction and a Yamaguchi[22] macrolactonization (varying only in protecting groups from Kigoshi's acid).

Synthesis of the THF core began with the optically active alcohol **31**, synthesized via an asymmetric aldol reaction between the O-TMS dienolate **29** and acrolein **30** using Carreira's aldol proceedure[23] and by kinetic resolution of racemic alcohol with Sharpless epoxidation.[24] The alcohol **31** was then heated in methanol and toluene to give a keto ester, which was reduced to the desired *syn*-diol **32**. The allylic alcohol was then transformed into the TBS protected propargyl alcohol **33** over 5 steps. Finally, an intramolecular iodoetherification[25] of compound **33** afforded the requisite tetrahydrofuran **34** in excellent yield. Using compound **34**, a sequential acetylation, oxidation, saponification, acetonide formation and silyl deprotection yielded the propargyl alcohol **35**. The alcohol **35** was subjected to reduction with Red-Al followed by NCS quench and then treated with MsCl and LiCl to afford the allyl chloride **36** (Scheme 2-3).

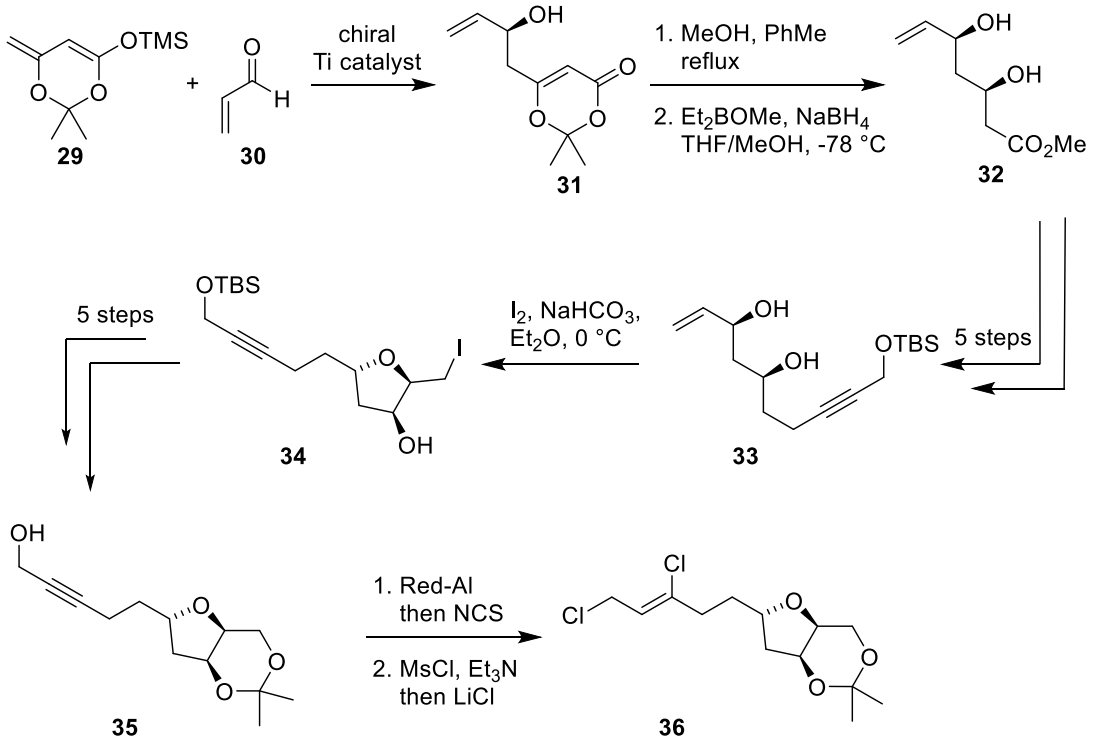

Scheme 2-3 Snider's route to the synthesis of allyl chloride

Synthesis of optically active vinyl stannane, **42** (Scheme 2.4) began with the commercially available propargyl alcohol **37,** which was subjected to Cu-catalyzed methylmagnesiation, followed by iodinolysis to afford the *Z*-methyl substituted iodo alkene **38**. The iodo-allylic alcohol was oxidized to the corresponding aldehyde, which then underwent an asymmetric aldol reaction in the presence of Kiyooka's[26-28] oxazaborolidine **40** to afford the β-hydroxy phenyl ester **41** in >80% ee. The allylic hydroxyl group was

protected as its TBS ether and the cross coupling of vinyl iodide with hexamethylditin under palladium catalysis furnished the desired vinyl stannane **42**.

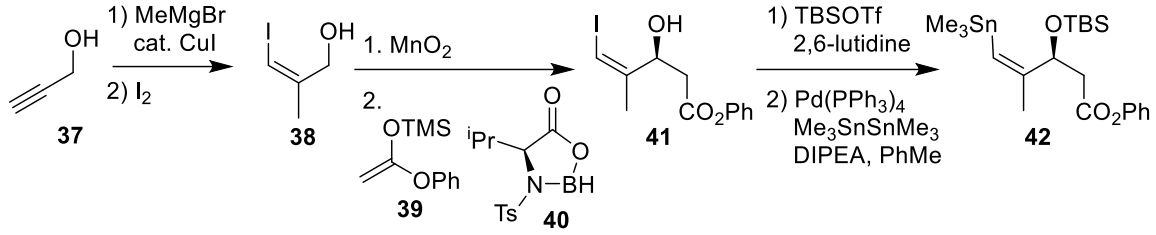

Scheme 2-4 Snider's synthesis of vinyl stannane

Stille coupling between vinyl stannane **42** and allyl chloride **36** using Farina's condition[29] afforded the requisite skipped diene **43** in 65% yield (Scheme 2.5). Acetonide deprotection under acidic conditions and selective reprotection of the primary hydroxyl group as its trityl ether was followed by phenyl ester hydrolysis, which furnished the seco acid **44**, setting the stage for macrocycle formation. Macrolactonization was achieved following Yamaguchi's protocol[22] to afford the macrocycle in 67% yield, along with dimer and trimer side product formation. The macrocycle was converted to Kigoshi's[7] intermediate **26** in 3 steps followed by NHK coupling with vinyl iodide **28** to afford *ent*-haterumalide NA methyl ester in 30-40 % yield. Overall, Snider's synthetic route was more efficient, and the total synthesis was completed in 27 steps (LLS) with 0.7% overall yield.

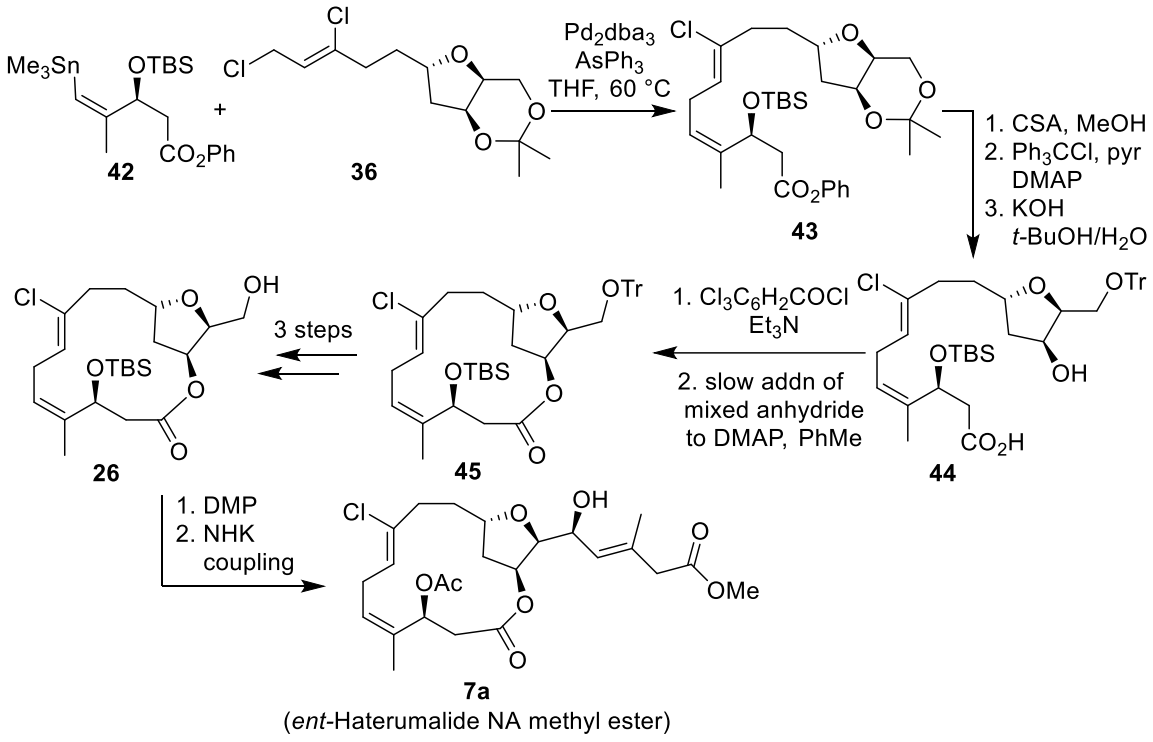

Scheme 2-5 Completion of Snider's synthesis

2.2.3. Hoye's Total Synthesis of Haterumalide NA

In 2005, Hoye and Wang[30] accomplished the first total synthesis of haterumalide NA with the correct configuration. This strategy involved Kaneda haloallylation[31] as a key step to introduce the vinyl chloride functionality and intramolecular cyclization to access the macrocycle. This synthesis begins with the construction of the desired tetrahydrofuran core **49** by following the methods previously reported by Roush and Micalizio (Scheme 2-6).[32] The Lewis acid catalyzed [3+2] annulation reaction of an allylsilane **47** and α-hydroxy aldehyde **48** afforded the desired THF motif **49**. The allylsilane **47** was made in six steps starting from compound **46**. The ene-yne **50** was made in 18 steps from compound **49**, setting the stage for a key intramolecular cyclization. Kaneda chloroallylation[31] of compound **50** in the presence of *bis*(benzonitrile)palladium chloride catalyst afforded the 14 membered macrocycle in a good overall yield as a 1:1.4 separable mixture of *Z* and *E* isomers (at C4/C5), with the *Z* being the desired isomer. Luche reduction of **51** yielded the desired single diasteromer at C3. Subsequent acetylation of alcohol **52** and removal of the PMB group gave the primary alcohol *ent*-**26**, which is an enantiomer of Kigoshi's key intermediate.

This material was oxidized to provide the aldehyde, followed by Nozaki-Hiyama-Kishi coupling with the iodide **53** gave the haterumalide NA PMB ester **54**. The deprotetction of the PMB ester **54** under mild conditions[33] afforded the required haterumalide NA (**1**) in 32 steps (LLS) with 0.2% overall yield.

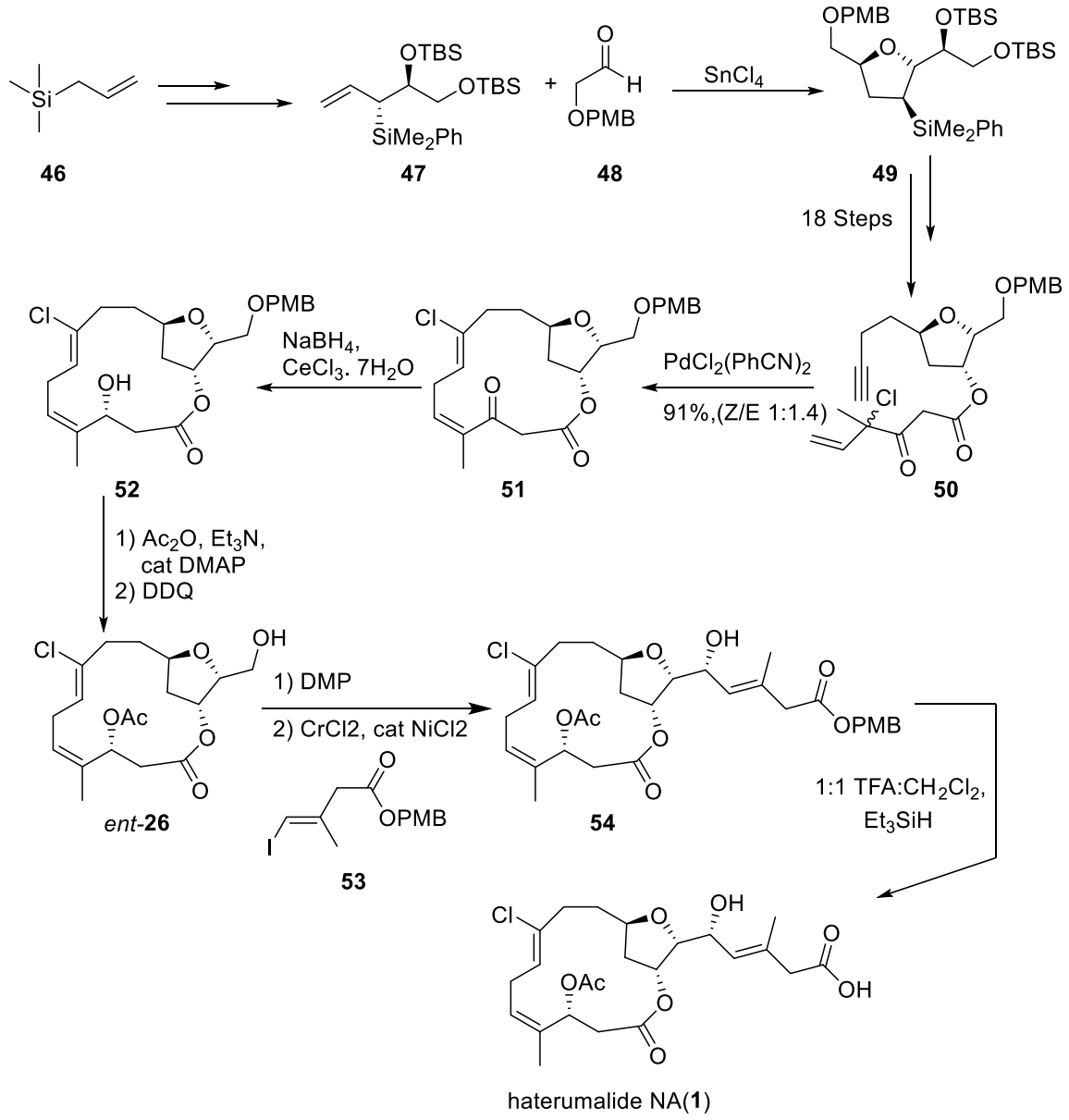

Scheme 2-6 Hoye's synthesis of haterumalide NA

2.2.4. Roulland's Synthesis of Haterumalide NA

In 2008, Roulland[34] reported the second total synthesis of haterumalide NA (**1**). The key step in their synthesis featured a Suzuki Miyaura cross-coupling[35] of the vinyl tetrahydrofuran building block **59** and an alkylboronate of the dichlorovinyl derivative **61** (Scheme 2-7).

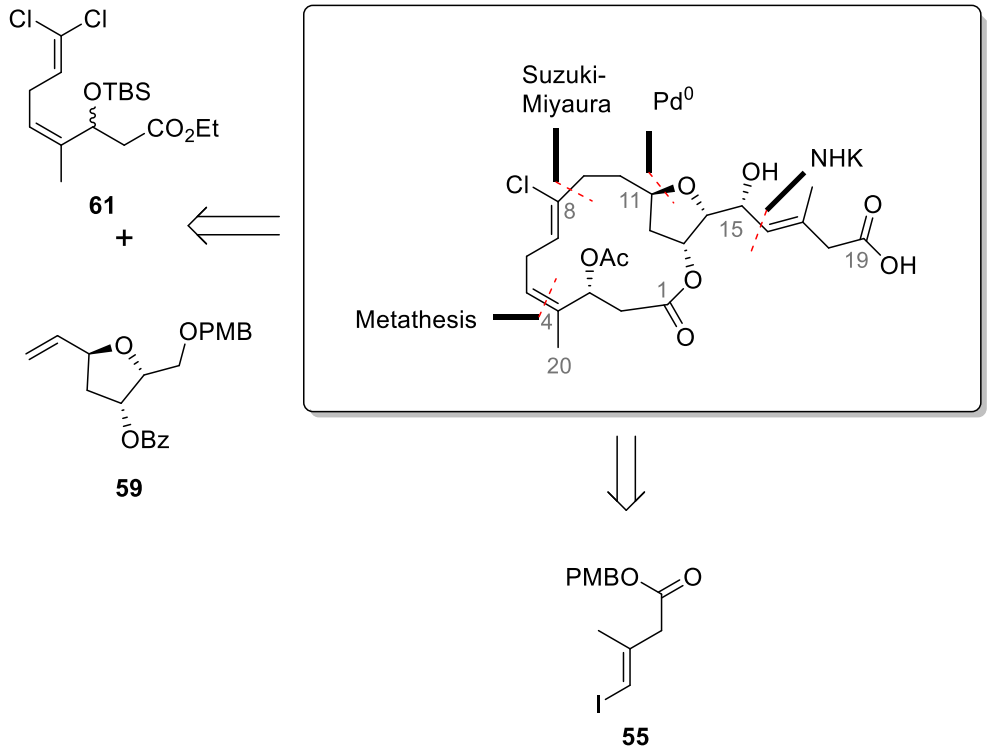

Scheme 2-7 Roulland's retrosynthetic analysis of haterumalide NA

The tetrahydrofuran **59** was synthesized starting from dimethyl D-tartrate (**56**), which constitutes the sole source of chirality in this synthesis. This material **56** was transformed in six steps to the diol **57** in good yield as an *E/Z* mixture (ca. 95:5) (Scheme 2-8). The intramolecular cyclization of the diol **57** in the presence of a palladium catalyst afforded the THF **58** with excellent diastereoselectivity (96:4). The two inseparable diastereomers **58a** and **58b** were converted to their corresponding benzoyl esters, which were separated after column chromatography. Thus, compound **59** was readily obtained as one of the precursors for Suzuki Miyaura cross-coupling.

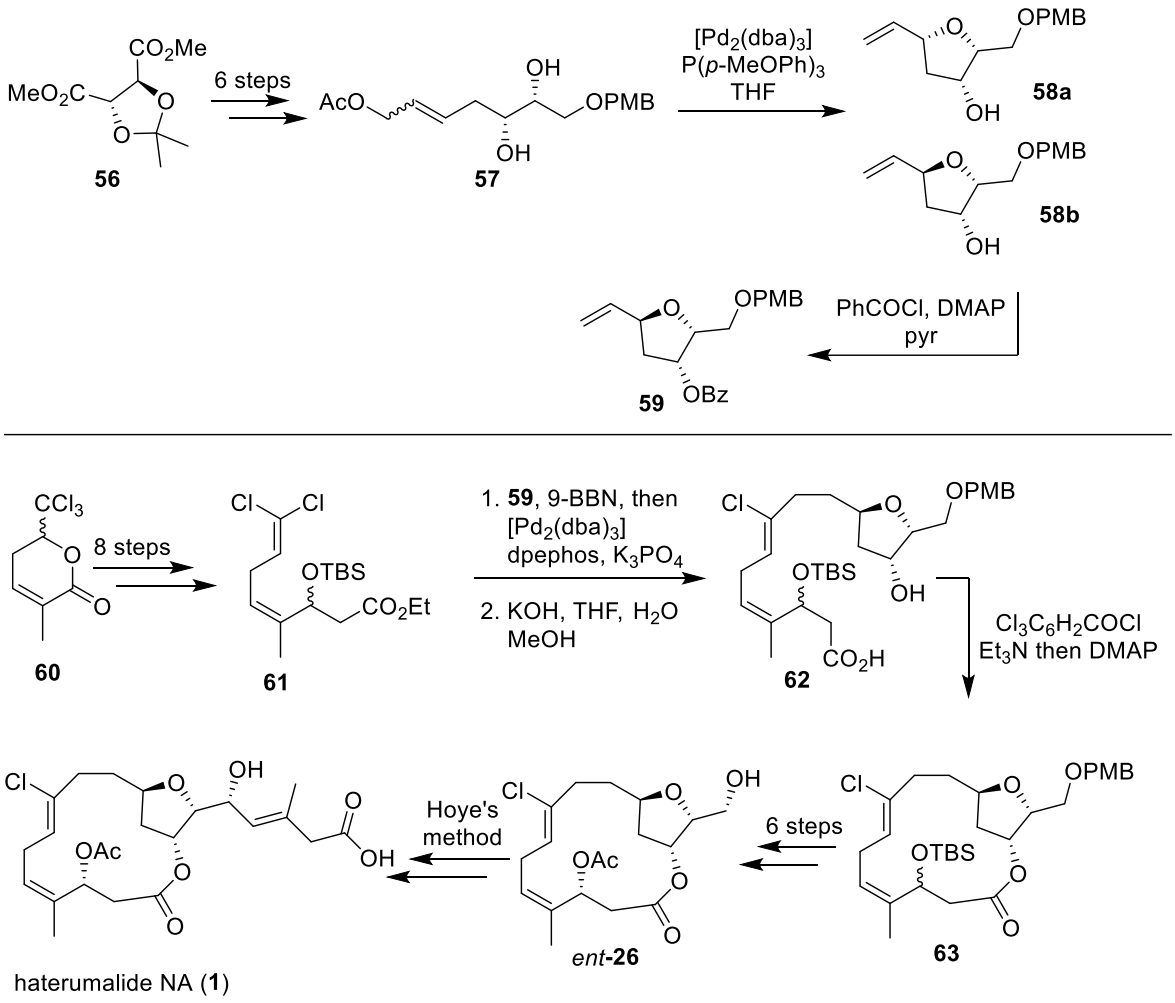

Scheme 2-8 Roulland's synthesis of hateuramalide NA

The other Suzuki Miyaura coupling partner, dichloro alkene **61** was synthesized in 8 steps (Scheme 2-7) from the precursor *α,β*-unsaturated lactone **60**. With both the compounds **59** and **61** in hand, Suzuki Miyaura[35] cross-coupling was performed using 9-BBN and a catalytic amount of [$Pd_2(dba)_3$], followed by hydrolysis which yielded the seco acid **62**. This material was later subjected to intramolecular macrolactonization using Yamaguchi's[22] conditions to produce macrolactone **63**. Subsequently, the macrolide **63** was transformed in 6 steps to give the Kigoshi intermediate[7] *ent*-**26**. The synthesis of haterumalide NA was completed from *ent*-**26** following the sequence developed by Hoye.[30] In conclusion, Roulland's synthesis of haterumalide NA was completed in 22 steps (LLS) in 4% overall yield.

2.2.5. Kigoshi's Synthesis of Haterumalide NA and B

In early 2008, shortly after Roulland's[34] synthesis was published, Kigoshi's[36] group reported an efficient second-generation total synthesis of haterumalide NA. Similar to Roulland's strategy, Kigoshi's synthesis incorporated Suzuki Miyaura cross coupling to form the C8-C9 bond. The synthesis commenced with commercially available D-mannose (**64**), which was transformed to the known glycal[37] **65** in two steps (Scheme 2-9). Protection of the secondary hydroxyl group as a 2,4-dimethoxybenzyl (DMPM) ether, followed by an oxymercuration-reduction sequence[38] and Wittig olefination of the hemiacetal gave the *α,β*-unsaturated ester **66**. Intramolecular oxy-Michael cyclization in the presence of Triton B in methanol afforded tetrahydrofuran **67** stereoselectively. Subsequently, ester **67** was reduced with $LiAlH_4$ and elimination gave the tetrahydrofuran **68** with the desired configuration at the three stereocentres. Hydroboration of compound **68** with 9-BBN dimer followed by *B*-alkyl Suzuki Miyaura[35] cross coupling with vinyl iodide **69** gave the desired vinyl silane **70** in good yield. Initial attempts to convert compound **70** to vinyl chloride **71** using modified Tamao[16] conditions, as reported by Kigoshi[7] previously, resulted in low and irreproducible yields. Optimized conditions with NCS and K_2CO_3 yielded **71** with the desired alkene geometry. Acid hydrolysis of the THP and acetonide groups followed by reprotection of the resulting diol as an acetonide group gave the alcohol **72**. Oxidation of the alcohol **72** followed by modified Horner-Wadsworth-Emmons[17] reaction and reduction of the resulting ester gave the allylic alcohol, which was oxidized to give the conjugated labile aldehyde **73**. This material over 8 steps was transformed into seco acid **74**, which was subjected to Yamaguchi macrolactonization[22] conditions to afford the macrocycle **75** as an inseparable mixture of diastereomers at C3. The removal of the TBS group afforded the free secondary hydroxyl alcohols **76**, which was resolved by column chromatography. The undesired alcohol was converted to the desired **76** by oxidation and Luche reduction.[39] The macrolide was subjected to acetylation and deprotection to give the intermediate *ent*-**26** and following Hoye's[30] endgame strategy, haterumalide NA was obtained in 32 steps (LLS) with 1.2% overall yield.

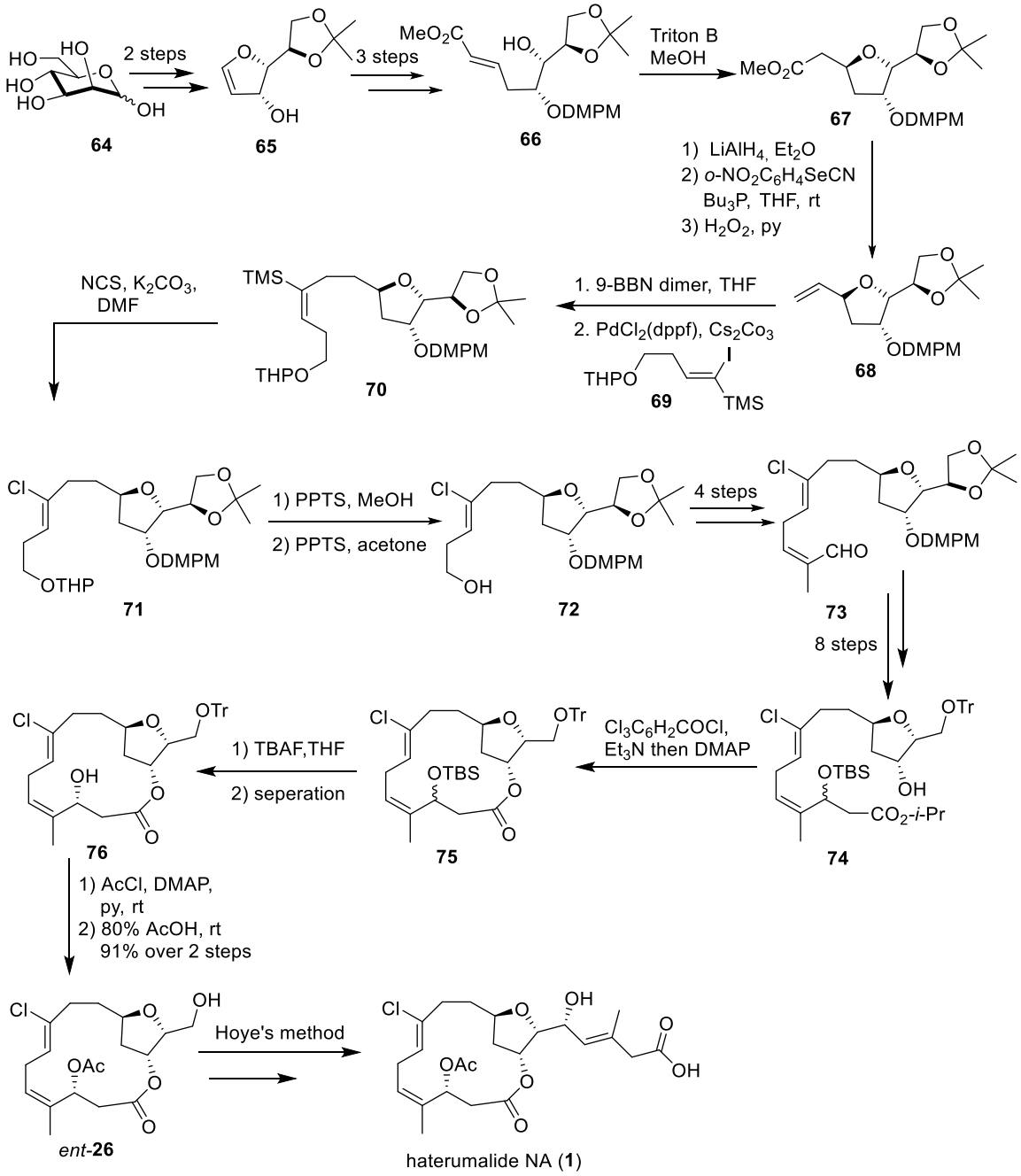

Scheme 2-9 Kigoshi's second generation synthesis of haterumalide NA

In 2009, Kigoshi *et al*.[40] reported the synthesis of haterumalide B (**6**). In comparison with their synthesis of haterumalide NA (**1**), this synthesis differs only by the coupling of side chain **79** used in the late stage Nozaki-Hiyama-Kishi[19,20] reaction (Scheme 2-10). Esterification of the (*E*)-iodo-acid **77** and the racemic mono protected diallyldiol **78** gave the racemic vinyl iodide **79**. Subsequently, NHK coupling of compound **79** with aldehyde

80, followed by removal of MPM group and selective oxidation of allylic alcohol afforded haterumalide NB (**6**) in 33 steps (LLS).

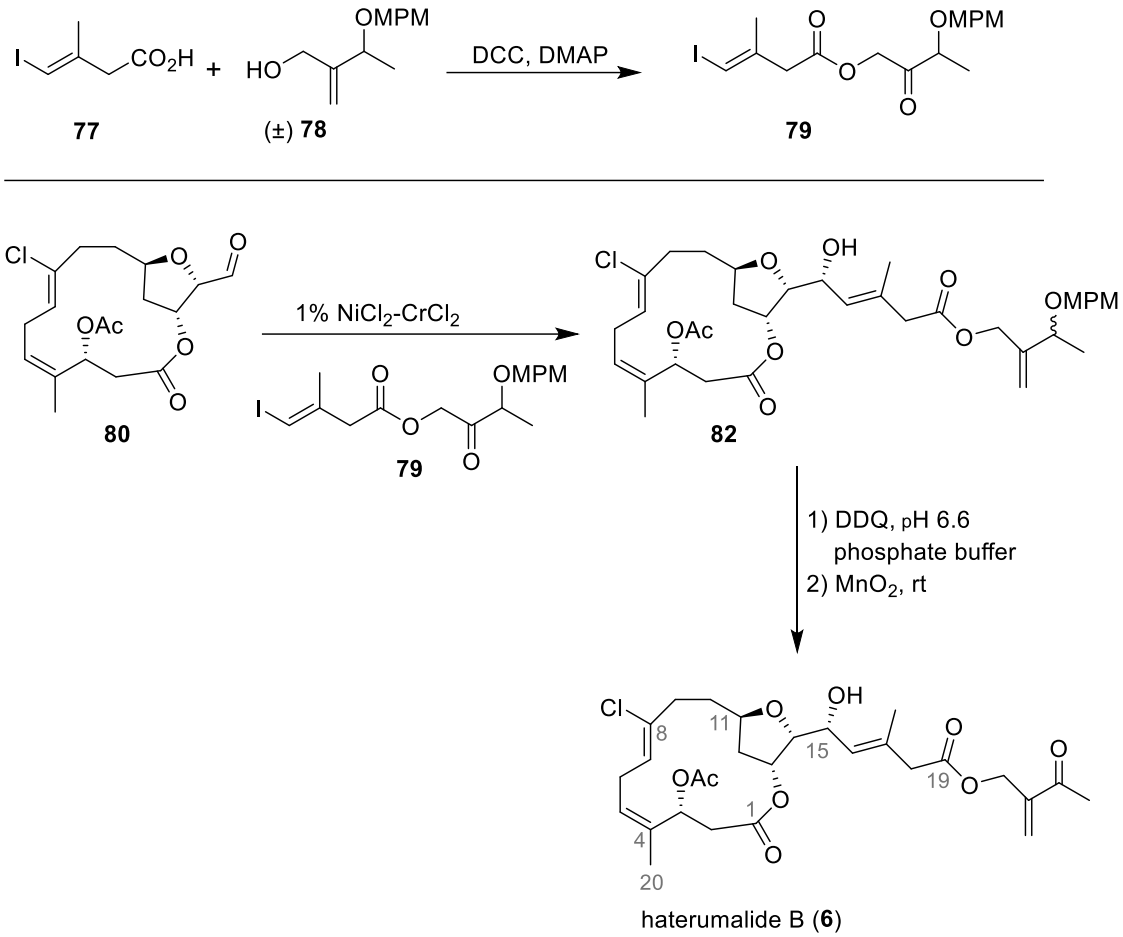

Scheme 2-10 Kigoshi's synthetic route to haterumalide B

2.2.6. Borhan's Total Synthesis of Haterumalide NC and Formal Synthesis of Haterumalide NA

In 2008, Borhan and Schomaker[41] accomplished the first total synthesis of haterumalide NC (**3**) (Scheme 2-11) and using this strategy they completed the formal synthesis of haterumalide NA. They utilized the chemistry of chlorovinylidene chromium carbenoids developed by Falck and Mioskowski[42] to construct the C8-C9 bond of the macrocycle. Enantioselective synthesis of the tetrahydrofuran **87** commenced with commercially available 2-deoxy-D-ribose (**86**), which was transformed over 5 steps to afford compound **87** (Scheme 2-11). Preparation of the protected hydroxy acid **85** began with the opening of the oxetane (**83**) with the anion of chloroform (generated via deprotonation of chloroform

with *n*BuLi), followed by Dess-Martin periodinane (DMP) oxidation,[43] Still-Gennari olefination[44] and DIBAL reduction of the corresponding ester furnished the desired alcohol **84**. Subsequent oxidation of the allylic alcohol **84** with manganese (IV) oxide followed by an asymmetric Mukiyama aldol reaction[45], silylation and saponification gave the seco acid **85** in good yield. Mitsunobu esterification[46] of alcohol **87** and seco acid **85** furnished the ester **88** with the required inverted stereochemistry at C13. After protecting group manipulations, selective dihydroxylation of the terminal alkene followed by oxidative cleavage yielded the corresponding aldehyde **89**. Next**,** intramolecular $CrCl_2$-mediated macrocyclization of aldehyde **89** furnished the macrocycle **90** in 54% yield (4:1 d.r.) with the required stereochemistry at the newly formed C9 centre. In the next four steps, **90** was transformed into aldehyde **91**, which was coupled to vinyl iodide **92** under Nozaki-Hiyama-Kishi conditions followed by desilylation with HF-pyridine to afford haterumalide NC (**3**). The total synthesis was completed in 16 steps (LLS) with 6% overall yield. Borhan's synthesis offered considerable improvement over the previuos routes with respect to step count. Additionally, the formal synthesis of haterumalide NA was achieved by subjecting macrocycle **90** to Barton-McCombie deoxygenation[47] of the C9-OH which furnished the advanced intermediate **93**, which was reported in prior syntheses of haterumalide NA (Scheme 2-12).

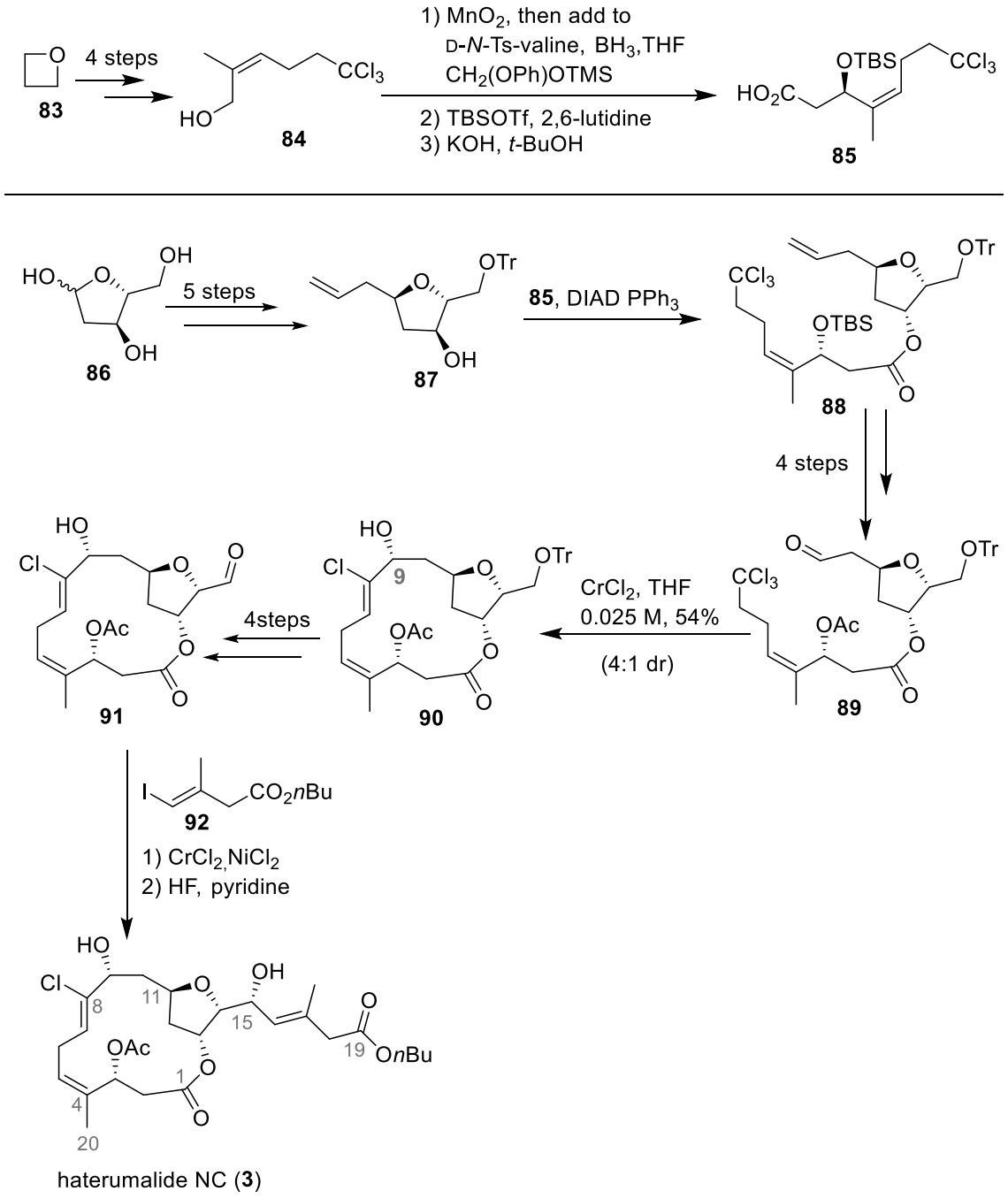

Scheme 2-11 Borhan's synthesis of haterumalide NC

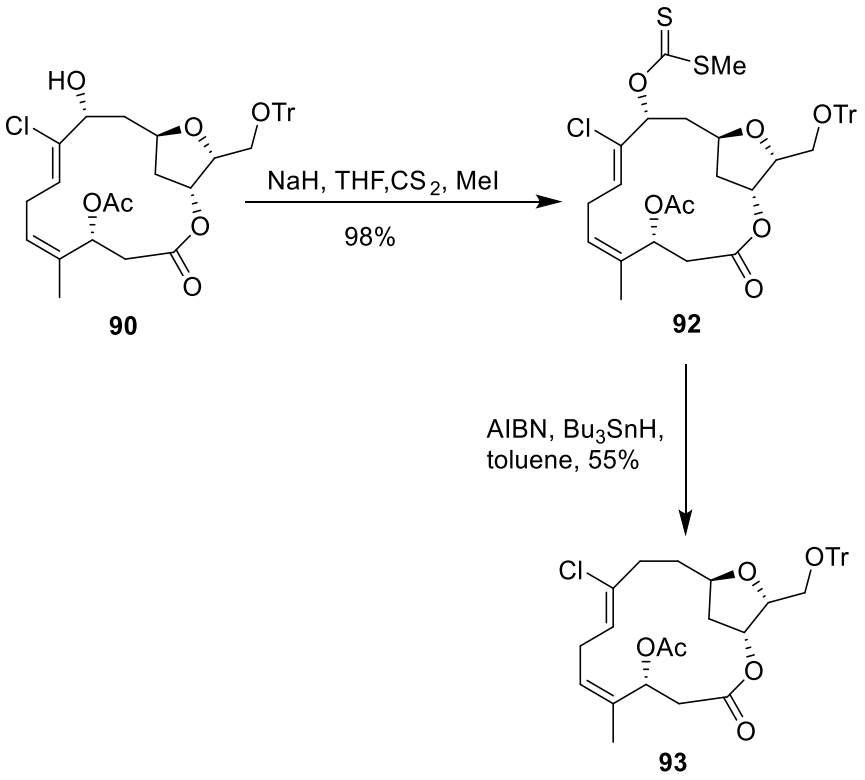

Scheme 2-12 Borhan's formal synthesis of haterumalide NA

2.2.7. Initial Studies Towards the Synthesis of Biselides by Kigoshi

In 2012, Kigoshi's[48] group reported their preliminary results towards the synthesis of biselides in two parts. They were able to achieve the synthesis of an important intermediate (**98**) but could not complete the total synthesis. In part 1, the synthesis began from the previously reported intermediate of haterumalide, alcohol **72**. The primary alcohol was oxidized to its corresponding aldehyde, followed by a Wittig reaction[49] to afford the iodo olefin **92** as a 3:1 mixture of *Z/E* isomers at the C4-C5 double bond (Scheme 2-13). The ethyl ester was then reduced with DIBALH to afford the desired *Z* isomer **93**, after column chromatography. Next, the C20 hydroxyl group was silylated with TBDPSCl to give vinyl iodide **94** followed by a key Stille coupling reaction with tributyl(vinyl)tin gave the skipped triene **95**. Subsequent dihydroxylation of terminal olefin of the diene moiety with OsO_4 was not selective and furnished the desired diol **97** (30%) and the undesired diol **96** (20%). Oxidative cleavage of the diol using $NaIO_4$ gave the corresponding α,β-unsaturated aldehyde, which was used immediately in a nonstereoselective aldol reaction of the lithium enolates derived from *i*-PrOAc, which afforded the β-hydroxy ester **98**. Thus Kigoshi *et al*.

were able to achieve the synthesis of key intermediate **98**, which incorporates the C1-C15 carbon framework of biselides A, B and C. However, lack of regioselectivity at the dihydroxylation step, low yield and non-selective aldol reactions were the major hurdles in completing the total synthesis of biselides.

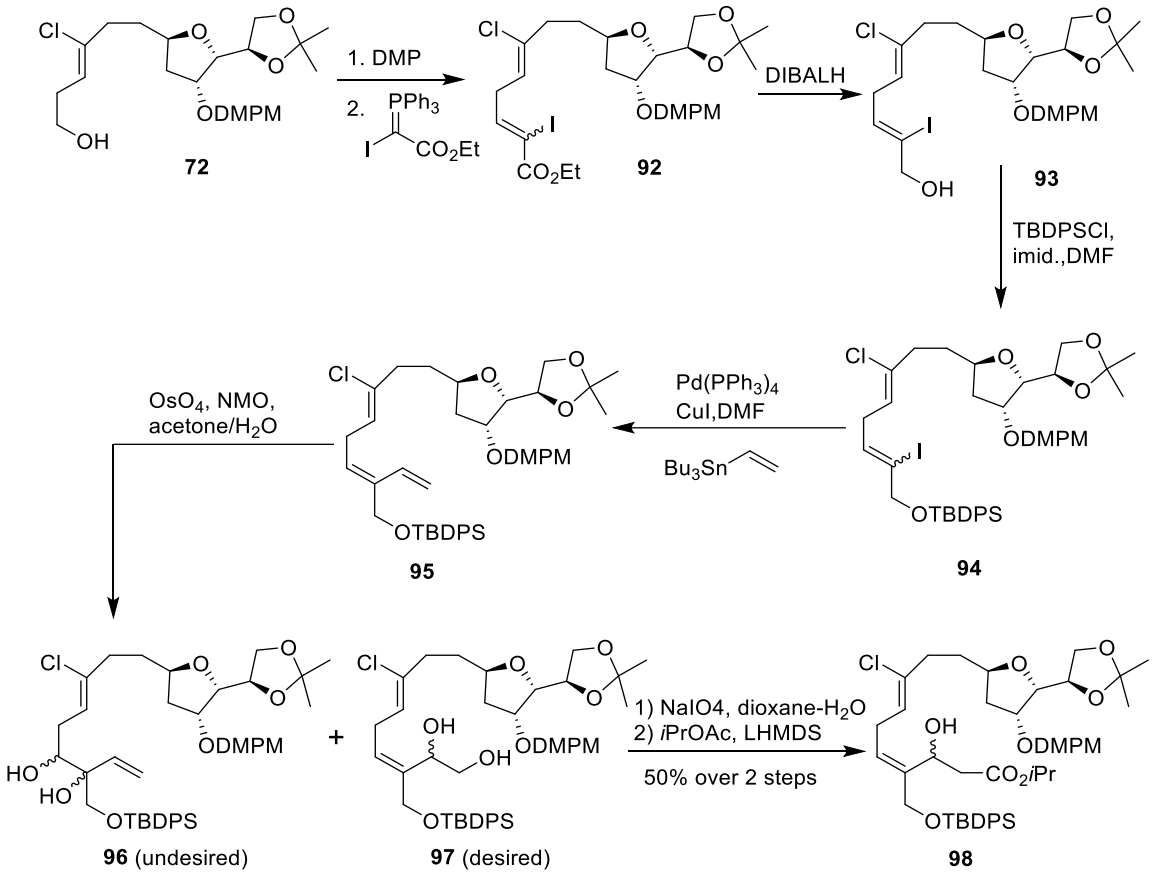

Scheme 2-13 Synthesis of biselide core using Stille coupling, Kigoshi 2012

In Part 2, Kigoshi *et al* [50]*.* reported an alternative route to access the macrocycle core of the biselides to circumvent the issues related to regioselective dihydroxylation and low yield from their previous synthesis (Scheme 2-13). This synthesis highlights their attempts to introduce the C20 hydroxyl group using regioselective allylic oxidation (Scheme 2-14). The synthesis began once again with the intermediate **72**, common to the synthesis of haterumalides. The primary alcohol **72** was converted to its *p*-nitrobenzoate ester **99** in 4 steps. These investigations revealed that the presence of the electron withdrawing *p*-nitrobenzoate group enhanced the regioselectivity of the allylic oxidation reaction. Thus, allylic oxidation of compound **99** with SeO_2 yielded the desired alcohol **100** in 35% yield and the undesired side product with oxygenation at C3 and an aldehyde at

C20 in 20% yield. Subsequently, the allylic hydroxyl group **100** was protected as its TBDPS ether, followed by removal of the p-nitrobenzoyl group and oxidation of the primary alcohol to give the aldehyde **101**, which was reacted with the lithium enolate derived from *i*-PrOAc, furnished the β-hydroxy ester **98** as a 1:1 diastereomeric mixture at C3. Compound **98** was converted to seco acid **102** in 6 steps, following the sequence previously reported in the synthesis of haterumalides. Yamaguchi macrolactonization[22] of the seco acid **102** afforded the macro lactone **103**. Next, the macrolide **103** was transformed to a diacetate in 4 steps, which is the desired fully substituted macrolactone part of biselides A, B and C. The synthesis was stopped at this stage and the authors did not cite the reasons for not completing the total synthesis. In conclusion, they completed the synthesis of the substituted macrolactone part of biselides in 32 steps (LLS) with a 0.25% overall yield.

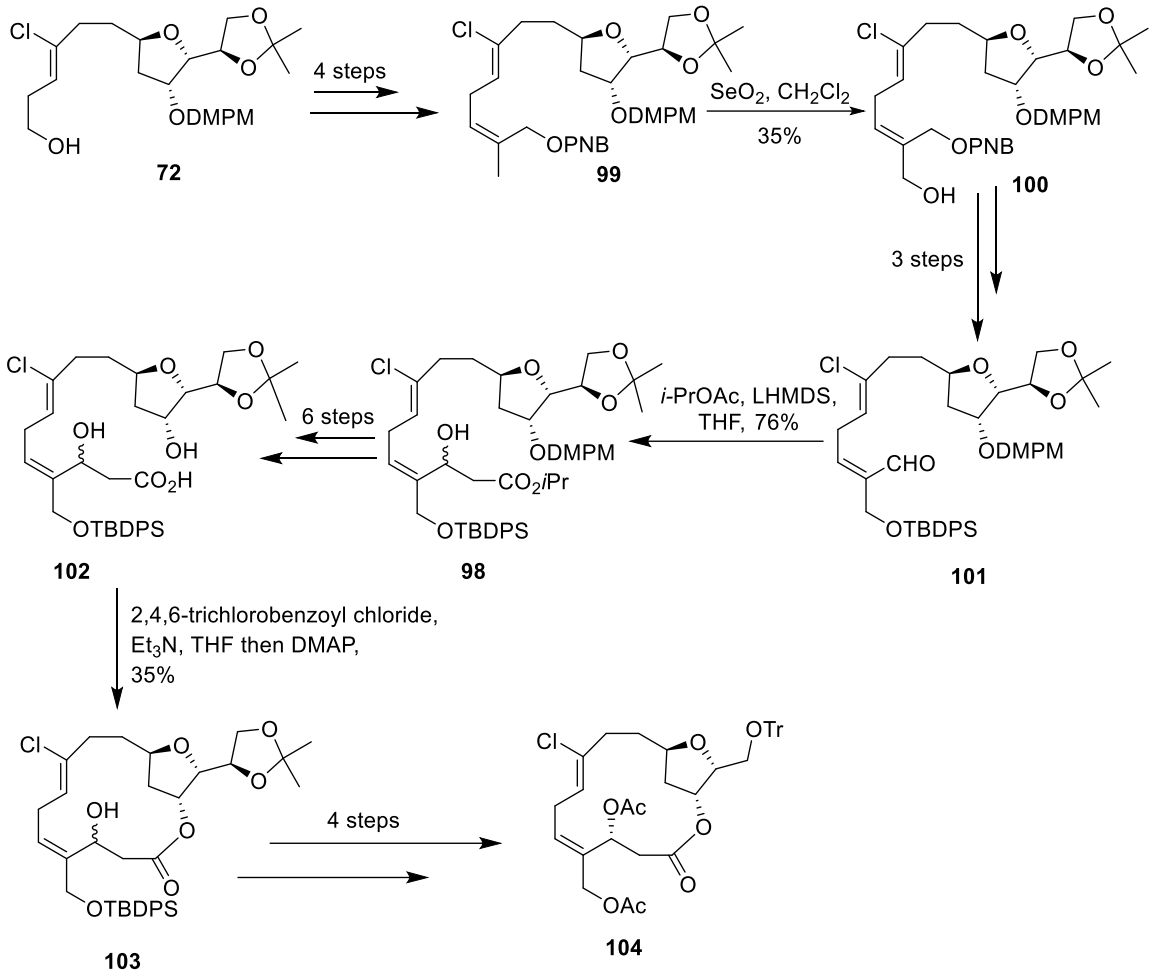

Scheme 2-14 Synthesis of biselide macrocyclic core using allylic oxidation

2.2.8. First Total Synthesis of Biselide A, Hayakawa 2017

In 2017, Hayakawa *et al*.[51] accomplished the first total synthesis of biselide A. In their previous synthesis[48,50] the authors reported preparation of key intermediate **98** via two alternative routes (Scheme 2-13 and 2-14). However, neither route was deemed practical due to low yields and selectivities. To overcome these problems, a regioselective enzymatic deacetylation was developed to introduce the C20 acetate group and a stereoselective aldol reaction to produce the C3 hydroxyl group as a single isomer.

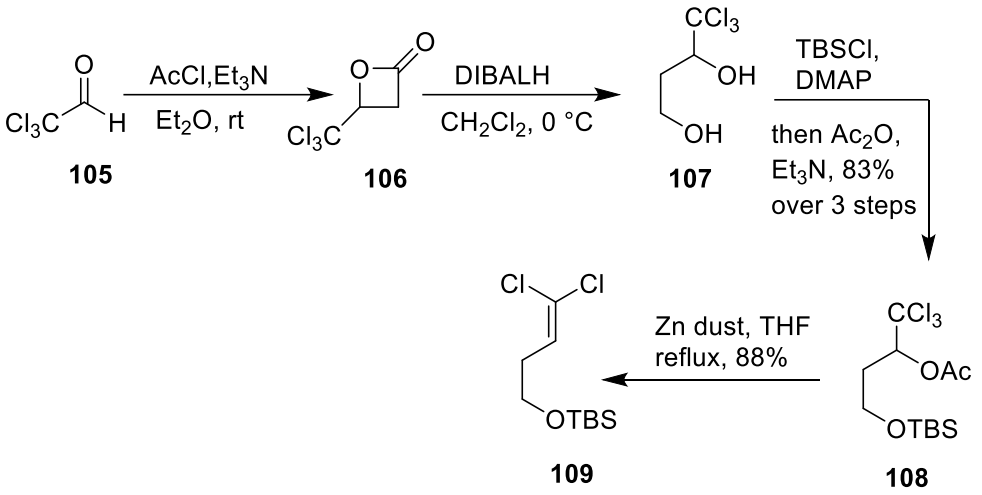

Scheme 2-15 Hayakawa's synthesis of dichloroolefin 109 as the C5-C8 segment

The synthesis began with the construction of the tetrahydrofuran **65** from D-mannose in 9 steps as reported in the previous synthesis of haterumalides[7] (Scheme 2-16). The dichloroolefin **109** was synthesized using a procedure reported by Roulland and Cossy[52] in 4 steps as shown in Scheme 2-15. Having both the coupling partners **65** and **109** in hand, a *B*-alkyl Suzuki Miyaura cross coupling was carried out using Roulland conditions[34] to give tetrahydrofuran **110** in quantitative yield. The coupled product was deprotected with TBAF and converted to alkyl iodide **111** using an Appel reaction followed by a Wittig reaction with diacetoxy acetone to afford the diacetate **112** in excellent yield. To carry out a regioselective enzymatic hydrolysis, a series of conditions were screened varying different solvents, buffers and enzymes (lipases). The best conditions involved stirring of compound **112** in phosphate buffer (pH 7.0) with porcine pancreas lipase (PPL) type II for 2 h at 27 °C, which afforded the allylic alcohol **113** in 45% yield. In a further 3 steps, the compound **113** was converted to (*Z*)-α,β-unsaturated aldehyde **114** (Scheme 2-17). The aldehyde was subjected to an asymmetric aldol reaction with 3-acetylthiazolidine thione (**115**) under Nago conditions[53] to furnish the C3 alcohol **116** as a single isomer. Over 7 further steps this material was elaborated into seco acid **117**. Intramolecular lactonization of seco acid **117** under Yamaguchi conditions[22] afforded the lactone **118** in 60% yield. The lactone was treated with TBAF to cleave the silyl protecting groups, followed by acetylation and removal of trityl group under acidic conditions to furnish the alcohol **119** in 85% yield over 3 steps. Subsequently, oxidation of the primary alcohol **119** to its corresponding aldehyde, followed by NHK coupling with vinyl iodide **120** and hydrolysis of a 2,4-dimethoxy benzoyl ester group afforded the mixture of biselide A

and C15-*epi* biselide A. After HPLC purification of this mixture, biselde A (**8**) was isolated in 50 % yield. The overall synthesis was completed in 32 steps (LLS).

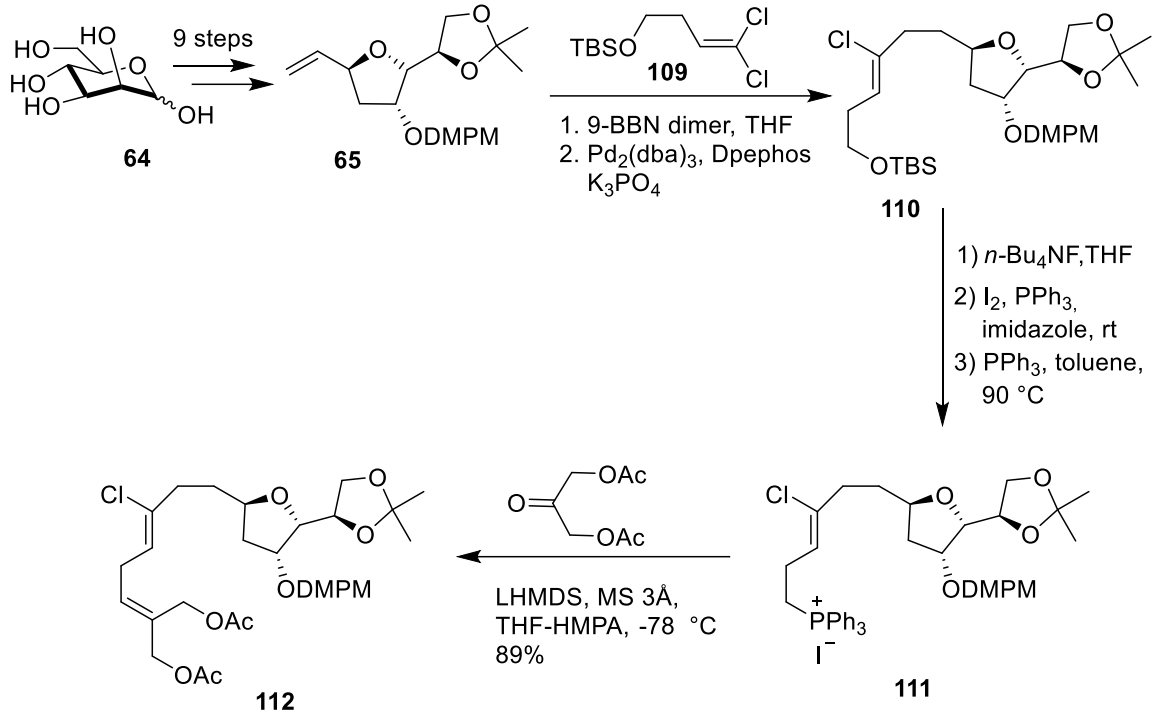

Scheme 2-16 Synthesis of diacetete 112 as a precursor for regioselective enzymatic hydrolysis

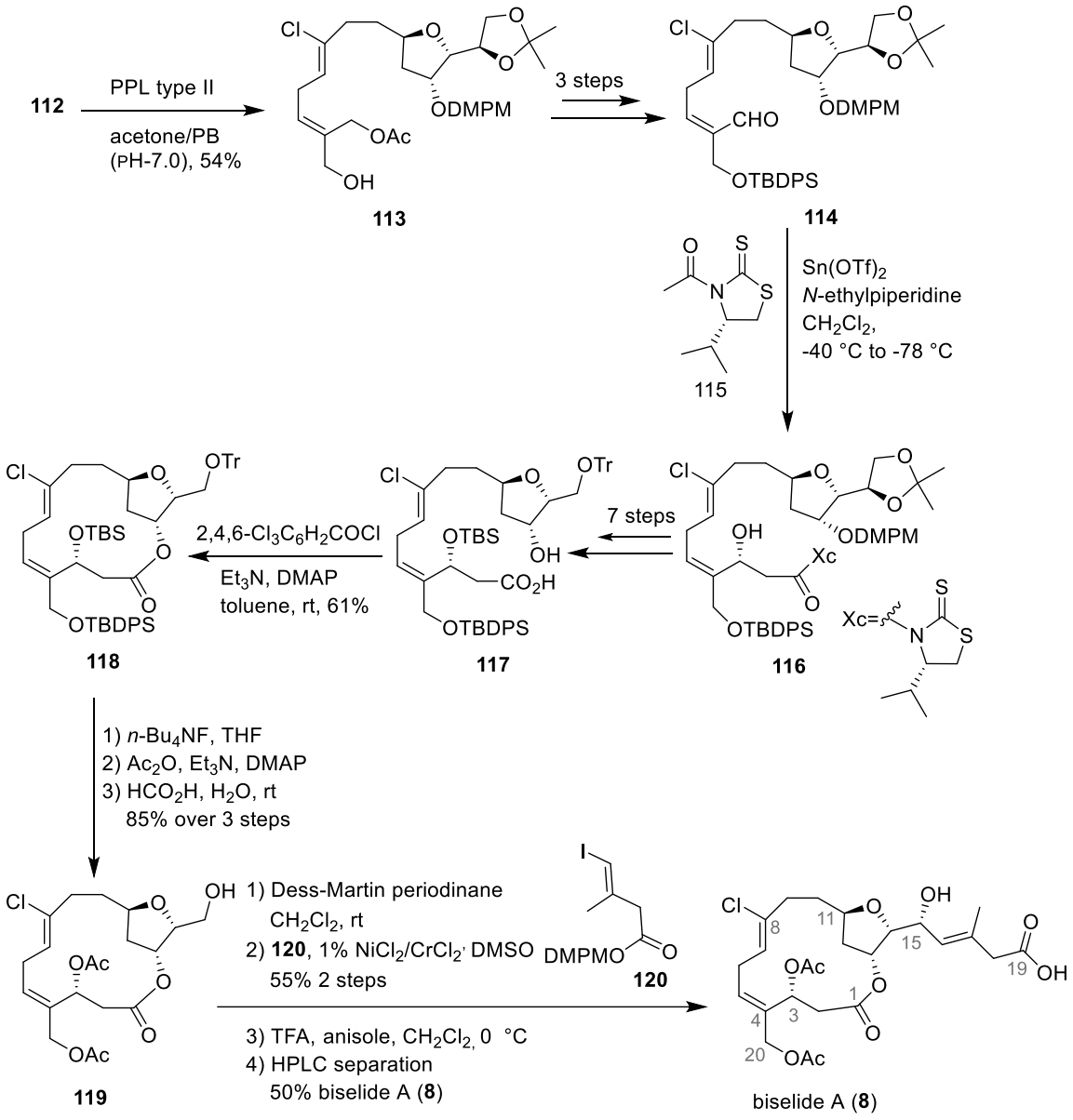

Scheme 2-17 Completion of Hayakawa's total synthesis of biselide A (8)

2.3. Previous Strategies for the Total Synthesis of Biselide A in the Britton Group

2.3.1. A Ring-Closing Metathesis Strategy to Access the Macrocycle Core of Biselide A

Studies directed towards the synthesis of biselides in the Britton group were commenced prior to the first reported synthesis of biselide A by Hayakawa[51] and co

workers in 2017. Previously in our group the synthetic studies towards biselide A were carried out by Dr. Baldip Kang[54], Hope Fan[55], Matthew Tarron[56] and Daniel Kwon[57]. Dr. Kang's strategy involved the group's previously reported chlorohydrin cyclization methodology[58-60] to construct the tetrahydrofuran core and a ring-closing metathesis strategy to access the C4-C5 alkene of the macrocycle. Further, his retrosynthetic proposal mirrors Hoye's[30] end game strategy to install the carboxylic acid component (Scheme 2-18).

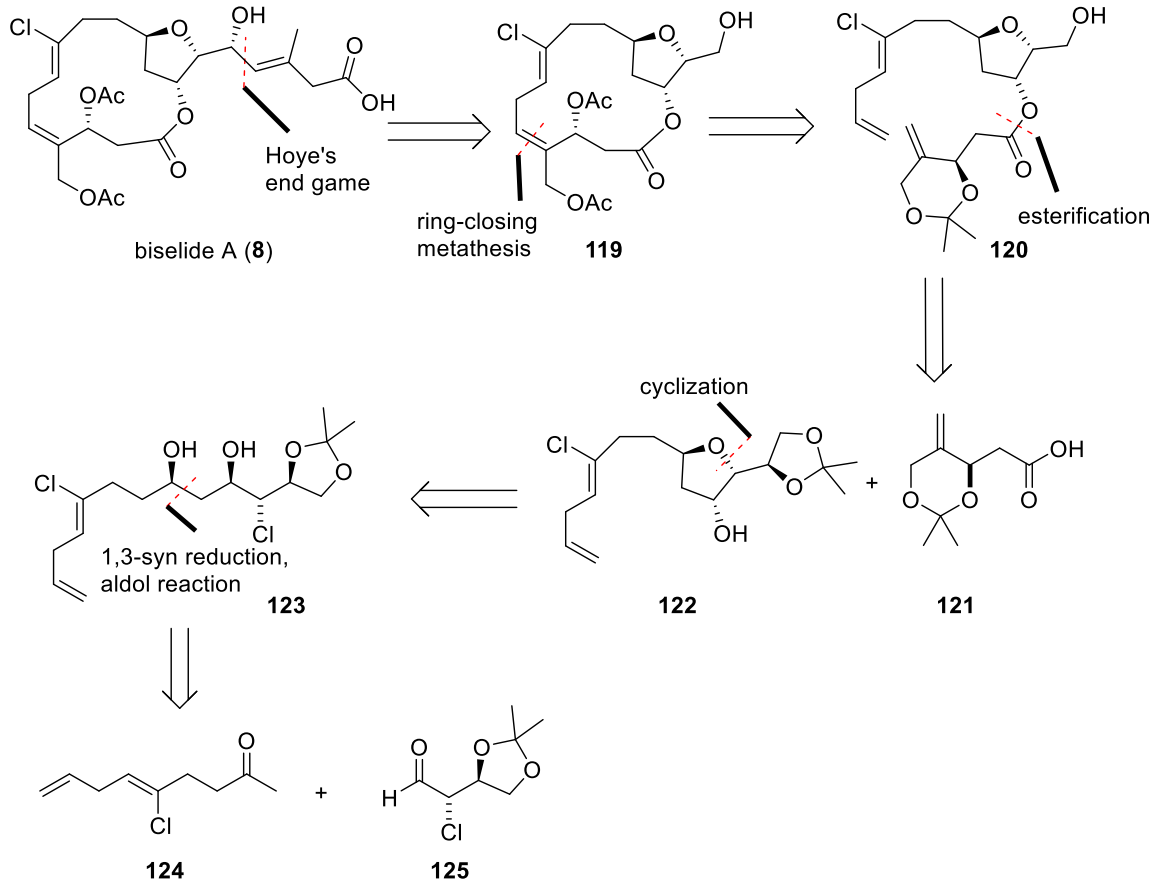

Scheme 2-18 Kang's initial retrosynthtic proposal involving key ring-closing metathesis step

Initial studies were directed towards an RCM strategy and began with the chlorination of the known aldehyde **126** using a catalytic amount of L-proline and *N*-chlorosuccinimide to give racemic α-chloroaldehyde (±)-**127**. Separately, Kaneda chloroallylation[31] of propargyl bromide (**128**) with allyl chloride (**129**) generated the desired skipped diene **130** in good diastereoselectivity. Subsequently, alkylation of compound **130** with ethyl acetoacetate, followed by decarboxylation afforded the methyl ketone **124**. This

intermediate **124** was subjected to a lithium enolate aldol reaction with α-chloroaldehyde (±)-**127** to produce the aldol adduct (±) **131** as a 6:1 mixture of *anti*:*syn* diastereomers. This adduct was reduced with DIBAL to produce the 1,3-s*yn* chlorohydrin (d.r 4:1) (±)-**132,** which was subjected to cyclization under microwave conditions in the presence of water to furnish the desired terahydrofuranol (±)-**133.** Next, selective protection of the primary hydroxyl group as its corresponding TBS ether afforded compound (±)-**134** (Scheme 2-19).

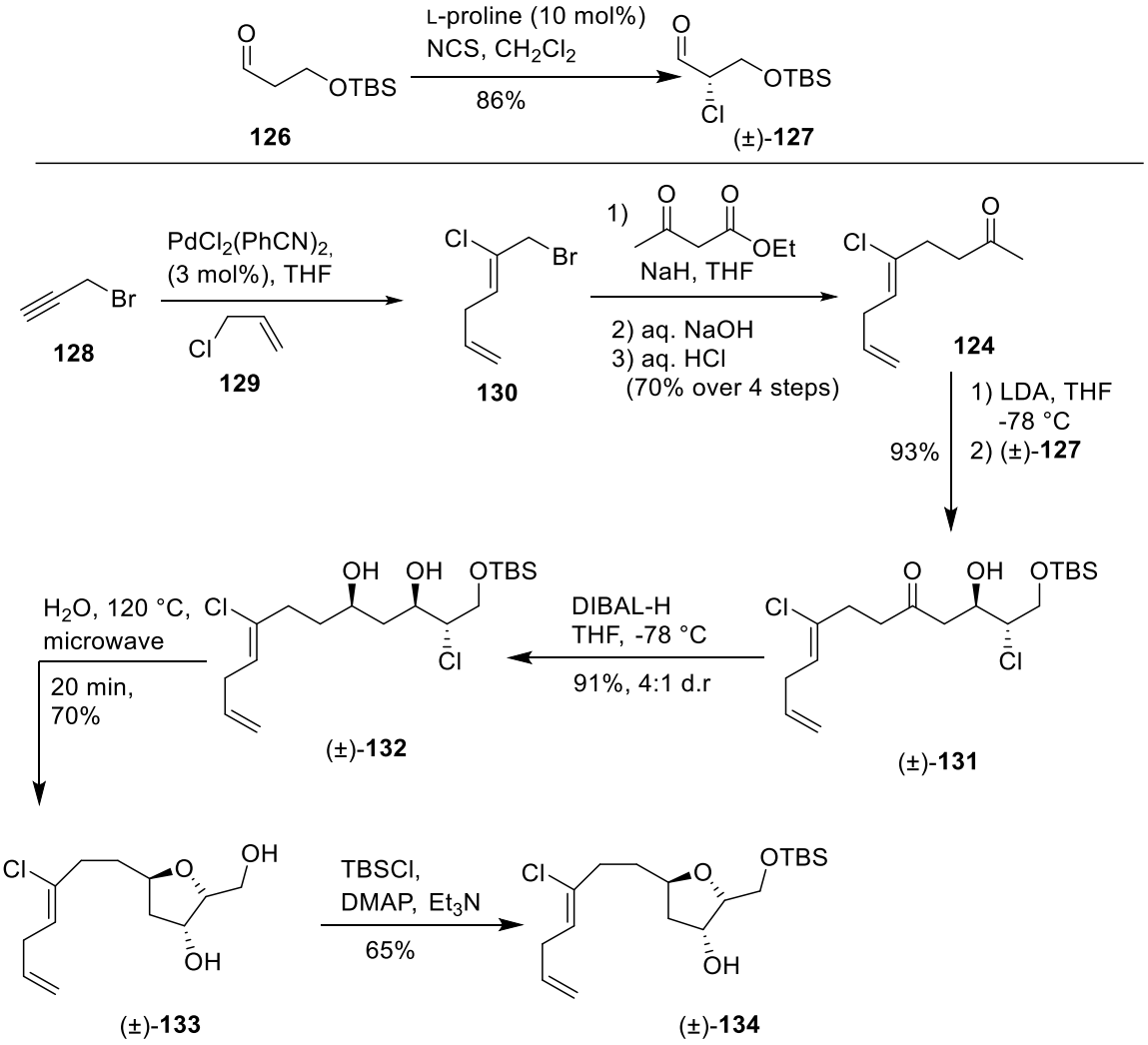

Scheme 2-19 Kang's synthesis of substituted tetrahydrofuranol 134

Over 4 steps the acid **136** was synthesized from the β-hydroxy ester **135**. Esterification between tetrahydrofuranol (±)-**134** and the acid **136** with DCC and DMAP furnished compound **137** as a precursor for the ring-closing metathesis reaction. Having

precursor **137** in hand, Kang attempted the ring-closing metathesis reaction (RCM) using different ruthenium metathesis catalysts under varied conditions. Unfortunately, the major product formed in this reaction was determined to be the metathesis dimer **138** and none of the desired product was formed (Scheme 2-20). The failure of this reaction was attributed to the reactivity differences between the two terminal alkenes and the *trans*-relationship between the side chains at C3/C5 position on the THF ring that presumably precludes the two alkenes from coming within close proximity of each other, which is required for the ring-closing metathesis reaction. Thus, this route was abandoned due to above-mentioned complications arising from the RCM reaction.

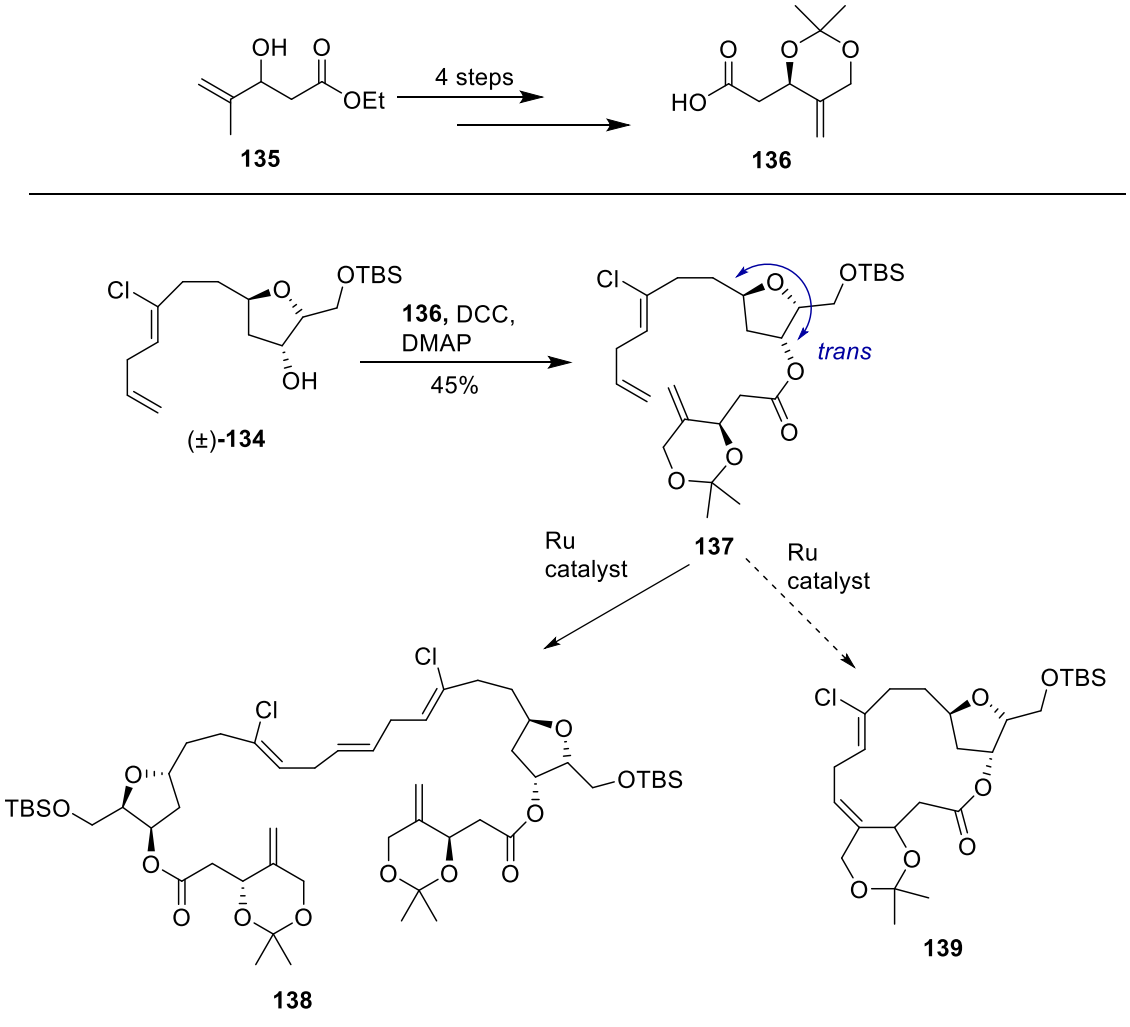

Scheme 2-20 synthesis of precursor 136 and intermolecular dimerization and intramolecular ring-closing pathways

2.3.2. A Relay Ring-Closing Metathesis-Based Strategy Towards the Macrocyclization of Biselide A.

Building on the studies of Kang, Fan envisioned that the removal of the THF ring may provide the flexibility in the carbon chain back bone required for a ring-closing metathesis reaction.[55] For a proof of concept studies, Fan synthesized two linear model substrates **140** and **142**, which upon successful RCM would give the 8-membered and 12-membered macrocycles **141** and **143** respectively (Scheme 2-21) Unfortunately, under varying conditions of concentration, solvent and catalyst, mostly the substrate **140** remained unreacted, while substrate **142** afforded small amounts of dimer **144** formation. In all cases no product formation was observed. These experimental results suggested the ring-closing metathesis reaction was impeded by a complex combination of lack of reactivity of terminal alkenes and steric strain between the side chains on the THF ring.

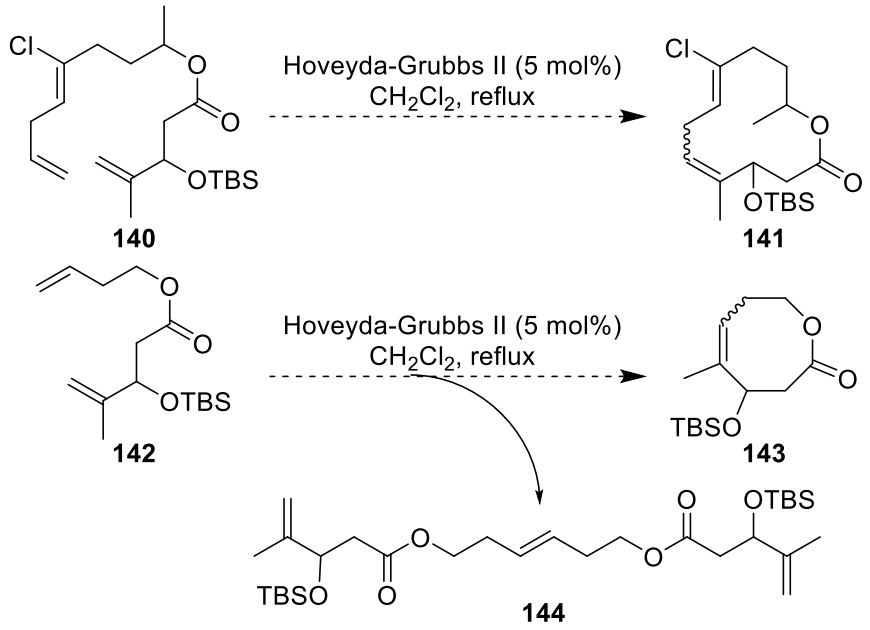

Scheme 2-21 Hope Fan's attempts for ring-closing metathesis with less rigid substrates.

Inspired by the success of Hoye[30,61] and Porco's[62] approach of relay ring-closing metathesis (RRCM) in the synthesis of natural products, Fan devised an alternative approach incorporating the RRCM (Scheme 2-23) as a key step to achieve the macrocyclization towards the synthesis of biselide A. This strategy would circumvent the lack of reactivity of the hindered alkene and give access to an expanded macrocycle,

followed by reduction of the ketone and thermal cyclization to form the tetrahydrofuran ring

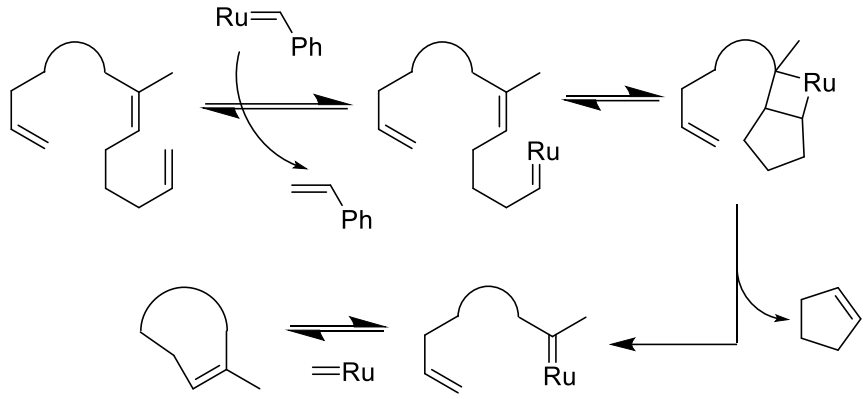

Figure 2-4 The relay ring-closing metathesis mechanism.

The RRCM precursor **149** was synthesized and subjected to a metathesis reaction in the presence of Grubbs II catalyst. Unfortunately, the major product formed in this reaction was the undesired *(E)*-alkene **151** (Scheme 2-24). Fan's efforts to optimize the reaction conditions to furnish the desired (*Z*)-alkene were not successful, suggesting that the reaction outcome was strictly substrate dependent. This precluded the application of RRCM strategy towards the synthesis of biselide A.

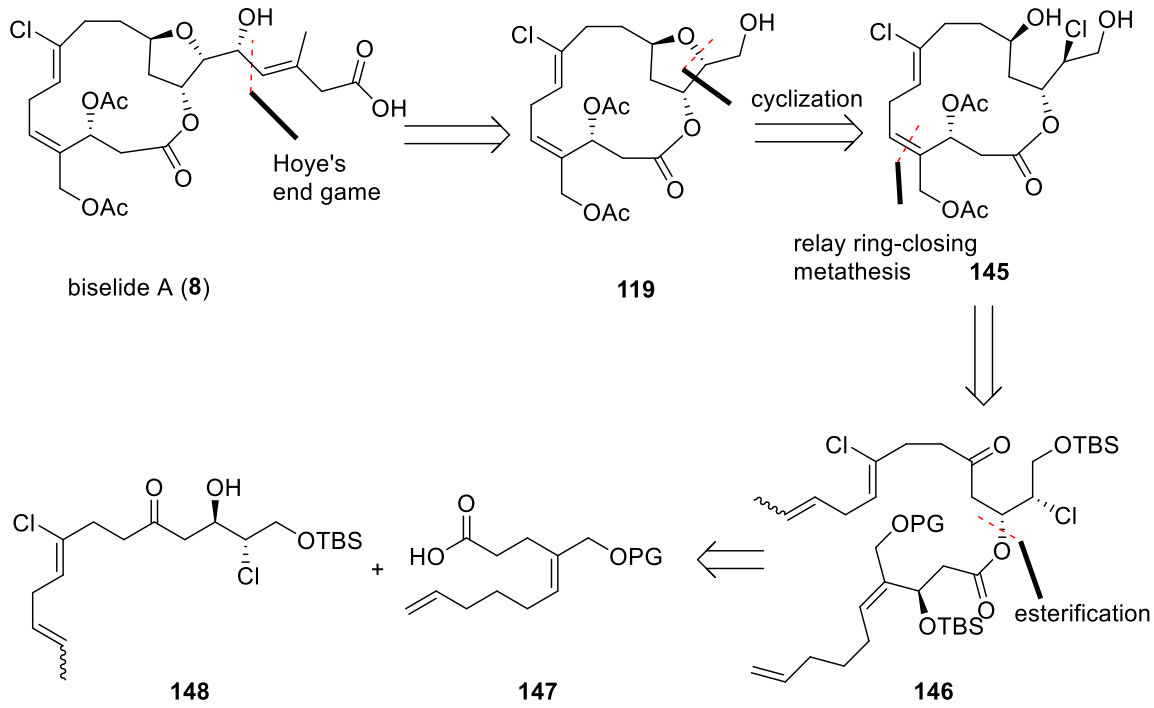

Scheme 2-22 Revised relay ring-closing metathesis strategy

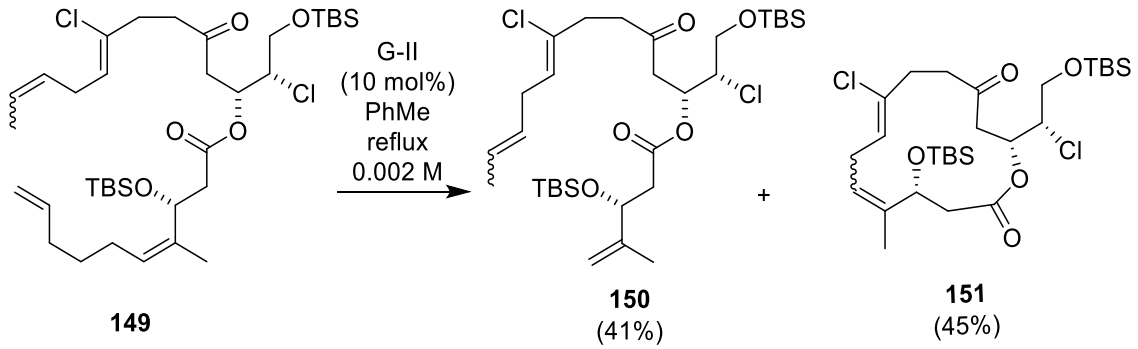

Scheme 2-23 The relay ring-closing metathesis reaction of substrate 149 giving the undesired (*E*)-isomer

2.3.3. A Horner-Wadsworth-Emmons Strategy Towards the Synthesis of Biselide A.

As a result of unsuccessful attempts to synthesize the macrocycle using the ring-closing metathesis strategy, a new retrosynthetic plan was devised by Taron incorporating macrolactonization and a key Horner-Wadsworth-Emmons (HWE)[17] reaction to install and elaborate the C4-C5 alkene towards the synthesis of biselide A (**8**) (Scheme 2-24). The retrosynthetic plan incorporated the use of Hoye's[30] end game strategy to install the carboxylic acid side chain. Taron planned to construct the C20-oxygenated macrocycle following the Yamaguchi macrolactonization[22] protocol as reported in the previous synthesis of the haterumalides. The precursor for macrolactonization could then be accessed using an HWE reaction between the aldehyde **153** and the phosphonate **152**. Selective oxidative cleavage of the terminal alkene **154** would finally provide the requisite aldehyde **153**, an intermediate in Kang's synthesis.[5]

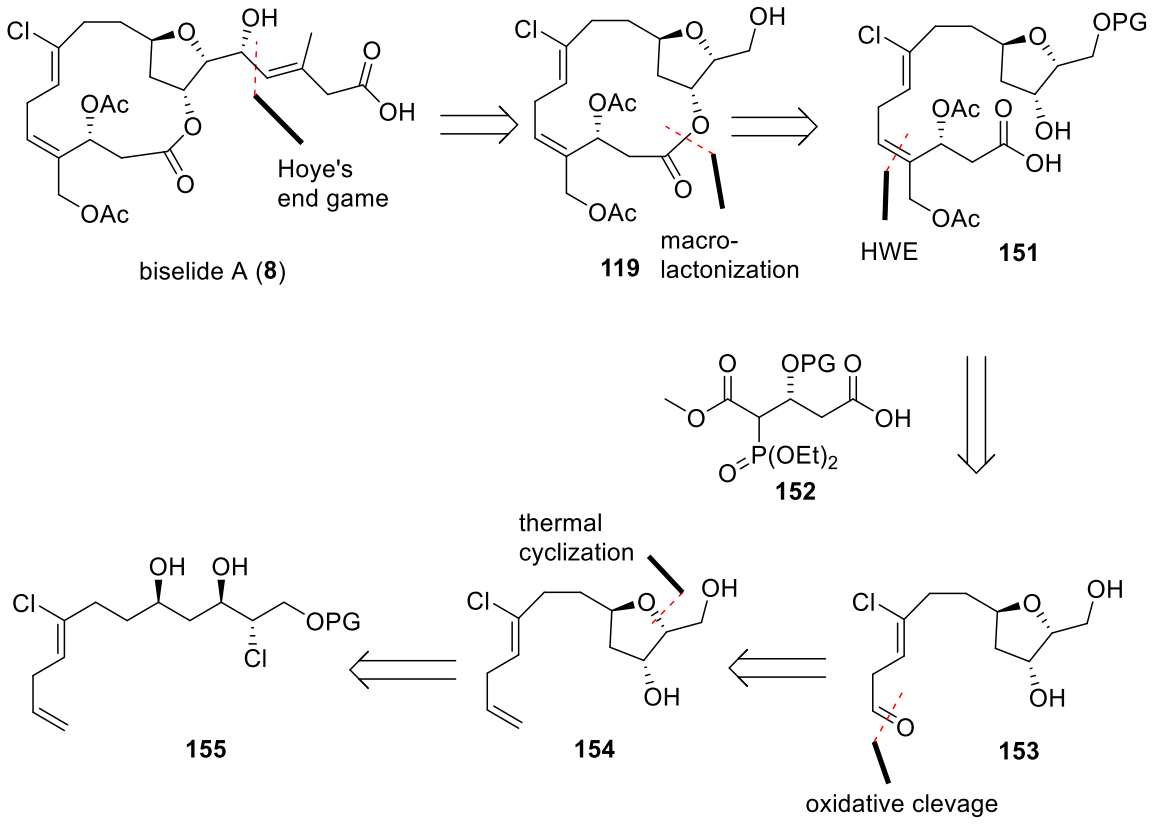

Scheme 2-24 Revised retrosynthesis for the Horner-Wadsworth-Emmons based strategy towards the syntheis of biselide A (8)

The synthesis began with the exposure of the skipped diene **156** to AD-mix (β), affording the terminal diol **157.** Oxidative cleavage of the diol **157** in the presence of sodium periodate furnished the desired aldehyde **158** with modest yield (Scheme 2-25).

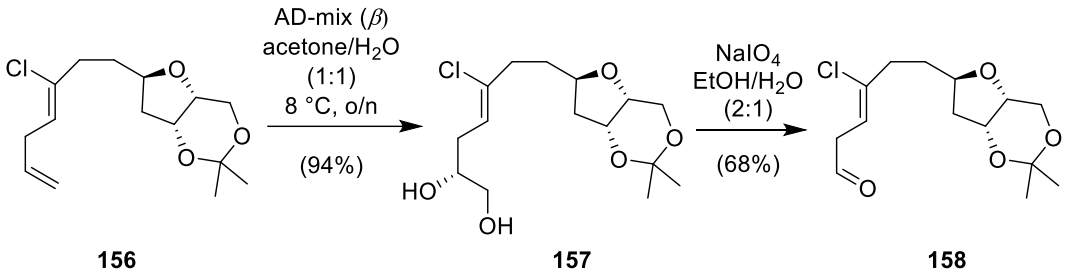

Scheme 2-25 Synthesis of the aldehyde 158

Unfortunately, efforts to access the phosphonate **159** were not successful. Moreover, a model HWE reaction between the aldehyde **158** and the phosphonate **161** with a free hydroxyl group afforded an intractable mixture of compounds. Decomposition of starting material was primarily observed through the elimination of the phosphonate group and therefore this route was not pursued further to elaborate the C4-C5 alkene (Scheme 2-27).

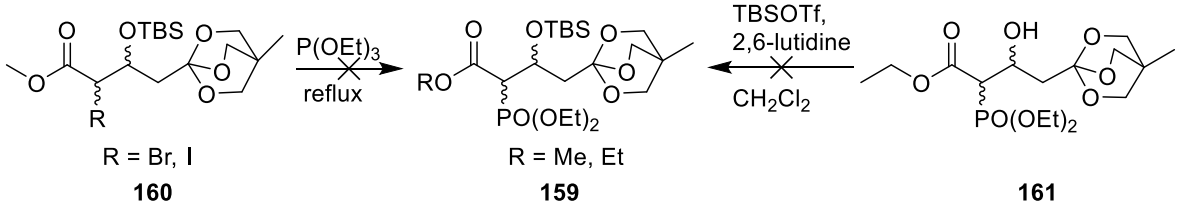

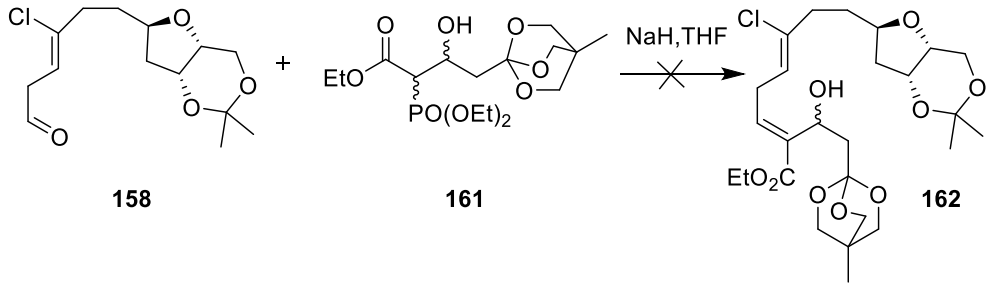

Scheme 2-26 Failure attemp to access the TBS protected phosphonate 159 and the Horner-Wadsworth-Emmons reaction.

2.3.4. A Cross Metathesis Strategy Towards the Total Synthesis of Biselide A

Considering the failures of the previous ring-closing metathesis, relay ring-closing metathesis and HWE approach, a revision of the synthetic strategy was required. Fan and Taron investigated an alternative strategy towards the synthesis of biselides. Their retrosynthesis[55-56] employed key chemical transformations including a cross metathesis to access the C4-C5 alkene, regioselective enzymatic acetylation (i.e.,installing the C20 functionality), asymmetric acetate aldol reaction (to install the C1 and C2 fragment of the macrocycle), Yamaguchi macrolactonization[22] and Nozaki-Hiyima-Kishi[19,20] coupling to complete the synthesis, which is a well precedented process (Scheme 2-28).

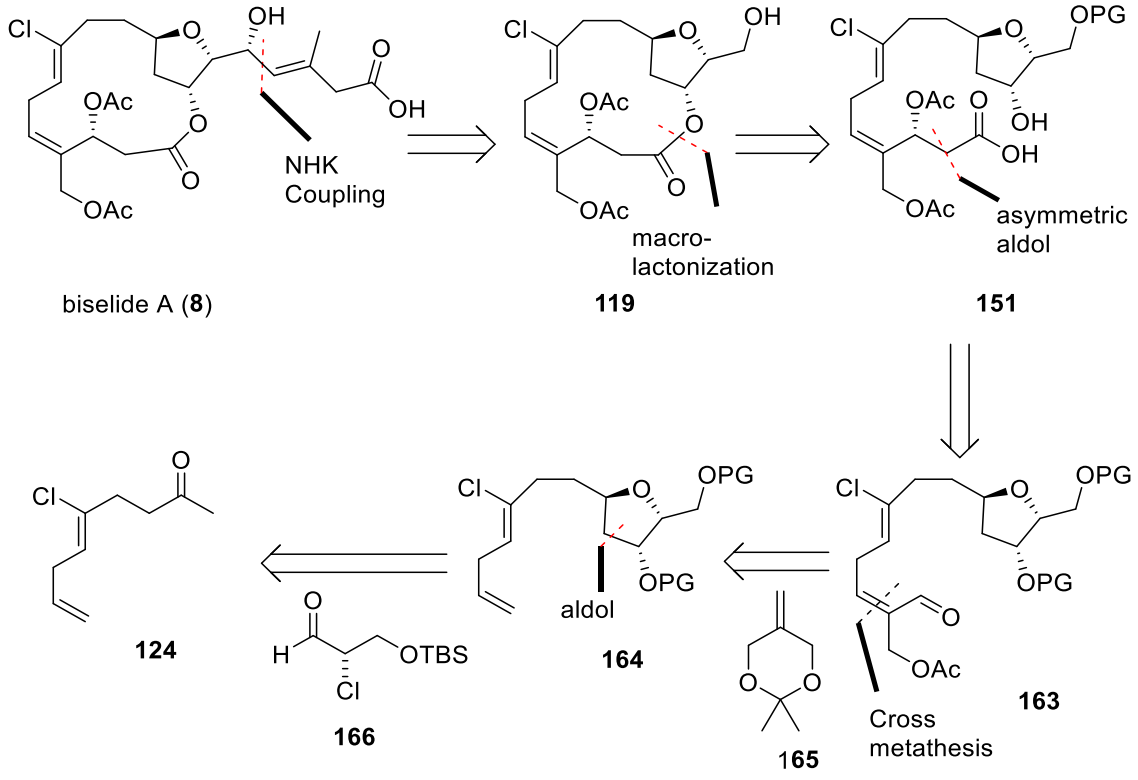

Scheme 2-27 A cross metathesis approach towards the syntheis of biselide A

The synthesis began from the intermediate diol **132** (Scheme 2-28) accessed by the methods developed by Kang.[54] Thermal cyclization of compound **132** under microwave conditions yielded the tetrahydrofuran diol **133** in 70% yield followed by disilylation to give the TBS ether **167** under standard conditions and in good yield. Next, cross metathesis using the optimized conditions between the acetonide **165** and the TBS

ether **167** afforded the desired diene **168,** albeit in modest yield. Selective cleavage of the allylic acetonide **168** under acidic conditions furnished the diol **169** in 70% yield. A subsequent regioselective enzymatic acetylation reaction following the conditions reported by Imai and coworkers furnished the cis-allylic alcohol **170** in 53% yield. Next, oxidation of alcohol **170** with Dess-Martin periodinane afforded the aldehyde **171.** With the aldehyde in hand, various lithium aldol reactions were carried out and several conditions were screened to access the seco acid as depicted in Scheme 2-29.

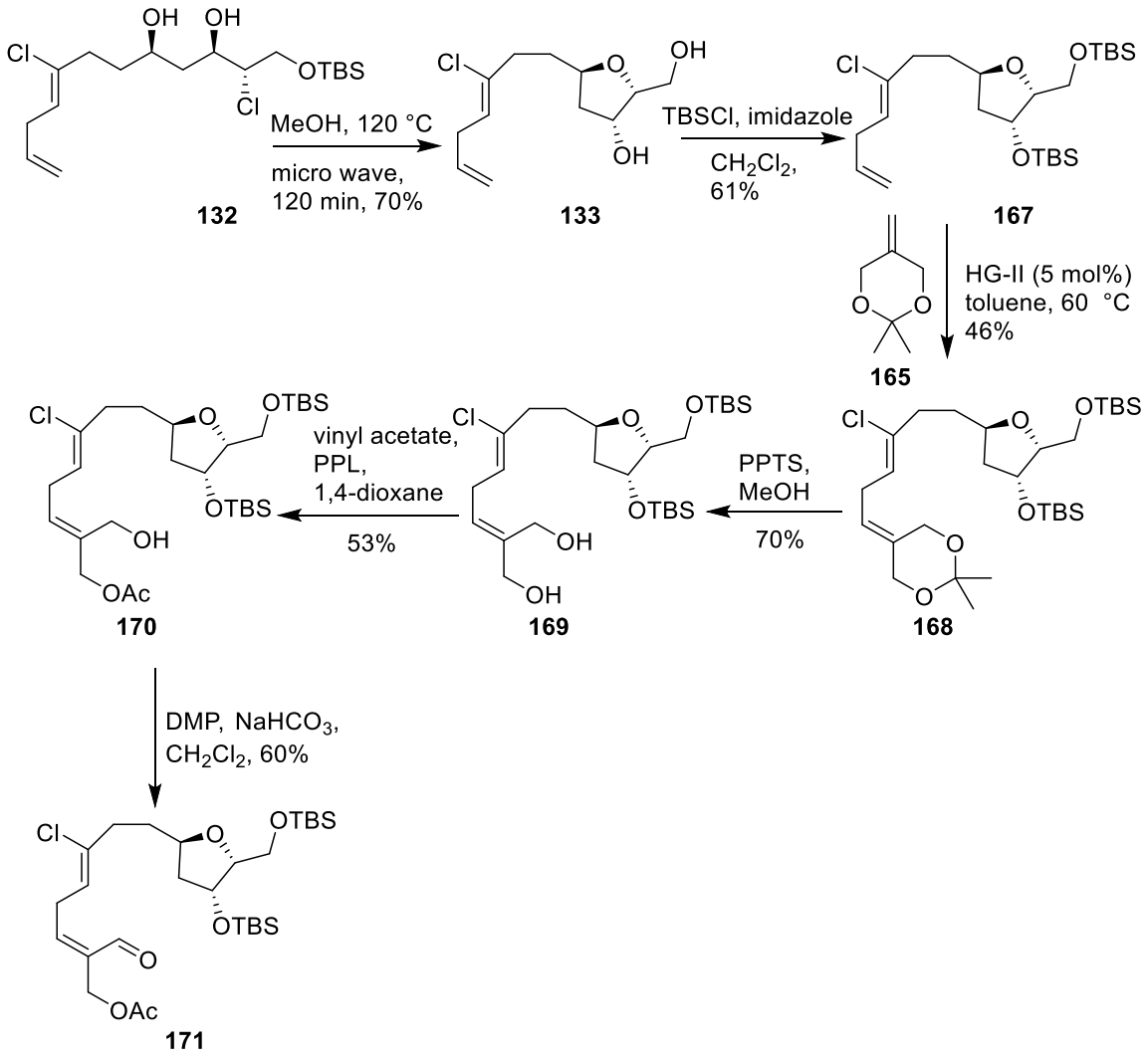

Scheme 2-28 Synthesis of the aldehyde 171 from the diol 132

The aldol reaction between the aldehyde **171** with the lithium enolate of ethyl acetate furnished the esters **172** diasteromeric at the C3 hydroxyl group. A subsequent basic hydrolysis of the ester **172** gave an intractable mixture of compounds that contained additional alkene functions (as observed by analysis of ^{1}H NMR spectra) suggesting that elimination of the β-hydroxyl group occurs in preference to the ester hydrolysis. As the basic ester hydrolysis conditions encouraged elimination, a tertiary butyl ester **175** was synthesized and anticipated that the acidic hydrolysis conditions would furnish the desired seco acid. Attempts to cleave the tertiary butyl ester under varied conditions were not successful and therefore the seco acid synthesis was not accomplished.

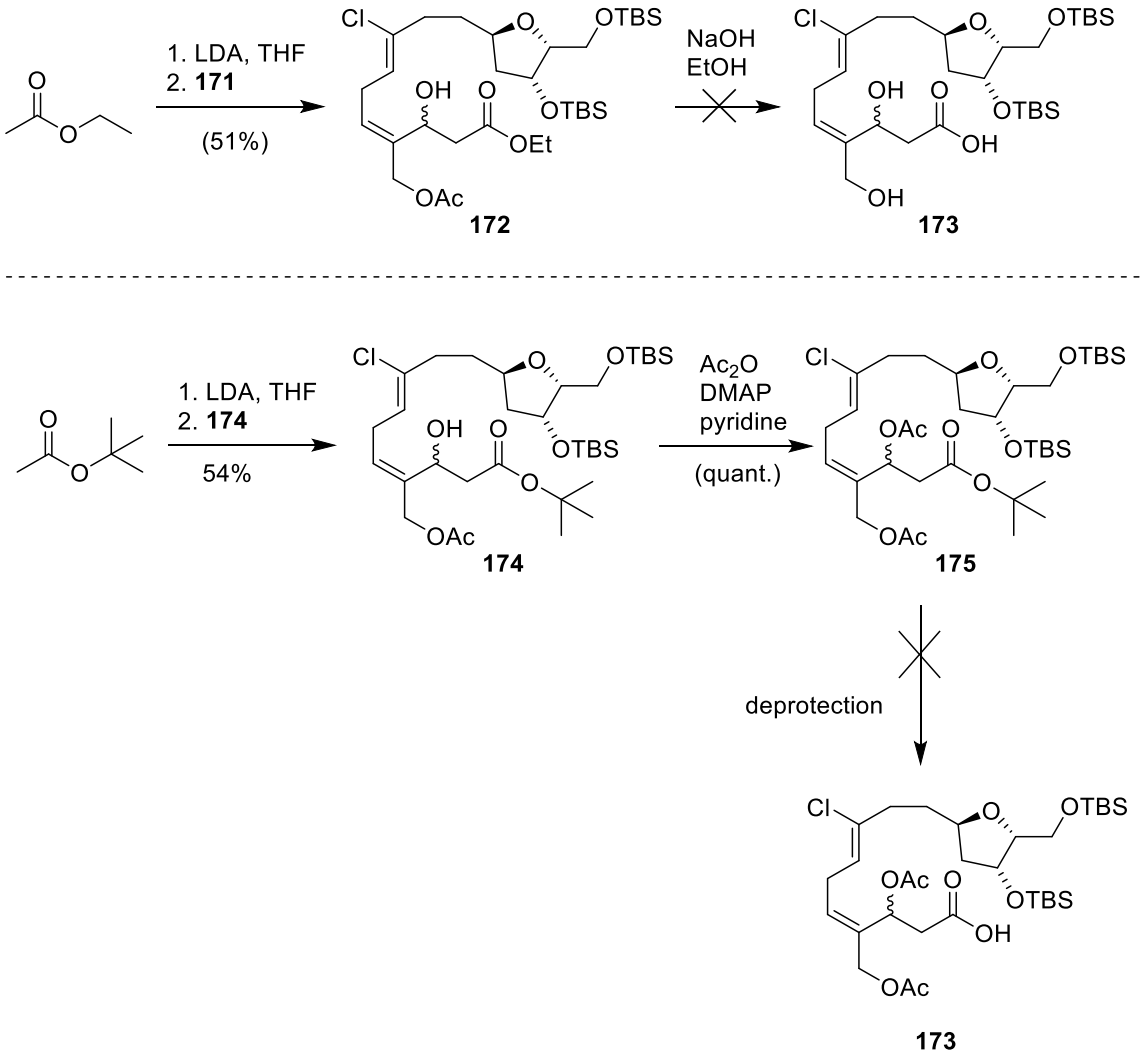

Scheme 2-29 Attempted synthesis of seco acid 173

2.3.5. A Revised Macrolactonization Strategy Towards the Synthesis of Biselide A

Building on lessons learned through the syntheses described above, Kwon devoted his efforts towards a detailed investigation of macrolactonization strategies. Based on the failings to access the seco acid for macrolactonization, there was a need to identify an acid protecting group that can be cleaved under mild conditions without affecting the neighboring acetate groups and TBS ethers.

The key intermediate aldehyde **171** was synthesized following previously developed methods[56] and subjected to an aldol reaction with the lithium enolate derived from methyl acetate (**176**) to afford the methyl ester **177.** The ester **177** was subjected to mild hydrolysis conditions developed by Nicolaou and co-workers[63] using trimethyltin hydroxide (Scheme 2-30). However, these conditions resulted in a complex mixture of products. Cleavage of phenyl esters under mild basic conditions (*e.g.*, H_2O_2 and $NaHCO_3$ at 0 °C) is well documented in the literature.[64] Thus, a 1:1 mixture of phenyl acetate (**178**) and the allylic alcohol **170** was stirred in a mixture of THF, H_2O, and H_2O_2 with $NaHCO_{3,}$. The analysis of the resulting crude mixture by ^{1}H NMR spectroscopy indicated complete hydrolysis of phenyl acetate (**178**) without affecting the primary allylic acetate group. However, attempts to hydrolyze the phenyl ester **180** were not successful. Considering the cleavage of *tert*-butyl thioesters can be accomplished utilizing silver salts, a thioester **183** was synthesized (Scheme 2-31) and upon treatment with silver (I) trifluroacetate under aqueous conditions at room temperature no reaction was observed. Increasing the temperature slowly to 80 °C resulted in the competitive clevage of the primary TBS ether, *tert*-butyl thioester and elimination of the β-acetoxy group to form compound **184** (Scheme 2-32). Maintaining this reaction for extended period of time at 40 °C resulted in decomposition. Several attempts to optimize the conditions to cleave the *tert*-butyl thioester were not successful. Inspired by the successful examples demonstrated by Masamune[65,66] directly using thioesters for macrolactonization in the synthesis of natural products, the *tert*- butyl thioester **183** was treated with several Cu(I) and Ag(I) salts. In all the cases, there was no conversion of starting material to the desired macrocycle, and this route was not pursued further.

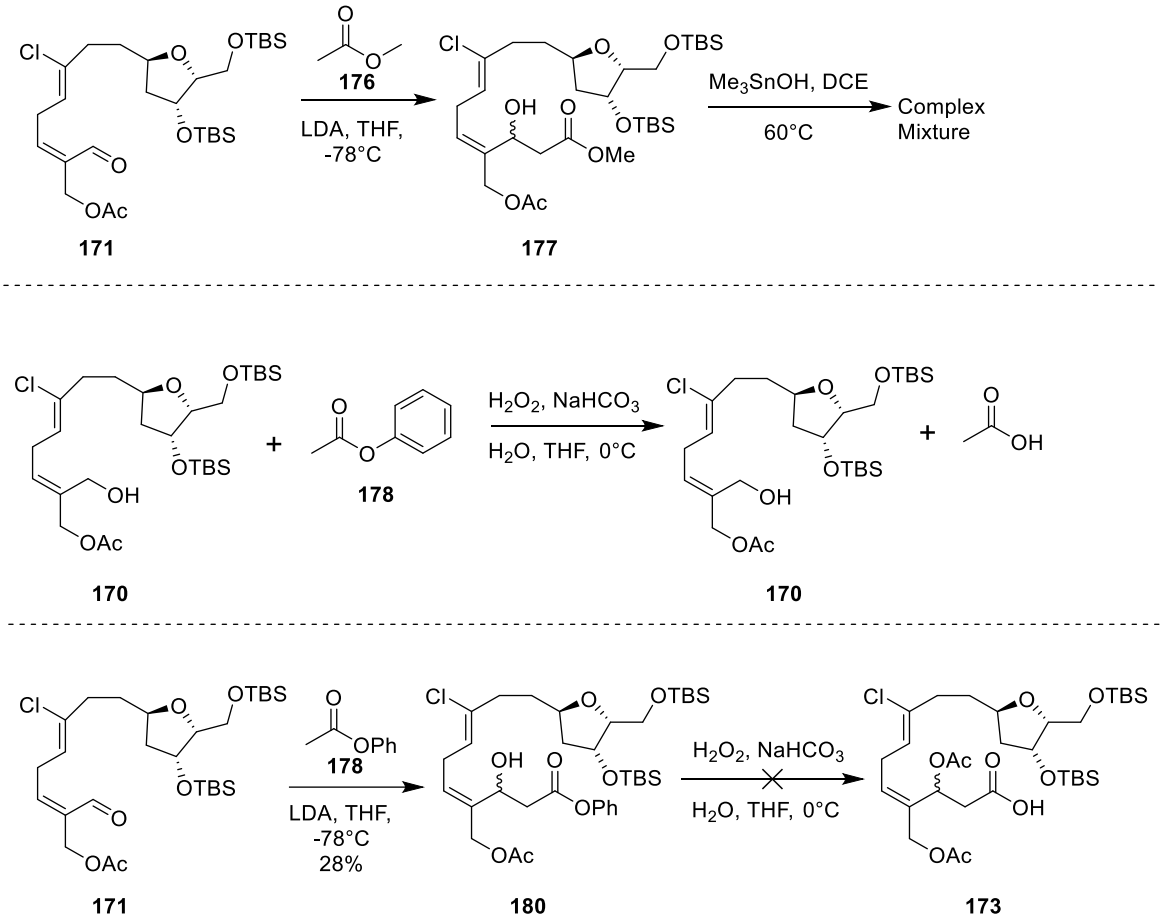

Scheme 2-30 Attempts to cleave methyl ester 177 and phenyl ester 180.

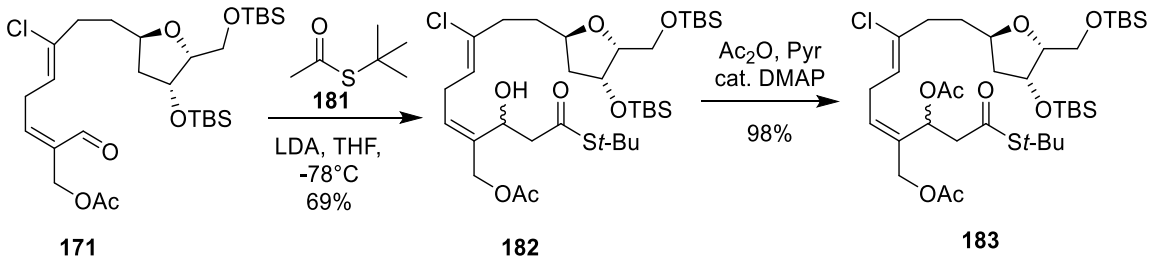

Scheme 2-31 Synthesis of *tert*-butyl thioester 183

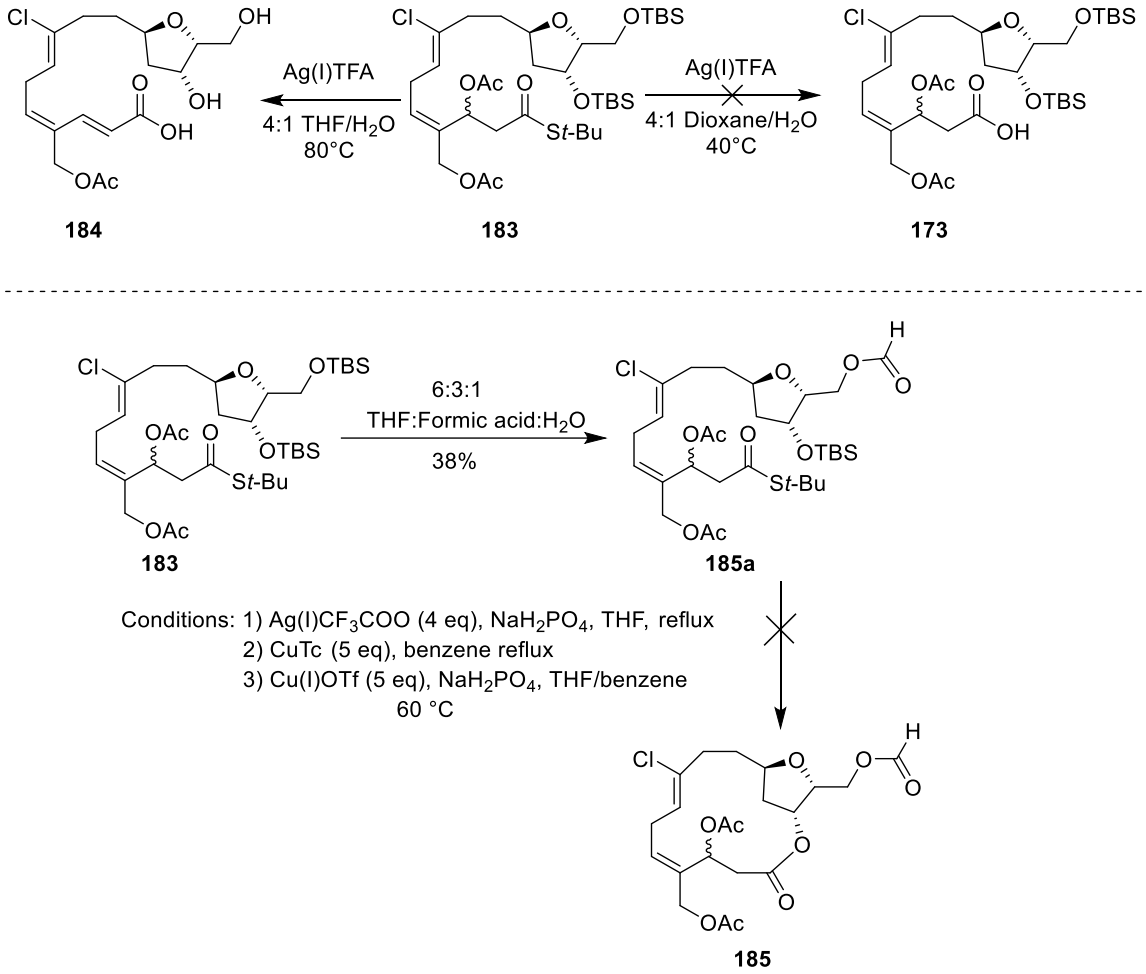

Scheme 2-32 Attempted hydrolysis of *tert*-butyl thioester 183 and failure to effect Masamune macrolactonization

In Hoye's synthesis[30] of haterumalide NA (**1**), a PMB ester was employed as a carboxylic acid protecting group and hydrolysis was effected under mild conditions without elimination of the secondary allylic acetate group. In light of this work, a PMB ester **187** was synthesized from the aldehyde **171** and PMB acetate **186** subjected to a lithium aldol reaction followed by acetylation and deprotection of the TBS ether to afford the diol **189** in excellent yield. The PMB ester **189** was stirred in a 3:1 solution of CH_2Cl_2:trifluoroacetic acid with 10 equivalents of triethylsilane at 0 °C, to furnish the desired seco acid **190** in moderate yield without any observed elimination of the β-acetoxy group or hydrolysis of primary/secondary allylic acetates (Scheme 2-33).

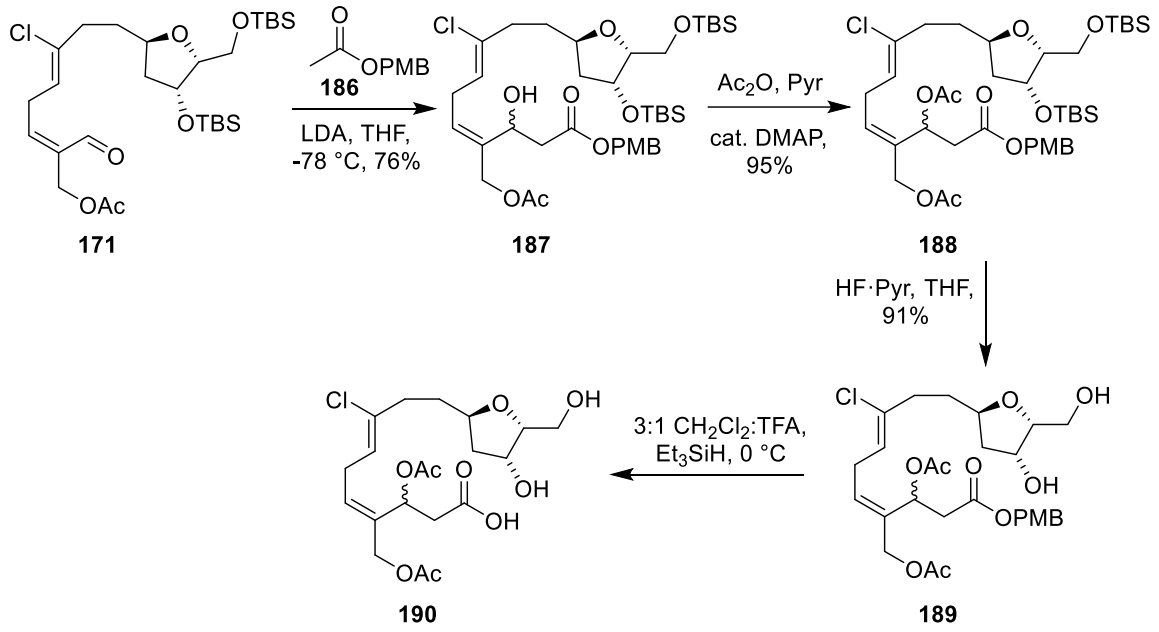

Scheme 2-33 Prepartion of Seco acid 190

The ^{1}H NMR spectrum of **190** in $CDCl_3$ showed marked differences in the chemical shifts of protons assigned to the two diastereomers **190a** and **190b** (Figure 2-5) on the THF ring. Given that these differences were not observed prior to the removal of PMB group and that the two diastereomers differ only in their relative stereochemistry at the remote C3 centre, this warranted further studies. A detailed investigation by ^{1}H NMR spectroscopy of **190** in different solvents suggested that the seco acid adopts a rigid conformation enforced by intramolecular hydrogen bonding between the free carboxylic acid and the oxygenated functionalities present on the THF ring as depicted in Figure 2-6. With these unexpected results, efforts were directed towards acid catalyzed hydrogen bond-templated[67] macrolactonization.

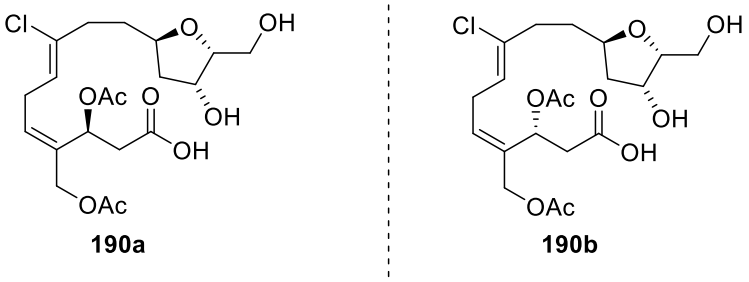

Figure 2-5 Diasteromers of the seco acid 190

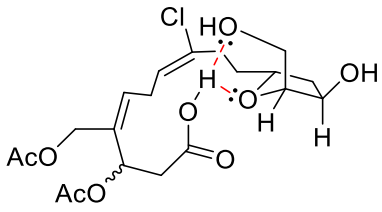

Figure 2-6 Proposed confirmation of seco acid 190

The seco acid **190**, stirred in $CDCl_3$ in the presence of a catalytic amount of PTSA, afforded only enone **184**. Next, seco acid **191** with a free primary hydroxyl group was subjected to acid catalyzed macrolactonization and afforded the primary macrolactone **192** in modest yield (Scheme 2-34). Encouraged by the success of this transformation, attention was directed towards translactonization to access the desired secondary macrolactone **193**. Reports from Corey[67] and Paterson[69] demonstrated the success of translactonization in the synthesis of large ring macrolactones in the synthesis of natural products. Unfortunately, employing similar procedures with **192** resulted in decomposition of the primary macrolactone and no isomerization was observed.

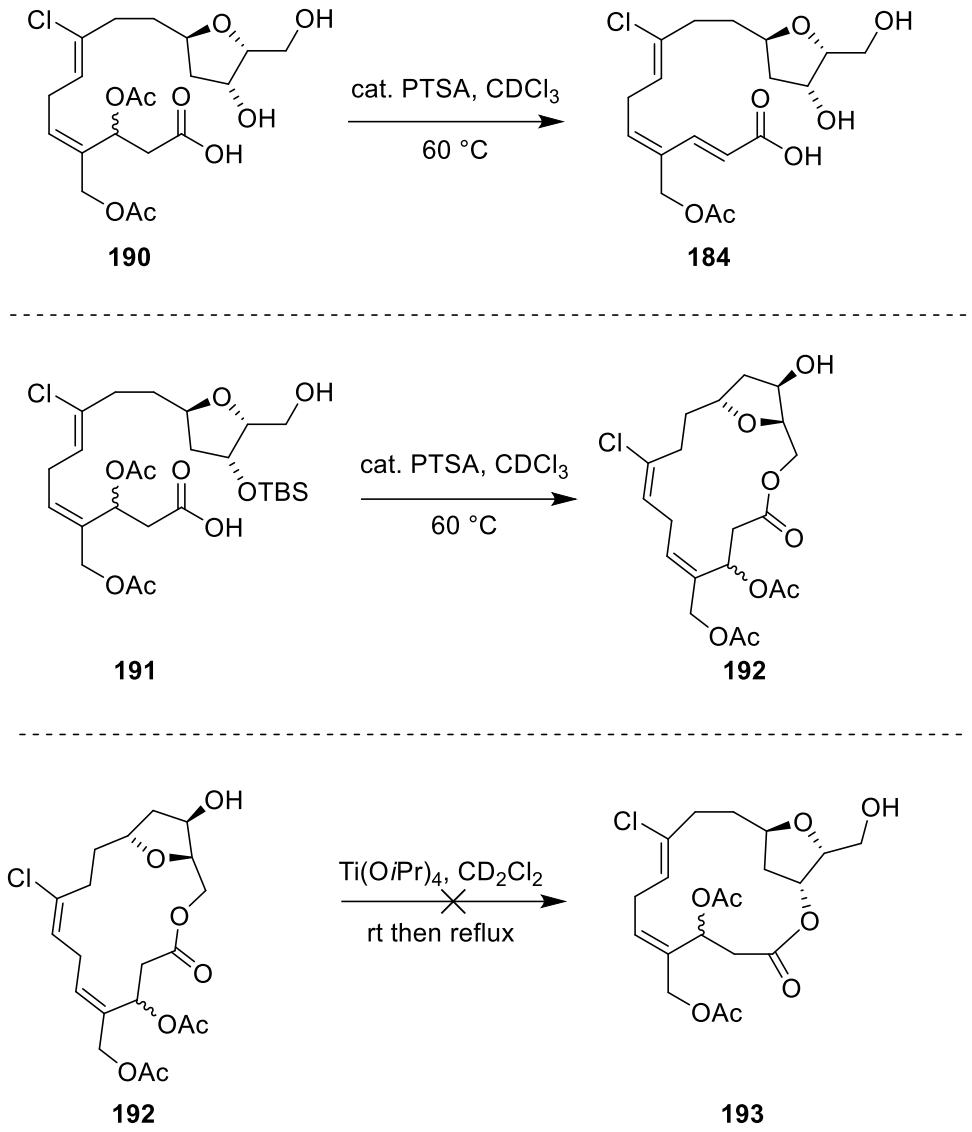

Scheme 2-34 Failure of hydrogen-bond template macrolactonization and translactonization

With the unsuccessful attempts to induce hydrogen-bond template macrolactonization and translactonization, as a last resort standard macrolactonization conditions were explored on seco acid **194**. A wide variety of conditions were screened ranging from Trost[69] and Yamamoto[70] acid catalyzed methods, Yamaguchi[22] and Boden-Keck[71] base catalyzed methods, and finally Corey-Nicolaou,[72] modified Mukaiyama[73-75] neutral or near neutral conditions. In all cases either a mixture of products was observed, or degradation dominated and the desired macrolactone **195** was not formed (Scheme 2-

35). These results suggest that seco acid **194** is too sensitive to participate in macrolactonization and therefore this route was not considered further.

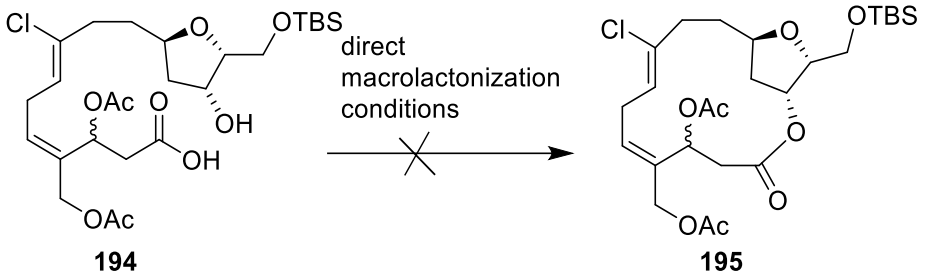

Scheme 2-35 Attempts to access the macrocycle 195

2.3.6. An Intramolecular Reformatsky type Macrocyclization Strategy

Considering the failures to engage seco acid **194** in macrolactonization, a new route was designed that would make use of an intramolecular Reformatsky type reaction to access the macrocycle towards the synthesis of biselide A. Following the same initial disconnection between C15-C16 gave the same macrolactone **119**. However, it was envisioned that intramolecular macrocylization would occur between the *α,β*-unsaturated aldehyde **196** and the bromo ester utilizing Reformatsky reaction as previously demonstrated by Kigoshi[7] in his synthesis of *ent*-haterumalide NA methyl ester. The aldehyde **196** can be achieved by methods described previously and the bromo acetate **197** would be synthesized by a DIC coupling reaction between the bromoacetic acid and the monosilylated tetrahydrofuran **198**. The THF **198** can be accessed from the thermal cyclization of the diol **132** (Scheme 2-36).

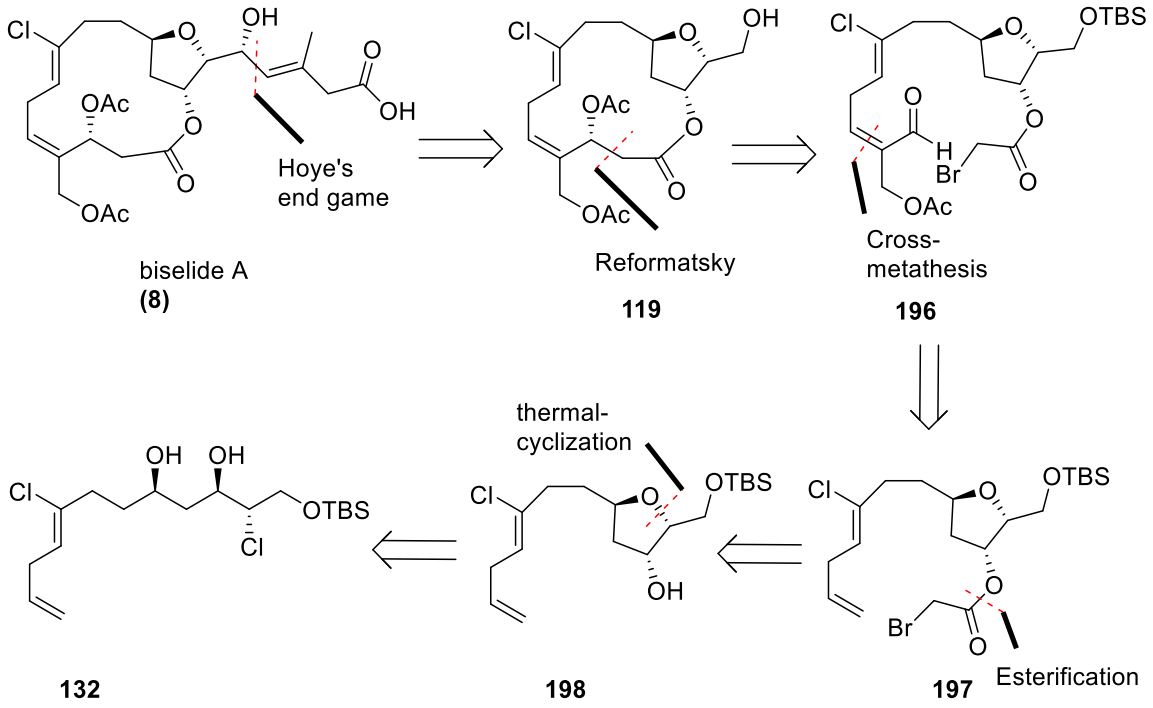

Scheme 2-36 Retrosynthesis of intramolecular Reformatsky strategy

With the aldehyde **196** in hand the stage was set for the intramolecular Reformatsky reaction to access the desired macrocycle **201** (Scheme 2-37). The aldehyde **196** was subjected to the conditions developed by Honda,[13] that includes slow addition of the aldehyde into a mixture of Wilkinson's catalyst and diethylzinc in THF/hexane at 0 °C. This reaction furnished the macrocycle as separable mixture of the undesired diastereomer **200** (42% yield) and desired diastereomer **201** (12% yield). Subjecting compound **200** to Mitsunobu conditions using triphenyl phosphine, DIAD and acetic acid afforded a 2:1:1 inseparable mixture of elimination product **202**, retention product **203**, and inversion product **204** (Scheme 2-38). The use of chloroacetic acid as a surrogate to acetic acid is well precedented to effect Mitsunobu inversion of hindered secondary alcohols. Thus, the macrocycle **201** was subjected to Mitsunobu inversion with chloroacetic acid,[76] which furnished a 2:1 mixture of inversion product **205** to elimination product **202**. Unfortunately, hydrolysis of chloroacetate **205** in the presence of a Zn/Cu couple[77] and NH_4Cl in methanol did not afford the desired alcohol **201**, but repetition of the same experiment under sonication conditions did yield the alcohol **201**, albeit in very low yield. Subsequently, the desired diastereomer **201** was acetylated followed by removal of the TBS ether to yield the alcohol **206**, which is an advanced intermediate in the synthesis of biselide A (Scheme 2-39).

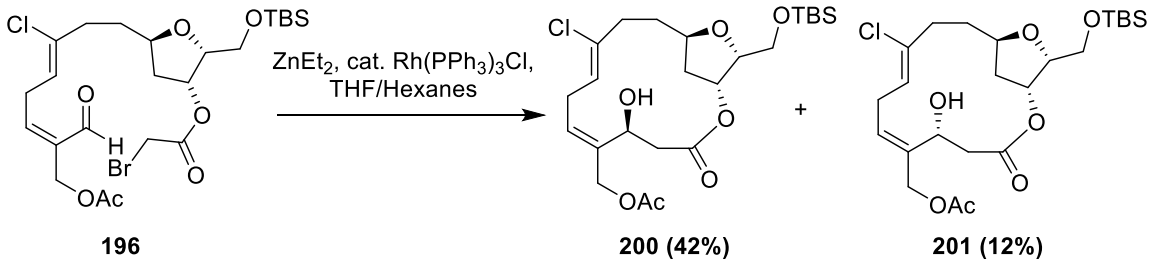

196 **200 (42%)** **201 (12%)**

Scheme 2-37 Intramolecular Reformatsky macrocylization

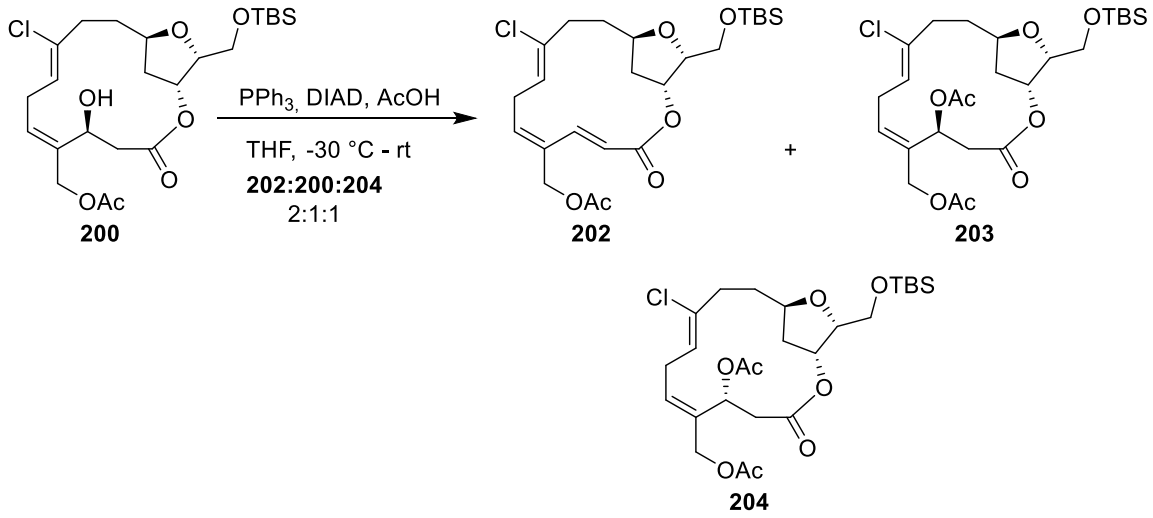

200 **202** **203** **204**

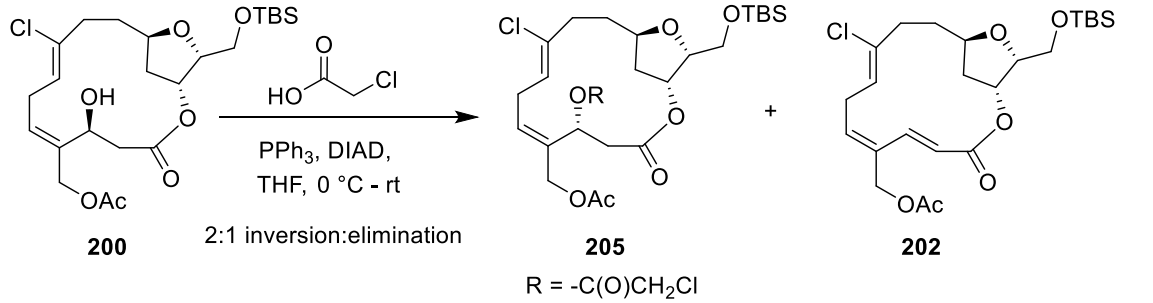

200 **205** **202**

R = -C(O)CH2Cl

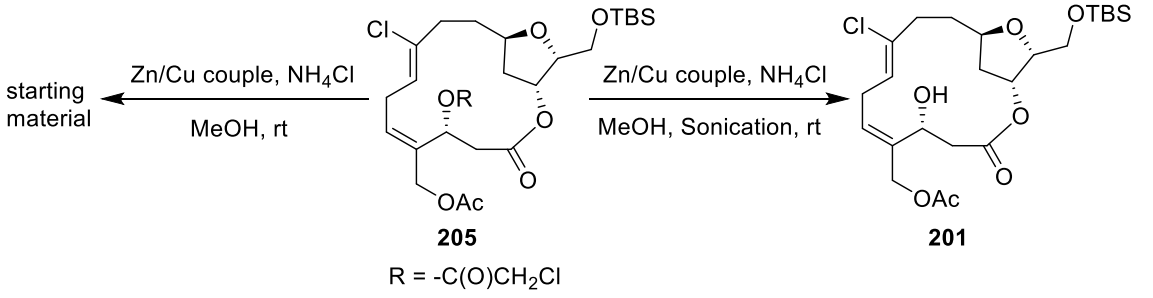

205 **201**

R = -C(O)CH2Cl

Scheme 2-38 Investigation of Mitsunobu inversion of C3 stereocentre

Owing to the sub milligram quantity of macrocycle **200** that was obtained, further optimization of hydrolysis of chloroacetate **205** and elaboration of the macrocycle to complete the synthesis of biselide A was not possible. However, a viable route was established to access the advanced macrocycle **119** towards the synthesis of biselide A (**8**).

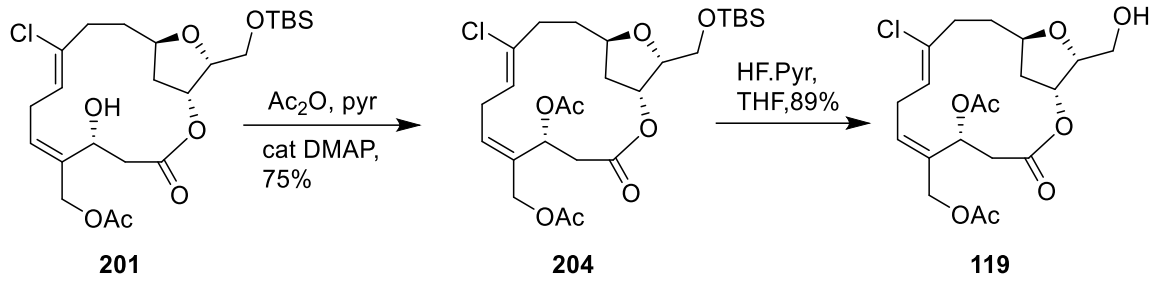

201 **204** **119**

Scheme 2-39 Synthesis of advanced macrocycle intermediate 119

2.4. Results and Discussion

2.4.1. A Scalable Approach and Optimization Studies Towards the Synthesis of Methyl Ketone 124 and the Tetrahydrofuran Diol 133

Our initial approach focused on the scale up of the previously developed synthesis, in order to access synthetically useful amounts of material to complete the total synthesis of biselide A (**8**). While Kwon's synthesis[57] offered considerable improvement over the previous routes with respect to accessing the macrocycle **119**, several key steps required improvement. Specifically, a robust process to provide the tetrahydrofuran diol **133** in gram quantities was required, optimization of the cross metathesis reaction was necessary and selective deprotection of the acetonide group to access the tetrahydrofuran diol **212** in consistent yield would improve material throughput. In addition, we planned on further exploring the Reformatsky macrocylization reaction in an effort to improve the yield of the desired diastereomers **201** or identify conditions to invert the C3 stereocentre of the undesired diastereomer **200** and finally complete the synthesis of biselide A. Based on these considerations our efforts commenced by accessing the methyl ketone **124** in gram quantities. A palladium-catalyzed Kaneda chloro allylation[31] between allyl chloride (**129)** and propargyl bromide (**128)** afforded vinyl chloride **130** as a 4:1 inseparable mixture of *Z/E* isomers. Alkylation of ethyl acetoacetate with vinyl chloride **130** in the presence of

sodium hydride followed by decarboxylation furnished the required methyl ketone **124** in 70% yield over 3 steps.[54,60] (Scheme 2-40). Here, we noted that the purity of compound **124** was critical for obtaining optimal yields in the subsequent lithium aldol reaction.

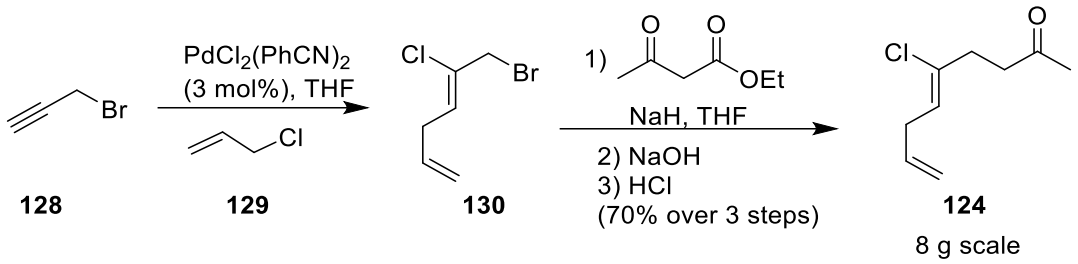

Scheme 2-40 Synthesis of the methyl ketone 124

^{1}H NMR spectroscopic analysis of the methyl ketone **124** revealed that the undesired *E* isomer generated during chloroallylation reaction was carried forward to the alkylation step and was not separated after column chromatography on SiO_2. Chromatography with silica gel impregnated with silver salts is a well known and established methodology for the separation of non-polar unsaturated compounds. This technique is well precedented in the separation of lipids, steroids and other terepenoids.[78-79] Based on this background, compound **124** was subjected to chromatography on silica gel impregnated with silver nitrate. The ^{1}H NMR spectroscopic analysis (Figure 2-7) of the purified product showed complete absence of the undesired *E* isomer. This was the first time that we were able to prepare compound **124** in its pure form.

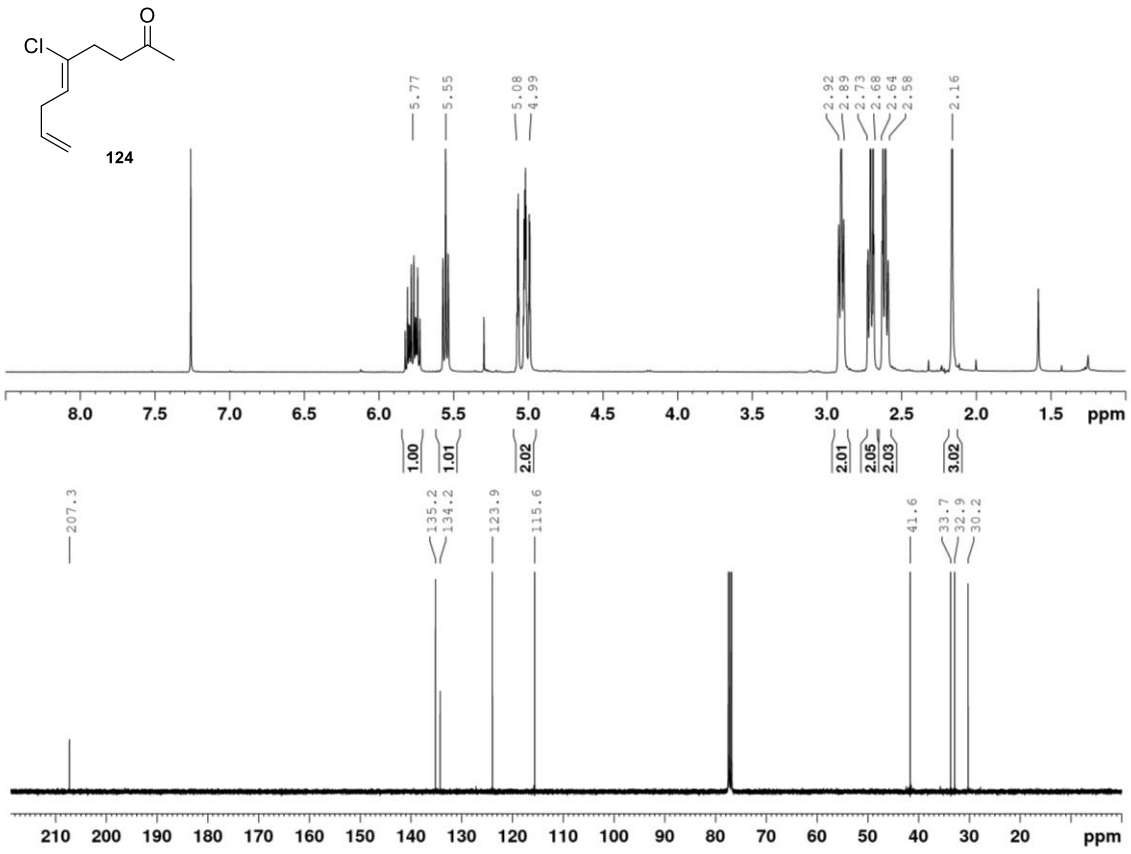

Figure 2-7 ^{1}H and ^{13}C NMR spectra of methyl ketone 124.

Next, we turned our attention towards the enantioselective synthesis of α-chloroaldehyde **127** (Scheme 2.40). Kang had previously developed a synthesis of aldehyde **127.**[54] Later, Fan optimized the final oxidation step in this sequence to prevent racemization at the chloromethine centre. Following the methods reported by De Kimpe,[80] L-Serine (**206**) was treated with $NaNO_2$ in 6N HCl at -10 to -5 °C to afford the α-chloroacid **207** with retention of stereochemistry in good yield. Fischer esterification of α-chloroacid **207** with methanol in the presence of catalytic amount of HCl furnished the methyl ester **208** with 88% yield. The primary hydroxyl group of the ester **208** was protected as its TBS ether using TBSCl and imidazole. The resulting TBS ester **209** was reduced with sodium borohydride under standard conditions to its corresponding alcohol **210**, followed by DMP oxidation to afford the desired optically enriched α-chloroaldehyde **127** in 85% yield. Scale up of the oxidation reaction following previous methods[55] often led to inconsistent yields ranging from 60-67%. The decrease in yield was mainly attributed to the emulsions formed during the work up of the reaction. Here, we found that emulsions could be prevented by

employing repetitive washings using 1:1:1 sat $NaHCO_3$: sat NaCl: water that improved the consistency and yield to 85%. Following this route, Fan had previously determined the enantiomeric excess of α-chloroaldehyde to be greater than 92%. Thus, the synthesis of the α-chloroaldehyde **127** was completed in 5 steps with 47% overall yield (Scheme 2-41).

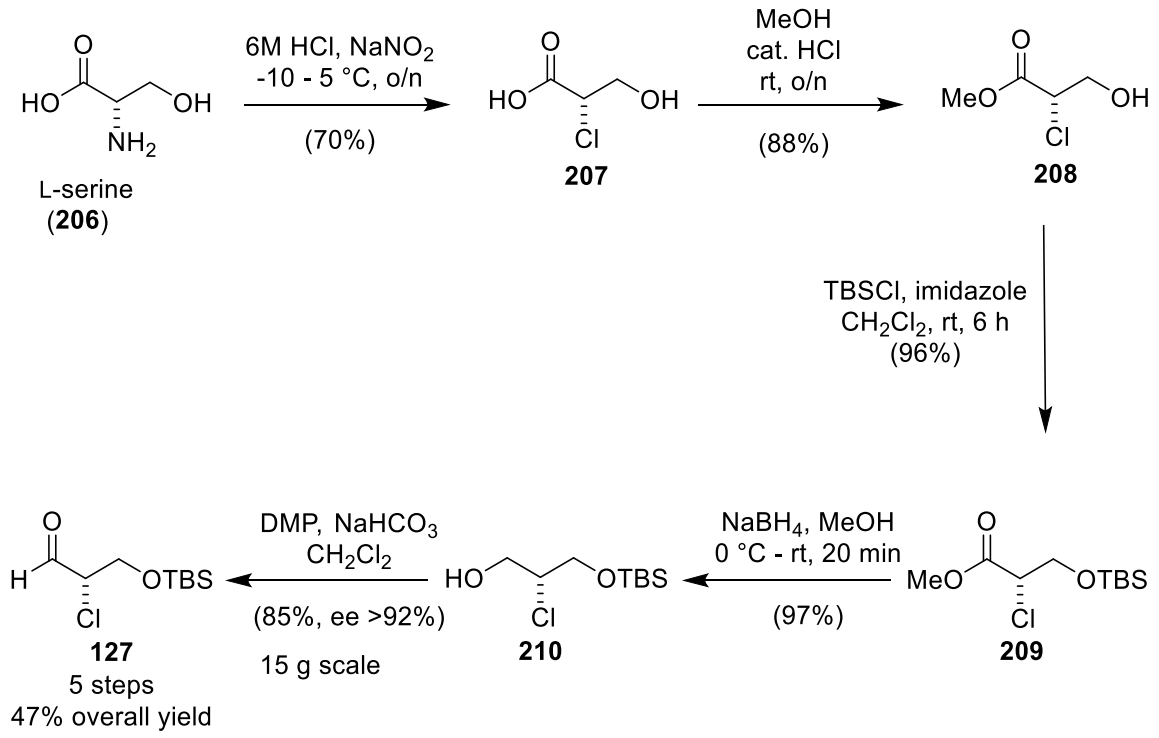

Scheme 2-41 Synthesis of α-chloroaldehyde 127

With the required building blocks in hand, we proceeded to synthesize the tetrahydrofuran diol **133** as shown in Scheme 2-42. The methyl ketone **124** was treated with lithium diisopropylamide, followed by slow addition of aldehyde **127** to afford the β-ketochlorohydrin **131**.[60] ^{1}H NMR spectroscopic analysis of the crude reaction mixture revealed a diastereomeric ratio (d.r) of approximately 6:1 (*anti:syn*). Upon purification by column chromatography, an 85% yield of the *anti*-ketochlorohydrin **131** was isolated with a d.r. of 8:1 (*anti:syn*). Next, 1,3-hydroxyl directed[81,82] reduction of the aldol adduct **131** with DIBAL afforded the desired chlorodiol **132** as a 4:1 mixture of *syn:anti* diol in 91% yield. The mixture of diastereomers could not be separated by column chromatography and were progressed together. Thus, the resultant mixture was subjected to thermal cyclization under microwave conditions to furnish the tetrahydrofuran diol **133** in 80 %

yield. With careful column chromatography, we were able to separate all the unreacted starting material and undesired isomers to afford the pure **133** as analyzed by ^{1}H NMR spectroscopy (Figure 2-8).

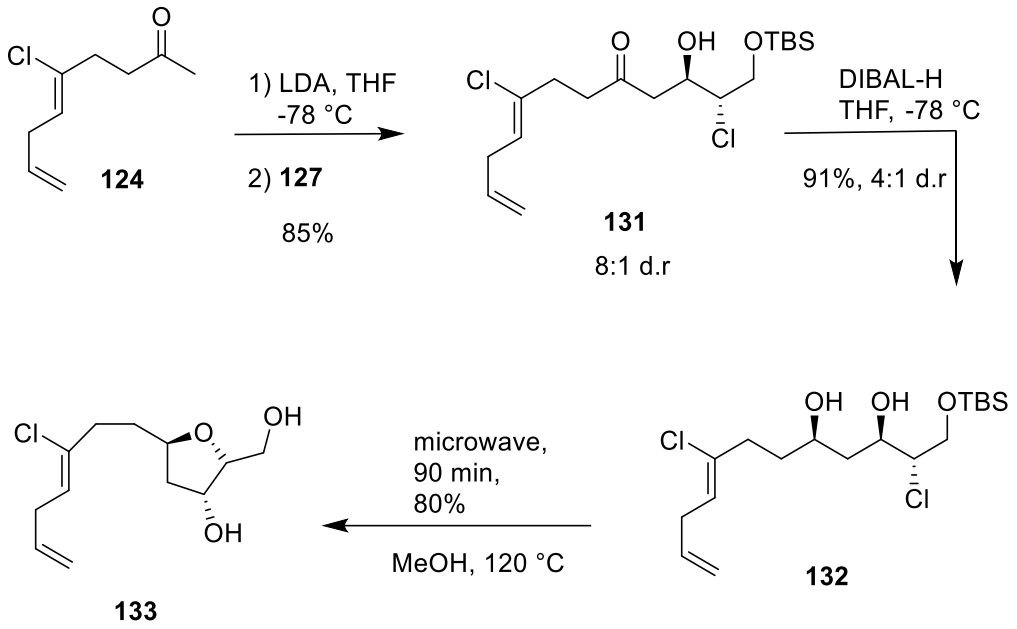

Scheme 2-42 Synthesis of tetrahydrofuran diol 133

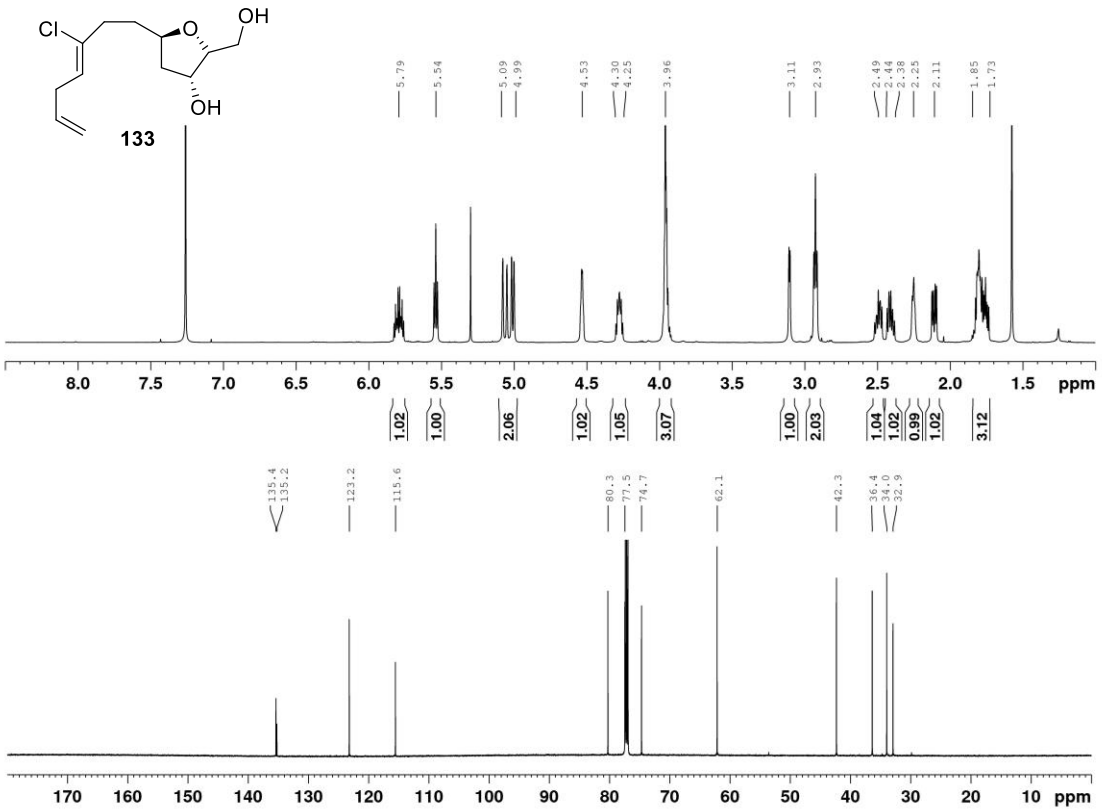

Figure 2-8 ^{1}H and ^{13}C NMR spectra of tetrahydrofuran diol 133

Selective monosilylation of the diol **133** with TBSCl and imidazole afforded the corresponding mono-TBS protected tetrahydrofuran **198** in 95% yield. Steglich[83] esterification between the resulting secondary alcohol **198** and bromoacetic acid in the presence of DIC and catalytic amount of DMAP afforded the required bromo ester **197**, a key precursor for a cross metathesis reaction in 85% yield. Subsequently, bromo ester **197** was subjected to a cross metathesis reaction with **165**, followed by acid catalyzed acetonide hydrolysis to afford the required diol **212** in 15-20% yield over two steps (Scheme 2-43) Unfortunately, the previously developed cross metathesis conditions (3 mol% Hoveyda-Grubbs II, 3 equivalents of acetonide **165**, 0.1 M concentration of CH_2Cl_2 at 40 °C provides **212** in 40% yield over two steps)[57] gave inconsistent conversion and yield in our hands. Furthermore, treating compound **211** with catalytic amount of PPTS in methanol led to the hydrolysis of both the acetonide and the primary TBS protecting group to give compound **213**. Attempts to optimize the reaction conditions to selectively hydrolyze the acetonide functionality were not successful. This method led to a mixture of compounds with the undesired compound **213** being the major product.

Unable to circumvent the formation of unwanted side-product, this synthetic route was abandoned.

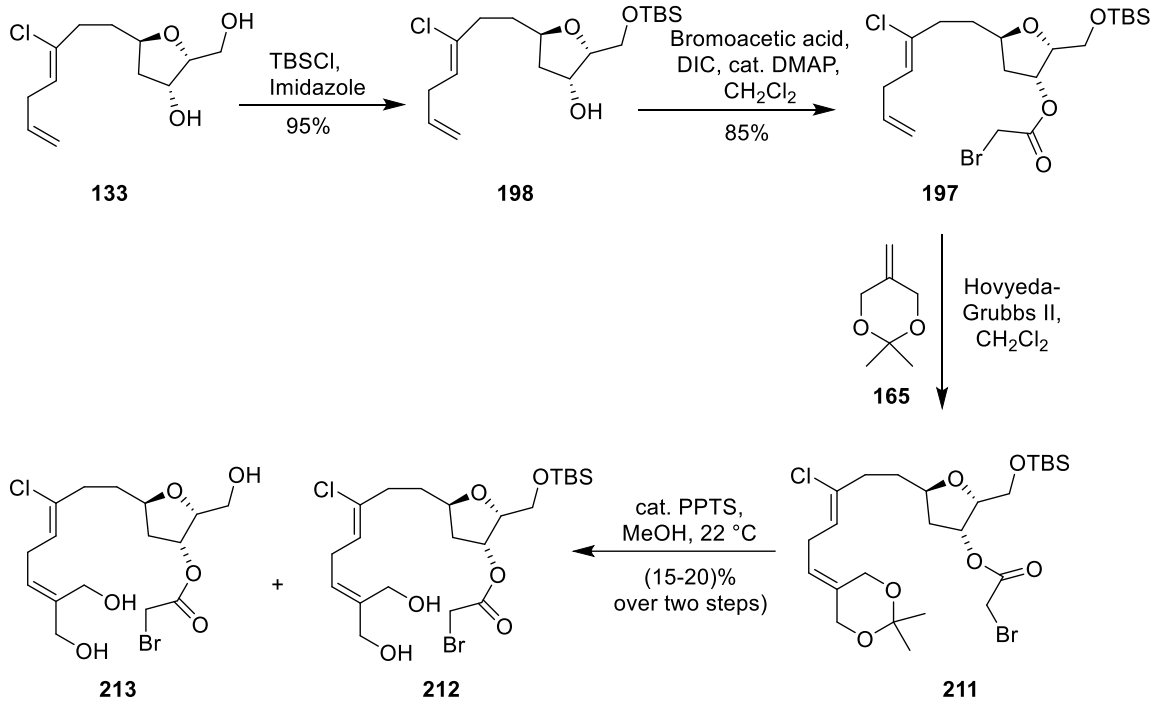

133 **198** **197** **165** **213** **212** **211**

Scheme 2-43 Synthesis of mono TBS protected tetrahydrofuran diol 212

2.4.2. Revised Protecting Group Strategy to Access the Macrocycle 219

Considering the challenges to selectively cleave the acetonide functionality after cross metathesis step, we envisioned that a protecting group switch would address the susceptibility of the primary TBS ether to undergo partial hydrolysis during acetonide deprotection. Based on the stability of silyl ethers towards acidic hydrolysis, we decided to protect the primary hydroxyl group of the tetrahydrofuran diol **133** as its *tert*-butyldiphenylsilyl (TBDPS) ether (Scheme 2-44). Our synthesis began by treating diol **133** with the TBDPS chloride and imidazole to afford the mono-TBDPS protected tetrahydrofuran **214** in 90% yield. Subsequent esterification of compound **214** with bromoacetic acid furnished the bromo ester **215** in 85% yield. This latter material was subjected to cross metathesis and the crude material was passed through a quick neutral alumina plug to remove the residual ruthenium complex. The resultant protected tetrahydrofuran **216** was stirred in methanol in the presence of 1 mol% PPTS. The reaction

was carefully monitored by TLC for completion. At this point, addition of an excess of 2 mol% PPTS afforded the diol **217** in 60% yield over two steps. The primary TBDPS ether was stable towards acidic reaction conditions and no hydrolysis product was observed. With the optimized conditions and relatively modest yield, we next turned our attention to elaborate the THF moiety towards accessing the C3-C2 carbon framework. Based on the conditions developed previously[51] for the regioselective enzymatic acetylation, the *trans* hydroxyl function of compound **217** was acetylated using Amano Lipase PS, and freshly distilled vinyl acetate in 1,4-dioxane afforded the allylic alcohol **218** in 80% yield. Oxidation of alcohol **218** with Dess-Martin periodinane under buffered conditions ($NaHCO_3$) provided the aldehyde **219** in good yield.

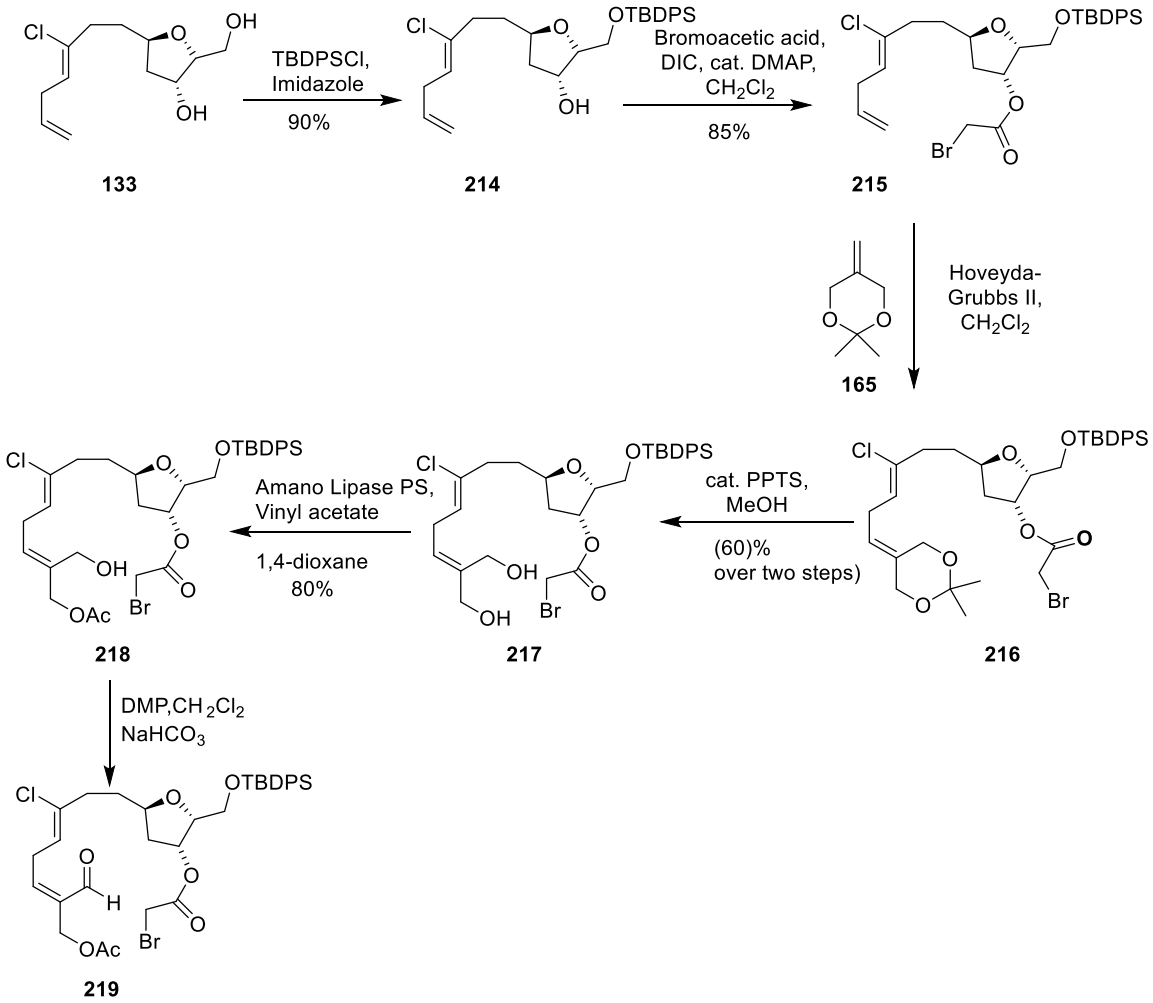

Scheme 2-44 Syntheis of TBDPS protected tetrahydrofuran 218

The ^{1}H NMR spectrum for the acetate **218** is depicted in the Figure 2-9. The C20 methylene protons resonate at δ 4.66 ppm (singlet) and the C3 methylene shows a characteristic resonance at δ 4.23 ppm (singlet). Additionally, the α-protons of the acetate group appear at δ 2.10 ppm (singlet), all of which confirmed that acetylation had occurred regioselctively. Additionally, a NOE correlation between the C20 methylene protons and the vinyl proton at δ 5.63 ppm (triplet) corroborates the regioselective acetylation of *trans*-hydroxyl group in compound **218.**

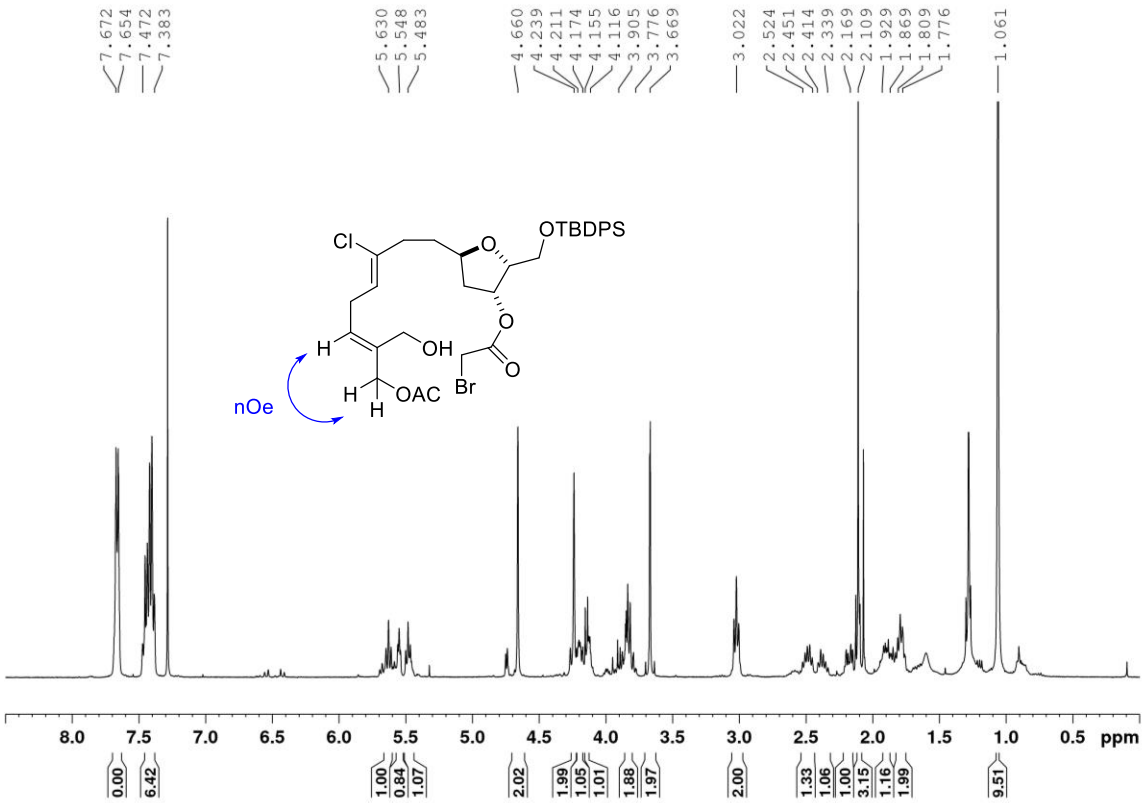

Figure 2-9 ^{1}H NMR spectrum of allylic acetate 218.

With aldehyde **219** in hand, the key intramolecular Reformatsky-type macrocyclization was investigated. The aldehyde **219** was subjected to previously optimized Honda's[13] conditions, however, no product formation was observed (Scheme 2-45). Unfortunately, attempts to effect this transformation by varying reaction concentration, temperature and catalyst loading primarily gave a mixture of decomposition products and failed to provide the desired product **220**. Interestingly, Kwon[57] had previously shown a similar Refortmatsky macrocyclization on intermediate **196** (Scheme 2-37), which differs

from **219** only in that the primary alcohol at C15 is protected as TBS ether rather than TBDPS ether. Notably, in Snider's[21] synthesis of *ent*-haterumalide NA methyl ester they were able to successfully accomplish Yamaguchi[22] macrolactonization of substrate **44** (Scheme 2-5), whereas in Kigoshi's[7] synthesis of haterumalide NA methyl ester they were unable to effect this transformation on a similar substrate **221**, which only differed in the presence of TBDPS protecting group at C15 rather than a trityl protecting group and the secondary hydroxyl group at C3 being protected as an acetate rather than a TBS ether as shown in Scheme 2-46. Although the role of protecting groups in the conformation of the macrocycle precursor is not clear, it is evident from our extensive experimental results and literature precedent that the choice of protecting group is crucial for the success of this unique macrocyclization. Considering our inability to effect macrocyclization with TBDPS protected aldehyde **219**, this route was not pursued further.

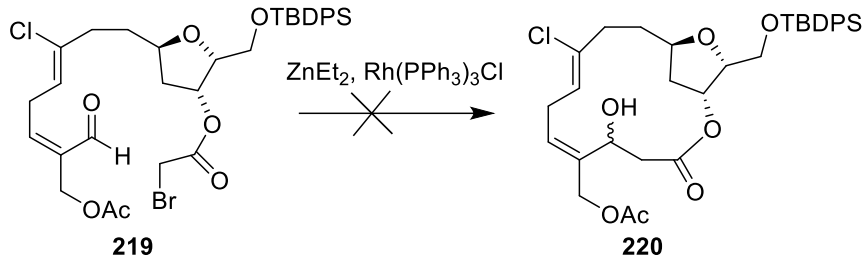

219 **220**

Scheme 2-45 Attempted macrocyclization with the aldehyde 219

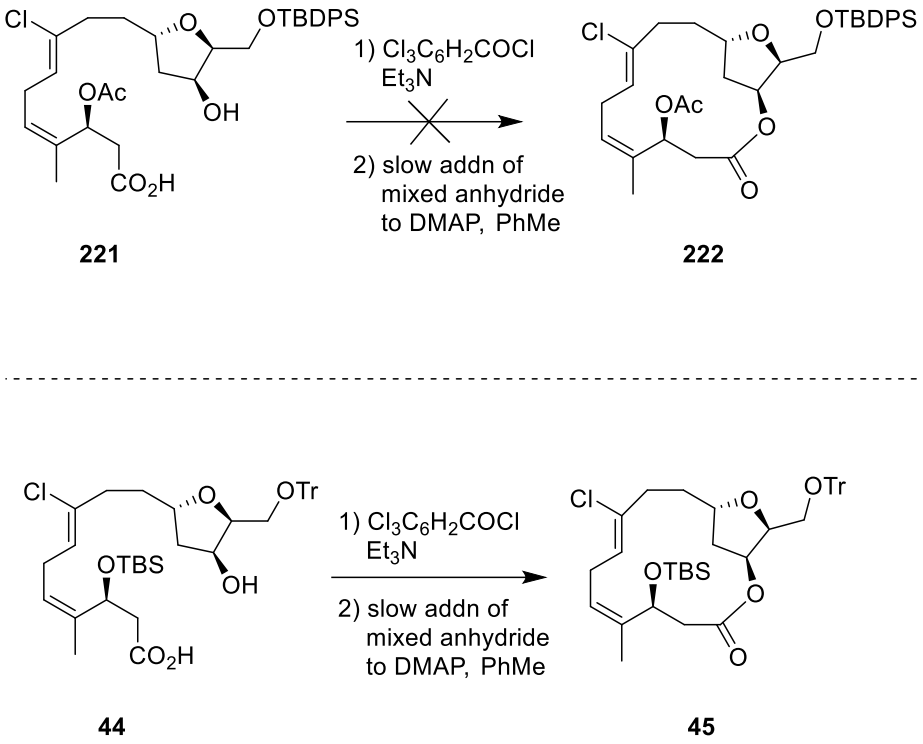

Scheme 2-46 Comparision of Kigoshi's and Snider's macrolactonization.

2.4.3. Optimization of the Cross Metathesis Reaction with TBS Protected tetrahydrofuran 197

Considering the ultimate failures of our protecting group manipulation strategy, we decided to explore and optimize the TBS protecting group route to access the macrocycle **201** in sufficient quantities to complete the synthesis of biselide A (**8**). The success of this route relies on addressing three major concerns; (1) improving the reaction conversion at the cross metathesis stage; (2) identifying robust workup conditions after the cross metathesis reaction that prevent hydrolysis of the bromo ester functionality; and (3) effecting selective hydrolysis of the acetonide group over the primary TBS ether in **211**.

Towards these goals, our synthesis commenced by treating the mono-TBS protected tetrahydrofuran **197** with the previously developed cross metathesis conditions. Unfortunately, the ^{1}H NMR spectrum of an aliquot of the reaction mixture after 12 hours showed the reaction conversion of 2:1 product to starting material. Attempts to promote further reaction by either extending the reaction time or through the addition of further portions of catalyst at different time intervals showed no effect on the reaction conversion.

Next, we looked at the effect of temperature on the reaction and observed that the increase in temperature from 40 °C to 60 °C enhanced the reaction conversion along with a significant formation of bromoester hydrolyzed by-product **223** (Scheme 2-47). These experimental results suggest that the bromoester functionality is sensitive to reaction temperatures > 45 °C and consequently we identified 40-45 °C as the optimum reaction temperature. After several experiments, we further identified the optimized reaction conditions of 8 mol% catalyst loading with 0.5 M reaction concentration in CH_2Cl_2 at 45 °C led to the reaction conversion of 7:1 (product to starting material ratio).

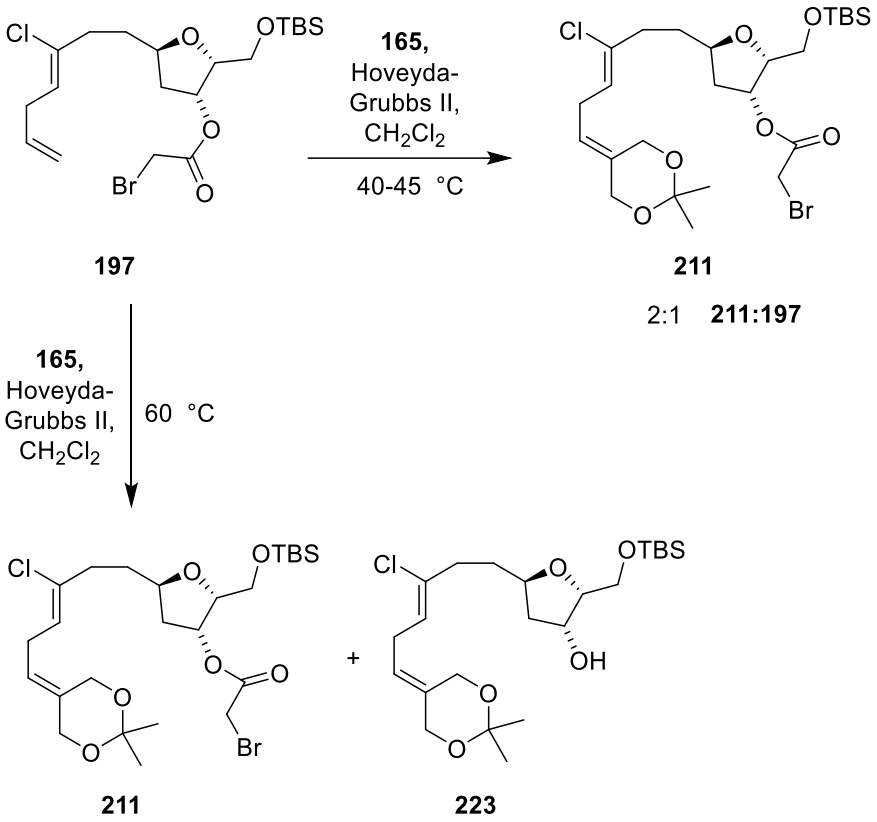

Scheme 2-47 Effect of temperature on cross metathesis reaction

With the increased catalyst loading, it was essential to effectively remove the residual ruthenium catalyst. Based on the previous studies from our group,[56,57] it was concluded that the presence of residual ruthenium complex in the cross metathesis product **211** would adversely effect the regioselective enzymatic acetylation at a later stage of the synthesis. Following the previous workup procedure, the crude material after cross metathesis was passed through a short neutral alumina plug and the desired product **211** was isolated in 20% yield along with a major byproduct formed by the deprotection of

the bromoester **223** in 40% yield. The ^{1}H NMR spectroscopic analysis of the crude material before and after purification via neutral alumina revealed that the tetrahydrofuran **211** was stable as a part of the crude reaction mixture but undergoes ester cleavage after purification with the neutral alumina. Use of silica gel or a pad of celite to filter the crude reaction mixture resulted in the increase in the amount of compound **223** isolated. It was speculated that the residual ruthenium or its byproducts in the presence of alumina or silica gel effects the cleavage of bromoester functionality in **211**. There are a few procedures reported in literature[84] to effectively remove the metathesis catalyst after reaction completion. Most of these methods either use a ligand or adsorbent that binds to ruthenium preferentially over the product, which aids in the removal of the catalyst. Georg *et al.,*[85] reported the use of either triphenylphosphine oxide or DMSO in effectively removing ruthenium catalyst /ruthenium byproducts after a metathesis reaction. Following a similar procedure, the crude material after metathesis was separated into two batches and stirred with 50 equivalents of DMSO and 50 equivalents of triphenylphosphine oxide respectively and passed through a small neutral alumina plug. While both the methods yielded colorless products neither prevented the formation of compound **223**. Paquette *et al.*[86] reported the use of $Pb(OAc)_4$, which oxidizes the ruthenium metal byproducts to unidentified products that can be removed by silica gel chromatography. Unfortunately, when compound **211** was subjected to the same conditions the hydrolysis product **223** was formed exclusively. Finally, we treated the crude **211** with a polar isocyanide $CNCH_2CO_2K$ which has been proven to effectively quench the ruthenium catalyst[87] after metatheses on various sensitive substrates, however these conditions also promoted decomposition of compound **211**.

Following the unsuccessful efforts to improve the metathesis workup, we envisaged that a change in the order of the reaction sequence would address the stability of bromoacetate functionality. We decided to subject compound **198** to cross metathesis prior to esterification and were optimistic that this route would allow us to perform a column purification after the metathesis reaction and isolate the product free from residual ruthenium byproducts (Scheme 2-48).

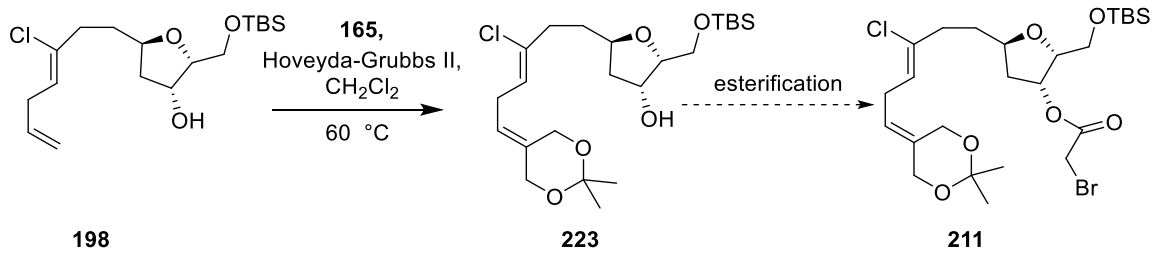

198 223 211

Scheme 2-48 Alternate route to access 211

Towards this goal, compound **198** (0.5 M in CH_2Cl_2) was treated with 8 mol% Hoveyda-Grubb's II catalyst, and 3 equivalents of the acetonide **165** at 60 °C for 12 hours. Upon completion of the reaction, the crude material was subjected to column chromatography on silica gel, affording the compound **223** as a colorless oil in 70% yield. Next, we investigated the conditions to facilitate the esterification reaction of compound **223**. The secondary hydroxyl functionality of compound **223** was subjected to Steglich esterification using bromoacetic acid, DIC and DMAP. Unfortunately, ^{1}H NMR analysis of the crude reaction mixture indicated deprotection of the acetonide group leading to the formation of a mixture of mono, di and tri-bromoacetylated products (**211**, **224**, **225** respectively). Attempts to optimize this reaction by varying the equivalents of DIC, lowering the reaction temperature and use of HATU as coupling agent resulted in a complex mixture of decomposition products and acetylated products. To facilitate ester formation prior to acetonide deprotection, **223** was treated with bromoacetyl bromide (**227**) in excess of pyridine at -20 °C. After only 10 minutes, the reaction had reached completion. Unfortunately, the major product observed in this reaction was the tri-bromoester **225** (Scheme 2-49).

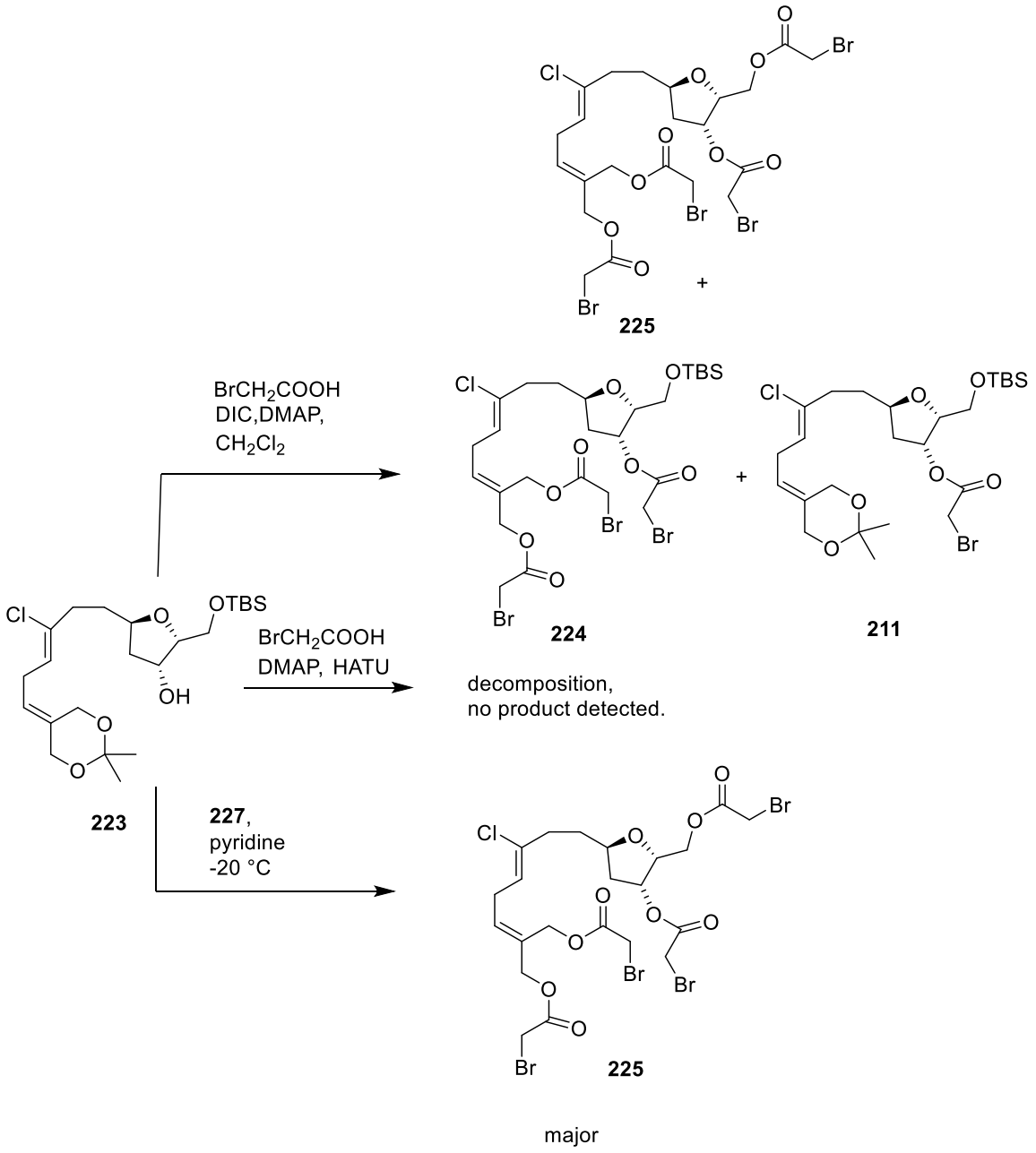

Scheme 2-49 Attempted esterification of compound 223.

Moving away from the acidic esterification conditions, we looked to effect this transformation under basic conditions to avoid acetonide deprotection. Bromoacetyl bromide (**227**) was treated with penatfluorophenol (**226**) in the presence of a base to afford its corresponding pentaflurophenyl ester **228**.[88] Subsequently, the alcohol **223** was subjected to esterification with **228** in the presence of DIPEA (Scheme 2-50). Unfortunately, TLC analysis revealed little to no change after a period of 4 hours. An

additional 12 hours at 40 °C led to an assortment of products as determined by TLC analysis. ^{1}H NMR spectroscopic analysis of the crude reaction mixture revealed no product formation. Considering these results, it is clear that the acetonide **223** is too sensitive to survive esterification under standard conditions. Consequently, this route was not pursued further.

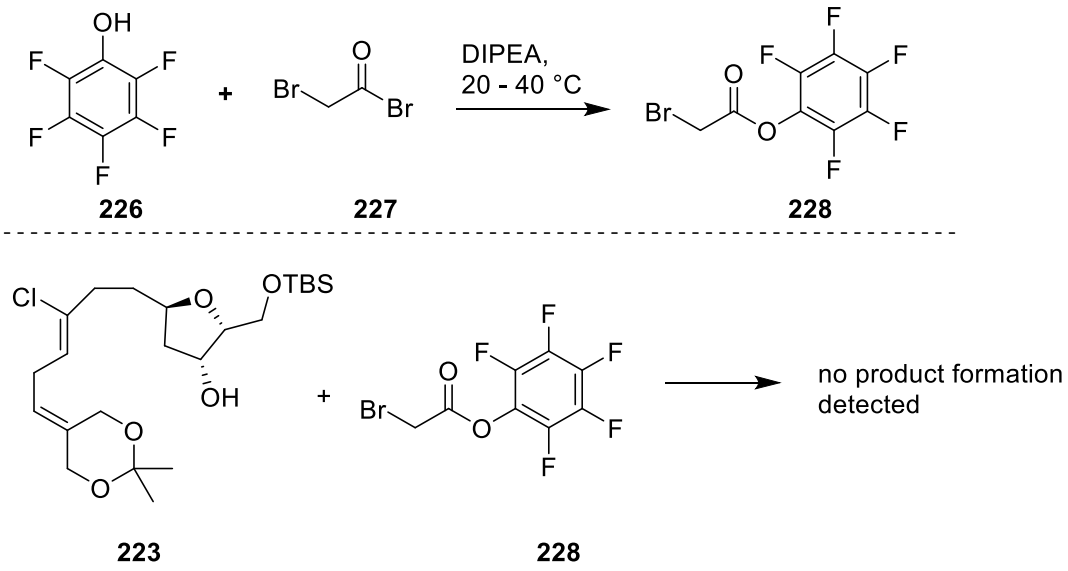

Scheme 2-50 Failed attempt to synthesize compound 211 with pentaflurophenyl ester 228.

Having abandoned the esterification route, we decided to revisit and optimize the cross metathesis workup. After extensive experimentation following reported methods, it was clear that we were unable to effectively remove ruthenium catalyst and prevent the cleavage of bromoester functionality in compound **211** after purification on neutral alumina. As a last resort, we tried an unprecedented technique of removing the metathesis catalyst by passing the crude reaction mixture through a Sephadex column. Despite small differences in the molecular weight and the sizes of the metathesis product **211** and Hoveyda-Grubbs II catalyst, we had hopes that size exclusion chromatography might separate the residual catalyst from the product. Also, moving away from alumina and silica gel as a stationary phase, we were curious to assess the stability of bromoester **211** on Sephadex, which is a resin made of cross-linked dextran gel. Thus, the crude metathesis product **211** was passed through a column packed with Sephadex LH-20 and eluted with methanol. We observed that the first few fractions displayed an intense dark brown color, indicative of the catalyst, and TLC analysis indicated no presence of the product. TLC

analysis of the later fractions which were slightly coloured confirmed the presence of only the desired product **212**. We observed that the bromoester functionality was stable to these conditions and thus circumvented the formation of the unwanted side product **223**. With these optimized conditions we were able to overcome the challenges of the cross-metathesis reaction and generate sufficient quantities of compound **211** to investigate selective TBS deprotection.

The acetonide **211** was treated with catalytic amount of PPTS in methanol at room temperature to afford a mixture of the desired diol **212** in 20% yield and the major TBS deprotected compound **213** in 40% yield over two steps. When the reaction was conducted at 0 °C, TLC indicated disappearance of starting material **211** after 30 minutes and presence of diol **212** as the major product. After basic workup, TLC analysis of crude reaction mixture indicated that a significant fraction of diol **212** underwent TBS ether deprotection to give compound **213**. To avoid the workup procedure, we introduced the use of polymer supported PPTS that was easily removed by filtration on a bed of celite at 0 °C after reaction completion. With these conditions we were able to reduce the formation of TBS deprotected product **213** to a great extent and finally achieve a significant improvement in the optimization of cross metathesis conditions and selective acetonide deprotection steps, that gave access to diol **212** in 75% yield over two steps (Scheme 2-51)

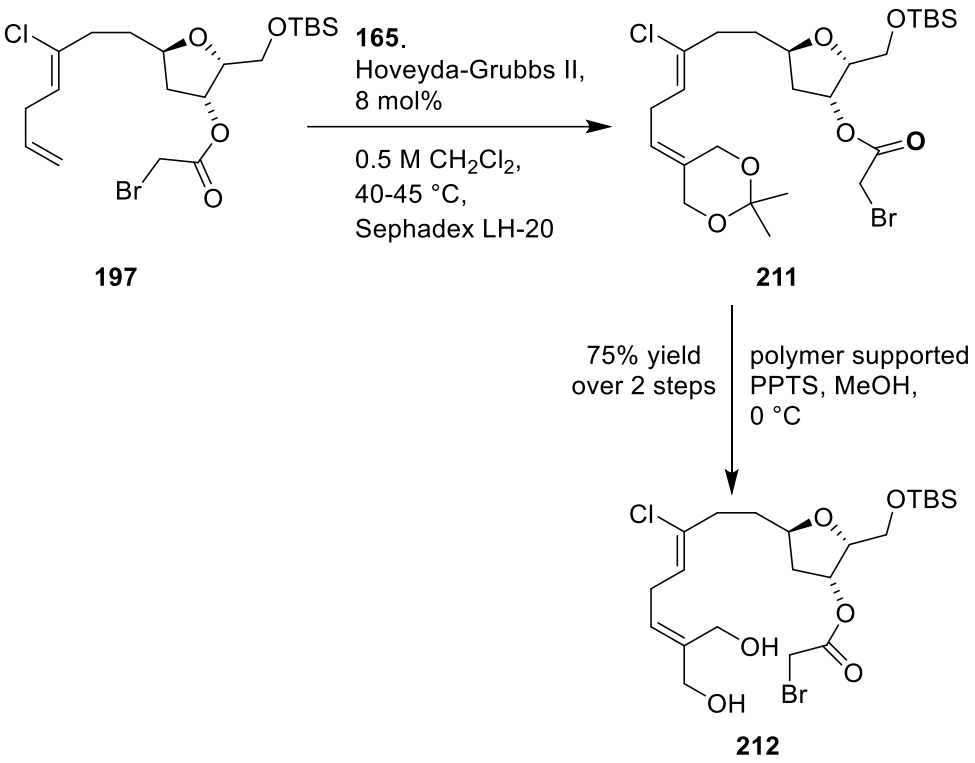

Scheme 2-51 Prepartion of tetrahydrofuran diol 212 via optimized cross metathesis reaction

2.4.4. Further Elaboration of Tetrahydrofuran diol 212 via Intramolecular Reformatsky-type Macrocyclization.

With the diol **212** in hand, we next tried to cyclize the 14-membered macrocycle using the intramolecular Reformatsky-type reaction. The trans-hydroxyl functionality of the diol **212**, was subjected to regioslelctive enzymatic acetylation using Amano Lipase PS, distilled vinyl acetate in dry 1,4-dioxane to afford the allylic acetate **226** at C20 as a single isomer in 80% yield. Notably, in Hayakawa's[51] synthesis of biselide A (**8**), the C20 oxygen functionality **113** was installed by regioselective enzymatic hydrolysis of diacetate **112** in 54% yield (Scheme 2.24). The allylic alcohol was oxidized with DMP to afford α,β-unsaturated aldehyde **196** in quantitative yield. No purification was necessary as the workup procedure yielded product of sufficient purity to carry on to the next step. However, we found that the *cis*-isomer **196** isomerizes to the undesired *trans*-isomer **227** on standing and also when subjected to column chromatography on silica gel. Thus, care had to be taken to immediately subject the unstable aldehyde **196** to the subsequent macrocyclization reaction (Scheme 2-52).

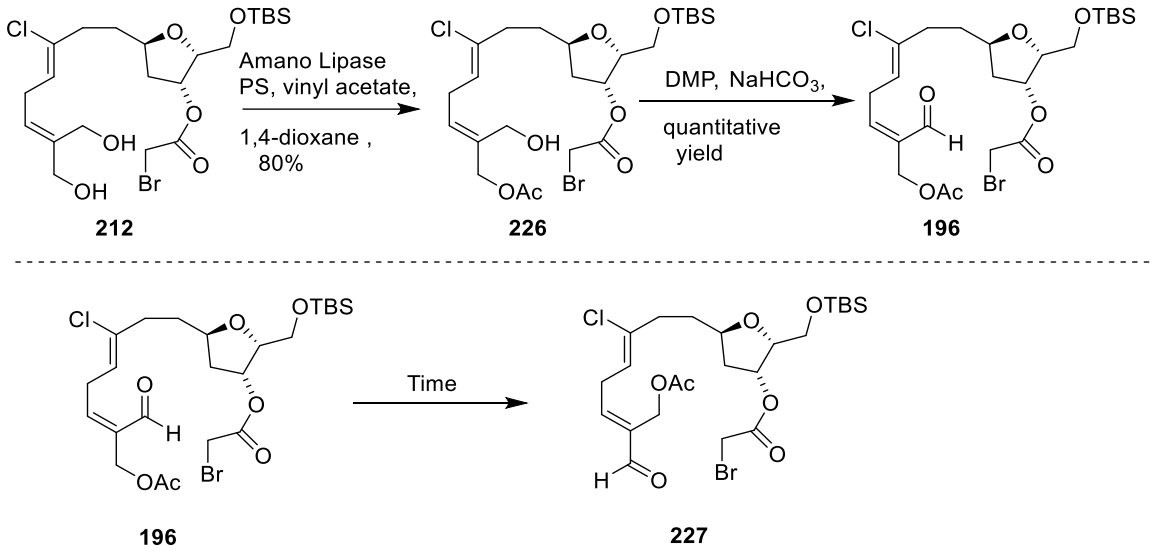

Scheme 2-52 Synthesis of aldehyde 196 and isomerization to *trans*-isomer 227

Having the aldehyde **196** in hand, the stage was set for intramolecular macrocyclization. The aldehyde **196**, was subjected to the previously optimized Honda's conditions.[13] Accordingly, aldehyde **196** was added via a syringe pump over 40 minutes to a mixture of Wilkinson's catalyst and $ZnEt_2$ in methyl *tert*-butyl ether (MTBE) at room temperature (RT), affording the macrocycle as a 2:1 (**200:201**) mixture of diastereomers at the newly generated C3 stereogenic centre in 40% yield for the undesired isomer **200** and 10% yield for the desired isomer **201** (Scheme 2-53). The two isomers were separated by column chromatography. ^{1}H NMR spectroscopic analysis of **200** and **201** revealed the presence of a *trans*-β-hydroxyl macrocycle **228**, which could not be separated by column chromatography. Presumably, this was formed from the *trans*-isomer **227.** We decided to carry forward with this mixture by-product and anticipated that we would be able to achieve separation at a later stage of the synthesis. Several attempts to change the diastereoselectivity of this transformation by varying temperature, mode of addition of aldehyde, and solvent were not successful.

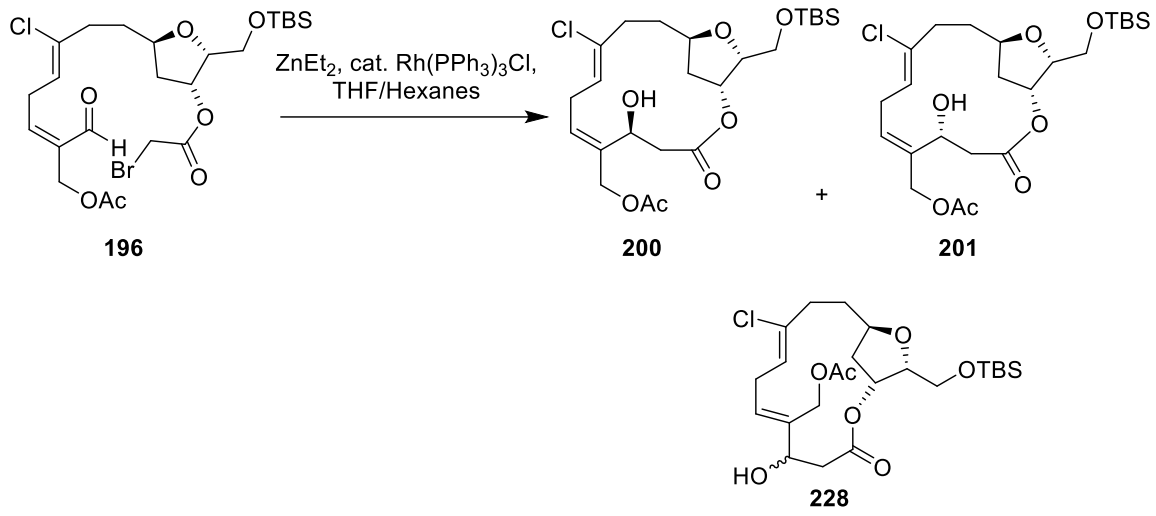

Scheme 2-53 Preparation of macrocycle via Reformtasky-type macrocyclization

2.4.5. Completion of Synthesis.

Considering the challenges to improve the ratio of diastereomers formed during the intramolecular macrocyclization, we next investigated the methods to convert the undesired isomer **200** to desired isomer **201**. Our previous attempts to invert the C3 stereogenic centre of compound **200** by Mitsunobu inversion were not successful (Scheme 2-38).[57] In Hoye's[30] synthesis of *ent*-haterumalide NA methyl ester, they achieved the desired C3-alcohol stereochemistry by subjecting the ketone **51** to Luche[39] reduction (Scheme 2-6). We decided to adopt the same strategy and the β-acetoxy alcohol **200** was subjected to DMP oxidation to give the corresponding C3 *Z*-ketomacrolactone **229** in 80% yield (Scheme 2-54). We found that the C3 *E* isomer **228** also underwent oxidation to give the C3 *trans*-ketomacrolactone **230**, which was separated by column purification. Thus, we were able to isolate compound **229** in its pure form. The C3 Z-ketomacrolactone **229** was subjected to Luche reduction using $NaBH_4$ and $CeCl_3.7H_2O$ to afford the desired C3-OH **201** exclusively as a single diastereomer in 90% yield. Interestingly, in Hayakawa's synthesis of biselide A, they were unable to invert the stereochemistry at C3 centre in compound **231** by this two step sequence (Scheme 2-55). It is notable that compound **231** differs from our substrate **229** only in that the primary alcohol at C15 is being protected as trityl ether rather than TBS ether and the C20 oxygen functionality is protected as TBDPS ether instead of an acetate group.

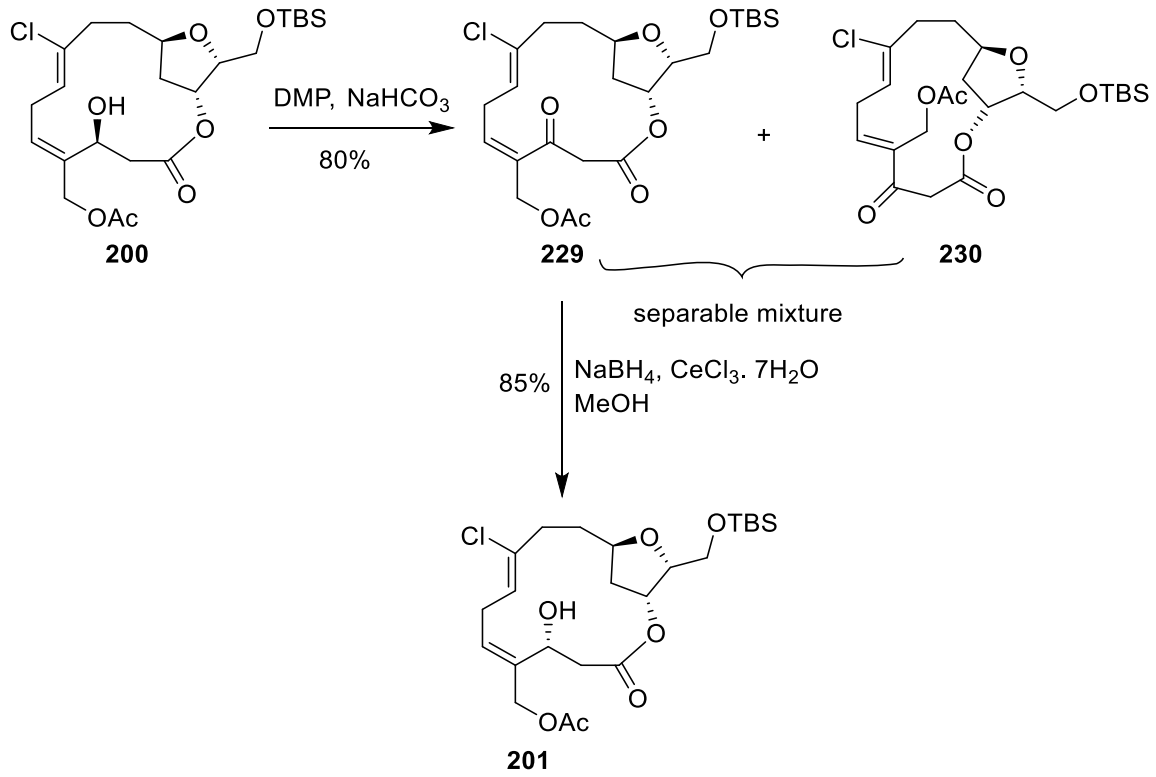

Scheme 2-54 Inversion of the C3 stereogenic centre in macrocycle 200

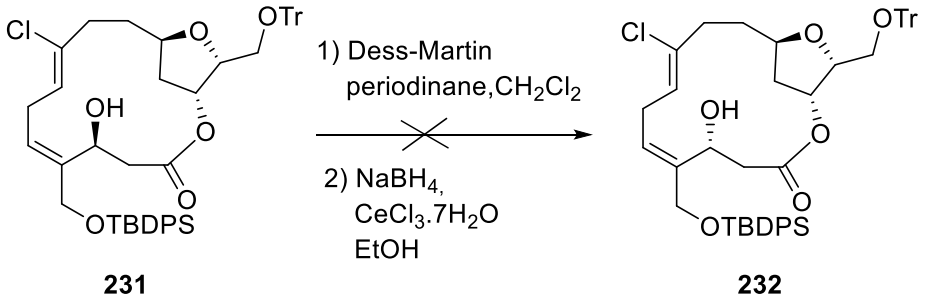

Scheme 2-55 Hayakawa's failed attempt to invert C3 stereogenic centre in 231

Next, the C3-alcohol **201** was acetylated under standard conditions using acetic anhydride and pyridine in CH_2Cl_2 to furnish the β-acetoxy macrocycle **204** in 90% yield. Subsequently, the primary TBS ether in **204** was carefully cleaved in the presence of 70% HF-pyridine, affording the primary alcohol **119** in 88% yield. The ^{1}H NMR spectral data were in agreement with that reported by Hayakawa[51] for **119**, which confirms the correct relative stereochemistry at C3 of our compound **119** in our synthesis. Subsequently, compound **119** was subjected to Dess-Martin oxidation to afford the aldehyde **233** in good

yield (Scheme 2-56). Next, the synthesis of the side chain began with carboalumination of 3-butyn-1-ol (**234**), followed by a Jones oxidation[89] as reported in the literature giving access to compound **77** (Scheme.2-57). Subsequently, esterification of acid **77** with 2,4-dimethoxybenzyl alcohol by a slightly modified literature[7] procedure using DMAP and DIC afforded compound **120** in 80% yield. (Compare to Kigoshi reported 54% yield for compound **120** using DMAP and PyBOP).

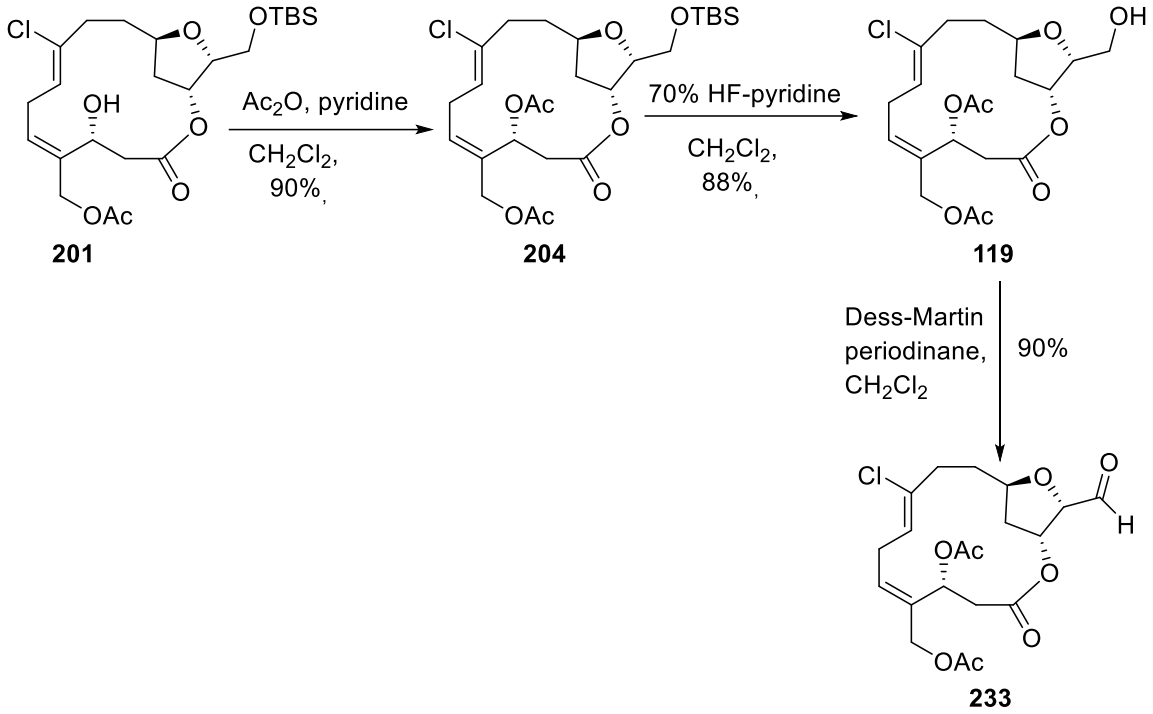

Scheme 2-56 Synthesis of aldehyde 233

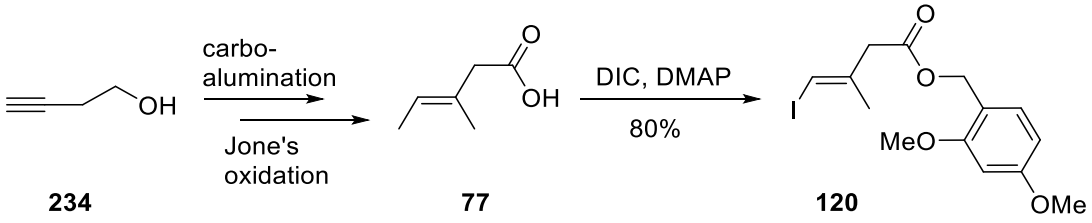

Scheme 2-57 Synthesis of the side chain 120

With the two key fragments **233** and **120** in hand, the stage was set for Ni/$CrCl_2$ mediated C-C bond formation to further elaborate the macrocycle *en route* to the total synthesis of biselide A (**8**). NHK coupling[19-20] between the aldehyde **233** and vinyl iodide **120** afforded the compound **234** as a diastereomeric mixture at the C15-OH (3:1 d.r.). This mixture was further treated with TFA in anisole at 0 °C for 1 hour to cleave the DMPM ether and purification by HPLC afforded biselide A (**8**) in 40% yield over two steps (Scheme 2-58). To our delight, the spectral properties of the synthetic biselide A (**8**) were identical in all respects to those reported for the natural material[2] (Table 2.3).

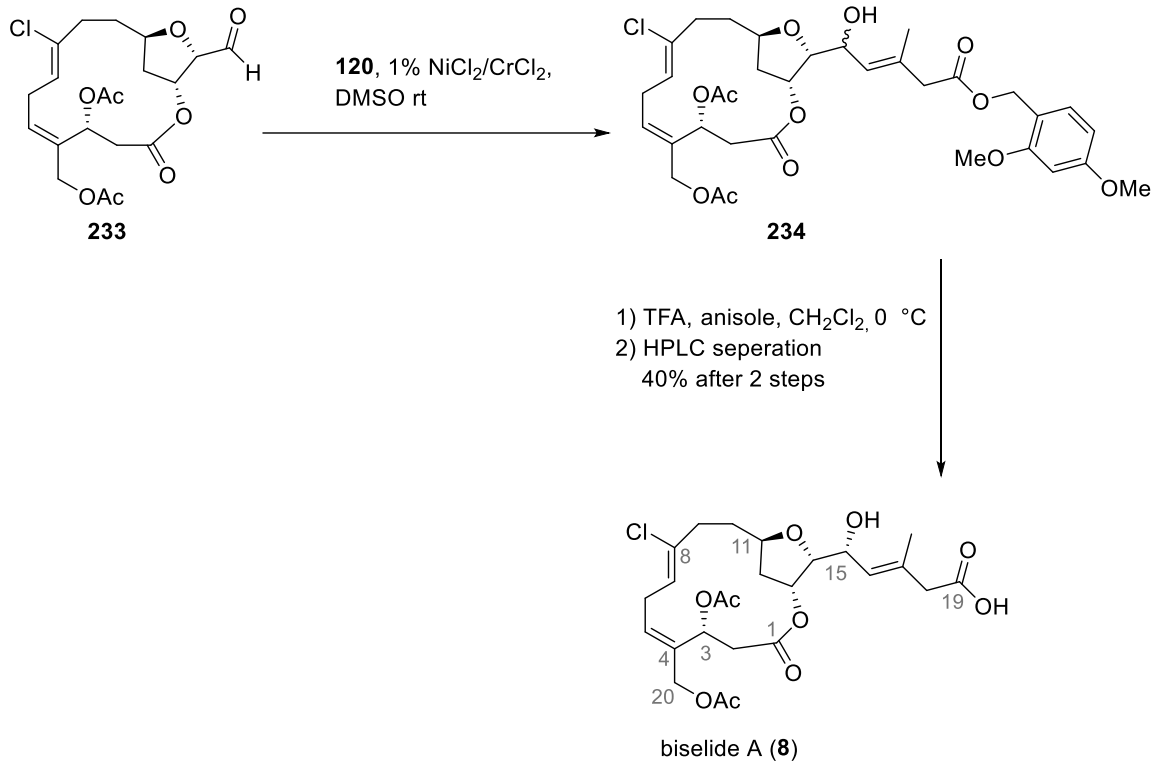

Scheme 2-58 Completion of biselide A (8) synthesis.

Table 2-2 Comparison of ^{1}H and ^{13}C NMR data between synthetic and natural biselide A (8) in CD_3OD.

Position	^{13}C (natural product)	^{13}C (synthetic)	Difference $\Delta\ \delta_{nat-\ syn}$	^{1}H (natural product)	^{1}H (synthetic)	Difference $\Delta\ \delta_{nat-\ syn}$
1	169.4	169.4	0			
2a	38.7	38.7	0	2.83 dd (12.0, 11.1)	2.85 dd (12.0, 11.1)	-0.02
2b				2.88 dd (12.0, 5.2)	2.89 dd (12.0, 5.1)	-0.01
3	67.8	67.7	0.06	5.84 dd (11.1, 5.2)	5.85 dd (11.2, 4.9)	-0.01
4	135.0	135.0	0			
5	133.9	133.9	0	6.08 dd (11.1, 7.1)	6.10 dd (10.9, 7.1)	-0.02
6a	27.7	27.7	0	2.61 m	2.62 m	-0.01
6b				3.55 m	3.56 m	-0.01
7	125.8	125.8	0	5.32 m	5.34 m	-0.01
8	133.6	133.6	0			
9a	35.5	35.5	0	2.31 m	2.33 m	-0.02
9b				2.45 m	2.47 m	-0.02
10a	29.0	29.0	0	1.39 m	1.41 m	-0.02
10b				2.28 m	2.30 m	-0.02
11	78.1	78.1	0	3.94 m	3.96 m	-0.02
12a	38.8	38.8	0	1.53 m	1.54 m	-0.01
12b				2.09 m	2.10 m	-0.01
13	76.7	76.7	0	5.30 m	5.32 m	-0.02
14	84.5	84.5	0	3.91 dd (8.6, 3.7)	3.92 dd (8.6, 3.7)	-0.01
15	66.5	66.5	0	4.53 t (8.6)	4.54 t (8.6)	-0.01
16	130.7	130.7	0	5.38 d (8.6)	5.39 dq (8.4, 1.3)	-0.01
17	135.9	135.9	0			
18	45.7	45.7	0	3.04 br s 2H	3.06 br s 2H	-0.02
19	175.4	175.4	0			
20a	65.5	65.5	0	4.70 d (12,9)	4.71 d (13.0)	-0.01
20b				4.96 d (12.9)	4.97 d (13.0)	-0.01

Position	^{13}C (natural product)	^{13}C (synthetic)	Difference $\Delta \delta_{nat-syn}$	^{1}H (natural product)	^{1}H (synthetic)	Difference $\Delta \delta_{nat-syn}$
21	17.3	17.3	0	1.82 br s 3H	1.84 d 3H (1.3)	-0.02
22	171.1	171.1	0			
23	21.0	21.0	0	2.02 s 3H	2.03 s 3H	-0.01
24	172.5	172.5	0			
25	20.9	21.0	-0.06	2.07 s 3H	2.08 s. 3H	-0.01

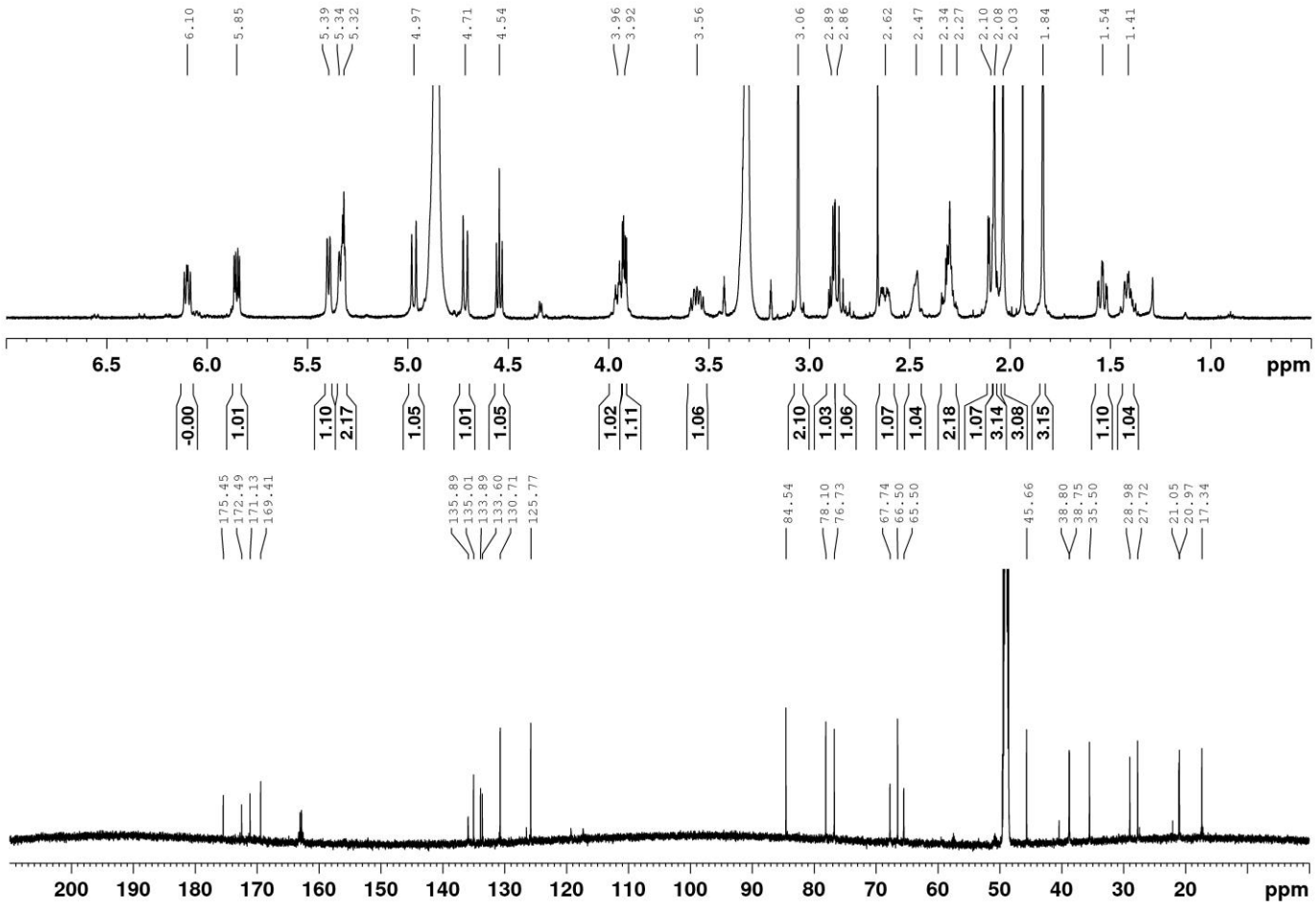

Figure 2-10 ^{1}H and ^{13}C NMR Spectra of synthetic biselide A (8) in CD_3OD

2.5. Conclusion

In conclusion, we have accomplished a concise total synthesis of biselide A (8) with the longest linear sequence (LLS) being 20 steps starting from commercially available L-serine. To access this potentially useful marine macrolide, we have developed a chlorohydrin-based strategy that affords rapid and stereo-controlled access to the tetrahydrofuran core. The key steps of our synthesis include a cross-metathesis reaction to access the C4-C5 alkene function and a regioselective enzymatic acetylation to install the C20 oxygen functionality. All of this was accomplished with minimal protecting group manipulations. The efficiency of our synthetic strategy should also enable us to access additional members of the biselide family of natural products and paves the way to study structure-activity relationship through the synthesis of unnatural analogues. Furthermore, the biological studies of biselide A (**8**) are currently underway.

2.6. Experimental

2.6.1. General Procedures

All reactions described were performed under an atmosphere of dry nitrogen using oven dried glassware unless otherwise specified. Flash chromatography was carried out with 230-400 mesh silica gel (Silicycle, SiliaFlash® P60). Concentration and removal of trace solvents was done via a Büchi rotary evaporator using a dry ice/acetone condenser and vacuum applied from a Büchi V-500 pump

All reagents and starting materials were purchased from Sigma Aldrich, Alfa Aesar, TCI America, AK Scientific or Strem and were used without further purification. All solvents were purchased from Sigma Aldrich, EMD, Anachemia, Caledon, Fisher or ACP and used without further purification unless otherwise specified. Diisopropylamine and CH_2Cl_2 were freshly distilled over calcium hydride. THF was freshly distilled over sodium metal/benzophenone. Cold temperatures were maintained by use of the following conditions: 5 °C, fridge (True Manufacturing, TS-49G); 0 °C, ice-water bath; −40 °C, acetonitrile-dry ice bath; −78 °C, acetone-dry ice bath; temperatures between −78 °C and 0 °C required for longer reaction times were maintained with a Neslab Cryocool Immersion Cooler (CC-100 II) in a ethanol/2-propanol bath.

Nuclear magnetic resonance (NMR) spectra were recorded using chloroform-*d* ($CDCl_3$), or methanol-d_4 (CD_3OD). Signal positions (δ) are given in parts per million from tetramethylsilane (δ 0) and were measured relative to the signal of the solvent (^{1}H NMR: $CDCl_3$: δ 7.26, CD_3OD: δ 3.35; ^{13}C NMR: $CDCl_3$: δ 77.16, CD_3OD: δ 49.3. Coupling constants (*J* values) are given in Hertz (Hz) and are reported to the nearest 0.1 Hz. ^{1}H NMR spectral data are tabulated in the order: multiplicity (s, singlet; d, doublet; t, triplet; q, quartet; quint, quintet; m, multiplet; b, broad), coupling constants, number of protons. NMR spectra were recorded on a Bruker Avance 600 equipped with a QNP or TCI cryoprobe (600 MHz), Bruker 500 (500 MHz), or Bruker 400 (400 MHz). Assignments of ^{1}H and ^{13}C NMR spectra are based on analysis of 1H-1H COSY, HSQC, HMBC, TOCSY and 1D NOESY spectra, where applicable.

Optical rotation was measured on a Perkin Elmer 341 Polarimeter at 589 nm.

Infrared (IR) spectra were recorded on a Perkin Elmer Spectrum Two™ Fourier transform spectrometer with neat samples. Only selected, characteristic absorption data are provided for each compound.

High resolution mass spectrometry was performed on an Agilent 6210 TOF LC/MS using ESI-MS or was carried out by the Notre Dame University Mass Spectrometry Department using EI technique.

High performance liquid chromatography (HPLC) was performed on an Agilent 1200 Series equipped with a variable wavelength UV-Vis detector (λ = 220 nm) and Daicel Chemical Industries, Ltd. Chiralpak® AD chiral column (4.6 × 250 mm).

2.6.2. Preparation of (*Z*)-5-Chlorononа-5,8-dien-2-one (124)

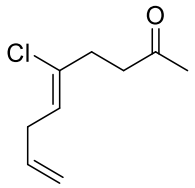

To a stirred solution of THF (200 mL) at -10 ^{o}C, sodium hydride (60% in oil, 3.0 g, 127.80 mmol) was added and stirred for 10 min. Ethyl acetoacetate (16.20 mL, 127.80 mmol) was added dropwise over 30 min. After this time freshly prepared bromide **130**[90] (25.0 g, 127.80 mmol, d.r 4:1) was added in one portion. The resulting mixture was allowed to warm to rt and stirred for 12 h. The reaction mixture was quenched with aqueous 1N. HCl (15 mL), diluted with Et_2O (150 mL), and the phases were separated. The aqueous phase was extracted with Et_2O (2 x 50 mL) and the combined organic phases were washed with brine (100 mL), dried (Na_2SO_4), filtered, and concentrated under reduced pressure to give a pale-yellow oil. This oil was suspended in MeOH (150 mL), aqueous 2N NaOH (50 mL) was added and the resulting mixture was stirred at rt for 12 h. The mixture was then acidified to pH-4.0 with concentrated HCl, diluted with Et_2O (150 mL) and the phases were separated. The aqueous phase was extracted with Et_2O (2 x 75 mL). The combined organic extracts were washed with water (50 mL), brine (75 mL), dried (Na_2SO_4), concentrated and purified by flash column chromatography (EtOAc/hexanes: 10% → 25%) over silica gel impregnated with silver nitrate to give the methyl ketone **124** (15.5 g, 70%) as a colorless oil. ~

^{1}H NMR (400 MHz, $CDCl_3$) δ 5.77 (ddt, *J* = 16.4, 10.1, 6.3 Hz, 1H), 5.55 (tt, *J* = 7.1, 1.0 Hz, 1H), 5.08 – 4.99 (m, 2H), 2.90 (ddt, *J* = 6.5, 4.8, 1.3 Hz, 2H), 2.72 – 2.67 (m, 2H), 2.63 – 2.58 (m, 2H), 2.16 (s, 3H).

^{13}C NMR (100 MHz, $CDCl_3$) δ 207.3, 135.2, 134.2, 123.9, 115.6, 41.6, 33.7, 32.9, 30.2.

IR (neat): 3080, 2978, 2920, 2227, 1718, 1432, 1362, 1162 cm^{-1}.

HRMS (ESI^{+}) calculated for $C_9H_{13}ClNaO$: 195.0547 $(M + Na)^{+}$; Found: 195.0559.

2.6.3. Preparation of (2*S*,3*R*,8*Z*)-1-((*tert*-Butyldimethylsilyl)oxy)-2,8-dichloro-3-hydroxydodeca-8,11-dien-5-one (131)

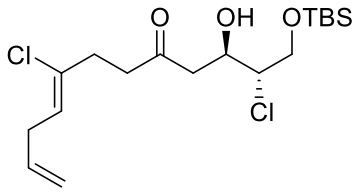

To a cold (-78 °C) stirred solution of *N,N*-diisopropylamine (2.0 mL, 14.90 mmol) in dry THF (200 mL) was added *n*-butyllithium (2.50 M in hexane, 6.20 mL, 15.20 mmol). The reaction mixture was warmed to 0 °C and stirred for 30 min. After this time, the reaction mixture was cooled to -78 °C and the methyl ketone **124** (2.0 g, 11.50 mmol) in THF (10.0 mL) was added dropwise over 15 min. The resulting mixture was stirred at -78 °C for 30 minutes and α- chloroaldehyde **127** (3.10 g, 13.90 mmol) was added. The solution was stirred at -78 °C for 1 h and the reaction was then quenched with a solution of saturated aqueous ammonium chloride (20 mL) and the phases were separated. The aqueous phase was extracted with ethyl acetate (3 x 15 mL) and the combined organic phases were washed with water (20 mL), brine (25 mL), dried (Na_2SO_4) filtered, and the solvent was removed *in vacuo*. Purification of the crude product by flash chromatography (EtOAc/hexanes: 10% → 30%) afforded the *anti*- ketochlorohydrin **131** (3.8 g, 85%, d.r 8:1, *anti/syn*) as a colourless oil.

^{1}H NMR (600 MHz, $CDCl_3$) δ 5.81 – 5.74 (m, 1H), 5.56 (td, *J* = 7.0, 1.0 Hz, 1H), 5.06 – 5.0 (m, 2H), 4.34 (ddd, *J* = 9.2, 6.5, 2.9 Hz, 1H), 3.97-3.86 (m, 3H), 2.92 – 2.62 (m, 8H), 0.90 (s, 9H), 0.09 (s, 6H).

^{13}C NMR (150 MHz, $CDCl_3$) δ 209.2, 135.1, 134.0, 124.2, 115.7, 69.7, 65.2, 63.2, 46.0, 41.7, 33.4, 32.9, 25.9 (4C), -5.3 (2C).

IR (neat): 3583, 3001, 2957, 2904, 2863, 2275, 1723, 1613, 1464, 1092 cm^{-1}.

HRMS (ESI^+) calculated for $C_{18}H_{32}Cl_2NaO_3Si$: 417.1390 $(M + Na)^+$; Found: 417.1384.

2.6.4. Preparation of (2*R*,3*R*,5*R*)-5-((*Z*)-3-Chlorohepta-3,6-dien-1-yl)-2-(hydroxymethyl)tetrahydrofuran-3-ol (133)

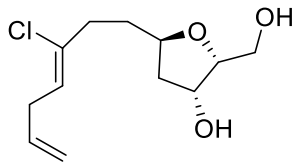

The chlorodiol **132** (2.0 g, 5.0 mmol) in methanol (50 mL) was added to a microwave vial. The vial was sealed in a CEM Discover LabMate microwave reactor and the reaction mixture was heated to 120 °C (as monitored by a vertically focussed IR temperature sensor) and maintained at this temperature for 1 h. The reaction mixture was cooled to rt and concentrated *in vacuo*. Purification by flash column chromatography (MeOH/$CHCl_3$: 0% → 10%) over silica gel afforded the diol **133** (1.0 g, 80%) as a colorless oil.

^{1}H NMR (600 MHz, $CDCl_3$) δ 5.79 (ddt, *J* = 16.6, 10.1, 6.3 Hz, 1H), 5.54 (t, *J* = 7.0 Hz, 1H), 5.08 – 4.98 (m, 2H), 4.53 (q, *J* = 3.9 Hz, 1H), 4.30 – 4.24 (m, 1H), 3.96 (m, 3H), 3.10 (d, *J* = 4.7 Hz, 1H), 2.93 (t, *J* = 6.7 Hz, 2H), 2.49 (ddd, *J* = 14.9, 8.9, 6.3 Hz, 1H), 2.43 – 2.37 (m, 1H), 2.25 (dd, *J* = 7.1, 4.5 Hz, 1H), 2.11 (ddd, *J* = 13.1, 5.7, 1.5 Hz, 1H), 1.88 – 1.66 (m, 3H).

^{13}C NMR (150 MHz, $CDCl_3$) δ: 135.4, 135.2, 123.2, 115.6, 80.3, 77.5, 74.7, 62.1, 42.3, 36.4, 34.0, 32.9.

IR (neat): 3453, 2952, 2857, 1658, 1639, 1430, 1255, 1087 cm^{-1}.

HRMS (ESI^+) calculated for $C_{12}H_{20}ClO_3$: 247.1095 $(M + H)^+$; Found: 247.1086.

$[\alpha]_D^{20}$ – 2.5 (*c* = 1.0, $CHCl_3$).

2.6.5. Preparation of (2*R*,3*R*,5*R*)-2-(((*tert*-Butyldiphenylsilyl)oxy)methyl)-5-((*Z*)-3-chlorohepta-3,6-dien-1-yl)tetrahydrofuran-3-ol (198)

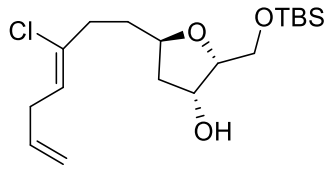

To a stirred solution of the diol **133** (2.50 g, 10.0 mmol) in dry dichloromethane (30 mL) was added *tert*-butyldimethylsilyl chloride (1.70 g, 11.10 mmol) and imidazole (2.80 g, 20.0 mmol). The reaction mixture was stirred for 12 h at rt. The reaction was then quenched with water (10 mL). The reaction mixture was extracted with dichloromethane (3 x 5 mL) and the combined organic phases were washed (brine 10 mL), dried (Na_2SO_4), filtered and the solvent was removed *in vacuo*. Purification of the crude product by flash column chromatography (EtOAc/hexanes: 5% → 25%) over silica gel afforded the compound **198** (3.48 g, 95%) as a colourless oil

^{1}H NMR (600 MHz, $CDCl_3$) δ 5.79 (ddt, *J* = 16.6, 10.1, 6.3 Hz, 1H), 5.52 (dd, *J* = 7.6, 6.5 Hz, 1H), 5.08 – 4.98 (m, 2H), 4.52 (td, *J* = 4.0, 2.6 Hz, 1H), 4.22 (dq, *J* = 9.8, 6.0 Hz, 1H), 3.97 – 3.89 (m, 3H), 3.56 (d, *J* = 3.9 Hz, 1H), 2.94 – 2.90 (m, 2H), 2.51 – 2.45 (m, 1H), 2.41 – 2.35 (m, 1H), 2.08 (ddd, *J* = 13.0, 5.4, 1.4 Hz, 1H), 1.80 – 1.75 (m, 2H), 1.71 – 1.66 (m, 1H), 0.90 (s, 9H), 0.10 (d, J = 2.9 Hz, 6H).

^{13}C NMR (150 MHz, $CDCl_3$) δ 135.4 (2C), 123.0, 115.5, 80.4, 77.5, 74.4, 63.0, 41.9, 36.5, 33.9, 32.9, 25.9 (3C), 18.26, -5.30, -5.36.

IR (thin film): 3530, 2953, 2857, 1472, 1089 cm^{-1}.

HRMS (ESI$^+$) calculated for $C_{18}H_{33}ClNaO_3Si$: 383.1780 $(M + Na)^+$; Found: 383.1775.

2.6.6. Preparation of (2*R*,3*R*,5*R*)-2-(((*tert*-Butyldimethylsilyl)oxy)methyl)-5-((*Z*)-3-chlorohepta-3,6-dien-1-yl)tetrahydrofuran-3-yl 2-bromoacetate (197)

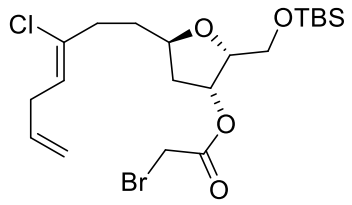

To a stirred solution of the mono-TBS tetrahydrofuranol **198** (3.0 g, 8.30 mmol) in dichloromethane (30 mL) at 0 °C, DMAP (0.10 g, 0.80 mmol), bromoacetic acid (1.38 g, 9.90 mmol), and DIC (1.90 mL, 12.40 mmol) were added successively and stirred for 15 min, after which time TLC analysis indicated the disappearance of compound **198**. The reaction mixture was diluted with water (15 mL) and the phases were separated. The organic phase was extracted with dichloromethane (2 x 10 mL). The combined organic phases were washed (aqueous Sat. $NaHCO_3$ 10 mL, brine 15 mL), dried (Na_2SO_4), concentrated and purified by flash column chromatography (EtOAc/hexanes: 0% → 15%) to give the compound **197** (3.40 g, 85%) as a clear oil.

^{1}H NMR (600 MHz, $CDCl_3$) δ: 5.78 (ddt, *J* = 6.2, 10.1, 16.3 Hz, 1 H), 5.53 (t, *J* = 7.0 Hz, 1 H), 5.49 (ddd, *J* = 1.1, 3.6, 5.2 Hz, 1 H), 5.03 (m, 2 H), 4.17 (dq, *J* = 6.0, 9.2 Hz, 1 H), 4.09 (ddd, *J* = 3.8, 5.9, 7.1 Hz, 1 H), 3.82 (s, 3 H), 3.79 (m, 1 H), 3.76 (dd, *J* = 2.9, 5.9 Hz, 1 H), 2.92 (t, *J* = 6.6 Hz, 2 H), 2.54-2.35 (m, 2 H), 2.15 (ddd, *J* = 1.4, 6.0, 14.0 Hz, 1 H), 1.86 (m, 1 H), 1.79 (dt, *J* = 6.6, 7.9 Hz, 2 H), 0.87 (s, 9 H), 0.49 (d, *J* = 3.3 Hz, 6 H).

^{13}C NMR (150 MHz, $CDCl_3$) δ: 166.5, 135.4, 135.1, 123.4, 115.5, 80.8, 77.0, 76.5, 61.1, 39.0, 36.4, 33.9, 32.9, 26.0 (3C), 25.9, -5.19, -5.26.

IR (thin film): 2928, 1738, 1275, 1089, 836, 777 cm^{-1}.

HRMS (ESI^+) calculated for $C_{20}H_{34}BrClNaO_4Si$: 503.0990(M+Na); Found: 503.0995.

$[\alpha]_D^{20}$ –20.0 (*c* = 0.10, $CHCl_3$).

2.6.7. Preparation of (2*R*,3*R*,5*R*)-2-(((*tert*-Butyldiphenylsilyl)oxy)methyl)-5-((*Z*)-3-chlorohepta-3,6-dien-1-yl)tetrahydrofuran-3-ol (214)

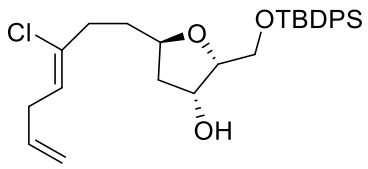

To a stirred solution of the diol **133** (1.0 g, 4.0 mmol) in dry dichloromethane (15 mL) was added *tert*-butyldiphenylsilyl chloride (1.23 g, 4.40 mmol) and imidazole (0.50 g, 8.0 mmol). The reaction mixture was stirred for 12 h at rt. The reaction was then quenched with water (10 mL). The reaction mixture was then extracted with dichloromethane (3 x 5 mL) and the combined organic phases were washed (brine 5 mL), dried (Na_2SO_4), filtered and the solvent was removed *in vacuo*. Purification of the crude product by flash column chromatography (EtOAc/hexanes: 5% → 30%) over silica gel afforded the compound **214** (1.77 g, 90%) as a colourless oil

^{1}H NMR (600 MHz, $CDCl_3$) δ 7.73 – 7.71 (m, 2H), 7.68 – 7.66 (m, 2H), 7.45 – 7.38 (m, 6H), 5.78 (ddt, *J* = 17.1, 10.2, 6.3 Hz, 1H), 5.52 (t, *J* = 7.0, 1.0 Hz, 1H), 5.07 – 4.98 (m, 2H), 4.60 – 4.57 (m, 1H), 4.26 (ddt, *J* = 10.1, 7.6, 5.1 Hz, 1H), 4.01 – 3.93 (m, 3H), 3.37(d, *J* = 3.5 Hz, 1H), 2.93 – 2.89 (m, 2H), 2.54 – 2.47 (m, 1H), 2.43 – 2.34 (m, 1H), 2.13 (ddd, *J* = 13.0, 5.3, 1.3 Hz, 1H), 1.83 – 1.67 (m, 3H), 1.06 (s, 9H).

^{13}C NMR (150 MHz, $CDCl_3$) δ 135.8 (2C), 135.6 (2C), 135.4 (2C), 130.1 (4C), 128.0 (4C), 123.0, 115.5, 80.5, 77.5, 74.3, 63.5, 41.8, 36.6, 34.0, 32.9, 26.9 (3C), 19.8.

IR (thin film): 3537, 2950, 2857, 1475, 1085 cm^{-1}.

HRMS (ESI$^+$) calculated for $C_{28}H_{38}ClO_3Si$: 485.2273 $(M + H)^+$; Found: 485.2269.

2.6.8. Preparation of (2*R*,3*R*,5*R*)-2-(((*tert* butyldiphenylsilyl)oxy)methyl)-5-((*Z*)-3-chlorohepta-3,6-dien-1-yl)tetrahydrofuran-3-yl 2-bromoacetate (215)

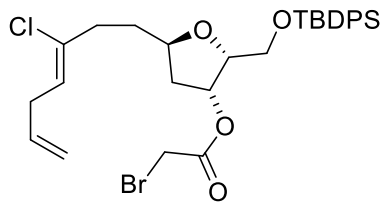

To a stirred solution of the mono-TBDPS tetrahydrofuranol **214** (1.50 g, 3.0 mmol) in dichloromethane (15 mL) at 0 °C, was added DMAP (38.0 mg, 0.30 mmol), bromoacetic acid (0.52 g, 3.70 mmol), and DIC (0.70 mL, 4.60 mmol) successively, stirred for 15 min, and gradually allowed to warm to rt. The mixture was stirred at rt for 1 h, after which time TLC analysis indicated the disappearance of **214**. The reaction mixture was diluted with water (15 mL) and the phases were separated. The organic phase was extracted with dichloromethane (2 x 10 mL). The combined organic phases were washed (aq. Sat. $NaHCO_3$, brine), dried (Na_2SO_4), filtered, concentrated and purified by flash column chromatography (EtOAc/hexanes: 0% → 10%) over silica gel to give the compound **215** (1.6 g, 85%) as a clear oil.

^{1}H NMR (600 MHz, $CDCl_3$) δ 7.65 – 7.36 (m, 10H), 5.78 (ddt, *J* = 16.7, 10.2, 6.3 Hz, 1H), 5.54 – 5.49 (m, 2H), 5.07 – 4.98 (m, 2H), 4.18 (ddd, *J* = 7.5, 5.6, 3.7 Hz, 1H), 4.12 (dq, *J* = 9.7, 6.1 Hz, 1H), 3.88 – 3.78 (m, 2H), 3.65 – 3.63 (m, 2H), 2.91 (t, *J* = 6.8 Hz, 2H), 2.48 (dt, *J* = 14.7, 7.6 Hz, 1H), 2.38 (dt, *J* = 15.1, 7.8 Hz, 1H), 2.18 – 2.13 (m, 1H), 1.89 – 1.82 (m, 1H), 1.80 – 1.75 (m, 2H), 1.04 (s, 9H).

^{13}C NMR (150 MHz, $CDCl_3$) δ 166.5, 135.8 (2C), 135.7(2C), 135.4, 135.1, 129.9 (4C), 127.9 (2C), 127.8 (2C), 123.3, 115.5, 80.6, 77.0, 76.5, 61.2, 39.1, 36.4, 33.9, 32.9, 26.9 (3C), 25.8, 19.3.

IR (thin film): 2920, 1732, 1279, 1075, 830, 775 cm^{-1}.

HRMS (ESI^+) calculated for $C_{30}H_{38}BrClNaO_4Si$: 629.1303 $(M+Na)^+$; Found: 629.1311.

2.6.9. Preparation of (2*R*,3*R*,5*R*)-2-(((*tert*-Butyldiphenylsilyl)oxy)methyl)-5-((*Z*)-3-chloro-8-hydroxy-7-(hydroxymethyl)octa-3,6-dien-1-yl)tetrahydrofuran-3-yl 2-bromoacetate (217)

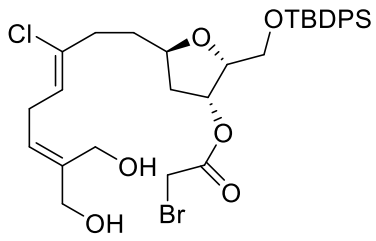

To a 25 mL 3-neck round bottom flask fitted with a reflux condesor and septa was charged the Hoveyda-Grubbs II catalyst (15.50 mg, 0.025 mmol). Acetonide **165** (190 mg, 1.50 mmol) in degassed dichloromethane (2.50 mL) and the diene **215** (300 mg, 0.50 mmol) in degassed dichloromethane (2.50 mL) were added simultaneously via a syringe to the round bottom flask through the septa. The reaction mixture was stirred for 12 h at 40 °C. The mixture was cooled to rt and the solvent was removed by rotaory evaporation to give a dark brown syrupy residue. This residue was passed through a 1.5-inch length neutral alumina plug (EtOAc/hexanes: 0% → 10%) and the solvent was removed *in vacuo* to give a brown oil. To this oil was added MeOH (5 mL), PPTS (3.80 mg, 0.015 mmol) and stirred for 30 min, after which time TLC analysis indicated the disappearance of compound **216**. The reaction mixture was filtered through a pad of celite with an additional aid of EtOAc (5 mL) and the filtrate was concentrated. Purification by flash colum chromatography (MeOH/$CHCl_3$: 0% → 10%) over silica gel afforded the diol **217** (197.0 mg, 60% over two steps) as a pale brown oil.

^{1}H NMR (600 MHz, $CDCl_3$) δ 7.65 – 7.63 (m, 4H), 7.44 – 7.41 (m, 2H), 7.39 – 7.36 (m, 4H), 5.53 – 5.50 (m, 2H), 5.46 (t, J = 7.1 Hz, 1H), 4.34 (br s, 1H), 4.21 (br s, 1H), 4.18 – 4.15 (m. 1H), 4.12 – 4.07 (m. 1H), 3.64 (d, *J* = 4.8 Hz, 2H), 2.96 (t, *J* = 7.2 Hz, 1H), 2.46 (dt, *J* = 14.7, 7.4 Hz, 1H), 2.34 (dt, *J* = 15.0, 7.7 Hz, 1H), 2.15 (ddd, *J* = 13.9, 5.8, 1.3 Hz, 1H), 1.86 (ddd, *J* = 14.2, 9.5, 4.9 Hz, 1H), 1.76 (dddd, *J* = 9.9, 8.2, 5.7, 2.2 Hz, 1H), 1.03 (s, 9H).

^{13}C NMR (150 MHz, $CDCl_3$) δ 167.6, 135.8, 135.7 (3C), 133.5, 133.4, 129.9 (4C), 127.8 (2C) 126.9 (2C), 123.3, 112.5, 80.5, 77.1, 76.5, 67.4, 61.6, 60.1, 39.1, 36.3, 33.8, 27.2, 26.9 (3C), 25.5, 19.3.

HRMS (ESI$^+$) calculated for $C_{32}H_{42}BrClNaO_6Si$: 687.1515 $(M+Na)^+$; Found: 687.1525.

2.6.10. Preparation of (2*R*,3*R*,5*R*)-5-((3*Z*,6*E*)-8-Acetoxy-3-chloro-7-(hydroxymethyl)octa-3,6-dien-1-yl)-2-(((tert-butyldiphenylsilyl)oxy)methyl)tetrahydrofuran-3-yl 2-bromoacetate (218)

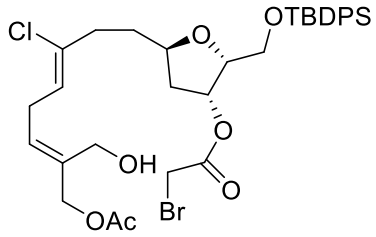

To a stirred solution of the diol **217** (50 mg, 0.075 mmol) in dry 1,4-dioxane (2.0 mL), 4 Å molecular sieves (50.0 mg) was added and stirred at rt for 20 min. To the resulting suspension vinyl acetate (20.0 µL, 0.225 mmol)) and Amano PS-D Lipase (5.0 mg) were added. The reaction mixture was stirred for 6 h at rt. To this mixture was then added EtOAc (3 mL), anhydrous magnesium sulphate and the mixture was filtered through a pad of celite with an additional quantity of EtOAc (3 mL). The solvent was removed *in vacuo* and purified by flash column chromatography (EtOAc/hexanes: 0% → 40%) over silica gel to give the monoacetylated compound **218** (43 mg, 80%) as a colorless oil.

^{1}H NMR (400 MHz, $CDCl_3$) δ 7.66 – 7.62 (m, 2H), 7.45 – 7.36 (m, 6H), 5.60 (t, *J* = 7.6 Hz, 1H), 5.52 (t, *J* = 4.2 Hz, 1H), 5.46 (t, *J* = 7.0 Hz, 1H), 4.63 (s, 2H), 4.21 (s, 2H), 4.20 – 4.15 (m, 1H), 4.13 – 4.09 (m, 1H), 3.88 – 3.77 (m, 2H), 3.64 (d, *J* = 1.8 Hz, 2H), 3.0 (t, *J* = 7.2 Hz, 2H), 2.46 (dt, *J* = 14.7, 7.4 Hz, 1H), 2.35 (dt, *J* = 14.8, 7.5 Hz, 1H), 2.15 (ddd, *J* = 14.0, 5.9, 1.4 Hz, 1H), 2.08 (s, 3H), 1.90 – 1.85 (m, 1H), 1.80 – 1.73 (m, 1H), 1.04 (s, 9H).

HRMS (ESI$^+$) calculated for $C_{34}H_{44}BrClNaO_7Si$: 729.1620 $(M+Na)^+$; Found: 729.1615.

2.6.11. Preparation of (2*R*,3*R*,5*R*)-2-(((*tert*-Butyldimethylsilyl)oxy)methyl)-5-((*Z*)-3-chloro-6-(2,2-dimethyl-1,3-dioxan-5-ylidene)hex-3-en-1-yl)tetrahydrofuran-3-yl 2-bromoacetate (212)

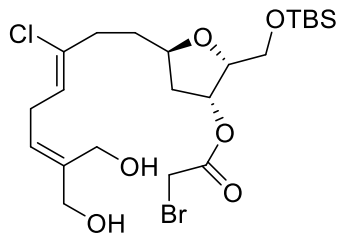

To a 25 mL 3-neck round bottom flask fitted with a reflux condensor and septa was charged the Hoveyda-Grubbs II catalyst (50 mg, 0.08 mmol). Acetonide **165** (0.40 g, 3.0 mmol) in degassed dichloromethane (1.0 mL) and the diene **197** (0.50 g, 1.0 mmol) in degassed dichloromethane (1.0 mL) were added simultaneously via a syringe to the round bottom flask through the septa. The reaction mixture was stirred for 12 h at reflux temperature. The mixture was cooled to rt and the solvent was removed by rotaory evaporation to give a dark brown syrupy residue. This residue was passed through a Sephadex LH-20 column (Methanol: 100%) and the solvent was removed *in vacuo* to give a colorless oil. To this oil was added methanol (3 mL), solid supported PPTS (7.50 mg, 0.03 mmol) at 0 °C and stirred for 30 min, after which time TLC analysis indicated the disappearance of compound **211**. The reaction mixture was filtered through a pad of celite with an additional quantity of EtOAc (5 mL) and the filtrate was concentrated, purified by flash column chromatography (MeOH/$CHCl_3$: 0% → 10%) over silica gel afforded the diol **212** (0.42 g, 75% over two steps) as a pale brown oil.

^{1}H NMR (400 MHz, $CDCl_3$) δ: 5.55 – 5.48 (m, 3 H), 4.36 (bs, 2 H), 4.23 (bs, 2 H), 4.18 c 4.13 (m, 1H), 4.11 – 4.06 (m, 1H), 3.83 (s, 2 H), 3.75 (dd, *J* = 6.3 , 2.4, Hz, 2 H), 2.97 (t, *J* = 7.4 Hz, 2 H), 2.51 – 2.43 (m, 1 H), 2.40 – 2.33 (m, 1 H), 2.15 (ddd, *J* = 14.0 , 5.8, 1.1Hz, 1 H), 1.88 – 1.82 (m, 1 H), 1.80 – 1.75 (m, 2 H), 0.87 (s, 9 H), 0.47 (d, *J* = 3.3 Hz, 6 H).

^{13}C NMR (150 MHz, $CDCl_3$) δ: 165.6, 137.5, 134.2, 125.9, 122.3, 79.8, 76.1, 75.6, 66.4, 60.1, 59.1, 38.0, 35.3, 32.8, 26.3, 24.9 (4C), -6.2, -6.3.

IR (thin film): 3366, 2928, 2856, 1739, 1462, 1277, 1256, 1092, 1007, 838, 778 cm^{-1}.

HRMS (ESI$^+$) calculated for $C_{22}H_{38}BrClNaO_6Si$: 563.1202 $(M+Na)^+$; Found: 563.1196.

$[\alpha]_D^{20}$ –22.7 (*c* = 0.30, $CHCl_3$).

2.6.12. Preparation of (2*R*,3*R*,5*R*)-5-((3*Z*,6*E*)-8-Acetoxy-3-chloro-7-(hydroxymethyl)octa-3,6-dien-1-yl)-2-(((*tert*-butyldimethylsilyl)oxy)methyl)tetrahydrofuran-3-yl 2-bromoacetate (226)

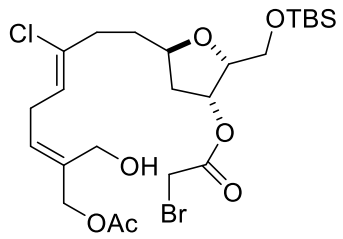

To a stirred solution of the diol **212** (200 mg, 0.37 mmol) in dry 1,4-dioxane (4.0 mL), was added 4 Å molecular sieves and stirred at rt for 20 min. To the resultant suspension, vinyl acetate (95.0 µL, 1.10 mmol)) and Amano PS-D Lipase (20.0 mg) were added. The reaction mixture was stirred for 6 h at rt. To this mixture was then added EtOAc (5 mL), anhydrous magnesium sulfate (100 mg) and the mixture was filtered through a pad of Celite with an additional quantity of EtOAc (3 mL). The solvent was removed *in vacuo* and purification by flash column chromatography (EtOAc/hexanes: 0% → 40%) over silica gel gave the monoacetyted compound **226** (170 mg, 80%) as a colorless oil.

^{1}H NMR (500 MHz, $CDCl_3$) δ 5.62 (t, *J* = 7.6 Hz, 1H), 5.49 – 5.47 (m, 2H), 4.65 (br s, 2H), 4.23 (d, *J* = 6.2 Hz, 2H), 4.19 – 4.14 (m, 1H), 4.09 – 4.07 (m, 1H), 3.83 (s, 2H), 3.75 (dd, *J* = 6.5, 4.4 Hz, 2H), 3.01 (t, *J* = 7.2 Hz, 2H), 2.48 (dt, *J* = 14.8, 7.4 Hz, 1H), 2.37 (dt, *J* = 14.8, 7.7 Hz, 1H), 2.19 – 2.13 (ddd, *J* = 13.9, 5.9, 1.3 Hz, 1H), 1.89 – 1.84 (m, 1H), 1.80 – 1.75 (m, 2H), 0.89 (s, 9H), 0.05 (d, *J* = 4.2 Hz, 6H).

^{13}C NMR (150 MHz, $CDCl_3$) δ: 171.4, 166.6, 135.4, 134.9, 130.2, 122.9, 80.8, 77.0, 76.5, 67.1, 61.1, 58.5, 39.0, 36.3, 33.9, 27.3, 25.9 (3C), 21.2, 18.4, -6.2, -6.3.

IR (thin film): 3366, 2928, 2856, 1739, 1462, 1277, 1256, 1092, 1007, 838, 778 cm^{-1}.

HRMS (ESI^+) calculated for $C_{22}H_{38}BrClNaO_6Si$: 605.1306 $(M+Na)^+$; Found: 605. 1297.

$[\alpha]_D^{20}$: –5.3 (*c* = 0.30, $CHCl_3$).

2.6.13. Preparation of ((1*R*,5*S*,6*Z*,9*Z*,13*R*,15*R*)-15-(((*tert*-Butyldimethylsilyl)oxy)methyl)-10-chloro-5-hydroxy-3-oxo-2,14-dioxabicyclo[11.2.1]hexadeca-6,9-dien-6-yl)methyl acetate (200) and ((1*R*,5*R*,6*Z*,9*Z*,13*R*,15*R*)-15-(((*tert*-butyldimethylsilyl)oxy)methyl)-10-chloro-5-hydroxy-3-oxo-2,14-dioxabicyclo[11.2.1]hexadeca-6,9-dien-6-yl)methyl acetate (201)

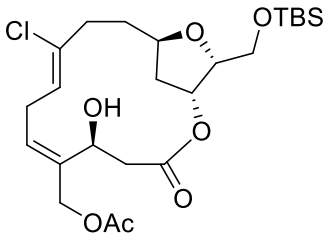

200
Major isomer

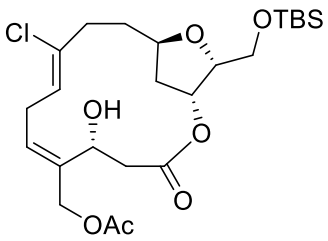

201
Minor isomer

To a stirred solution of monoacetate **226** (25.0 mg, 42.0 µmol) and $NaHCO_3$ (10 mg, 126.0 µmol) in dichloromethane (0.5 mL) was added Dess-Martin periodinane (21 mg, 51.3 µmol) and stirred for 45 minutes. The reaction mixture was then quenched with a mixture of water/aqueous saturated $NaHCO_3$/brine (1 mL; v/v 1:1:1) and phases were seperated. The aqueous phase was extracted with dichloromethane (3 x 0.5 mL). The combined organic phases were then washed (brine 1 mL), dried (Na_2SO_4), and concentrated to give the crude aldehyde **196**. Which was used immediately in the next step.

To a suspension of $Rh(PPh_3)_3Cl$ (6.2 mg, 64.4 µmol) in *tert*-butyl methylether (11.0 mL) was added $ZnEt_2$ (15% in toluene , 0.75 mL, 858.0 µmol) and stirred vigorously. A solution of aldehyde **196** (25.0 mg, 42.9 µmol) in *tert*-butyl methylether (3.0 mL) was added dropwise into the stirred solution over a period of 1 h. After addition, the reaction mixture was stirred for 1 h at rt. The reaction was then quenched with an aqueous solution of saturated ammonium chloride (5 mL) and filtered through a pad of Celite with an additional quantity of EtOAc (5 mL). The phases were separated, and the organic phase was extracted with EtOAc (3 x 2 mL). The combined organic phases were washed (brine 5 mL), dried (Na_2SO_4), concentrated and purified by flash chromatography (EtOAc/hexanes: 0% → 30%) over silica gel to afford the undesired major diastereomer **200** (8.5 mg, 40%)

as a colourless oil, and the desired minor diastereomer **201** (2.5 mg, 10%) as a colourless oil.

Major undesired diastereomer **200**:

^{1}H NMR (400 MHz, $CDCl_3$) δ: 6.10 (dd, *J* =9.2, 7.1 Hz, 1 H), 5.55 (t, *J* = 6.9 Hz, 1 H), 5.29 (t, *J* = 3.8 Hz, 1 H), 4.81 (d, *J* = 12.4 Hz, 1 H), 4.79 (m, 1 H), 4.59 (d, *J* = 12.4 Hz, 1 H), 4.18 (dt, *J* = 7.2 ,4.2 Hz, 1 H), 3.8 (m, 1 H), 3.72 (dd, *J* = 6.2 ,5.3 Hz, 2 H), 3.11 (m, 1 H), 2.89 (m, 1 H), 2.74 (dd, *J* = 12.7 , 7.8, Hz, 1 H), 2.67 (dd, *J* = 12.7 , 5.8 Hz, 1 H), 2.47-2.34 (m, 1 H), 2.30-2.19 (m, 2 H), 2.10 (s, 3 H), 1.59-1.47 (m, 3 H), 0.87 (s, 9 H), 0.06 (d, *J* = 1.6 Hz, 6 H).

^{13}C NMR (150 MHz, $CDCl_3$) δ 170.5, 170.4, 134.4, 134.2, 131.1, 123.2, 80.6, 76.4, 75.9, 66.5, 65.4, 61.2, 41.4, 38.6, 34.0, 29.6, 28.6, 26.3 (3C), 21.0, 18.3, -5.2, -5.4.

IR: 3448, 2967, 2932, 2859, 1734, 1472, 1366, 1255, 1234, 1136, 1080, 837, 777 cm^{-1}.

HRMS: m/z calcd for $C_{24}H_{39}ClO_7Si$: 525.2046 (M+Na); Found: 525.2049 (M+Na).

$[\alpha]_D^{20}$ +6.0 (*c* = 0.10, $CHCl_3$)

Minor desired diasteromer **201**:

^{1}H NMR (600 MHz, $CDCl_3$) δ 6.0 (dd, *J* = 10.8, 7.2 Hz, 1H), 5.23 (t, *J* = 3.5 Hz, 1H), 5.17 (ddd, *J* = 8.3, 2.6, 1.4 Hz, 1H), 5.02 (d, *J* = 12.9 Hz, 1H), 4.72 – 4.69 (m, 1H), 4.67 (d, *J* = 13.0 Hz, 1H), 4.13 (td, *J* = 7.0, 3.8 Hz, 1H), 3.86 (ddt, *J* = 11.7, 7.8, 3.9 Hz, 1H), 3.77 (d, J = 7.0 Hz, 2H), 3.38 – 3.32 (m, 1H), 2.86 (dd, *J* = 11.7, 4.1 Hz, 1H), 2.71 – 2.65 (m, 2H), 2.54 – 2.49 (m, 1H), 2.41 (d, *J* = 6.2 Hz, 1H), 2.37 (dt, *J* = 12.7, 5.1 Hz, 1H), 2.16 (ddd, *J* = 13.9, 12.6, 5.5 Hz, 1H), 2.10 (s, 3H), 2.01 (dd, *J* = 12.7, 3.4 Hz, 1H), 1.48 – 1.42 (m, 2H), 0.86 (s, 8H), 0.04 (d, *J* = 1.8 Hz, 6H).

^{13}C NMR (150 MHz, $CDCl_3$) δ 171.0, 169.0, 136.3, 132.9 (2C), 124.2, 80.6, 76.3, 75.3, 65.8, 65.3, 61.0, 40.8, 37.8, 35.0, 28.1, 26.5, 26.0 (3C), 21.3, 18.4, -5.2, -5.3.

IR (thin film): 3460, 2955, 2930, 2857, 1737, 1464, 1377, 1250, 1081, 837, 778 cm^{-1} .

HRMS (ESI^+) calculated for $C_{24}H_{39}ClNaO_7Si$: 525.2046 (M+Na); Found: 525.2041.

$[\alpha]_D^{20}$ –11.7 (*c* = 0.70, $CHCl_3$)

2.6.14. Preparation of ((1*R*,5*R*,6*Z*,9*Z*,13*R*,15*R*)-5-acetoxy-15-(((*tert*-Butyldimethylsilyl)oxy)methyl)-10-chloro-3-oxo-2,14-dioxabicyclo[11.2.1]hexadeca-6,9-dien-6-yl)methyl acetate (204)

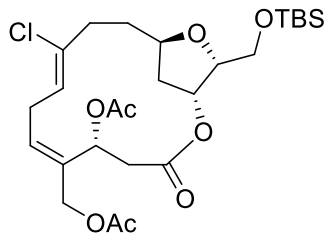

To a stirred solution of macrocycle **201** (8.3 mg, 16.4 µmol) in dichloromethane (0.5 mL) at rt was added a catalytic amount of DMAP (1.0 mg), acetic anhydride (2.5 µL, 24.7 µmol) and pyridine (4.0 µL, 49.4 µmol). The reaction mixture was stirred for 5 h and then the solvent was removed *in vacuo*. Purification of the crude product by flash column chromatography (EtOAc/hexanes: 0% → 25%) over silica gel afforded compound **204** (8.0 mg, 90%) as a pale-yellow oil.

^{1}H NMR (600 MHz, $CDCl_3$) δ 6.05 (dd, *J* = 11.0, 7.0 Hz, 1H), 5.82 (dd, *J* = 11.9, 4.6 Hz, 1H), 5.26 (t, *J* = 3.5 Hz, 1H), 5.20 (br d, *J* = 7.3 Hz, 1H), 4.96 (d, *J* = 13.3 Hz, 1H), 4.73 (d, *J* = 13.4 Hz, 1H), 4.13 (td, *J* = 7.1, 3.8 Hz, 1H), 3.90 (ddt, *J* = 11.6, 7.7, 3.9 Hz, 1H), 3.77 (d, *J* = 7.2 Hz 2H), 3.65 – 3.60 (m, 1H), 2.83 (t, *J* = 11.8 Hz, 1H), 2.74 (dd, *J* = 11.9, 4.6 Hz, 1H), 2.69 – 2.63 (m, 1H), 2.54 – 2.49 (m, 1H), 2.38 (dtd, *J* = 13.9, 10.7, 8.8, 4.3 Hz, 1H), 2.17 (td, *J* = 13.3, 5.4 Hz, 1H), 2.09 (s, 3H), 2.09 – 2.06 (m, 1H), 2.04 (s, 3H),1.48 – 1.42 (m, 2H), 0.86 (s, 9H), 0.04 (d, *J* = 3.8 Hz, 6H).

^{13}C NMR (150 MHz, $CDCl_3$) δ 170.7, 169.4, 168.0, 13403, 133.0, 132.1, 124.3, 80.7, 76.3, 75.7, 66.5, 64.2, 60.9, 38.0, 37.8, 35.0, 28.0, 26.9, 26.0 (3C), 21.3, 21.2, 18.4, -5.2, -5.3.

IR (thin film): 2959, 2929, 1739, 1433, 1373, 1229, 1079, 838, 780 cm^{-1}.

HRMS (ESI^+) calculated for $C_{24}H_{41}ClNaO_8Si$: 567.2151 $(M+Na)^+$; Found: 567.2161.

$[\alpha]_D^{20}$ –14.1 (*c* = 0.31, $CHCl_3$).

2.6.15. Preparation of ((1*R*,5*R*,6*Z*,9*Z*,13*R*,15*R*)-5-Acetoxy-10-chloro-15-(hydroxymethyl)-3-oxo-2,14-dioxabicyclo[11.2.1]hexadeca-6,9-dien-6-yl)methyl acetate (119)

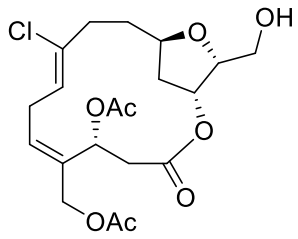

To a stirred solution of macrocycle **204** (8 mg, 14.6 µmol) in THF (0.5 mL) was added HF·py (60 µL). The reaction mixture was stirred at rt for 1 h and quenched with aqueous saturated $NaHCO_3$ (1 mL). The mixture was extracted with EtOAc (3 × 3 mL) and the combined organic extracts were dried (Na_2SO_4), filtered, concentrated and purified by flash column chromatography (EtOAc/hexanes: 0% → 60%) over silica gel afforded the compound **119** (5.5 mg, 88%) as clear oil.

^{1}H NMR (600 MHz, $CDCl_3$) δ 6.09 – 6.03 (dd, *J* = 11.1, 7.0 Hz, 1H), 5.84 – 5.77 (dd, *J* = 11.7, 4.5 Hz, 1H), 5.28 – 5.25 (t, *J* = 3.8 Hz, 1H), 5.24 – 5.20 (ddd, *J* = 8.0, 2.9, 1.3 Hz, 1H), 4.95 – 4.88 (dt, *J* = 13.1, 1.1 Hz, 1H), 4.75 – 4.70 (dd, *J* = 13.2, 1.1 Hz, 1H), 4.28 – 4.16 (dt, *J* = 7.6, 4.5 Hz, 1H), 3.95 – 3.89 (tt, *J* = 11.6, 3.8 Hz, 1H), 3.89 – 3.83 (ddd, *J* = 11.0, 7.6, 2.8 Hz, 1H), 3.70 – 3.64 (ddd, *J* = 11.9, 7.5, 4.7 Hz, 1H), 3.61 – 3.53 (ddd, *J* = 18.2, 11.0, 8.0 Hz, 1H), 2.88 – 2.79 (t, *J* = 12.0 Hz, 1H), 2.77 – 2.72 (dd, *J* = 12.2, 4.5 Hz, 1H), 2.70 – 2.64 (m, 1H), 2.57 – 2.50 (d, *J* = 14.3 Hz, 1H), 2.45 – 2.38 (tt, *J* = 12.8, 5.2 Hz, 1H), 2.23 – 2.16 (ddd, *J* = 13.8, 12.6, 5.5 Hz, 1H), 2.05 – 2.03 (s, 3H), 1.53 – 1.42 (m, 2H).

^{13}C NMR (150 MHz, $CDCl_3$) δ 170.7, 169.5, 168.1, 134.8, 133.1, 132.0, 124.3, 80.8, 76.2, 76.1, 66.4, 64.3, 61.7, 38.1, 38.0, 35.1, 27.8, 26.9, 21.2 (2C).

IR (thin film): 3454, 2956, 2855, 1736, 1232, 1047, 930, 838, 777 cm^{-1}.

HRMS (ESI$^+$) calculated for $C_{20}H_{27}ClNaO_8$: 453.1283 $(M+Na)^+$; Found: 453.1287.

$[\alpha]_D^{20}$ +6.8 (*c* = 0.22, $CHCl_3$).

2.6.16. Preparation of 2,4-dimethoxybenzyl (*E*)-4-Iodo-3-methylbut-3-enoate (120)

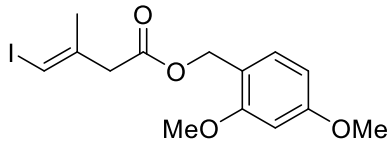

To a stirred solution of the acid **77** (100 mg, 0.47 mmol) in dichloromethane (2.0 mL) at 0 °C, DMAP (17.0 mg, 0.13 mmol), 2,4-dimethoxybenzyl alcohol (95.0 mg, 0.55 mmol), and DIC (150 µL, 0.83mmol) were added successively and stirred for 1 h, after which time TLC analysis indicated the disappearance of compound **77**. The reaction mixture was diluted with brine (5 mL) and the phases were separated. The aqueous phase was extracted with dichloromethane (2 x 3 mL). The combined organic phases were washed (aqueous saturated $NaHCO_3$ 3 mL, brine 3 mL), dried (Na_2SO_4), concentrated and purified by flash column chromatography (EtOAc/hexanes: 0% → 20%) to give the compound **120** (130 mg, 80%) as a colorless oil.

^{1}H NMR (600 MHz, $CDCl_3$) δ 7.22 (d, *J* = 8.9 Hz), 6.49 – 6.38 (m, 2H), 6.13 (br d, *J* = 1.1 Hz, 1H), 5.10 (s, 2H), 3.82 (s, 6H), 3.21 (d, *J* = 1.1 Hz, 2H), 1.90 (d, *J* = 1.1 Hz, 3H).

^{13}C NMR (150 MHz, $CDCl_3$) δ 170.2, 161.6, 159.2, 140.7, 131.2, 116.8, 104.1, 98.7, 80.2, 62.5, 55.6, 55.5, 44.4, 24.1.

Data in agreement with that reported by Kigoshi *et al*.[36]

2.6.17. Preparation of ((1*R*,5*R*,6*Z*,9*Z*,13*R*,15*S*)-5-Acetoxy-10-chloro-15-formyl-3-oxo-2,14-dioxabicyclo[11.2.1]hexadeca-6,9-dien-6-yl)methyl acetate (196)

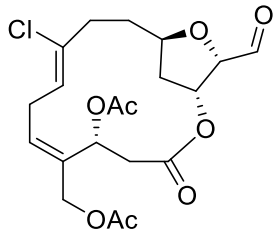

To a stirred solution of the macrocycle **119** (5.5 mg, 12.8 µmol) and $NaHCO_3$ (3.5 mg, 34.8 µmol) in dichloromethane (0.3 mL) was added Dess-Martin periodinane (8.2 mg, 19.2 µmol) and the reaction mixture was stirred for 45 minutes. The reaction mixture was then quenched with a mixture of water/aqueous saturated $NaHCO_3$/brine (1 mL; v/v - 1:1:1) and separated the phases. The aqueous phase was extracted with dichloromethane (3 x 0.5 mL). The combined organic phases were washed (brine 1 mL), dried (Na_2SO_4), and concentrated to give the crude aldehyde **196** (5.0 mg), which was used immediately in the next step

^{1}H NMR (500 MHz, $CDCl_3$) δ 9.68 (d, *J* = 1.9 Hz, 1H), 6.06 (dd, *J* = 11.1, 7.1 Hz, 1H), 5.77 (dd, *J* = 11.9, 4.5 Hz, 1H), 5.51 (t, *J* = 4.1 Hz, 1H), 5.23 (br d, *J* = 8.3 Hz, 1H), 4.90 (d, *J* = 13.2 Hz, 1H), 4.69 (d, *J* = 13.2 Hz, 1H), 4.40 (dd, *J* = 4.7, 1.9 Hz, 1H), 4.15 – 4.09 (m, 1H), 3.61 (ddd, *J* = 18.2, 10.9, 8.1 Hz, 1H), 2.82 (t, *J* = 11.9 Hz, 1H), 2.71 – 2.65 (m, 2H), 2.61 – 2.50 (m, 2H), 2.24 – 2.16 (m, 2H), 2.09 (s, 3H), 2.03 (s, 3H), 1.54 – 1.44 (m, 2H).

2.6.18. Preparation of 2,4-dimethoxybenzyl (*R,E*)-5-((1*R*,5*R*,6*Z*,9*Z*,13*R*,15*R*)-5-acetoxy-6-(acetoxymethyl)-10-chloro-3-oxo-2,14-dioxabicyclo[11.2.1]hexadeca-6,9-dien-15-yl)-5-hydroxy-3-methylpent-3-enoate (234)

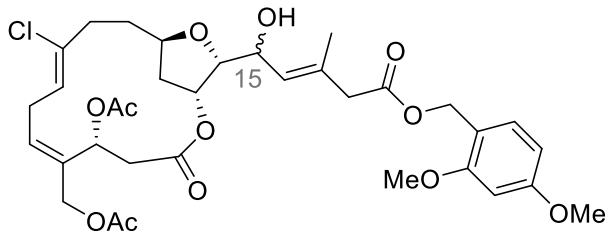

To a stirred solution of the above crude aldehyde **233** (5 mg, 11.6 µmol), and vinyl iodide **120** (13.0 mg, 35 µmol) in degassed DMSO (0.4 mL) was added $CrCl_2$, doped with $NiCl_2$ (1.0 % wt/wt, 14.2 mg, 116 µmol). The reaction was stirred for 12 h at rt. The mixture was cooled to 0 °C, diluted with water (2 mL), and extracted with Et_2O (8 x 5 mL). The combined organic extracts were dried (Na_2SO_4) concentrated and purified by flash column chromatography (EtOAc/hexanes: 30% → 80%) to afford the compound **234** (3.5 mg, 45%) as a diasteromeric mixture (3:1) at C15.

^{1}H NMR (600 MHz, $CDCl_3$) δ 7.23 (d, *J* = 9.0 Hz, 1H), 6.46 (m, 2H), 6.06 (dd, *J* = 10.9, 7.2 Hz, 1H), 5.82 (dd, *J* = 11.5, 4.7 Hz, 1H), 5.45 – 5.40 (m, 1H), 5.42 (d, *J* = 7.9, Hz, 1H), 5.31 (m, 1H), 5.20 (m, 1H), 5.09 (s, 2H), 4.92 (d, *J* = 13.0 Hz, 1H), 4.73 (d, *J* = 13.2 Hz, 1H), 4.58 (t, *J* = 8.0 Hz, 1H), 3.94 (dd, *J* = 7.8, 3.7 Hz, 2H), 3.81 (d, *J* = 3.1 Hz, 9H), 3.60 (m, 1H), 3.08(s, 2H), 2.87 – 2.79 (m, 2H), 2.66 (m, 1H), 2.51 (m, 1H), 2.39(m, 1H), 2.17 (m, 1H), 2.10 (m, 1H), 2.09 (s, 3H), 2.04 (s, 3H), 1.83 (s, 3H), 1.50 – 1.39m (m, 2H).

HRMS (ESI$^+$) calculated for $C_{34}H_{47}ClNO_{12}$: 696.2781 $(M+NH_4)^+$; Found: 696.2775

Data in agreement with that reported by Hayakawa *et al*.[51]

2.6.19. Biselide A (8)

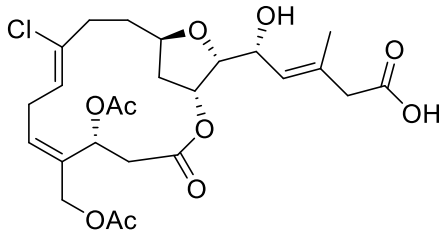

To a stirred solution of the ester **234** (3.2 mg, 47.1 µmol) in dichloromethane (0.2 mL) at 0 °C, anisole (1M, solution in CH_2Cl_2, 50 µL), and TFA (1M, solution in CH_2Cl_2, 50 µL) were added. The reaction mixture was stirred for 4 h at the same temperature after which the solvent was removed by rotary evaporation. The crude compound was purified by HPLC to afford biselide A (1.1 mg, 40%) as a colorless oil.

^{1}H NMR (600 MHz, MeOD) δ 6.10 (dd, *J* = 10.9, 7.1 Hz, 1H), 5.85 (dd, *J* = 11.2, 4.9 Hz, 1H), 5.39 (dq, *J* = 8.4, 1.3 Hz, 1H), 5.34 – 5.32 (m, 2H), 4.97 (d, *J* = 13.0 Hz, 1H), 4.71 (d, *J* = 13.0 Hz, 1H), 4.54 (t, *J* = 8.6 Hz, 1H), 3.96 (m, 1H), 3.92 (dd, *J* = 8.6, 3.7 Hz, 1H), 3.56 (m, 1H), 3.06 (br s, 2H), 2.89 (dd, *J* = 12.0, 5.1 Hz, 1H), 2.85 (dd, *J* = 12.0, 11.1 Hz, 1H), 2.62 (m, 1H), 2.47 (m, 1H), 2.34 – 2.27 (m, 2H), 2.10 (m, 1H), 2.08 (s, 3H), 2.03 (s, 3H), 1.84 (d, *J* = 1.3 Hz, 3H), 1.54 (m, 1H), 1.41 (m, 1H).

^{13}C NMR (150 MHz, MeOD) δ 175.4, 172.5, 171.1, 169.4, 135.9, 135.0, 133.9, 133.6, 130.7, 125.8, 84.5, 78.1, 76.7, 67.7, 66.5, 65.5, 45.7, 38.8, 38.7, 35.5, 29.0, 27.7, 21.0 (2C), 17.3.

IR (thin film): 3430, 3020, 2929, 1741, 1704, 1237, 1030 cm^{-1}.

HRMS (ESI$^+$) calculated for $C_{25}H_{33}ClNaO_{10}$: 551.1660 $(M+Na)^+$; Found: 551.1654.

<u>Purification of Synthetic Biselide A</u>: The final reaction product was purified by RP-HPLC (Phenomenex Kinetix XB-C_{18} 4.6 x 250 mm, 5 µm) using a gradient of MeCN: H_2O with 0.1% TFA (0-5 min. 15% MeCN, 5-25 min. 15-50% MeCN, 25.1-30 min. 100% MeCN, 30-38 min. 15% MeCN) at a flow rate of 1.25 mL min^{-1}, monitoring UV wavelength 210 nm to give 1.1 mg of the final compound biselide A (t_R = 22.5).

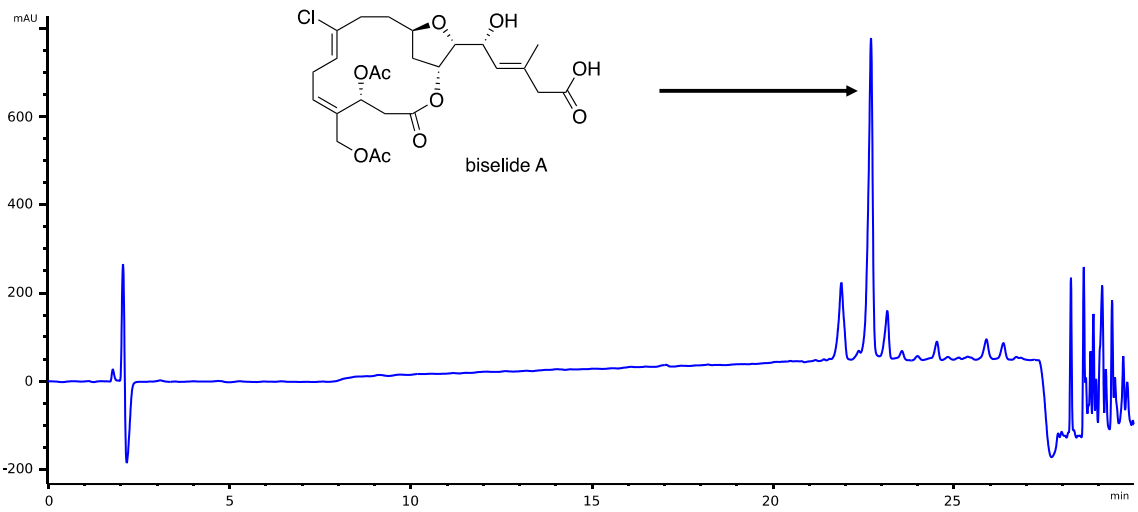

Figure 2-11 RP-HPLC trace of synthetic biselide A. Absorbance displayed at 210 nm with reference set at 360 nm, Bw 100 nm.

HR-MS of Synthetic Biselide A: Measurement of biselide A (**8**) was performed with an Acquity UPLC H-Class (Waters) using an HSS C18, 100 mm x 2.1 mm, 1.7 μm column (Waters). Separation of 5 μL sample was achieved by a gradient of (A) H_2O + 0.1% FA to (B) MeCN + 0.1% FA at a flow rate of 500 μL/min and 45°C for 7.5 min (0-0.3 min 5% MeCN, 0.3-4.7 min 5-90% MeCN, 4.7-5.5 min 90-98% MeCN, 5.5-5.8 min 98% MeCN, 5.81-7.5 min 5% MeCN). The LC flow was split to 5 μL/min into a Synapt G2-Si operated in positive ion mode. Analysis was conducted using the MS^E mode which was set to alternate between collision energies of 0eV and 30eV every 0.3 sec. The instrument was operated in electrospray mode with 20 μg/mL leucine enkephalin lockspray infusion enabled every 10 sec. Mass spectra were acquired from 50-1500 m/z at 2Hz scan rate in centroid mode with automatic lockmass correction.

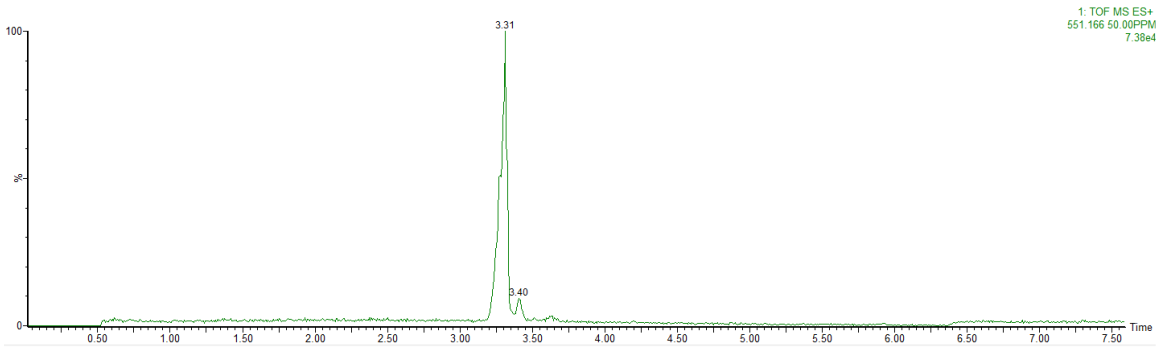

EIC for *m/z* 551.166 $[M+Na]^+$ with 50 ppm window of value for $C_{25}H_{33}ClO_{10}Na$ $[M+Na]^+$.

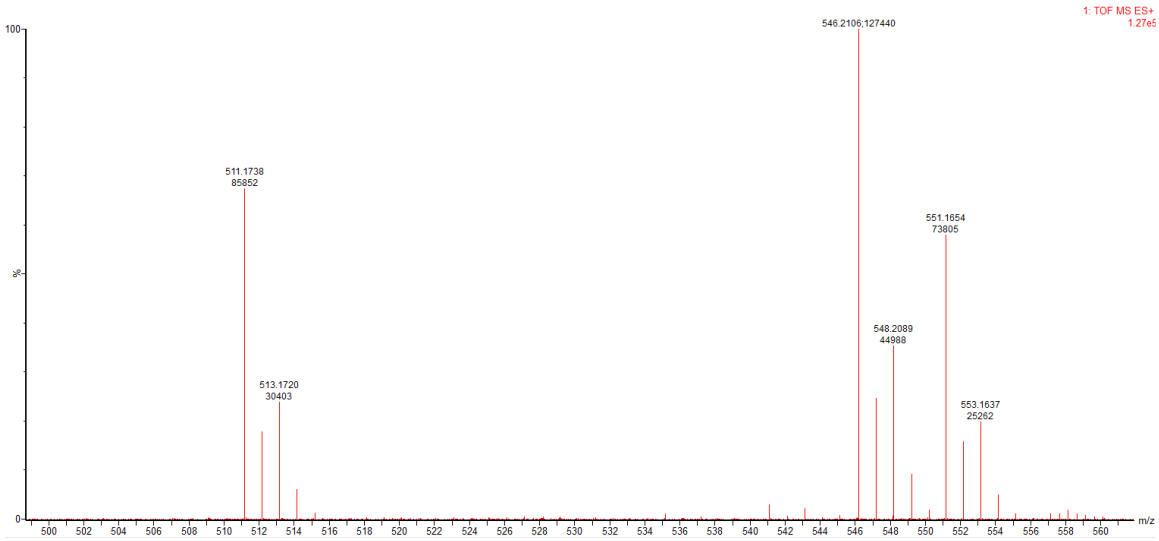

Expansion of MS spectrum at 3.31 minutes. Shown are values corresponding to biselide A: *m/z* 551.1654 $[M+Na]^+$, calcd 551.1654 $C_{25}H_{33}ClO_{10}Na$; *m/z* 546.2106 $[M+NH_4]^+$, calcd 546.2101 for $C_{25}H_{33}ClO_{10}NH_4$; *m/z* 511.1738 $[M+H-H_2O]^+$, calcd 511.1729 for $C_{25}H_{32}ClO_9$ $[M+H-H_2O]^+$.

Circular dichroism: Synthetic biselide A was diluted in MeOH to a concentration of 1 mg/mL. From the prepared sample, 600 µL was transferred to quartz cuvettes (path length 2.0 mm) for circular dichroism (CD) analysis. The spectrum was acquired on a Chirascan qCD from 400 nm to 200 nm at a 1 nm resolution at a scan rate of 0.5 scans/sec. The methanol blank scans were automatically subtracted and the average of three scans is reported below with a maximum of +4.22 millidegrees at 209 nm.

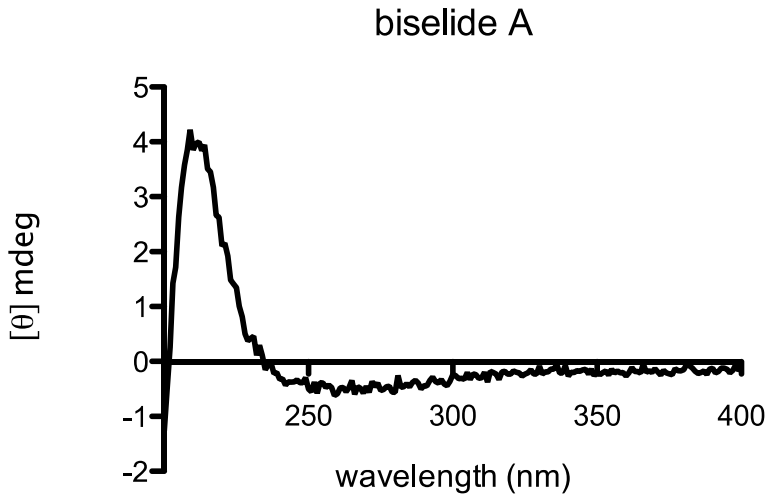

References

(1) Ueda, K.; Hu, Y. *Tetrahedron Lett.***1999**; *40*, 6305-6308

(2) Takada, N.; Sato, H.; Suenaga, K.; Arimoto, H.; Yamada, K.; Ueda, K.; Uemura, D. *Tetrahedron Lett.* **1999**, *40*, 6309–6312.

(3) Strobel, G.; Li, J. Y.; Sugawara, F.; Koshino, H.; Harper, J.; Hess, W. M. *Microbiology* **1999**, *145*, 3557–3564.

(4) Levenfors, J. J.; Hedman, R.; Thaning, C.; Gerhardson, B.; Welch, C. J. *Soil Biol. Biochem.* **2004**, *36*, 677–685.

(5) Thaning, C.; Welch, C. J.; Borowicz, J. J.; Hedman, R.; Gerhardson, B. *Soil Biol. Biochem.* **2001**, *33*, 1817–1826.

(6) Lorente, A.; Lamariano-Merketegi, J.; Albericio, F.; Álvarez, M. *Chem. Rev.* **2013**, *113*, 4567–4610.

(7) Kigoshi, H.; Kita, M.; Ogawa, S.; Itoh, M.; Uemura, D. *Org. Lett.* **2003**, *5*, 957–960.

(8) Teruya, T.; Shimogawa, H.; Suenaga, K.; Kigoshi, H. *Chemistry lett.* **2004**, 33, 1184–1185.

(9) Teruya, T; Suenaga, K.; Maruyama, S.; Kurotaki, M.; Kigoshi, H. *Tetrahedron*, **2005**, *61*, 6561-6567

(10) Sato. B.; nakajima, H.; Fujita, T.; Takase, S.; Yoshimura, S.; Kinoshita, T.; Terano, H. *J. Antibiot.* **2005**, *58*, 634–639.

(11) Inami, M.; Kawamura, I.; Tsujimoto, S.; Yasuno, T.; Lacey, E.; Hirosumi, J.; Takakura, S.; Nishigaki, F.; Naoe, Y.; Manda, T.; Mutoh, S. *J. Antibiot.* **2005**, *58*, 640–647.

(12) Kobayashi, M.; Sato, K.; Yoshimura, S.; Yamaoka, M.; Takase, S.; Ohkubo, M.; Nakajima, H. *J. Antibiot.* **2005**, *58*, 648–653.

(13) Yamaoka, M.; Sato, K.; Kobayashi, M.; Nishio, N.; Ohkubo, M.; Fujii, T.; Nakajima, H. *J. Antibiot.* **2005**, *58*, 654–662.

(14) Yadav, J. S.; Deshpande, P. K.; Sharma, G. V. M. *Tetrahedron* **1990**, *46*, 7033–7046.

(15) Dondoni, A.; Fentin, G.; Fogagnolo, M.; Merino, P. *Tetrahedron Lett.* **1990**, *31*, 4513–4516.

(16) Tamao, K.; Akita, M.; Maeda, K.; Kumada, M. *J. Org. Chem.* **1987**, *52*, 1100–1106.

(17) Ando, K. *J. Org. Chem.* **1998**, *63*, 8411–8416.

(18) Kanai, K.; Wakabayashi, H.; Honda, T. *Org. Lett.* **2000**, *2* (16), 2549–2551.

(19) Takai, K.; Kimura, K.; Kuroda, T.; Hiyama, T.; Nozaki, H. *Tetrahedron Lett.* **1983**, *24*, 5281–5284.

(20) Takai, K.; Tagashira, M.; Kuroda, T.; Oshima, K.; Utimoto, K.; Nozaki, H. *J. Am. Chem. Soc.* **1986**, *108*, 6048–6050.

(21) Gu, Y.; Snider, B. B. *Org. Lett.* **2003**, *5*, 4385–4388

(22) Inanaga, J.; Hirata, K.; Saeki, H.; Katsuki, T.; Yamaguchi, M. *Bull. Chem. Soc. Jpn*. **1979**, *52*, 1989–1993.

(23) Singer, R. A.; Carreira, E. M. *J. Am. Chem. Soc.* **1995**, *117*, 12360–12361.

(24) (a) Sharpless, K. B.; Akashi, K. *J. Am. Chem. Soc.* **1976**, *98*, 1986–1987; (b) Hentges, S. G.; Sharpless, K. B. *J. Am. Chem. Soc.* **1980**, *102*, 4263–4265.

(25) Tamaru, Y.; Hojo, M.; Kawamura, S. I.; Sawada, S.; Yoshida, Z. I. *J. Org. Chem.* **1987**, *52*, 4062–4072.

(26) Kiyooka, S. ichi; Kaneko, Y.; Komura, M.; Matsuo, H.; Nakano, *J. Org. Chem.* **1991**, *56*, 2276–2278.

(27) Kiyooka, S.; Kaneko, Y.; Kume, K. *Tetrahedron Lett.* **1992**, *33*, 4927–4930.

(28) Fustero, S.; García De La Torre, M.; Pina, B.; Fuentes, A. S. *J. Org. Chem.* **1999**, *64*, 5551–5556.

(29) Farina, V.; Krishnan, B. *J. Am. Chem. Soc.* **1991**, *113*, 9585–9595.

(30) Hoye, T. R.; Wang, J. *J. Am. Chem. Soc.* **2005**, *127*, 6950–6951.

(31) Kaneda, K.; Uchiyama, T.; Fujiwara, Y.; Imanaka, T.; Teranishi, S. *J. Org. Chem.* **1979**, *44*, 55–63.

(32) Micalizio, G. C.; Roush, W. R. *Org. Lett.* **2001**, *3*, 1949–1952.

(33) Pearson, D. A.; Blanchette', M.; Baker, M. Lou; Guindon, C. A. *Tetrahedron. Lett*. **1989**, *30*, 2739–2742.

(34) Roulland, E. *Angew. Chem. Int. Ed.* **2008**, *47,* 3762–3765

(35) Miyaura, N.; Suzuki, A. *Chem. Rev.* **1995**; *95*, 245–2483.

(36) Hayakawa, I.; Ueda, M.; Yamaura, M.; Ikeda, Y.; Suzuki, Y.; Yoshizato, K.; Kigoshi, H. *Org. Lett.* **2008**, *10*, 1859–1862.

(37) Ireland, R. E.; Thaisrivongs, S.; Vanier, N.; Wilcox, C. S. *J. Org. Chem.* ***1980,*** 45*,* 48–61.

(38) Oishi, T.; Takeshi Oishi, al; Ando, K.; Inomiya, K.; Sato, H.; Iida, M.; Chida, N. *Bull. Chem. Soc. Jpn.* **2002**, *75*, 1927–1947.

(39) Gemal, A. L.; Luche, J.-L. *J. Am. Chem. Soc.* **1981**, *103*, 5454–5459.

(40) Ueda, M.; Yamaura, M.; Ikeda, Y.; Suzuki, Y.; Yoshizato, K.; Hayakawa, I.; Kigoshi, H. *J. Org. Chem.* **2009**, *74*, 3370–3377.

(41) Schomaker, J. M.; Borhan, B. *J. Am. Chem. Soc.* **2008**, *130*, 12228–12229.

(42) (a) Baati, R.; Barma, D. K.; Falck, J. R.; Mioskowski, C. *Tetrahedron Lett.* **2002**, *43*, 2179–2181; (b) Baati, R.; Barma, D. K.; Falck, J. R.; Mioskowski, C. *J. Am. Chem. Soc.* **2001**, *123*, 9196–9197

(43) Dess, D. B.; Martin, J. C. *J. Org. Chem.* **1983**, *48*, 4155–4156.

(44) Still, W. C.; Gennari, C. *Tetrahedron Lett.* **1983**, *24*, 4405–4408.

(45) Kiyooka, S.; Kaneko, Y.; Komura, M.; Matsuo, H.; Nakano, M. *J. Org. Chem.* **1991**, *56*, 2276–2278.

(46) Mitsunobu, O.; Yamada, M. *Bull. Chem. Soc. Jpn.* **1967**, *40*, 2380–2382.

(47) Barton, D.; McCombie, S. *J. Chem. Soc. Perkin Trans. 1* **1975**, 1574–1585.

(48) Satoh, Y.; Kawamura, D.; Yamaura, M.; Ikeda, Y.; Ochiai, Y.; Hayakawa, I.; Kigoshi, H. *Tetrahedron Lett.* **2012**, *53*, 1390–1392.

(49) (a) Wittig, G.; Schöllkopf, U. *Chem. Ber.* **1954**, *87*, 1318–1330; (b) Inhoffen, H. H.; Kath, J. F.; Brückner, K. *Angew. Chem*. **1955**, *67*, 276–278.

(50) Satoh, Y.; Yamada, T.; Onozaki, Y.; Kawamura, D.; Hayakawa, I.; Kigoshi, H. *Tetrahedron Lett.* **2012**, *53*, 1393–1396.

(51) Hayakawa, I.; Okamura, M.; Suzuki, K.; Shimanuki, M.; Kimura, K.; Yamada, T.; Ohyoshi, T.; Kigoshi, H. *Synthesis.* **2017**, *49*, 2958–2970.

(52) Liron, F.; Fosse, C.; Pernolet, A.; Roulland, E. *J. Org. Chem*. **2007**, *72*, 2220–2223.

(53) Nagao, Y.; Hagiwara, Y.; Kumagai, T.; Ochiai, M.; Inoue, T.; Hashimoto, K.; Fujita, E. *J. Org. Chem*. **1986**, *51*, 2391–2393.

(54) Kang, B. Applications of α-Chloroaldehydes toward the Synthesis of Natural Products, Ph.D. Thesis, Simon Fraser University, 2012, pp 1-325.

(55) Fan, H. Studies Toward the Total Synthesis of Biselides & Radical Fluorination of Aliphatic Compounds, M.Sc. Thesis, Simon Fraser University, 2014, pp. 1–96.

(56) Taron, M. Studies Toward the Total Synthesis of Biselide A, M.Sc. Thesis, Simon Fraser University, 2011, pp1–77.

(57) Kwon, D.Studies Towards the Total Synthesis of tetrahydrofuran-Containing Natural Products, M.Sc. Thesis, Simon Fraser University, 2016, pp 1–109.

(58) Kang, B.; Mowat, J.; Pinter, T.; Britton, R. *Org. Lett.* **2009**, *11*, 1717–1720.

(59) Kang, B.; Chang, S.; Decker, S.; Britton, R. *Org. Lett*. **2010**, *12*, 1716–1719.

(60) Halperin, S.; Kang, B.; Britton, R. *Syn.* **2011**, *12*, 1946–1953.

(61) Hoye, T. R.; Jeffrey, C. S.; Tennakoon, M.; Wang, J.; Zhao, H. *J. Am. Chem. Soc.* **2004**, *126*, 10210–10211.

(62) Wang, X.; Bowman, E. J.; Bowman, B. J.; Porco, J. A. *Angew. Chem. Int. Ed.* **2004**, *43*, 3601–3605.

(63) Nicolaou, K. C.; Estrada, A. A.; Zak, M.; Lee, S. H.; Safina, B. S. *Angew. Chem.Int. Ed.* **2005**, *44*, 1378–1382.

(64) Kenner, G. W.; Seely, J. H. *J. Am. Chem. Soc.* **1972**, *94*, 3259–3260.

(65) Masamune, S.; Bates, G. S.; Corcoran, J. W. *Angew. Chem. Int. Ed.* **1977**, *16*,585–607.

(66) Masamune, S.; Hayase, Y.; Schilling, W.; Chan, W. K.; Bates, G. S. *J. Am. Chem.Soc.* **1977**, *99*, 6756–6758.

(67) Corey, E. J.; Brunelle, D. J.; Nicolaou, K. C. *J. Am. Chem. Soc.* **1977**, *99*, 7359–7360.

(68) Paterson, I.; Watson, C.; Yeung, K.; Wallace, P. A.; Ward, R. A. *J. Org. Chem.* **1997**, *62*, 452–453.

(69) Trost, B. M.; Chisholm, J. D. *Org. Lett.* **2002**, *4*, 3743–3745.

(70) Ishihara, K.; Kubota, M.; Kurihara, H.; Yamamoto, H. *J. Org. Chem.* **1996**, *61*, 4560–4567.

(71) Boden, E. P.; Keck, G. E. *J. Org. Chem.* **1985**, *50*, 2394–2395.

(72) Corey, E. J.; Nicolaou, K. C. *J. Am. Chem. Soc.* **1974**, *96*, 5614–5616

(73) Smith, A. B.; Dong, S.; Brenneman, J. B.; Fox, R. J. *J. Am. Chem. Soc.* **2009**,*131*, 12109–12111.

(74) Mukaiyama, T.; Usui, M.; Saigo, K. *Chem. Lett.* **1976**, 49–50.

(75) Li, P.; Xu, J.-C. *Tetrahedron* **2000**, *56*, 8119–8131.

(76) Hughes, D. L.; Reamer, R. A. *J. Org. Chem.* **1996**, *61*, 2967–2971.

(77) Orsini, F.; Pelizzoni, F.; Ricca, G. *Tetrahedron Lett.* **1982**, *23*, 3945–3948.

(78) Gupta, A.S.; Dev, S. *J. Chromatogr.* **1963**, *12*,189–190.

(79) Ozcimder, M.; Hammers, W. E. *J. Chromatogr.,* **1980**, *187*, 307-310.

(80) Matthias, D.; Brabandt, W. Van; Dekeukeleire, S.; Dejaegher, Y.; Kimpe, N. De. *Chem. Eur. J.* **2008**, *14*, 6336–6340.

(81) Narasaka, K.; Pai, H. C. *Chem. Lett.* **1980**, 1415–1418.

(82) Chen, K. M.; Hardtmann, G. E.; Prasad, K.; Repi, O.; Shapiro, M. J. *Tetrahedron Lett.* **1987**, *28*, 155–158.

(83) Neises, B.; Steglich, W. *Angew. Chem. Int. Ed.* **1978**, *17*, 522–524.

(84) (a) Vougioukalakis, G. C. *Chem. Eur. J.* **2012**, *18*, 8868–8880; (b) Higman, C. S.; Lummiss, J. A. M.; Fogg, D. E. *Angew. Chem. Int. Ed.* **2016**, *55*, 3552–3565. (c) (1) Wheeler, P.; Phillips, J. H.; Pederson, R. L. *Org. Process Res. Dev.* **2016**, *20* (7), 1182–1190.

(85) Mi Ahn, Y.; Yang, K.; Georg, G. I. *Org. Lett*. **2001**, *3*, 1411–1413.

(86) Paquette, L. A.; Schloss, J. D.; Efremov, I.; Fabris, F.; Gallou, F.; Amdino, J. M.; Yang, J. *Org. Lett*. **2000***, 2*, 1259–1261.

(87) Galan, B. R.; Kalbarczyk, K. P.; Szczepankiewicz, S.; Keister, J. B.; Diver, S. T. *Org. Lett*. **2007***, 9*, 1203-1206.

(88) Heine, N.; Ast, T.; Schneider-Mergener, J.; Reineke, U.; Germeroth, L.; Wenschuh, H. *Tetrahedron* **2003**, *59* (50), 9919–9930.

(89) Bowden, K.; Heilbron, I. M.; Jones, E. R. H.; Weedon, B. C. L. *J. Chem. Soc.* **1946**, *39*; (b) Djerassi, C.; Engle, R. R.; Bowers, A. *J. Org. Chem. **1956**, 21,* 1547–1549.

Chapter 3.

A Counterintuitive Stereochemical Outcome from a Chelation-Controlled Vinylmetal Aldehyde Addition Leads to the Configurational Reassignment of Phormidolide A

This chapter contains the manuscript "***A counterintuitive stereochemical outcome from a chelation-controlled vinylmetal aldehyde addition leads to the configurational reassignment of phormidolide A***", which was published in Chemical Communications (**2019**, *55*, 9717-9720). Headings ('Abstract', 'Introduction', 'Results and discussion' and 'Conclusion') not present in the manuscript are included herein for clarity.

Nelson Y. S. Lam[A]†, Garrett Muir[B]†, Venugopal Rao Challa[B], Robert Britton[B]* and Ian Paterson[A]*

[A]University Chemical Laboratory, Lensfield Road, Cambridge, CB2 1EW, UK.

[B]Department of Chemistry, Simon Fraser University, 8888 University Drive, Burnaby, British Columbia, V5A 1S6, Canada.

The thesis author contributed laboratory work (experiments, optimization of conditions, purification and characterization of compounds **8**-**13,** as shown in scheme 3.2). All other laboratory work and detailed NMR spectroscopic studies were performed by Garrett Muir and Nelson Y.S. Lam.

3.1. Abstract

As part of our ongoing studies towards the total synthesis of phormidolide A (1), we explored the chelation-controlled vinylmetal addition of fragment **2** to aldehyde **3** to install the reported 17*S* configuration. While the stereochemical outcome of this reaction was opposite to that expected, detailed NMR comparisons with the previously reported triacetonide derivative of phormidolide A (**18**) highlighted that the major adduct was a better match to the natural product. The synthesis of three model acetonides and detailed spectroscopic comparisons to the triacetonide derivative of phormidolide A supports a reassignment of seven of the 11 stereocentres in phormidolide A (**1a**).

3.2. Introduction

Phormidolide A (**1**, Fig. 3-1) is a complex polyketide isolated by the Gerwick group in 2002 from the marine cyanobacterium *Leptolyngbya* sp. collected off the coast of Sulawesi, Indonesia.[1,2] It possesses 11 stereocentres, four in the tetrahydrofuran-embedded macrolactone and seven in the elaborate polyol side chain, terminating in the signature bromomethoxydiene motif. Phormidolide A was reported to be inactive in the NCI 60 cell line assay, though it exhibited potent brine shrimp toxicity.[1] Interestingly, the structurally related natural products phormidolide B and C showed micromolar toxicity across various cancer cell lines,[3] potentially suggesting a yet unknown mechanism of action in eukaryotic cells for phormidolide A. At the time of its isolation, the relative stereochemistry of phormidolide A was wholly determined through application of Murata's *J*-based method,[4] taking into account NOE correlations, $^{2/3}J$ homo and heteronuclear coupling constants to ascertain the configuration of all 11 stereogenic centres. The relative stereochemistry of the all-*syn* polyol side chain was corroborated through the preparation of the corresponding diacetonide, with the absolute configuration initially determined through a variable-temperature NMR experiment with a methoxyphenyl acetic acid derivative of the C7 alcohol,[1] and subsequently by the preparation and analysis of the two diastereomeric Mosher esters of a phormidolide A triacetonide derivative at the same position.[2] Through the synthesis of a series of model C10-C23 diacetonides and detailed NMR spectroscopic comparisons with the triacetonide derivative of phormidolide A, we herein report the stereochemical reassignment of phormidolide A from **1** to **1a**

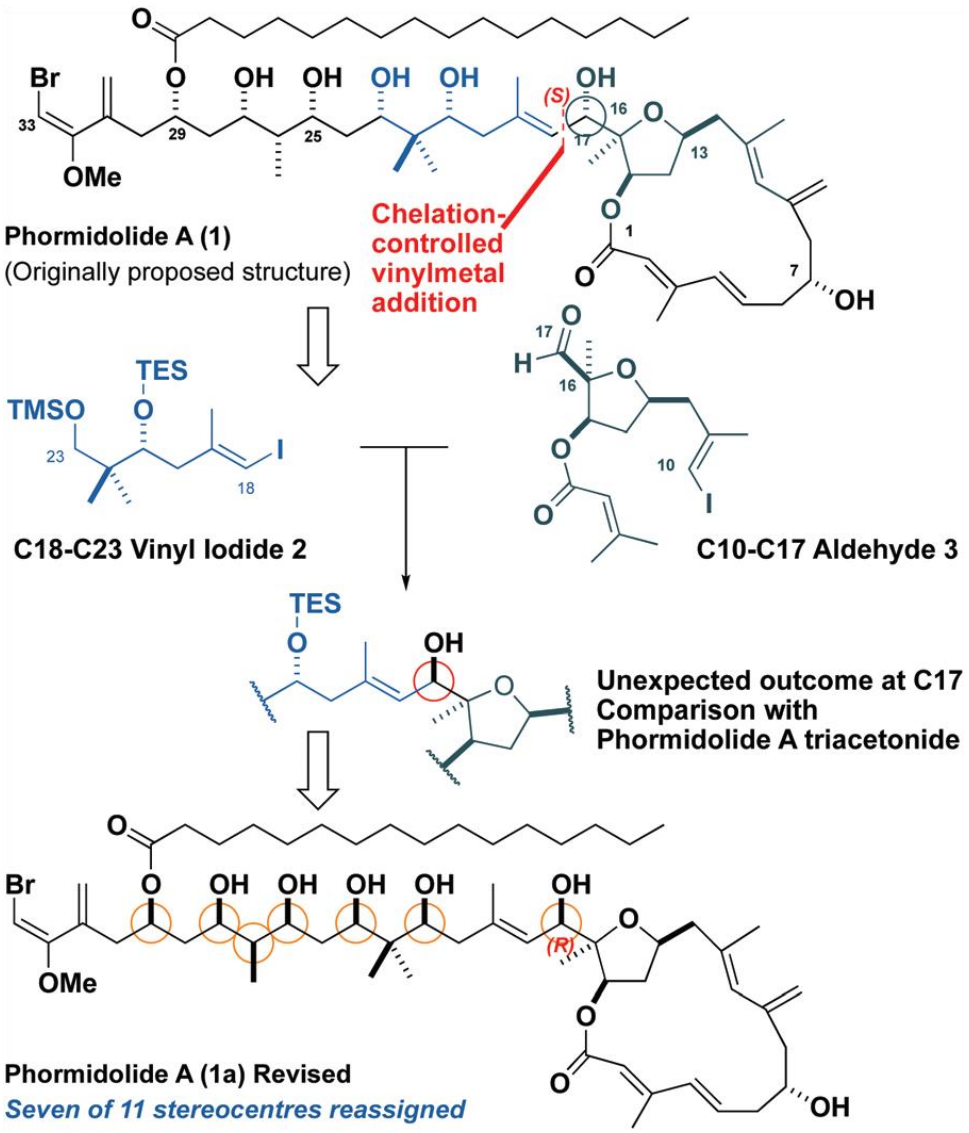

Figure 3-1 The originally proposed structure for phormidolide A (1).

Our approach to phormidolide A (**1**) hinges upon a chelation-controlled vinylmetal aldehyde addition to give the reported 17S configuration. The unexpected outcome favouring 17*R* from this reaction led us to reassign seven of the 11 stereocentres of phormidolide A. (**1a**)

3.3. Results and Discussion.

Drawn to its gamut of structural features and elusive but potentially interesting biological activity, we sought to embark on a synthetic campaign towards phormidolide A.[5] Noting that the side chain was a conserved structural feature across related congeners (including oscillariolide),[3] we chose to disconnect across C17-C18 via a vinylmetal

addition[6] to reveal the macrolactone C17 aldehyde and the C18-C33 side chain. We surmised that the reported 17*S* configuration could be set up *via* a chelation-controlled aldehyde addition with the nucleophile selectively approaching from the side of the small methyl substituent at C16.

To test this rationale, a facile route to the truncated C18-C23 vinyl iodide **2** and C10-C17 aldehyde **3** was developed. Vinyl iodide **2** (Scheme 3-1) was obtained from a Negishi carbalumination[7] of 3-butyn-1-ol followed by oxidation to afford the sensitive aldehyde **4**. An asymmetric Mukaiyama aldol reaction[8] with silyl ketene acetal **5** mediated by the chiral Lewis acid **6**[9] gave adduct **7** (91% *ee*, see the ESI). Subsequent TES ether formation, reduction (DIBAL) and TMS protection afforded the C18-C23 vinyl iodide **2** in six steps.

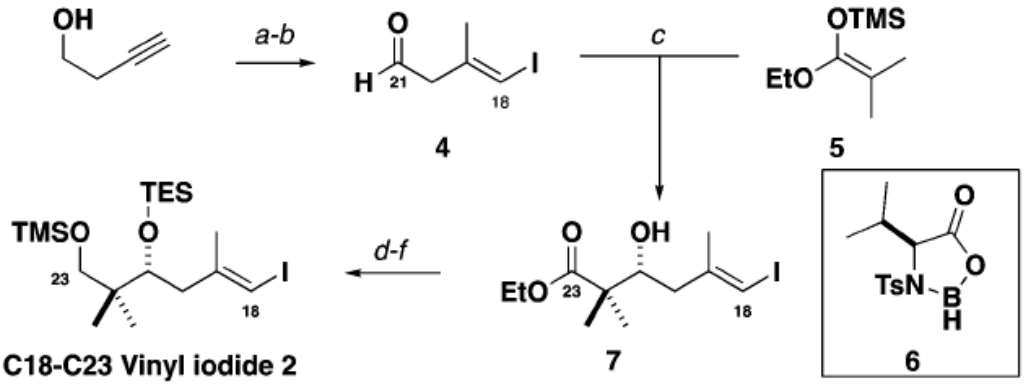

Scheme 3-1 Synthesis of the C18-C23 vinyl iodide 2

Reagents and conditions: (a) Cp_2ZrCl_2 (20 mol%), $AlMe_3$, H_2O, CH_2Cl_2, –20 °C to r.t.; I_2, Et_2O, –20 °C to r.t., 87% (b) DMP, $NaHCO_3$, CH_2Cl_2; (c) L-Ts-valine, $BH_3{\cdot}SMe_2$, CH_2Cl_2/THF (9:1), 0 °C; **4**, **5**, –78 °C, 67% over two steps, 91% *ee*; (d) TESOTf, 2,6-lutidine, CH_2Cl_2, –78 °C, 98%; (e) DIBAL, CH_2Cl_2, –78 to –20 °C, 90% brsm; (f) TMSCl, Et_3N, DMAP, CH_2Cl_2, 91%

Synthesis of the C10-C17 aldehyde **3** (Scheme 3-2) commenced with a Negishi carbalumination of 4-pentyn-1-ol, followed by oxidation to provide aldehyde **8**. At this point, an L-proline-catalysed tandem α-chlorination/aldol reaction[10] with ketone **9** that proceeds *via* a dynamic kinetic resolution was employed to generate the chlorohydrin **10** as a separable mixture of diastereomers (98% *ee*, 5.3:1 *dr*, see the ESI). Subsequent Grignard addition (MeMgBr) provided alcohol **11** (6:1 *dr*), whereby an S_N2 displacement and *in situ*

acetal deprotection under microwave conditions gave triol **12**. This was then protected as the cyclic siloxane, triflated (Tf_2O, py) and reduced ($[Bu_4N][BH_4]$) to afford **13**. Recognising that the configuration at C15 needed to be inverted, a global desilylation (TBAF), monoprotection (TBSCl), then oxidation of alcohol **14** followed by reduction (DIBAL) afforded the epimeric alcohol **15** as a single diastereomer. Noting that the natural product contains an α,β-unsaturated ester motif at C15 and recognising that our model system required suitable functionalities to mirror the natural product, we transformed alcohol **15** into the dimethylacrylate ester **16** (DCC, DMAP, DMAP·HCl).[11,12] Finally, desilylation of **16** followed by a Dess-Martin oxidation gave the C10-C17 aldehyde **3** in 12 steps.

With both C18-C23 vinyl iodide **2** and C10-C17 aldehyde **3** in hand, we explored the planned vinylmetal addition using the in situ generated Grignard species (Scheme 3-3, Method a).[6] Encouragingly, we obtained a 5:1 mixture of alcohols, epimeric at C17 in 77% yield. To unambiguously ascertain the stereochemistry and noting that the triacetonide derivative of phormidolide A (**18**) was known,[2] we transformed **17a** into the corresponding diacetonide (PPTS, MeOH; K_2CO_3, MeOH; PPTS, $(MeO)_2CMe_2$). Unexpectedly, analysis of the ^{13}C chemical shifts and NOE enhancements from the diacetonide revealed that we had in fact formed the 15, 17-*anti* acetonide *anti*-**19a**, corresponding to the 17*R* configuration (i.e. the epimer of the expected structure). Next, we conducted the vinyl lithium addition by omitting $MgBr_2·OEt_2$ (Method b), expecting to favour the 17*S* adduct dictated by polar Felkin-Anh rather than chelation control.

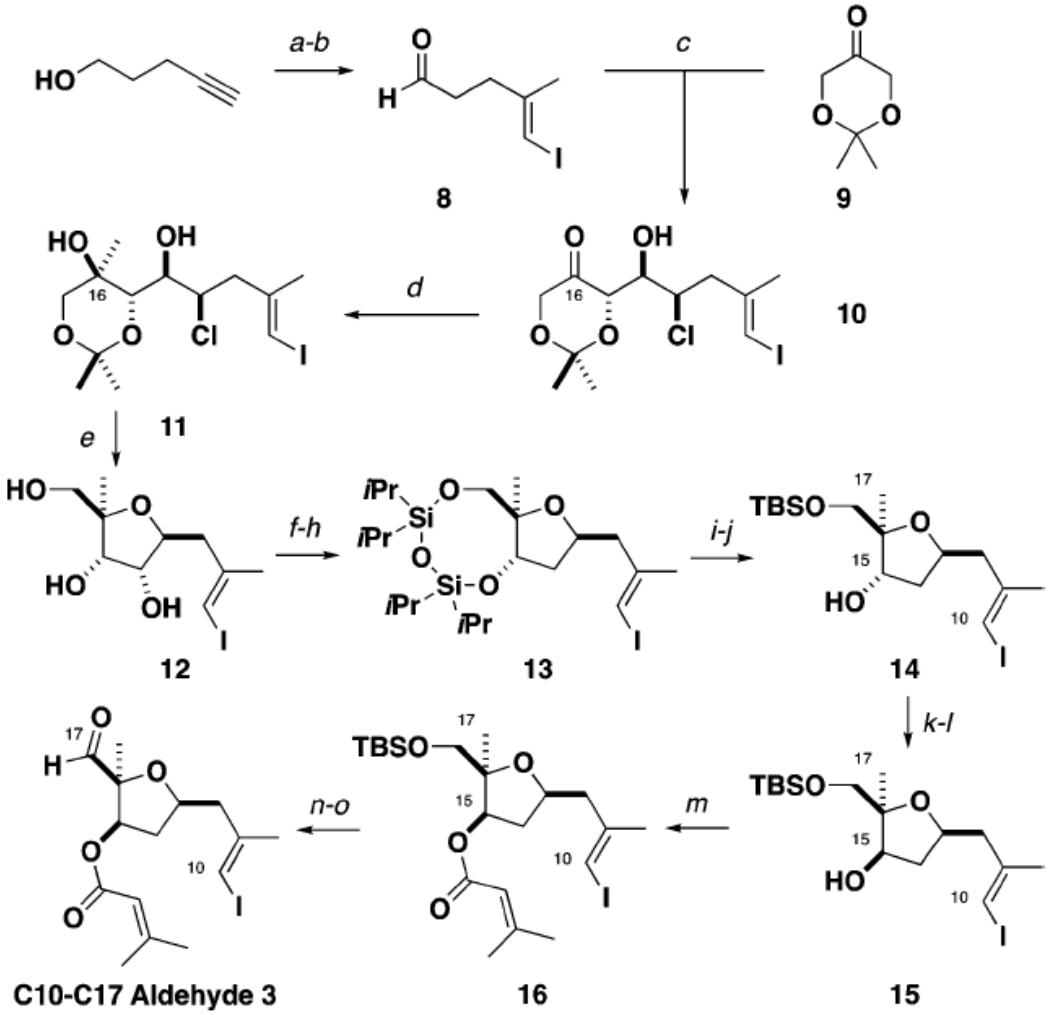

Scheme 3-2 Synthesis of the C10-C17 aldehyde 3

Reagents and conditions: (a) Cp_2ZrCl_2 (30 mol%), $AlMe_3$, H_2O, CH_2Cl_2, –20 °C to r.t.; I_2, Et_2O, –20 °C to r.t., 87% (b) DMP, $NaHCO_3$, CH_2Cl_2, 95%; (c), **8**, NCS, L-Proline, CH_2Cl_2; **9**, CH_2Cl_2, 47%, 98% *ee*, 5.3:1 *dr*; (d) MeMgI, CH_2Cl_2, –78 °C, 49%, 6:1 *dr*; (e) MeOH, µwave, 110 °C, 67%; (f) TIPSDSiCl$_2$, py, CH_2Cl_2, 89%; (g) Tf_2O, py, CH_2Cl_2 (h) [*n*Bu_4N][BH_4], PhMe, 55 °C, 68% over two steps; (i) HCl, MeOH, 84%; (j) TBSCl, imid., CH_2Cl_2, 83%; (k) DMP, $NaHCO_3$, CH_2Cl_2, 99%; (l) DIBAL, CH_2Cl_2, –78 °C, 99%, >20:1 *dr*; (m) 3,3-dimethylacrylic acid, DCC, DMAP, DMAP·HCl, CH_2Cl_2, 93%; (n) TsOH·H_2O, CH_2Cl_2/MeOH (1:1), 68%; (o) DMP, $NaHCO_3$, CH_2Cl_2, 86%, brsm

The vinyl lithium addition indeed delivered the other epimer **17b**, which yielded the diacetonide *syn*-**19b** corresponding to the originally proposed 17*S* configuration for phormidolide A (see the ESI). Interestingly, the NMR data for 15, 17-*syn*-**19b** did not match that reported for the analogous region of triacetonide **18**. In particular, through

Rychnovsky's acetonide analysis,[13] the ^{13}C NMR shifts for the two acetonide methyl groups (19.2 and 30.0 ppm for *syn*-**19b**) compared with **18** (25.3 and 23.7 ppm for **18**) appeared to us to be diagnostic for the 15,17-*anti* rather than the originally proposed 15, 17-*syn* stereochemistry.

At this juncture, it appeared that the configuration of one of the two stereocentres in the 15, 17-acetonide in **18** was misassigned. Analysis of chemical shifts, NOE data and comparison between intermediates **14**, **15** and the natural product supports the configuration at C15 (see the ESI), leaving C17 as the likely suspect stereocentre. A reanalysis of the reported $^{3}J_{CH}$, $^{3}J_{HH}$ and NOE data for phormidolide A indeed provided evidence that the natural product possessed the 17*R* configuration rather than the reported 17*S* configuration. This observation suggested that the Grignard nucleophile in the chelation-controlled addition preferentially approached the C17 carbonyl from the face opposite the C16 methyl group (Scheme 3- 4, TS-I), indicating that it was exerting a disproportionately large steric influence over the preferred trajectory of the incoming nucleophile, so disfavouring TS-II.[14]

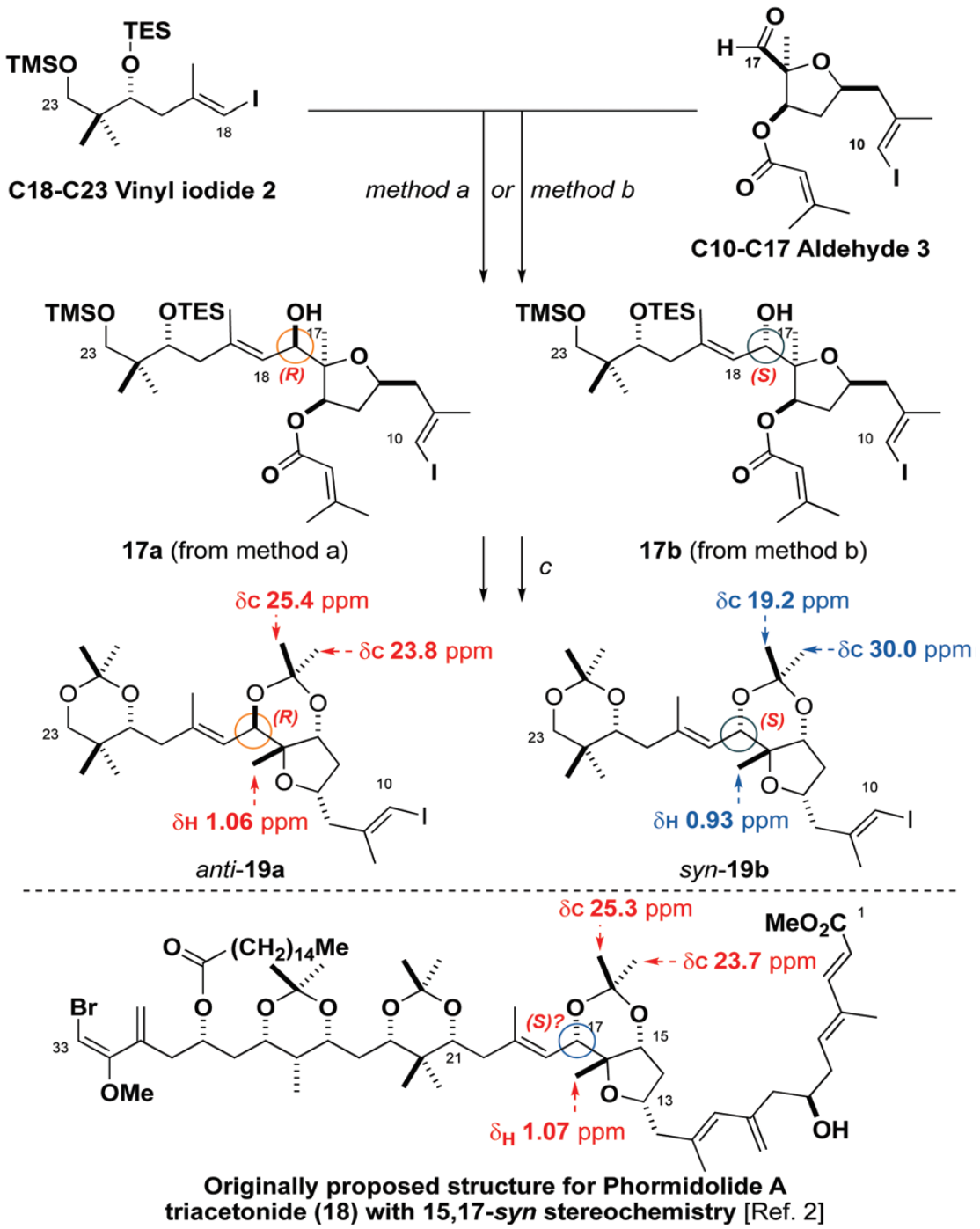

Scheme 3-3 Synthesis of diastereomeric acetonides *anti*-19a and *syn*-19b

Reagents and conditions: (a) **2**, *t*BuLi, Et_2O, –78 °C; $MgBr_2{\cdot}OEt_2$, Et_2O, –78 °C ; **3**, CH_2Cl_2, –78 °C, 77%, 5:1 *dr*; (b) **2**, *t*BuLi, Et_2O, –78 °C; 3, CH_2Cl_2, –78 °C, 37%, 4:1 *dr*; (c) PPTS, MeOH; K_2CO_3, MeOH; PPTS, 2,2-dimethoxypropane, CH_2Cl_2, 24% over three steps for *anti*-**19a**, 69% over three steps for *syn*-**19b**. The structure and the diagnostic ^{13}C and ^{1}H NMR shifts reported for phormidolide A triacetonide **18** are shown for comparision.

Following our reassignment of C17 to the *R* configuration, it was prudent to check whether or not C21, and the remainder of the side chain were configured correctly. In pursuit of this, the enantiomeric C18-C23 vinyl iodide *ent*-**2** was prepared. A chelation-controlled vinyl Grignard addition gave predominantly the alcohol **17c** (Scheme 3-4), and the corresponding diacetonide 21-*epi*-*anti*-**19c** was prepared.

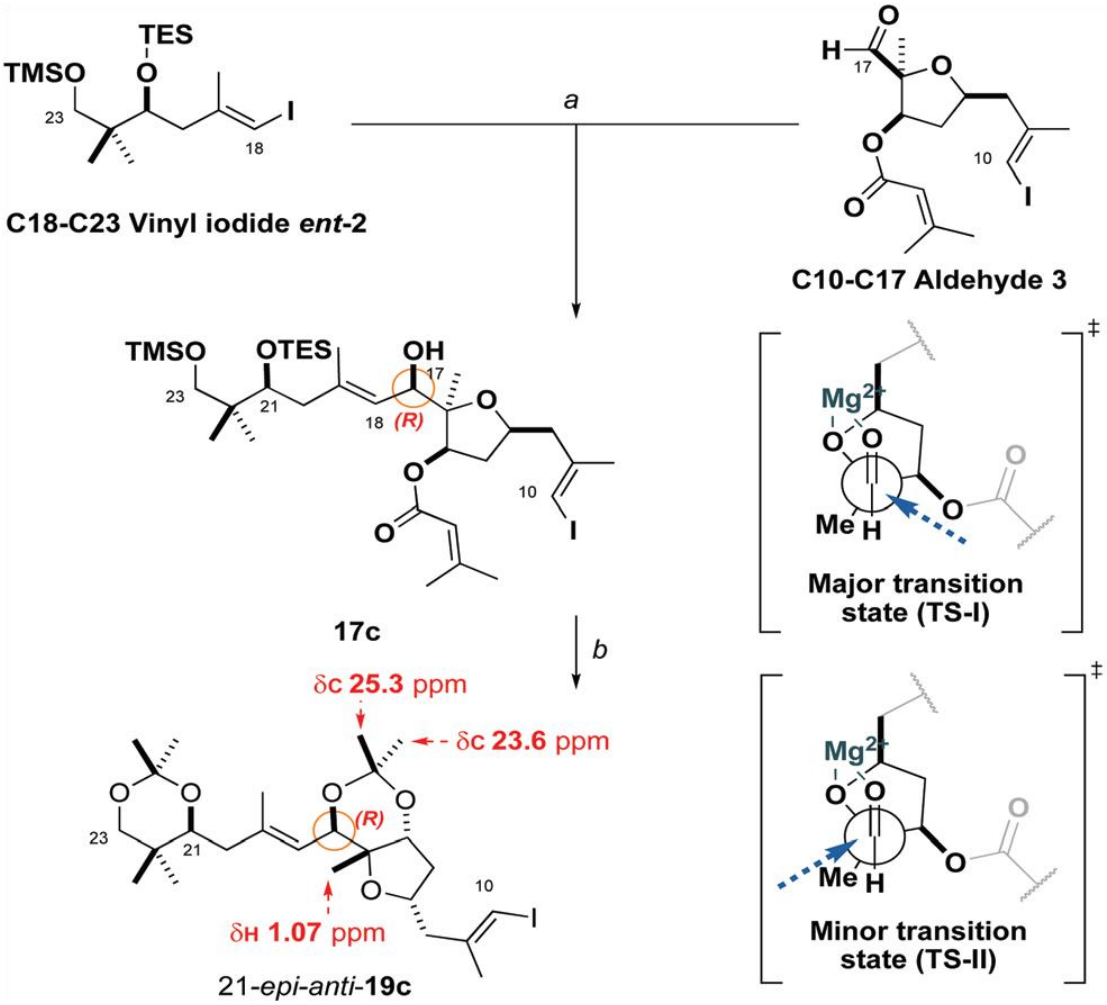

Scheme 3-4 Synthesis of 21-*epi*-*anti*-19c

Reagents and conditions: (a) *ent*-**2**, *t*BuLi, Et_2O, –78 °C; $MgBr_2 \cdot OEt_2$, Et_2O, –78 °C ; **3**, CH_2Cl_2, –78 °C, 77%, 5:1 *dr*; (b) PPTS, MeOH; K_2CO_3, MeOH; PPTS, 2,2-dimethoxypropane, CH_2Cl_2, 48% over three steps. The major transition state TS-I is proposed outlining the observed diastereoselectivity of the vinylmetal addition into aldehyde **3**

With the three diastereomeric diacetonides in hand, a thorough spectroscopic comparison to the phormidolide A triacetonide **18** was undertaken. Analysis of ^{1}H and ^{13}C NMR shifts revealed that the diacetonide 21-*epi*-*anti*-**19c** (Table 3-1, entry 1) matched the triacetonide derivative of the natural product much better than diacetonide *anti*-**19a** (Table 3-1, entry 2 and Fig.3- 2). Notably, diacetonide *syn*-**19b** corresponding to the originally proposed (17*S*, 21*R*) configuration was the poorest match (Table 3-1, entry 3), even by excluding the signals attributed to the acetonide (Fig. 3-2). As the relative configuration of the remainder of the side chain was relayed back to C21 *via J*-based methods,[1] and confirmed *via* the previously synthesised diacetonide derivative of phormidolide A,[1,2] we propose that the configuration of **1** should be reassigned to 21*S*, 23*R*, 25*S*, 26*R*, 27*R* and 29*R*, as shown in **1a** (Fig. 3-1).

Subsequent to their isolation paper, the Gerwick group reported a detailed analysis of the biosynthesis of phormidolide A. Here, they noted that the ketoreductases responsible for setting carbinol configuration were inconsistent with the absolute stereochemistry proposed for the natural product.[2] Specifically, it was noted that Type B-like ketoreductases present in the phormidolide A polyketide synthase system catalyse the formation of D-OHs in polyketide motifs.[15] However, the original isolation report presents all 10 carbinol stereocentres as L configured. Our proposed reassignment of the six carbinol stereocentres as D-configured in **1a** is also consistent with the stereochemistry predicted by analysis of the ketoreductase domain (see the ESI), which now gives a better rationalisation for the biosynthesis of phormidolide A.

Table 3-1 Sum of absolute errors |Δ| (ppm)[a][b] for each diastereomer compared to the reported spectra of phormidolide triacetonide 18.[2]

Entry		Sum |Δ| ^{1}H	Max |Δ| ^{1}H	Sum |Δ| ^{13}C	Max |Δ| ^{13}C
1.	21-*epi*-*anti*-**19C**	**0.24**	**0.08**	**3.2**	**1.5**
2.	*anti*-**19a**	0.32	0.11	8.2	2.7
3.	*syn*-**19b**	1.34	0.37	30.0	8.2

[a] Absolute errors taken for NMR shifts between H/C10-H/C21 inclusive of acetonide proton and carbons
[b] |Δ| = δ(Experimental shift) – δ (Reported shift), errors in ppm

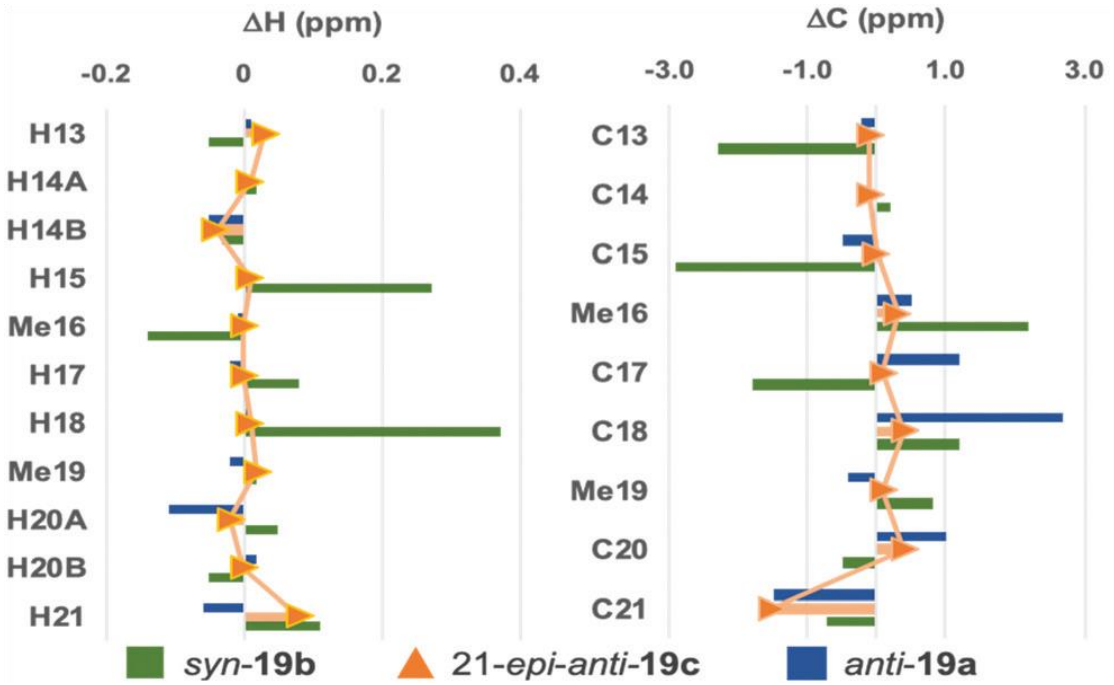

Figure 3-2 Bar graph highlighting the ^{1}H (left) and ^{13}C (right) NMR chemical shift differences between diacetonides *syn*-**19b**, *anti*-**19a**, 21-*epi*-*anti*-**20c** with phormidolide A triacetonide **18** between H10/C10 and H21/C21, overlaid with a line graph for 21-*epi*-*anti*-**19c.** The errors for the acetonide methyl groups and C16 are omitted as the very large errors caused by *syn*-**19b** obfuscates the deviations for the remainder of the ^{1}H and ^{13}C signals.

3.4. Conclusion

In summary, an unexpected stereochemical outcome from a chelation-controlled vinyl Grignard addition of **2** into aldehyde **3** prompted a re-examination of the stereochemical assignment of phormidolide A. Subsequent NMR analyses of three diastereomeric diacetonides *anti*-**19a**, *syn*-**19b** and 21-*epi*-*anti*-**19c** revealed the relative configuration between C21, C17 and the macrolactone. Combining this with the previously reported analysis then resulted in the reassignment of seven of the 11 stereocentres, leading to the revised structure **1a**. Importantly, this work validates the choice of suitable fragments as well as a key fragment union strategy for our on-going total synthesis campaign directed at **1a**, and reaffirms the power of synthesis in its role in the unambiguous stereochemical elucidation of complex natural products.[16]

3.5. Experimental

3.5.1. General Procedures

Unless the reaction contained aqueous reagents or otherwise stated, all reactions were carried out under an atmosphere of argon, using oven dried glassware and standard techniques for handling air sensitive chemicals.

Reagents were purified using standard laboratory procedures; benzene, dichloromethane and dichloroethane were distilled from CaH_2 and stored under argon. THF and Et_2O were distilled from potassium or sodium wire/benzophenone ketyl radical and stored under argon, 2,6-lutidine, *i*Pr_2NH, DIPEA and Et_3N were distilled from CaH_2 and stored over CaH_2 under argon. DMF was distilled from $MgSO_4$ and stored over 4 Å molecular sieves. Solvents used for extraction and chromatography were distilled. All other chemicals were used as received from the supplier unless otherwise stated. Aqueous solutions of ammonium chloride (NH_4Cl), sodium bicarbonate ($NaHCO_3$), sodium thiosulfate ($Na_2S_2O_3$), brine (NaCl) and sodium/potassium (Na/K) tartrate were saturated. Buffer solutions were prepared as directed from stock tablets.

Flash column chromatography was carried out using Kieselgel 60 (230-400 mesh) and a positive solvent pressure. TLC was carried out using Merck Kieselgel 60 F_{254} plates, which were visualised under UV light (254 nm) and stained with potassium permanganate or phosphomolybdic acid/$Ce_2(SO_4)_3$ dips.

NMR spectra were recorded using the following machines: Bruker Avance II (600 MHz), Bruker Avance 500 BB (500 MHz), Avance TCI cryoprobe (500 MHz) and Avance 400 DRX (400 MHz). ^{1}H spectra were recorded at 298 K with an internal deuterium lock for the residual undeuterated solvent: $CDCl_3$ (δ_H = 7.26 ppm) and DMSO-d_6 (δ_H = 2.50 ppm). ^{1}H data are presented as: chemical shift (δ / ppm), relative to tetramethylsilane (δ_{TMS} = 0 ppm), integration, multiplicity (s = singlet, d = doublet, t = triplet, q = quartet, qn = quintet, sext = sextet, sept = septet, m = multiplet, br = broad, app = apparent, obs = obscured) and coupling constants (*J* in Hz). Signals are assigned according to the numbering scheme for phormidolide (*vide infra*) unless otherwise indicated. Assignments have been made based on 1D data presented along with 2D spectra and comparison with fully assigned spectra for similar compounds. ^{13}C NMR spectra were recorded at 298 K

with broadband proton decoupling and an internal deuterium lock for ^{13}C: $CDCl_3$ (δ_C = 77.0 ppm) or DMSO-d_6 (δ_H = 39.5 ppm). Data are listed by chemical shift (δ / ppm) relative to tetramethylsilane ($\delta_{TMS} = 0$ ppm).

Fourier transform IR spectroscopy (FT-IR) was carried out using a Perkin-Elmer Spectrum-One spectrometer and spectra were recorded as a thin film. Wavelengths of maximum absorption (ν_{max}) are reported in wavenumbers (cm^{-1}). Optical rotations were measured using a Perkin-Elmer 241 polarimeter at the sodium D-line (589 nm) and are reported as $[\alpha]_D^{20}$, concentration (*c* in g/100 mL) and solvent used. High resolution mass spectrometry (HRMS) was carried out by the EPSRC National Mass Spectrometry Facility (Swansea, UK) using electrospray ionisation (ESI). The parent ion $[M+H]^+$ or $[M+Na]^+$ is quoted. Chiral HPLC was carried out on a Shimadzu XR-LC system, using a Chiralpak® IA column and a solvent system of mixed hexanes and isopropanol.

The numbering system used for the carbon skeleton of phormidolide A follows that of Williamson *et al.*[1], with the exception of skeletal substitutions (e.g. hydroxyl, methyl, methoxy and methylene groups), which are denoted by the skeletal carbon to which they are attached. The complete numbering scheme for phormidolide A (**1**) is shown below:

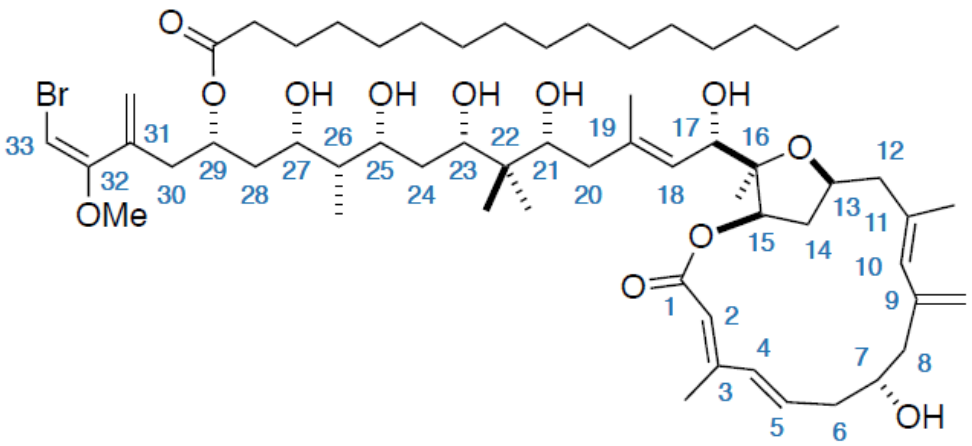

*Numbering scheme for the originally proposed structure of phormidolide A (**1**)*

3.5.2. Synthesis of the C18-C23 Vinyl Iodide

Alcohol – 4a

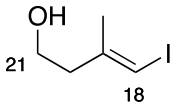

$AlMe_3$ (47.0 mL, 93.9 mmol) was added to a solution of Cp_2ZrCl_2 (1.95 g, 6.67 mmol) in CH_2Cl_2 (90 mL) at –20 ˚C. The solution was stirred for 10 min at –20 ˚C, before the addition of water (845 µL, 47.0 mmol). The pale-yellow suspension was stirred for 10 min at –20 ˚C. A solution of 3-butyn-1-ol (2.12 g, 30.3 mmol) in CH_2Cl_2 (20 mL) was treated with $AlMe_3$ (4.70 ml, 9.39 mmol) and transferred *via* cannula into the reaction. The reaction mixture was stirred for 16 h, with gradual warming to r.t., during which a yellow suspension formed. A solution of I_2 (9.16 g, 36.4 mmol) in Et_2O (200 mL) was transferred *via* cannula to the mixture at –20 ˚C, resulting in a colour change to vivid yellow, then brown. The reaction mixture was allowed to warm to r.t. and stirred for 2 h. The reaction was quenched by addition of Na/K tartrate (200 mL) and Et_2O (200 mL) and vigorously stirred at r.t. for 1.5 h. The layers were separated, and the aqueous phase was extracted with Et_2O (3 × 100 mL), dried ($MgSO_4$) and the solvent removed under reduced pressure to afford a yellow liquid. Purification by flash column chromatography (Et_2O/PE 30-40: 20% → 30%) afforded the product **4a** as a pale-yellow oil (5.22 g, 26.4 mmol, 87%).

R_f (Et_2O/PE 30-40: 50%) = 0.54

^{1}H NMR (400 MHz, $CDCl_3$) δ_H 6.01 (1H, q, *J* = 1.0 Hz, H18), 3.72 (2H, t, *J* = 6.3 Hz, H21), 2.48 (2H, t, *J* = 6.3, H20), 1.87 (3H, s, Me19).

^{13}C NMR (125 MHz, $CDCl_3$) δ_C 144.5, 76.8, 60.1, 42.4, 23.8.

Data in agreement with that presented by Penner[17]

Hydroxyester – 7 and *ent*-7

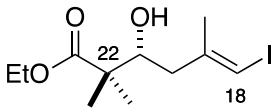

Dess-Martin Periodinane (2.50 g, 5.89 mmol) was added to a stirred suspension of alcohol **4a** (500 mg, 2.35 mmol) and $NaHCO_3$ (1.50 g, 17.8 mmol) in wet CH_2Cl_2 (25 mL). The reaction mixture was stirred at r.t. until TLC monitoring indicated full consumption of the starting material (ca. 1.5 h). The reaction was quenched by the addition of $NaHCO_3$ (20 mL) and $Na_2S_2O_3$ solution (20 mL) and stirred at r.t. for 30 min. The layers were separated, and the aqueous phase was extracted with CH_2Cl_2 (3 × 10 mL). The combined organic phases were washed with brine (50 mL), dried ($MgSO_4$) and concentrated under reduced pressure to ca. 10 mL. The solution of the crude aldehyde **4** was dried over 4 Å molecular sieves and directly used in the subsequent step without further purification. Aldehyde **4** was both volatile and highly prone to degradation, and an analytically pure sample was not obtained.

$BH_3 \cdot SMe_2$ (279 μL, 2.95 mmol) was added dropwise to a stirred solution of *N*-tosyl-L-valine[18] (799 mg, 2.95 mmol) in CH_2Cl_2 (7 mL) and THF (1 mL) at 0 °C. The solution was stirred at 0 °C for 1 h before cooling to –78 °C. A combined solution of the crude aldehyde **4** and the silyl ketene acetal **5**[19] (1.11 g, 5.89 mmol, dried over CaH_2) in CH_2Cl_2 (15 mL) was added *via* cannula to the reaction mixture. The reaction mixture was stirred at –78 °C for 3 h before quenching with $NaHCO_3$ solution. Upon warming to r.t., the layers were separated and the aqueous phase extracted with CH_2Cl_2 (3 × 40 mL). The combined organic phases were washed with brine (100 mL), dried ($MgSO_4$), and the solvent removed under reduced pressure. Purification by flash column chromatography (EtOAc/PE 40-60: 5%) afforded the product **7** as an orange oil (516 mg, 3.95 mmol, 67% over 2 steps, 91% e.e.).

The enantiomeric compound ***ent*-7** was analogously prepared from alcohol **4a** (1.00 g, 4.71 mmol), employing *N*-tosyl-D-valine (1.92 g, 7.07 mmol) as an orange oil (818 mg, 2.51 mmol, 53%)

R_f (EtOAc/PE 40-60: 30%) = 0.57

^{1}H NMR (400 MHz, $CDCl_3$) δ_H 6.02 (1H, q, *J* = 0.9 Hz, H18), 4.16 (2H, q, *J* = 7.1 Hz, $CH_3\underline{CH_2}O$), 3.81 (1H, ddd, *J* = 10.0, 5.6, 2.5 Hz, H21), 2.39 (1H, d, *J* = 5.6 Hz, OH), 2.33 (1H, br d, *J* = 13.2 Hz, H20a), 2.26 (1H, dd, *J* = 13.9, 10.0 Hz, H20b), 1.90 (3H, d, *J* = 0.9 Hz, Me19), 1.27 (3H, t, *J* = 7.1 Hz, $\underline{CH_3}CH_2O$), 1.20 (3H, s, Me22a), 1.20 (3H, s, Me22b).

^{13}C NMR (125 MHz, $CDCl_3$) δ_C 177.1, 145.1, 73.7, 60.8, 46.7, 42.0, 23.9, 21.6, 20.7, 14.2, 14.1.

IR (thin film): ν_{max} 3526, 2984, 1716, 1469, 1386, 1269, 1134, 1070.

$[\alpha]_D^{20}$ +13.9 (**7**, *c* 1.0, $CHCl_3$); $[\alpha]_D^{20}$ –12.6 (***ent*-7**, *c* 0.26, $CHCl_3$).

Chiral HPLC (Chiralpak® IA, *i*PrOH : *n*-hexane: 5%) R_T (major) 10.02 min, R_T (minor) 10.74 min.

HRMS (ESI^+) calculated for $C_{11}H_{20}O_3I$ $[M+H]^+$ 327.0452, found 327.0451.

Proof of absolute configuration at C21

Attempts at confirming the anticipated configuration[20,21] of hydroxyester **7** from the diastereomeric MTPA esters was inconclusive, yielding inconsistent signs across both sides of the MTPA esters. The absolute configuration at C21 was unambiguously ascertained through the synthesis of the corresponding MTPA esters of ketone **7b**. Experimental procedures for the synthesis of the diastereomeric MTPA esters are outlined below:

Ketone – 7b

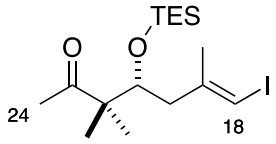

A solution of ester **7a** (42.5 mg, 0.182 mmol) in toluene (0.5 mL) was added *via* cannula to a stirred solution of methylmagnesium bromide (130 µL, 0.886 mmol, 3 M in Et_2O) and triethylamine (255 µL, 1.82 mmol) in toluene (2.5 mL). The mixture was heated to 80 °C and stirred until TLC monitoring indicated complete consumption of the starting material (ca. 4 h). The mixture was allowed to cool to r.t. and quenched with NH_4Cl solution

(2 mL). The layers were separated, and the aqueous phase extracted with Et_2O (3 × 3 mL). The combined organic phases were dried ($MgSO_4$) and the solvent removed under reduced pressure. Purification by flash column chromatography (EtOAc/PE 40-60: 4%) afforded the product **7b** as a pale-yellow oil (36.5 mg, 0.168 mmol, 92%).

R_f (EtOAc/PE 40-60: 30%) = 0.78

^{1}H NMR (400 MHz, $CDCl_3$) δ_H 5.93 (1H, q, *J* = 1.0 Hz, H18), 4.08 (1H, t, *J* = 5.7 Hz, H21), 2.20 (2H, d, *J* = 5.7 Hz, H20), 2.15 (3H, s, H24), 1.84 (3H, d, *J* = 1.0 Hz, Me19), 1.12 (3H, s, Me22a), 1.10 (3H, s, Me22b) 0.94 (9H, t, *J* = 8.0 Hz, $Si(CH_2\underline{CH_3})_3$), 0.57 (6H, q, *J* = 8.0 Hz, $Si(\underline{CH_2}CH_3)_3$).

^{13}C NMR (125 MHz, $CDCl_3$) δ_C 213.3, 144.5, 78.4, 74.6, 52.9, 44.4, 27.0, 23.9, 22.2, 19.8, 7.1, 5.4.

IR (thin film): ν_{max} 2945, 2910, 2876, 1702, 1459, 1353, 1238, 1088, 1004.

$[\alpha]_D^{20}$ +16.4 (*c* 0.5, $CHCl_3$).

HRMS (ESI$^+$) calculated for $C_{16}H_{32}O_2SiI$ $[M+H]^+$ 411.1211, found 411.1206.

Mosher esters – (*R*)-MTPA-7c and (*S*)-MTPA-7c

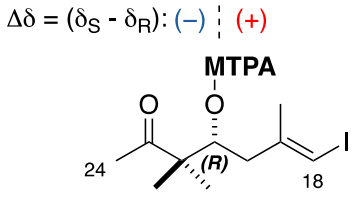

A solution of TBAF (54 µL, 53.6 µmol, 1 M in THF) was added to a stirred solution of TES ether **7b** (20 mg, 48.7 µmol) in THF (0.5 mL). The pale-yellow solution was stirred for 1 h at r.t. before being quenched with a solution of NH_4Cl (0.5 mL). The layers were separated, and the aqueous phase was extracted with Et_2O (3 × 1 mL). The combined organic phases were dried ($MgSO_4$) and the solvent removed under reduced pressure to afford the crude hydroxyketone (11 mg, 38.5 µmol, 79%), which was used directly in subsequent steps without purification.

***(R)-Mosher ester* – (R)-MTPA-7c**

DCC (54 µL, 54.0 µmol, 1 M in CH_2Cl_2) was added in portion to a stirred solution of crude hydroxyketone (4.0 mg, 13.5 µmol), *(R)*-MTPA (12 mg, 54.0 µmol) and DMAP (one crystal) in CH_2Cl_2 (500 µL). The mixture was stirred for 24 h at r.t., during which the solution became a white suspension. The mixture was filtered through cotton wool and the filtrate reduced to dryness. Purification by flash chromatography (EtOAc/PE 40-60: 10%) afforded the product **(*R*)-7c** as a colourless oil (4.0 mg, 7.80 µmol, 58%).

R_f (EtOAc/PE 40-60: 20%) = 0.48

^{1}H NMR (400 MHz, $CDCl_3$) δ_H 7.48-7.40 (5H, m, ArH), 5.94 (1H, s, H18), 5.66 (1H, dd, *J* = 9.8, 2.4 Hz, H21), 3.43 (3H, s, OMe), 2.43 (1H, dd, *J* = 14.3, 9.8 Hz, H20a), 2.31 (1H, d br, *J* = 14.3 Hz, H20b), 2.13 (3H, s, H24), 1.93 (3H, s, Me19), 1.17 (3H, s, Me22a), 1.15 (3H, s, Me22b).

***(S)-Mosher ester – (S)*-MTPA-7c**

DCC (54 µL, 54.0 µmol, 1 M in CH_2Cl_2) was added in portion to a stirred solution of crude hydroxyketone (4.0 mg, 13.5 µmol), *(S)*-MTPA (12 mg, 54.0 µmol) and DMAP (one crystal) in CH_2Cl_2 (500 µL). The mixture was stirred for 24 h at r.t., during which the solution became a white suspension. The mixture was filtered through cotton wool and the filtrate reduced to dryness. Purification by flash chromatography (EtOAc/PE 40-60: 10%) afforded the product **(*S*)-7c** as a colourless oil (4.6 mg, 8.97 µmol, 66%).

R_f (EtOAc/PE 40-60: 20%) = 0.48

^{1}H NMR (400 MHz, $CDCl_3$) δ_H 7.49-7.41 (5H, m, ArH), 5.95 (1H, s, H18), 5.69 (1H, dd, *J* = 10.1, 2.3 Hz, H21), 3.49 (3H, s, OMe), 2.45 (1H, dd, *J* = 14.4, 10.1 Hz, H20a), 2.30 (1H, br d, *J* = 14.4 Hz, H20b), 2.11 (3H, s, H24), 1.94 (3H, s, Me19), 1.13 (3H, s, Me22a), 1.12 (3H, s, Me22b).

Following the advanced Mosher model described by Hoye *et al.*,[22] the C21 centre arising from the enantioselective Mukaiyama aldol reaction was assigned as 21*R*.

Table 3-2 Diagnostic ^{1}H NMR signals for the configurational assignment of 21*R*

Proton	δH (*S*)-MTPA (ppm)	δH (*R*)-MTPA (ppm)	$\Delta\delta_{S-R}$ (ppm)
H24	2.11	2.13	–0.02
Me22a	1.13	1.17	–0.04
Me22b	1.12	1.15	–0.03
H21	5.69	5.66	+0.03
H20a	2.45	2.43	+0.02
H20b	2.32	2.31	+0.01
Me19	1.94	1.93	+0.01
H18	5.95	5.94	+0.01

Alcohol 7d and *ent*-7d

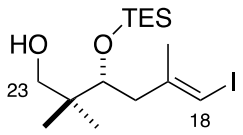

DIBAL (8.31 mL, 8.31 mmol, 1 M solution in hexanes) was added dropwise to a stirred solution of the ester **7a** (1.80 g, 4.16 mmol) in dichloromethane (42 mL) at –78 ˚C. The reaction mixture was stirred at –78 ˚C for 30 min before the addition of an extra aliquot of DIBAL (4.16 mL, 4.16 mmol, 1 M solution in hexanes). The reaction mixture was warmed to –40 ˚C over 1 h before quenching with the successive addition of MeOH (2 mL) and Na/K tartrate (30 mL). The mixture was allowed to warm to r.t. and stirred for 2 h. The layers were separated, and the aqueous phase extracted with dichloromethane (3 × 20 mL). The combined organic phases were washed with brine (20 mL), dried ($MgSO_4$) and the solvent removed under reduced pressure. Purification by flash column chromatography (EtOAc/PE 40-60: 10% → 20%) afforded the product **7d** as a colourless oil (1.31 g, 3.30 mmol, 79%, 90% brsm).

The enantiomeric alcohol ***ent*-7d** was analogously prepared from ester ***ent*-7a** (1.00 g, 2.27 mmol) as a colourless oil (720 mg, 1.82 mmol, 73%).

R_f (EtOAc/PE 40-60: 30%) = 0.80

^{1}H NMR (500 MHz, $CDCl_3$) δ_H 5.98 (1H, s, H18), 3.72 (1H, dd, *J* = 8.6, 2.6 Hz, H21), 3.67 (1H, dd, *J* = 10.7, 3.2 Hz, H23a), 3.28 (1H, dd, *J* = 10.7, 7.4 Hz, H23b), 2.66 (1H, dd, *J* = 7.4, 3.4 Hz, OH), 2.48 (1H, dd, *J* = 14.1, 2.6 Hz, H20a), 2.36 (1H, dd, *J* = 14.1, 8.6 Hz, H20b), 1.85 (3H, d, *J* = 0.6 Hz, Me19), 1.04 (3H, s, Me22a), 0.96 (9H, t, *J* = 8.1 Hz, $Si(CH_2\underline{CH_3})_3$), 0.80 (3H, s, Me22b), 0.59, 0.58 (6H, app dq, *J* = 8.0 Hz, $Si(\underline{CH_2}CH_3)_3$).

^{13}C NMR (125 MHz, $CDCl_3$) δ_C 144.8, 78.2, 78.0, 70.0, 43.7, 39.5, 24.0, 23.3, 21.5, 7.1, 5.4

IR (thin film): ν_{max} 3477, 2955, 2927, 1459, 1318, 1274, 1090, 1006.

$[\alpha]_D^{20}$ +17.8 (**7d**, *c* 0.15, $CHCl_3$); $[\alpha]_D^{20}$ −14.7 (***ent*-7d**, *c* 0.30, $CHCl_3$)

HRMS (ESI$^+$) calculated for $C_{15}H_{31}O_2SiIH$ $[M+H]^+$ 399.1216, found 399.1217.

C18-C23 vinyl iodide 2 and *ent*-2

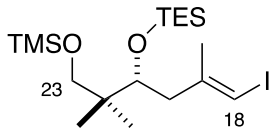

TMSCl (342 μL, 2.70 mmol) was added to a stirred solution of alcohol **7d** (855 mg, 2.16 mmol), Et_3N (451 μL, 3.24 mmol) and DMAP (26.0 mg, 21.6 μmol) in dichloromethane (25 mL) at r.t.. The reaction was stirred at r.t. for 1 h before quenching with MeOH (1 mL). The solvent was removed under reduced pressure and the residue resuspended in PE 40-60 before filtering over a pad of silica, eluting with PE 40-60. Removal of the solvent under reduced pressure afforded the C18-C23 vinyl iodide **2** as a colourless oil (924 mg, 1.96 mmol, 91%).

The enantiomeric C18-C23 vinyl iodide ***ent*-2** was analogously prepared from alcohol ***ent*-7d** (100 mg, 252 μmol) to afford the product as a colourless oil (89 mg, 189 μmol, 75%).

R_f (EtOAc/PE 40-60: 20%) = 0.66

^{1}H NMR (500 MHz, $CDCl_3$) δ_H 5.88 (1H, s, H18), 3.77 (1H, dd, *J* = 8.8, 2.4 Hz, H21), 3.34 (1H, d, *J* = 9.6 Hz, H23a), 3.22 (1H, d, *J* = 9.6 Hz, H23b), 2.37 (1H, dd, *J* = 13.6, 2.4 Hz,

H20a), 2.24 (1H, dd, *J* = 13.6, 8.8 Hz, H20b), 1.83 (3H, s, Me19), 0.94 (9H, t, *J* = 9.4 Hz, $Si(\underline{CH_2}CH_3)_3$), 0.82 (3H, s, Me22a), 0.79 (3H, s, Me22b), 0.55 (6H, q, *J* = 9.4 Hz, $Si(\underline{CH_2}CH_3)_3$), 0.08 (9H, s, $Si(CH_3)_3$)

^{13}C NMR (125 MHz, $CDCl_3$) δ_C 145.8, 74.0, 69.2, 43.4, 40.3, 24.0, 21.1, 20.2, 7.2, 5.5, –0.6;

IR (thin film): ν_{max} 2877, 2597, 1251, 1092, 1013, 874

$[\alpha]_D^{20}$ +9.6 (**2**, *c* 0.28, $CHCl_3$); $[\alpha]_D^{20}$ –9.0 (***ent*-2**, *c* 0.32, $CHCl_3$)

HRMS (ESI^+) calculated for $C_{18}H_{39}O_2Si_2IH$ $[M+H]^+$ 471.1612, found 471.1615.

3.5.3. Synthesis of C10-C17 Aldehyde

Vinyl iodide 8a

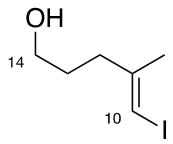

$AlMe_3$ (89 mL, 178 mmol, 2.0 M solution in hexane) was added dropwise to a stirred solution of Cp_2ZrCl_2 (5.20 g, 17.8 mmol) in dichloroethane (200 mL) at –30 °C. The solution was stirred at –30 °C for 5 min before the dropwise addition of H_2O (535 μL, 29.7 mmol) into the reaction mixture. The resultant mixture was allowed to warm to r.t. over 10 min before cooling to –30 °C. A solution of 4-pentyn-1-ol (5.53 ml, 59.4 mmol) in dichloroethane (97 mL) was added dropwise *via* cannula to the reaction mixture at –30 °C. The reaction mixture was allowed to warm to r.t. and stirred at r.t. for 20 h before cooling to – 30°C. A solution of I_2 (30.1 g, 119 mmol) in THF (59 mL) was added dropwise *via* cannula to the reaction mixture. The resulting mixture was stirred at – 30°C for a further 2 h before quenching with Na/K tartrate (200 mL), warming to r.t. and stirred for 16 h at r.t.. The resulting suspension was filtered to remove excess salts and the layers were separated. The aqueous layer was extracted with dichloromethane (3 × 100mL) and the combined organic phases were washed with brine (300 mL), dried ($MgSO_4$), and the solvent removed under reduced pressure. Purification by flash chromatography

(EtOAc/hexanes: 30% → 50%) gave the vinyl iodide **8a** as an orange oil (11.72 g, 51.8 mmol, 87%).

R_f (EtOAc/hexanes: 50%) = 0.40

^{1}H NMR (400 MHz, $CDCl_3$) δ_H 5.94 (1H, q, *J* = 1.2 Hz, H10), 3.65 (2H, t, *J* = 6.4 Hz, H14), 2.32 (2H, td, *J* = 7.5, 1.1 Hz, H12), 1.87 (3H, d, *J* = 1.2 Hz, Me11), 1.76-1.68 (2H, m, H13).

Data in agreement as presented by Clausen *et al.*[23]

Chlorohydrin 10

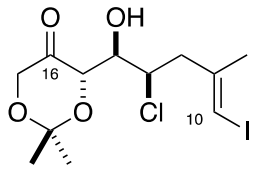

Dess-Martin Periodinane (18.87 g, 44.5 mmol) was added to a stirred suspension of alcohol **8a** (8.40 g, 37.1 mmol), $NaHCO_3$ (9.33 g, 111.0 mmol) in dichloromethane (123 mL). The reaction mixture was stirred at r.t. for 1 h before quenching with the addition of $NaHCO_3$ (50 mL), $Na_2S_2O_3$ (50 mL) and H_2O (50 mL). The mixture was stirred for 2 h before the layers were separated. The aqueous layer was extracted with dichloromethane (3 × 100 mL). The combined organic phases were washed with brine (300 mL), dried ($MgSO_4$), and the solvent removed under reduced pressure to afford the crude aldehyde **9** (8.04 g, 35.9 mmol, 95%), which was used directly in subsequent steps without purification.

NCS (4.31 g, 32.3 mmol) was added to a stirred solution of aldehyde **9** (8.04 g, 35.9 mmol), L-proline (3.72 g, 32.3 mmol) in dichloromethane (120 mL). The reaction was stirred at r.t. until complete chlorination of the aldehyde was observed by NMR (*ca.* 2 h). At this point, 2,2-dimethyl-1,3-dioxan-5-one (5.62 g, 43.1 mmol) was added and the reaction mixture was stirred at r.t. for 24 h. The reaction was quenched by addition of brine (100 mL) and the layers separated. The organic phase was washed with brine (100 mL) and the combined aqueous phases were extracted with dichloromethane (3 × 150 mL). The combined organic phases were dried ($MgSO_4$), and the solvent removed under reduced pressure. Purification by flash chromatography (EtOAc/hexanes: 10% → 25%)

afforded chlorohydrin **10** as a yellow oil (6.56 g, 16.9 mmol, 47%, 98% *ee*) as a separable 5.3 : 1 mixture of diastereomers.

R_f (EtOAc/hexanes: 20%) = 0.35

^{1}H NMR (600 MHz, $CDCl_3$) δ_H 6.15 (1H, q, *J* = 1.2 Hz, H10), 4.39 (1H, dd, *J* = 8.9, 1.5 Hz, H15), 4.33–4.26 (2H, m, H13, H17a), 4.08 (1H, d, *J* = 17.6 Hz, H17b), 3.88 (1H, ddd, *J* = 8.9, 3.0, 1.7 Hz, H14), 3.39 (1H, dd, J = 3.0, 1.4 Hz, OH), 2.80 (2H, dt, *J* = 7.7, 1.3 Hz, H12), 1.88 (3H, d, *J* = 1.1 Hz, Me11), 1.51 (3H, s, $\underline{Me}_AMe_BCO_2$), 1.43 (s, 3H, $Me_A\underline{Me}_BCO_2$).

^{13}C NMR (150 MHz, CDCl3) δ_c 212.4, 143.2, 101.8, 79.5, 72.8, 70.6, 66.5, 58.6, 43.8, 24.0, 23.9, 23.5.

IR : ν_{max} 3513, 2987, 1738, 1376, 1222, 1086, 863.

$[\alpha]_D^{20}$ –68.2 (*c* 1.54, $CHCl_3$).

Chiral HPLC (Chiralpak® IG, *i*PrOH : *n*-hexane: 1%) R_T (major) 3.47 min, R_T (minor) 2.98 min.

HRMS (ESI$^+$) calculated for $C_{12}H_{18}ClIO_4Na$ $[M+Na]^+$ 410.9830, found 410.9841.

Alcohol 11

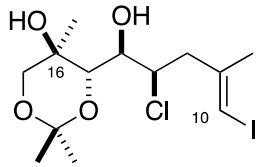

MeMgI (27.6 mL, 82.8 mmol, 3.0 M solution in Et_2O) was added dropwise to a stirred solution of chlorohydrin **9** (9.17 g, 23.6 mmol) in dichloromethane (79 mL) at –78 °C. The reaction was stirred at –78 °C for 24 h before quenching with HCl (100 mL, 1.0 M solution in H_2O) and warmed to r.t. The layers were separated, and the aqueous phase was extracted with dichloromethane (3 × 100 mL). The combined organic phases were washed with brine (300 mL), dried ($MgSO_4$), and the solvent removed under reduced pressure to afford the crude alcohol as a 6:1 mixture of diastereomers at C16. Purification

by flash chromatography (EtOAc/PE 40-60: 20% → 30%) afforded alcohol **11** as an off-white solid (4.69 g, 11.6 mmol, 49%) as a single diastereomer.

R_f (EtOAc/PE 40-60: 30%) = 0.39

^{1}H NMR (600 MHz, $CDCl_3$) δ_H 6.14 (1H, q, *J* = 1.2 Hz, H10), 4.41 (1H, ddd, *J* = 9.0, 6.1, 1.4 Hz, H13), 3.79 (1H, d, *J* = 9.2 Hz, H15), 3.74-3.69 (2H, m, H14, H17a), 3.49 (1H, d, *J* = 11.3 Hz, H17b), 2.76 (1H, ddd, *J* = 14.3, 9.0, 1.0 Hz, H12a), 2.74 (1H, s, OH16), 2.70 (1H, ddd, *J* = 14.3, 6.1, 1.2 Hz, H12b), 2.47 (1H, d, *J* = 8.6 Hz, OH14), 1.89 (3H, d, *J* = 1.1 Hz, Me11), 1.47 (3H, s, $\underline{Me}_AMe_BCO_2$), 1.41 (3H, s, Me16), 1.38 (s, 3H, $Me_A\underline{Me}_BCO_2$).

^{13}C NMR (150 MHz, $CDCl_3$) δ_c 143.2, 99.7, 79.3, 73.6, 72.9, 70.3, 68.2, 60.8, 44.3, 28.9, 23.8, 20.5, 19.2.

IR ν_{max} 3397, 3320, 2998, 2876, 1377, 1146, 1080, 1043, 860, 519; $[\alpha]_D^{20}$ –8.7 (*c* 1.3, $CHCl_3$).

HRMS (ESI$^+$) calculated for $C_{13}H_{22}ClIO_4Na$ $[M+Na]^+$ 427.0149, found 427.0155.

Proof of absolute configuration at C14

The absolute configuration at C14 arising from the L-proline-catalyzed aldol reaction was determined by synthesizing the diastereomeric Mosher esters ***(R)***- and ***(S)***-**MTPA**-11 from alcohol 11.

Mosher esters – *(R)*-MTPA-11 and *(S)*-MTPA-11

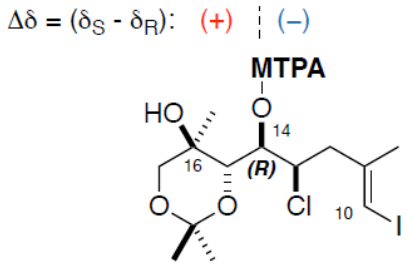

(R)-Mosher ester **– *(R)*-MTPA-11**

A stock solution of DMAP (1.2 mg) in CH_2Cl_2 (1 mL) was separately prepared, of which an aliquot of the DMAP stock solution (250 µL) was used to dissolve alcohol **11** (10.0 mg, 24.7 µmol). DIC (5.7 µL, 37 µmol) and *(R)*- MTPA (8.7 mg, 37 µmol) was added to this solution and the resulting mixture was stirred at r.t. for 24 h, after which the product formation was observed by TLC. The solution was diluted with CH_2Cl_2 (1 mL) and quenched with sat. $NaHCO_3$ (1 mL) was added. The layers were separated, and the aqueous phase was extracted with CH_2Cl_2 (2 x 2 mL) The organic layers were combined, washed with brine (5 mL), dried (Na_2SO_4), and concentrated. Purification by flash chromatography (EtOAc/hexanes 40-60: 10% → 20%) afforded the product **(*R*)-MTPA-11** as a colourless oil (3.4 mg, 5.4 µmol, 23%).

R_f (EtOAc/hexanes: 30%) = 0.48

^{1}H NMR (601 MHz, Chloroform-d) δ 7.65 (dd, J = 7.1, 2.8 Hz, 2H, ArH), 7.47 – 7.42 (m, 3H, ArH), 6.03 (q, J = 1.1 Hz, 1H, H10), 5.19 (dd, J = 9.1, 1.4 Hz, 1H, H10), 4.43 (ddd, J = 10.4, 4.3, 1.3 Hz, 1H, H13), 4.11 (d, J = 9.1 Hz, 1H, H15), 3.65 (s, 3H, OMe), 3.60 (d, J = 11.8 Hz, 1H, H17a), 3.34 (d, J = 11.4 Hz, 1H, H17b), 2.60 (m, 1H, H12a), 2.40 (ddd, J = 14.6, 10.4, 0.8 Hz, 1H, H12b), 1.86 (d, J = 1.0 Hz, 3H, Me11), 1.46 (s, 3H, $\underline{Me}_AMe_BCO_2$), 1.38 (s, 3H, $Me_A\underline{Me}_BCO_2$), 1.14 (s, 3H, Me16).

(S)-Mosher ester **– *(S)*-MTPA-11**

DIC (122 µL, 0.79 mmol) was added to a stirred solution of *(S)*-MTPA (92.5 mg, 0.395 mol) and DMAP (96.5 mg, 0.79 mmol) in CH_2Cl_2 (400 µL). Alcohol **11** (16 mg, 39.5 µmol) was added to this solution. The mixture was stirred for 5h at r.t., to the point when

product was observed by TLC. The solution was diluted with CH_2Cl_2 (1 mL) and sat. $NaHCO_3$ (1 mL) was added. The layers were separated, and the aqueous phase was extracted with CH_2Cl_2 (2 x 2 mL). The organic layers were combined, washed with brine (5 mL), dried (Na_2SO_4), and concentrated. Purification by flash chromatography (EtOAc/hexanes: 10%) afforded the product **(*S*)-MTPA-11** as a colourless oil.

R_f (EtOAc/hexanes: 30%) = 0.70

^{1}H NMR (500 MHz, Chloroform-d) δ 7.69 – 7.64 (m, 2H, ArH), 7.46 – 7.40 (m, 3H, ArH), 5.82 (q, J = 1.1 Hz, 1H, H10), 5.16 (dd, J = 9.2, 1.4 Hz, 1H, H14), 4.37 (ddd, J = 10.8, 3.9, 1.4 Hz, 1H, H13), 4.20 (d, J = 9.1 Hz, 1H, H15), 3.70 (d, J = 11.5 Hz, 1H, 17a), 3.47 (d, J = 1.3 Hz, 3H, OMe), 3.45 (d, J = 11.5 Hz, 1H, 17b), 2.48 (ddd, J = 14.7, 4.0, 1.3 Hz, 1H, 12a), 2.11 (dd, J = 14.5, 10.8 Hz, 1H, 12b), 1.80 (d, J = 1.1 Hz, 3H, Me11), 1.48 (s, 3H, $\underline{Me}_AMe_BCO_2$), 1.40 (s, 3H, $Me_A\underline{Me}_BCO_2$), 1.29 (s, 3H, Me16).

Following the advanced Mosher model described by Hoye *et al.*,[22] the C14 centre arising from the enantioselective Mukaiyama aldol reaction was assigned as 14*R*.

Table 3-3 Diagnostic ^{1}H NMR signals for the configurational assignment of 14*R*

Proton	**δH (*S*)-MTPA** (ppm)	**δH (*R*)-MTPA** (ppm)	$\Delta\delta_{S-R}$ (ppm)
Me11	1.80	1.86	-0.06
H12b	2.11	2.40	-0.29
H12a	2.48	2.60	-0.12
H13	4.37	4.43	-0.06
H14	5.16	5.19	-0.03
H15	4.20	4.11	0.09
Me16	1.29	1.14	0.15
H17a	3.70	3.60	0.10
H17b	3.45	3.34	0.11

Triol 12

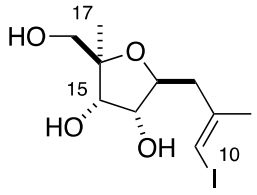

Alcohol **11** (1.48 g, 3.66 mmol) was dissolved in MeOH (50 mL) in a pressurized vessel and heated to 120 ˚C over 15 minutes in a microwave, reaching a pressure of 250 psi. The reaction was maintained at 120 ˚C at 250 psi for 110 minutes before cooling to r.t. The solvent was removed under reduced pressure and the product was purified by flash chromatography (EtOAc: 100%) to afford triol **12** as an off-white solid (0.804 g, 2.45 mmol, 67%).

R_f (CH_2Cl_2/MeOH: 10%) = 0.42

^{1}H NMR (600 MHz, $CDCl_3$) δ_H 6.05 (1H, q, *J* = 1.2 Hz, H10), 4.09 (1H, d, *J* = 6.3 Hz, H15), 3.96 (1H, ddd, *J* = 7.5, 6.1, 5.3 Hz, H13), 3.83 (1H, t, *J* = 6.2 Hz, H14), 3.49 (1H, d, *J* = 11.6 Hz, H17a), 3.44 (1H, d, *J* = 11.6 Hz, H17b), 2.52 (1H, ddd, *J* = 14.5, 5.3, 1.2 Hz, H12a), 2.44 (1H, ddd, *J* = 14.5, 7.5, 1.2 Hz, H12b), 1.90 (3H, d, *J* = 1.1 Hz, Me11), 1.19 (3H, s, Me16).

^{13}C NMR (150 MHz, $CDCl_3$) δ_c 144.7, 84.8, 79.6, 77.3, 75.4, 72.2, 67.8, 43.3, 24.8, 17.3.

IR ν_{max} 3301, 2924, 1105, 1045, 1023, 761, 676, 574, 558.

$[\alpha]_D^{20}$ -22.1 (*c* 1.63, MeOH).

HRM**S** (ESI$^+$) calculated for $C_{10}H_{17}IO_4Na$ $[M+Na]^+$ 351.0063, found 351.0078.

The relative configuration in triol **12** was confirmed by observing a NOE enhancement between H13 and Me16, placing H13 and Me16 in a *syn* configuration. Additionally, no NOE enhancements were observed between H13 and H14, as well as H15 and Me16. This supports that H13, OH14, OH15 and Me16 are in a *syn* relationship around the THF ring (Figure 3-3). This result is also supported by NOE data obtained for alcohol **14** (*vide infra*).

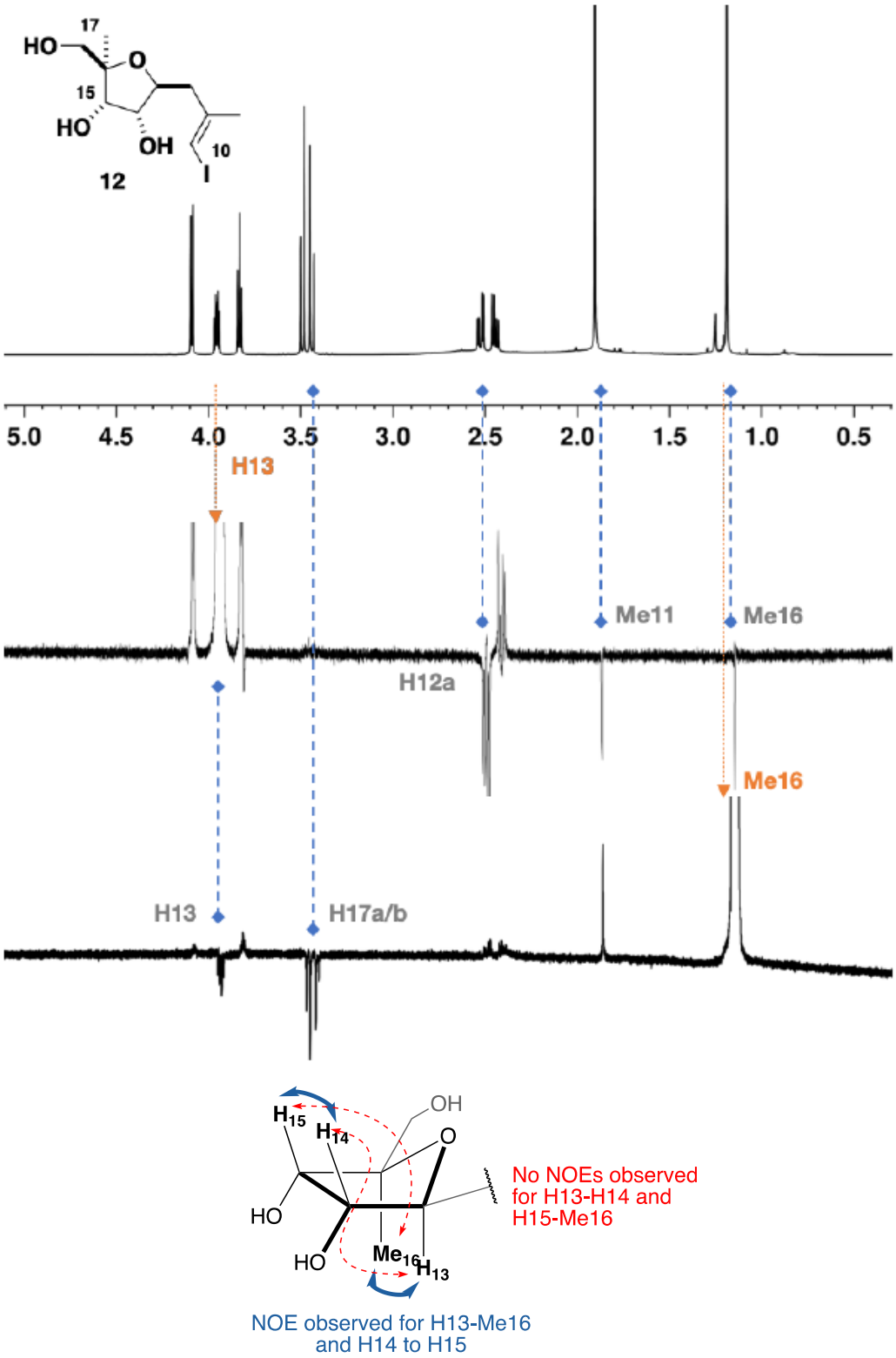

Figure 3-3. Observed NOE correlations confirming the relative configuration of triol 12

Alcohol 12a

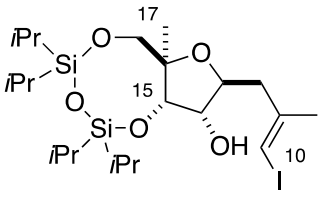

1,3-Dichloro-1,1,3,3-tetraisopropyldisiloxane (1.88 mL, 5.88 mmol) was added dropwise to a stirred solution of triol **12** (1.607 g, 4.90 mmol) in dichloromethane (18 mL) and pyridine (6 mL) at 0 °C. The solution was allowed to warm to r.t. and stirred for 48 h at r.t. before quenching with NH_4Cl (25 mL). The layers were separated, and the organic phase was washed with NH_4Cl (25 mL). The combined aqueous phase was extracted with dichloromethane (2 × 50 mL) and the combined organic phases were washed with brine (50 mL), dried ($MgSO_4$) and concentrated under reduced pressure. Purification by flash chromatography (EtOAc/hexanes: 5% → 10%) afforded alcohol **12a** as a yellow oil (2.49 g, 4.36 mmol, 89%).

R_f (EtOAc/hexanes: 20%) = 0.72

^{1}H NMR (600 MHz, $CDCl_3$) δ_H 6.02 (1H, q, *J* = 1.2 Hz, H10), 4.13-4.07 (2H, m, H13, H15), 3.80 (1H, dd, *J* = 6.9, 2.9 Hz, H14), 3.66 (2H, d, *J* = 2.3 Hz, H17), 2.86 (1H, s, OH), 2.47-2.39 (2H, m, H12), 1.90 (3H, d, *J* = 1.1 Hz, Me11), 1.24 (3H, s, Me16), 1.12-0.97 (24H, m, *i*PrSi).

^{13}C NMR (150 MHz, $CDCl_3$) δ_c 144.5, 83.1, 81.1, 77.4, 75.0, 74.8, 69.8, 44.0, 25.0, 17.6, 17.7, 17.6, 17.5, 17.4, 17.3, 17.3, 17.2, 17.1, 13.5, 13.0, 13.0, 12.8.

IR ν_{max} 2944, 2867, 1464, 1113, 1035, 885, 867, 692.

$[\alpha]_D^{20}$ –10.6 (*c* 0.82, $CHCl_3$).

HRMS (ESI$^+$) calculated for $C_{22}H_{43}IO_5Si_2H$ $[M+H]^+$ 571.1766, found 571.1776.

Siloxane 13

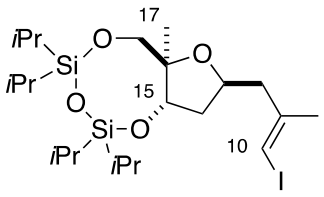

Pyridine (1.9 mL, 23.5 mmol) was added to a solution of alcohol **12a** (2.68 g, 4.70 mmol) in dichloromethane (24 mL) and the solution was cooled to 0 °C, to which Tf_2O (1.98 mL, 11.75 mmol) was added dropwise to the stirred solution at 0 °C. Upon completion, the stirred solution was allowed to warm to r.t. over 1 h before quenching with $NaHCO_3$ (25 mL). The layers were separated, and the aqueous layer was extracted with dichloromethane (3 × 25 mL). The organic layers were combined, washed with brine (100 mL), dried ($MgSO_4$), and the solvent removed under reduced pressure. The crude product was filtered over a plug of silica, eluting with dichloromethane (100 mL). Owing to the instability of the product, triflate **12b** was used immediately in the subsequent step without further purification.

nBu_4BH_4 (3.63 g, 14.1 mmol) was added to a stirred solution of the crude triflate **12b** (3.21g) in PhMe (24 mL) at r.t.. The mixture was heated to 50 °C and stirred for 1 h before the addition of NH_4Cl (25 mL) and allowing the mixture to cool to r.t.. The layers were separated, and the aqueous phase extracted with EtOAc (3 × 25 mL). The combined organic phases were washed with brune (100 mL), dried ($MgSO_4$), and the solvent removed under reduced pressure. Purification by flash chromatography (EtOAc/hexanes: 2% → 5%) afforded siloxane **13** as a clear oil (1.75 g, 3.15 mmol, 68% over two steps).

R_f (EtOAc/hexanes: 10%) = 0.53

^{1}H NMR (600 MHz, $CDCl_3$) δ_H 5.94 (1H, q, *J* = 1.1 Hz, H10), 4.29 (1H, t, *J* = 8.8 Hz, H15), 4.19 (1H, dddd, *J* = 9.2, 6.9, 5.9, 3.6 Hz, H13), 3.69 (1H, d, *J* = 11.7 Hz, H17a), 3.64 (1H, d, *J* = 11.7 Hz, H17b), 2.43 (1H, ddd, *J* = 14.0, 5.9, 1.2 Hz, H12a), 2.28 (1H, ddd, J = 14.0, 7.0, 1.0 Hz, H12b), 2.13-2.04 (1H, m, H14a), 1.94-1.84 (1H, m, H14b), 1.86 (3H, d, J = 1.1 Hz, Me11), 1.11 (3Hm s, 3H, Me16), 1.13-1.01 (28H, m, *i*PrSi).

^{13}C NMR (150 MHz, $CDCl_3$) δ_c 145.0, 83.1, 77.1, 73.0, 72.0, 68.4, 46.8, 37.3, 24.9, 17.7, 17.6, 17.6, 17.6, 17.6, 17.5, 17.4, 17.3, 17.3, 17.2, 16.4, 13.6, 13.2, 12.8, 12.8.

IR ν_{max} 2943, 2867, 1464, 1105, 1032, 885, 692.

$[\alpha]_D^{20}$ –7.2 (*c* 0.93, $CHCl_3$).

HRMS (ESI$^+$) calculated for $C_{22}H_{43}IO_4Si_2H$ $[M+H]^+$ 555.1817, found 555.1803.

Diol 13a

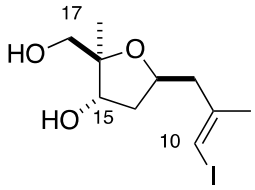

Siloxane **13** (1.16 g, 2.09 mmol) was dissolved in a solution of HCl in MeOH (21 mL, 21.0 mmol, 0.1 M) and stirred at 50 °C for 7 h. The reaction was quenched by the addition of solid $NaHCO_3$ (*ca.* 3 g) and the mixture diluted with CH_2Cl_2 (60 mL). The solids were filtered off, the filtrate collected, and the solvents removed under reduced pressure. Purification by flash chromatography (EtOAc/hexanes: 80%) afforded diol **13a** as clear oil (548 mg, 1.75 mmol, 84%).

R_f (EtOAc)= 0.52

^{1}H NMR (600 MHz, $CDCl_3$) δ_H 5.99 (1H, q, *J* = 1.0 Hz, H10), 4.31 (1H, qn, *J* = 6.8 Hz, H13), 4.25 (1Hm, dd, *J* = 6.8, 4.6 Hz, H15), 3.45 (1H, d, *J* = 11.2 Hz, H17a), 3.41 (1H, d, *J* = 11.3 Hz, H17b), 2.46 (1H, dd, *J* = 14.1, 6.8 Hz, H12a), 2.33 (1H, dd, *J* = 14.1, 6.2 Hz, H12b), 2.09-1.96 (3H, m, H14a, OH, OH), 1.89 (1H, dd, *J* = 13.7, 6.5 Hz, H14b), 1.86 (3H, d, *J* = 1.0 Hz, Me11), 1.16 (3H, s, Me16).

^{13}C NMR (150 MHz, $CDCl_3$) δ_C 144.8, 85.5, 77.2, 74.1, 73.4, 67.8, 46.1, 40.2, 24.6, 17.1.

IR ν_{max} 3377, 2933, 1376, 1274, 1044, 769, 669.

$[\alpha]_D^{20}$ +6.5 (*c* 1.0, MeOH)

HRMS (ESI$^+$) calculated for $C_{10}H_{17}IO_3NH_4$ $[M+NH_4]^+$ 330.0566, found 330.0526.

TBS ether 14

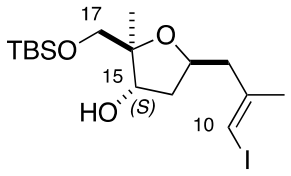

Diol **13**a (707 mg, 2.26 mmol) and imidazole (462 mg, 6.78 mmol) were dissolved in CH_2Cl_2 (23 mL) and cooled to 0 °C. TBSCl (406 mg, 2.71 mmol) was added and the solution was allowed to warm to r.t. over 2 h before quenching with NH_4Cl (20 mL). The layers were separated, and the aqueous layer was extracted with CH_2Cl_2 (3 × 20 mL). The organic layers were combined, washed with brine (60 mL), dried ($MgSO_4$), and the solvent removed under reduced pressure. Purification by flash chromatography (EtOAc/hexanes: 10% → 30%) afforded TBS ether **14** as a clear oil (802 mg, 1.88 mmol, 83%).

R_f (EtOAc/hexanes: 20%) = 0.53

^{1}H NMR (500 MHz, $CDCl_3$) δ_H 5.96 (1H, q, *J* = 1.0 Hz, H10), 4.29 (1H, ddd, *J* = 13.0, 7.3, 6.6 Hz, H13), 4.24 (1H, dt, *J* = 6.4, 4.0 Hz, H15), 3.47 (1H, d, *J* = 9.8 Hz, H17a), 3.36 (1H, d, *J* = 9.8 Hz, H17b), 2.48 (1H, dd, *J* = 13.9, 6.4 Hz, H12a), 2.31 (1H, dd, *J* = 13.9, 6.7 Hz, H12b), 1.95* (1H, ddd, *J* = 13.0, 6.5, 4.2 Hz, H14a), 1.92-1.87* (1H, m, H14b), 1.86 (3H, d, *J* = 1.0 Hz, Me11), 1.65 (1H, d, *J* = 4.3 Hz, OH), 1.19 (3H, s, Me16), 0.89 (9H, s, $SiMe_2$*t*Bu), 0.06 (6H, s, $SiMe_2$*t*Bu).

^{13}C NMR (125 MHz, $CDCl_3$) δ_C 144.9, 83.4, 79.3, 74.1, 67.9, 46.0, 41.0, 25.7, 24.3, 22.5, 18.0, –5.5, –5.8.

IR (thin film): ν_{max} 3439, 2928, 2857, 1463, 1258, 1088 779.

$[\alpha]_D^{20}$ –1.7 (*c* 0.24, $CHCl_3$).

HRMS (ESI$^+$) calculated for $C_{16}H_{31}O_3SiIH$ $[M+H]^+$ 427.1165, found 427.1162.

*H14 signals that are particularly characteristic ***against*** a 15*S* assignment in phormidolide A (H14: 2.33 and 1.57 ppm for H14a and H14b respectively in phormidolide A *vs.* 1.95 and 1.90 ppm for H14a and H14b in **14**). For comparison, H14a and H14b appears at 2.36 and 1.69 ppm in alcohol **15** possessing the 15*R* configuration, which is

the configuration reported in phormidolide A (*vide infra*). NOE analysis of alcohol **14**, compared with the reported NOE enhancements observed in phormidolide A also supports our conclusion.

*NOE analysis of TBS ether **14***

1. Correlations were observed in the ^{1}H-^{1}H NOESY spectrum between H15 and H12/H17, showing that H15 lies on the same side as the two alkyl substituents. *This correlation is not seen in alcohol 15 where the C15 configuration is inverted (vide infra)*

2. Correlation was observed between H13 and Me16, positioning the two substituents *syn* to each other.

3. No correlations were observed between H15 and Me16, suggesting that H15 and Me16 lie *anti* to each other.

These observations suggest that H15 lie *anti* to both H13 and Me16, placing H15 in an *S* configuration (Figure 3-4). In phormidolide A, NOE enhancements were observed for H15 to H14b and Me16, with H14b correlating to H13. H14a reported no NOE enhancements to any THF signals. These differential results, alongside with chemical shift analysis, confirm that phormidolide does not contain the *S* configuration at C15

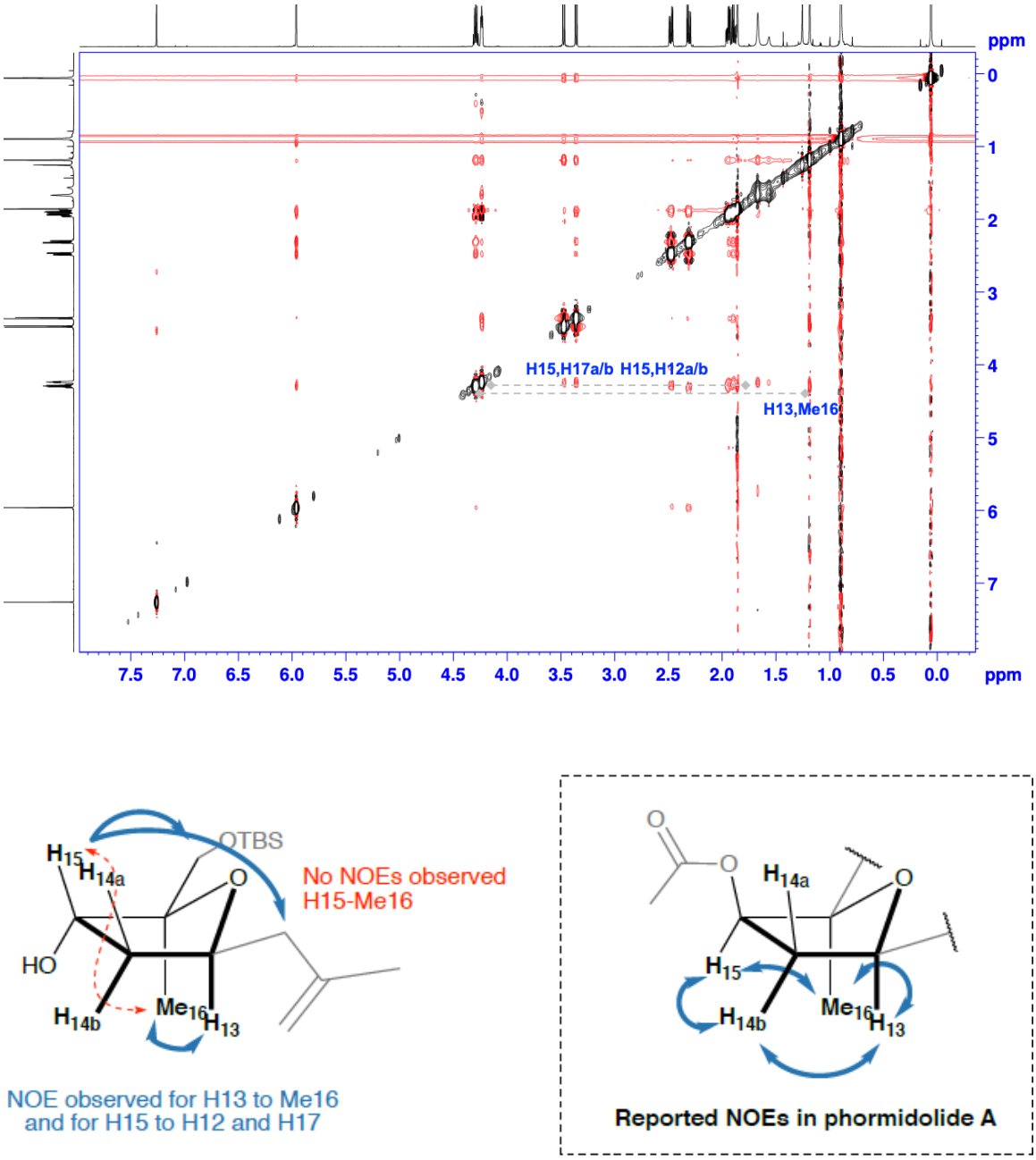

Figure 3-4. **Diagram highlighting the NOE correlations observed for alcohol 14. The reported NOE enhancements for phormidolide A is presented alongside for comparison.**

Ketone 14a

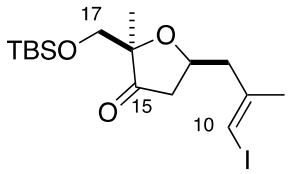

Dess-Martin Periodinane (311 mg, 733 μmol) was added to a stirred suspension of alcohol **14** (125 mg, 293 μmol) and $NaHCO_3$ (100 mg, 1.17 mmol) in wet CH_2Cl_2 (4 mL). The reaction mixture was stirred at r.t. until TLC monitoring indicated full consumption of the starting material (ca. 30 min). The reaction mixture was quenched by the addition of $NaHCO_3$ (2 mL) and $Na_2S_2O_3$ solution (2 mL) and stirred at r.t. for 30 min. The layers were separated, and the aqueous phase was extracted with CH_2Cl_2 (3 × 2 mL). The combined organic phases were dried ($MgSO_4$) and concentrated under reduced pressure. Purification by flash column chromatography (EtOAc/PE 40-60: 0% → 5%) afforded the product **14a** as a colourless oil (123 mg, 290 μmol, 99%).

R_f (EtOAc/PE 40-60: 20%) = 0.71

^{1}H NMR (500 MHz, $CDCl_3$) δ_H 6.03 (1H, q, *J* = 0.9 Hz, H10), 4.33 (1H, app dq, *J* = 10.5, 6.1 Hz, H13), 3.64 (1H, d, *J* = 10.5 Hz, H17a), 3.53 (1H, d, *J* = 10.5 Hz, H17b), 2.71 (1H, dd, *J* = 14.3, 6.1 Hz, H14a), 2.55 (1H, dd, *J* = 14.3, 6.1 Hz, H14b), 2.48 (1H, dd, *J* = 17.4, 5.8 Hz, H12a), 2.19 (1H, dd, *J* = 17.4, 10.5 Hz, H12b), 1.92, (3H, d, *J* = 0.9 Hz, Me11), 1.09 (3H, s, Me16), 0.87 (9H, s, $SiMe_2tBu$), 0.05 (3H, s, $SiMe_2tBu$), 0.02 (3H, s, $SiMe_2tBu$).

^{13}C NMR (125 MHz, $CDCl_3$) δ_C 216.2, 144.1, 84.8, 77.5, 71.6, 67.3, 45.6, 43.3, 25.9, 24.6, 18.3, 17.7, –5.3, –5.6.

IR (thin film): ν_{max} 2948, 2867, 1762, 1454, 1253, 1098, 898.

$[\alpha]_D^{20}$ +16.3 (*c* 0.95, $CHCl_3$).

HRMS (ESI$^+$) calculated for $C_{16}H_{29}O_3SiIH$ $[M+H]^+$ 425.1009, found 425.1006.

Alcohol 15

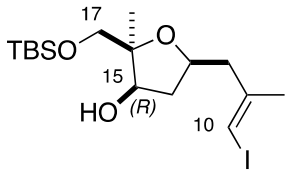

DIBAL (1.69 mL, 1.69 mmol, 1 M solution in hexanes) was added dropwise to a stirred solution of ketone **14a** (239 mg, 563 μmol) in dichloromethane (6 mL) at –78 ˚C. The reaction mixture was stirred at –78 ˚C for 1 h before quenching with MeOH (500 μL), Na/K tartrate (5 mL) and the stirred mixture allowed to warm to r.t. over 3 h. The layers were separated, and the aqueous phase was extracted with CH_2Cl_2 (3 × 5 mL). The combined organic phases were dried ($MgSO_4$) and concentrated under reduced pressure. Purification by flash column chromatography (EtOAc/PE 40-60: 2%) afforded the product **15** as a colourless oil (238 mg, 559 μmol, 99%) as a single diastereomer.

R_f (EtOAc/PE 40-60: 20%) = 0.53

^{1}H NMR (500 MHz, $CDCl_3$) δ_H 5.99 (1H, s, H10), 4.14-4.11 (2H, m, H13, H15), 3.76 (1H, d, *J* = 10.3 Hz, H17a), 3.67 (1H, d, *J* = 10.3 Hz, H17b), 3.55 (1H, d, *J* = 6.2 Hz, OH15), 2.59 (1H, dd, *J* = 13.9, 6.8 Hz, H12a), 2.43 (1H, dd, *J* = 13.9, 6.3 Hz, H12b), 2.39-2.32* (1H, m, H14a), 1.88 (3H, s, Me11), 1.70-1.64* (1H, m, H14b), 1.15 (3H, s, Me16), 0.93 (9H, s, $SiMe_2$*t*Bu), 0.13 (3H, s, $SiMe_2$*t*Bu), 0.12 (3H, s, $SiMe_2$*t*Bu).

^{13}C NMR (125 MHz, $CDCl_3$) δ_C 144.9, 83.4, 79.3, 74.1, 67.9, 46.0, 41.0, 25.7, 24.3, 22.5, 18.0, –5.5, –5.8.

IR (thin film): ν_{max} 3439, 2928, 2857, 1463, 1258, 1088 779.

$[\alpha]_D^{20}$ –1.7 (*c* 0.24, $CHCl_3$).

HRMS (ESI$^+$) calculated for $C_{16}H_{31}O_3SiIH$ $[M+H]^+$ 427.1165, found 427.1162.

*H14 signals that are particularly characteristic in support of the reported 15*R* assignment present in phormidolide A (2.33 and 1.57 ppm for H14a and H14b respectively in phormidolide A *vs.* 2.36 and 1.69 ppm for H14a and H14b in **15**). For comparison, H14a and H14b appears at 1.95 and 1.90 ppm in alcohol **14** possessing the 15*S* configuration

(*vide supra*). All subsequent intermediates bearing the reported 15*R* configuration contain a signal at *ca.*2.30- 2.40 ppm, and another at 1.60-1.70 ppm for the diastereotopic protons of H14, which favourably compares with the ones reported for phormidolide A but not with structures bearing the 14*S* configuration.

*NOE analysis of alcohol **15***

1) Correlations were observed between H15 to H14a and Me16, suggesting the three groups are positioned *syn* to each other

2) Correlations were observed between H13 and Me16, suggesting that H13 and Me16 are positioned *syn* to each other. This also means that H15, H14a and H13 are positioned *syn* to each other

3) No Correlations were observed for either H13/H15 or Me16 to H14b,

This suggests that the H13 and H15 lies *syn* to H14a and Me16, giving the 15*R* configuration (Figure 3-5). Notably, the observed correlations are in contrast to the ones observed for alcohol 14 (*vide supra*). The chemical shift values, alongside with NOE enhancements match very favourably to the ones reported in phormidolide A, giving strong evidence that the relative configuration in the THF, especially at C15, is configured correctly as the 15*R* configuration.

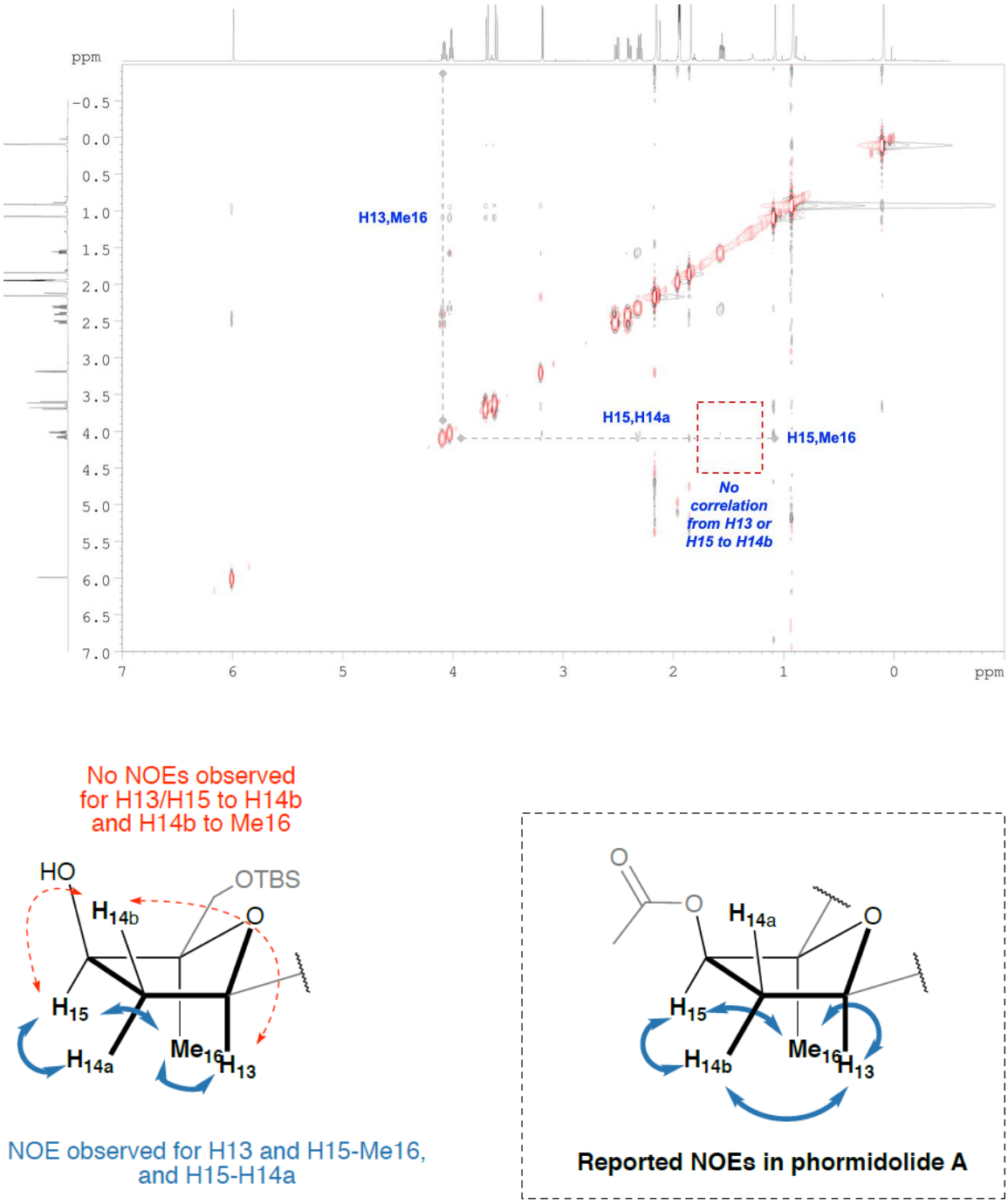

Figure 3-5 **NOE correlations observed for alcohol 15 (spectrum acquired in d_3-MeCN to separate the superimposed H13 and H15) in support of the 15 *R* configuration.**

Ester 16

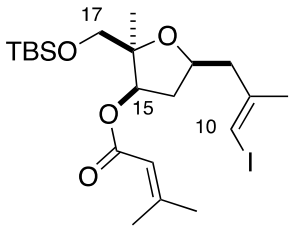

DCC (2.27 mL, 2.27 mmol, 1 M solution in dichloromethane) was added in one portion to a stirred solution of alcohol **15** (160 mg, 378 μmol), dimethylacrylic acid (227 mg, 2.27 mmol), DMAP (277 mg, 2.27 mmol) and DMAP·HCl (359 mg, 2.27 mmol) in dichloromethane (4 mL) at r.t.. The cloudy white suspension was stirred at r.t. for 24 h before quenching with NH_4Cl (5 mL). The layers were separated, and the aqueous phase was extracted with Et_2O (3 × 5 mL). The combined organic phases were dried ($MgSO_4$) and concentrated under reduced pressure. Purification by flash column chromatography (EtOAc/PE 40-60: 0% → 5%) afforded the product **16** as a colourless oil (178 mg, 350 μmol, 93%).

R_f (EtOAc/PE 40-60: 20%) = 0.72

^{1}H NMR (500 MHz, $CDCl_3$) δ_H 5.94 (1H, d, *J* = 1.0 Hz, H10), 5.66 (1H, sept, *J* = 1.2 Hz, =CH), 5.10 (1H, dd, *J* = 6.4, 3.9 Hz, H15), 4.22 (1H, ddt, *J* = 7.5, 6.8, 6.5 Hz, H13), 3.70 (1H, d, *J* = 9.7 Hz, H17a), 3.50 (1H, d, *J* = 9.7 Hz, H17b), 2.56 (1H, dd, *J* = 13.9, 6.8 Hz, H12a), 2.46 (1H, ddd, *J* = 13.8, 7.5, 6.6 Hz, H14a), 2.38 (1H, dd, *J* = 13.9, 6.6 Hz, H12b), 2.17 (3H, d, *J* = 1.7 Hz, =CMe$_a$Me$_b$), 1.91 (3H, d, *J* = 1.2 Hz, =CMe$_a$<u>Me</u>$_b$), 1.85 (3H, d, *J* = 1.0 Hz, Me11), 1.70 (1H, ddd, *J* = 13.9, 6.4, 3.9 Hz, H14b), 1.20 (3H, s, Me16), 0.86 (9H, s, SiMe$_2$*t*Bu), 0.03 (3H, s, SiMe$_2$*t*Bu), 0.01 (3H, s, SiMe$_2$*t*Bu).

^{13}C NMR (125 MHz, $CDCl_3$) δ_C 165.7, 157.4, 144.9, 116.0, 84.5, 77.2, 74.5, 66.0, 46.3, 37.6, 27.4, 25.8, 24.5, 21.7, 20.3, 18.2, –5.5, –5.6.

IR (thin film): ν_{max} 2927, 2853, 1723, 1561, 1444, 1144,1103.

$[\alpha]_D^{20}$ –13.0 (*c* 0.30, $CHCl_3$).

HRMS (ESI$^+$) calculated for $C_{21}H_{37}O_4SiIH$ $[M+H]^+$ 509.1579, found 509.1572.

Alcohol 16a

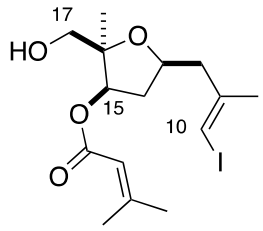

TsOH·H_2O (3.5 mg, 20.3 μmol) was added to a stirred solution of TBS ether **16** (103 mg, 203 μmol) in MeOH (1 mL) and dichloromethane (1 mL) at r.t.. The reaction mixture was stirred for 3 h at r.t., after which it was diluted with dichloromethane (5 mL) and quenched by the addition of $NaHCO_3$ (10 mL). The layers were separated, and the aqueous phase was extracted with dichloromethane (3 × 5 mL). The combined organic phases were dried ($MgSO_4$) and concentrated under reduced pressure. Purification by flash column chromatography (EtOAc/PE 40-60: 20%) afforded the product **16a** as a colourless oil (54.6 mg, 138 μmol, 68%).

R_f (EtOAc/PE 40-60: 20%) = 0.23

^{1}H NMR (400 MHz, $CDCl_3$) δ_H 5.99 (1H, s, H10), 5.70 (1H, s, =CH), 5.08 (1H, dd, *J* = 6.8, 4.9 Hz, H15), 4.22 (1H, app qn, *J* = 6.8 Hz, H13), 3.57 (1H, dd, *J* = 11.8, 6.3 Hz, H17a), 3.51 (1H, dd, *J* = 11.8, 6.2 Hz, H17b), 2.57 (1H, dd, *J* = 13.9, 6.4 Hz, H12a), 2.52 (1H, ddd, *J* = 13.6, 6.8, 6.8 Hz, H14a), 2.42 (1H, dd, *J* = 13.9, 6.3 Hz, H12b), 2.18 (3H, s, $=CMe_aMe_b$), 1.93 (3H, s, $=CMe_a\underline{Me}_b$), 1.87 (3H, s, Me11), 1.72 (1H, ddd, *J* = 13.5, 7.1, 4.9 Hz, H14b), 1.26 (3H, s, Me16).

^{13}C NMR (100 MHz, $CDCl_3$) δ_C 166.4, 159.1 144.6, 115.3, 84.1, 78.1, 77.2, 74.1, 65.8, 46.0, 37.7, 27.6, 24.5, 21.7, 20.4.

IR (thin film): ν_{max} 3511, 2919, 1717, 1649, 1377, 1228, 1145, 1008;

$[\alpha]_D^{20}$ +2.2 (*c* 0.19, $CHCl_3$).

HRMS (ESI^+) calculated for $C_{15}H_{23}O_4INa$ $[M+Na]^+$ 417.0539, found 417.0535.

C10-C17 Aldehyde 3

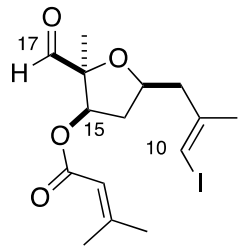

Dess-Martin Periodinane (250 mg, 583 μmol) was added to a stirred suspension of alcohol **16a** (46.0 mg, 117 μmol) and $NaHCO_3$ (48 mg, 1.17 mmol) in wet CH_2Cl_2 (2 mL). The reaction mixture was stirred at r.t. for 30 min before quenching by the addition of $NaHCO_3$ (2 mL) and $Na_2S_2O_3$ solution (2 mL) and stirred at r.t. for 30 min. The layers were separated, and the aqueous phase was extracted with CH_2Cl_2 (3 × 2 mL). The combined organic phases were dried ($MgSO_4$) and concentrated under reduced pressure. Purification by flash column chromatography (EtOAc/PE 40-60: 0% → 5%) afforded the product **3** as a colourless oil (30.3 mg, 77.2 μmol, 86% brsm), alongside with 20-30% of the C10 protodeiodinated product that is inseperable at this stage.

R_f (EtOAc/PE 40-60: 20%) = 0.35;

^{1}H NMR (500 MHz, $CDCl_3$) δ_H 9.63 (1H, s, H17), 6.03 (1H, q, *J* = 1.1 Hz, H10), 5.59 (1H, s, =CH), 5.19 (1H, dd, *J* = 6.4, 4.1 Hz, H15), 4.41 (1H, dt, *J* = 13.7, 6.6 Hz, H13), 2.70 (1H, dd, *J* = 14.0, 6.7 Hz, H12a), 2.55 (1H, ddd, *J* = 13.7, 7.2, 6.4 Hz, H14a), 2.50 (1H, dd, *J* = 14.0, 6.4 Hz, H12b), 2.15 (3H, d, *J* = 1.3 Hz, =C<u>Me</u>$_a$Me$_b$), 1.90 (6H, s, Me11, =CMe$_a$<u>Me</u>$_b$), 1.79 (1H, ddd, *J* = 13.7, 6.2, 4.1 Hz, H14b), 1.31 (3H, s, Me16).

^{13}C NMR (125 MHz, $CDCl_3$) δ_C 201.0, 165.1, 159.3, 144.4, 114.9, 87.6, 79.7, 77.6, 76.8, 45.9, 37.7, 27.5, 24.4, 20.4, 19.6.

IR (thin film): ν_{max} 2918, 1738, 1723, 1649, 1443, 1377, 1224, 1138, 1076.

$[\alpha]_D^{20}$ –3.4 (*c* 0.29, $CHCl_3$).

HRMS (ESI$^+$) calculated for $C_{15}H_{21}IO_4Na$ $[M+Na]^+$ 415.0382, found 415.0373.

3.5.4. Vinyl Metal Addition and Acetonide formation

General procedure for the vinylmetal addition of vinyl iodide 2 to aldehyde 3

*t*BuLi (13 eq., molarity in pentane titrated before use) was added dropwise (down the side of the flask) to a stirred solution of vinyl iodide **2** or ***ent*-2** (6.5 eq., dried by azeotroping with PhH and over CaH_2) in Et_2O (0.1 M relative to vinyl iodide) at –78 °C, taking care that the reaction temperature does not exceed –78 °C. The solution was stirred for 30 seconds before the dropwise addition of a freshly prepared solution of $MgBr_2 \cdot OEt_2$ (19 eq., 0.6 M in Et_2O) into the reaction mixture at –78 °C. The mixture was stirred for 5 min at –78 °C before the dropwise addition of aldehyde **3** (1 eq., dried by azeotroping with PhH × 3) in dichloromethane (0.1 M relative to aldehyde) *via* cannula (down the side of the flask). The pale-yellow reaction mixture was stirred at –78 °C for 1 h before quenching with NH_4Cl (3 mL) and warmed to r.t.. The layers were separated, and the aqueous phase was extracted with CH_2Cl_2. The combined organic phases were dried ($MgSO_4$) and concentrated under reduced pressure. Purification by flash column chromatography (Et_2O/PE 40-60: 0% → 5%) afforded the crude product as a colourless oil as an inseparable mixture of diastereomers, alongside with their C10 protodeiodinated counterparts. The crude product mixture was subjected to the acetonide formation sequence outlined below.

General procedure for the synthesis of diacetonides *anti*-19a, *syn*-19b and 21-*epi*-*anti*-19c

PPTS (one crystal) was added to a stirred solution of *bis*-silyl ethers **17a**, **17b** or **17c** (1 eq.) in dichloromethane (100 μL) and methanol (100 μL) at r.t.. The reaction mixture was stirred for 16 h at r.t. before quenching with $NaHCO_3$ and diluting with EtOAc. The layers were separated, and the aqueous phase was extracted with EtOAc. The combined organic phases were dried ($MgSO_4$) and concentrated under reduced pressure. The crude triol was dissolved in MeOH (150 μL) and K_2CO_3 (6 mg, ca. 10 eq.) was added. The pale-yellow mixture was stirred overnight at r.t. before quenching with NH_4Cl and diluted with EtOAc. The layers were separated, and the aqueous phase was extracted with EtOAc. The combined organic phases were dried ($MgSO_4$) and concentrated under reduced pressure. The crude tetraol was redissolved in dichloromethane (100 μL) and 2,2-dimethoxypropane (100 μL) and PPTS (one crystal) was added. The solution was stirred

for a further 16 h before quenching with $NaHCO_3$ and diluting with EtOAc. The layers were separated, and the aqueous phase was extracted with EtOAc. The combined organic phases were dried ($MgSO_4$) and concentrated under reduced pressure. Purification by preparative thin layer chromatography (EtOAc/PE 40-60: 20%) afforded the diacetonide as a colourless oil.

Alcohol 17a and 15,17-*anti* acetonide *anti*-19a

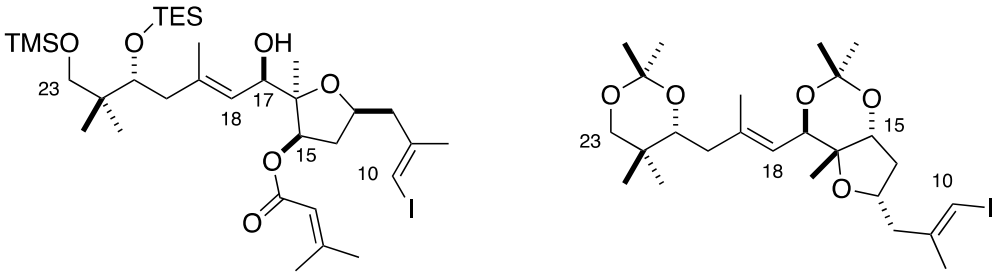

The addition reaction was performed according to the general procedure described above, using vinyl iodide **2** (42.0 mg, 88.9 μmol), *t*BuLi (120 μL, 185 μmol, 1.5 M in pentane), $MgBr_2 \cdot OEt_2$ (381 μL, 229 μmol, 0.6 M solution in Et_2O), and aldehyde **3** (4.9 mg, 12.7 μmol) to afford the crude product **17a** (7.2 mg, 9.78 μmol, 77%), a colourless oil as an inseparable 5 : 1 mixture of diastereomers at C17. alongside with the C10 protodeiodinated material.

The crude product was transformed to the corresponding acetonide *anti*-**19a** according to the general procedure described above to afford the pure diacetonide ***anti*-19a** as a colourless oil (1.3 mg, 2.37 mmol, 24% over three steps)

R_f (EtOAc/PE 40-60: 20%) = 0.85

^{1}H NMR (500 MHz, $CDCl_3$) δ_H 5.97 (1H, q, *J* = 0.9 Hz, H10), 5.19 (1H, dq, *J* = 8.6, 1.0 Hz, H18), 4.40 (1H, d, *J* = 8.6 Hz, H17), 4.21-4.14 (1H, m, H13), 3.94 (1H, dd, *J* = 7.0, 2.1 Hz, H15), 3.64 (1H, dd, *J* = 9.0, 2.7 Hz, H21), 3.61 (1H, d, *J* = 11.4 Hz, H23a), 3.28 (1H, d, *J* = 11.4 Hz, H23b), 2.63 (1H, dd, *J* = 13.9, 7.7 Hz, H12a), 2.48 (1H, dd, *J* = 13.9, 5.5 Hz, H12b), 2.32 (1H, app dt, *J* = 13.9, 7.0 Hz, H14a), 2.11-2.01 (2H, m, H20), 1.85 (3H, d, *J* = 0.9 Hz, Me11), 1.73-1.65 (4H, m, H14b, Me19), 1.39 (3H, s, $\underline{Me}_A Me_B CO(O))^A$, 1.38 (3H,

s, $\underline{Me}_A Me_B CO(O))^B$, 1.36 (3H, s, $Me_A\underline{Me}_B CO(O))^B$, 1.34 (3H, s, $Me_A\underline{Me}_B CO(O))^A$, 1.06 (3H, s, Me16), 1.01 (3H, s, Me22a), 0.74 (3H, s, Me22b).

^{13}C NMR (125 MHz, $CDCl_3$) δ_C 145.3, 137.6, 123.0, 100.3^A, 98.6^B, 87.0, 77.7, 76.6, 76.1, 75.5, 73.0, 46.4, 39.9, 38.7, 36.7, 32.9, 31.9, 29.7^B, 25.4^A, 24.2, 23.8^A, 21.8, 18.9^B, 18.5, 18.0, 17.8.

IR (thin film): ν_{max} 2925, 1460, 1375, 1223, 1100.

$[\alpha]_D^{20}$ +19.5 (*c* 0.06, $CHCl_3$).

HRMS (ESI$^+$) calculated for $C_{25}H_{41}O_5IH$ $[M+H]^+$ 549.2077, found 549.2082.

^{A}Signals attributed to the C15, C17 acetonide,

^{B}Signals attributed to the C21, C23 acetonide

The 15,17-*anti* configuration in *anti*-**19a** was confirmed firstly by observing the ^{13}C chemical shifts for the acetonide Me (25.4 and 23.8 ppm) and acetal centre (100.3 ppm), both of which were strongly indicative for the 15,17-*anti* stereochemistry adopted as a result of the twist-boat conformation of the acetonide, placing the two acetonide Me groups in a *pseudo* equivalent chemical environment (3-6).[10] This was corroborated by running a series of NOE experiments. Notably:

1) No NOE correlation was observed between Me16 and H17, indicating a *trans* relationship between Me16 and H17

2) H15 show strong NOE enhancements to Me16 and *one* of the acetonide Me, while H17 shows a strong NOE enhancement to the other acetonide Me, indicating that H15 and Me16 sit on one side of the acetonide, while H17 sits on the other. This places H15 and H17 *trans* to each other in this ring, and therefore a 15,17-*anti* relationship exists between them

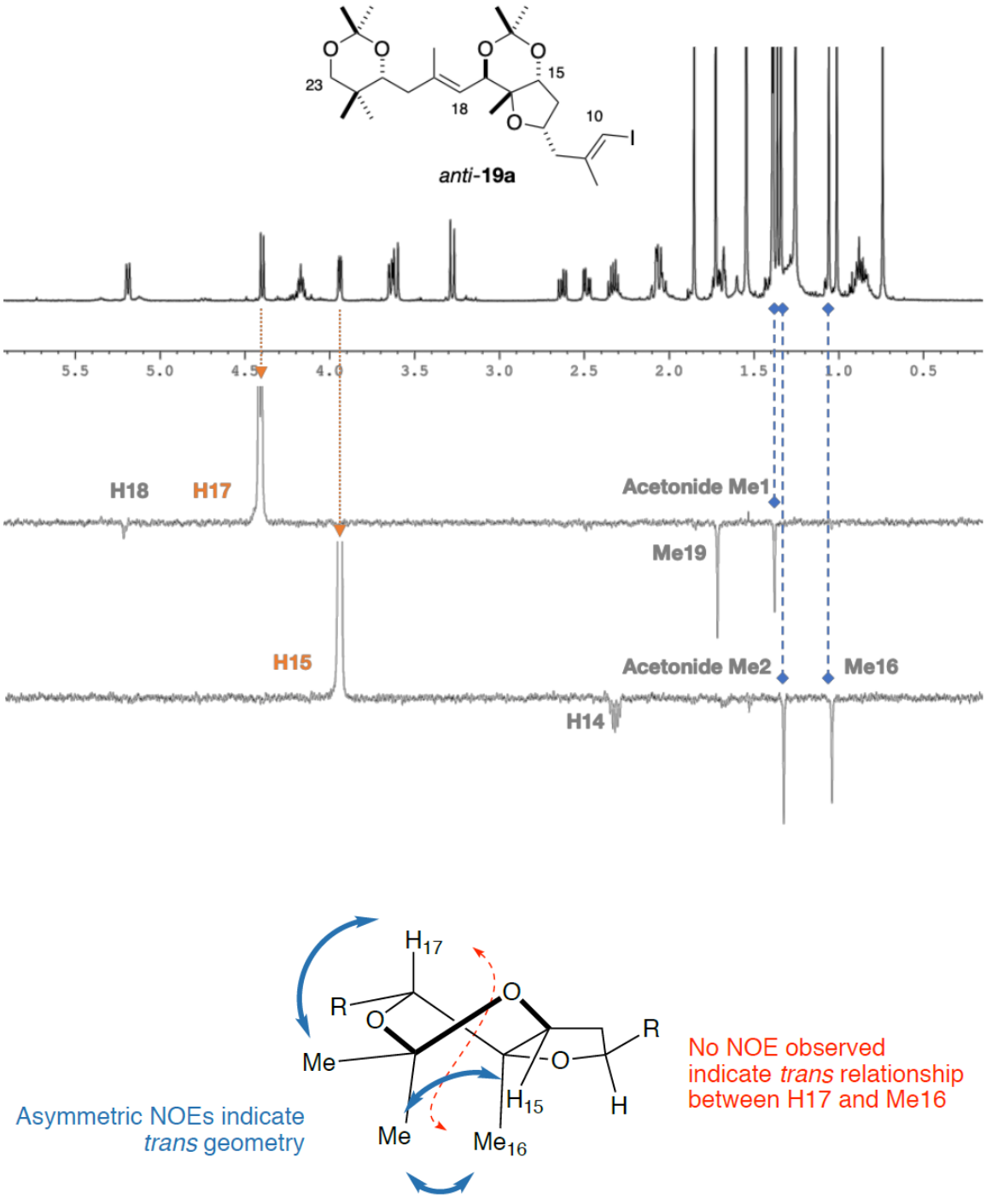

Figure 3-6 **Observed NOE correlations for anti-19a. Irradiated signals are denoted in orange, while observed NOE correlations from the irradiated signals are denoted in grey.**

Alcohol 17b and 15,17-*syn* acetonide *syn*-19b

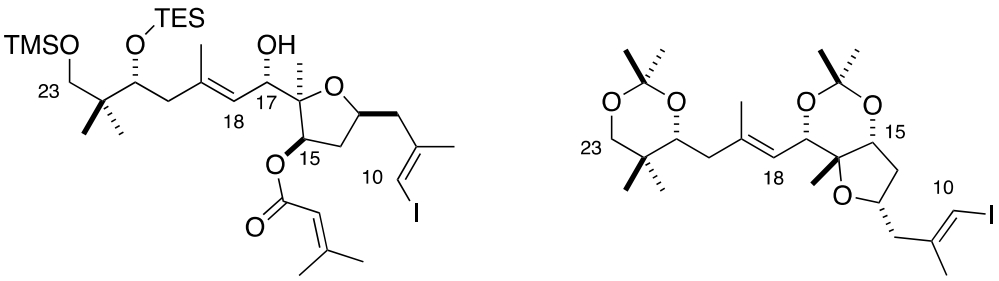

The addition reaction was performed according to the general procedure described above except omitting the addition of $MgBr_2OEt_2$, using vinyl iodide **2** (42.0 mg, 88.9 μmol), *t*BuLi (97 μL, 185 μmol, 1.9 M in pentane), and aldehyde **3** (4.9 mg, 12.7 μmol) to afford the crude product **17b** (3.5 mg, 4.74 μmol, 37%), a colourless oil as an inseperable 4 : 1 mixture of diastereomers at C17, alongside with the C10 protodeiodinated material.

The crude product was transformed to the corresponding acetonide *syn*-**19b** according to the general procedure described above to afford the pure diacetonide as a colourless oil (1.8 mg, 3.28 mmol, 69% over three steps). Owing to competing lithium/iodine exchange at C10 from the formed vinyllithium species in the previous step, the product acetonide contains a 1 : 1 mixture of the C10 protodeiodinated species that was inseparable.

R_f (EtOAc/PE 40-60: 20%) = 0.87

^{1}H NMR (500 MHz, $CDCl_3$) δ_H 5.98 (1H, s, H10), 5.55 (1H, d, *J* = 8.6 Hz, H18), 4.50 (1H, d, *J* = 8.6 Hz, H17), 4.22-4.19 (1H, m, H13), 4.11 (1H, app d, *J* = 4.5 Hz, H15), 3.81 (1H, dd, *J* = 7.0, 2.2 Hz, H21), 3.66 (1H, d, *J* = 11.6 Hz, H23a), 3.27 (1H, d, *J* = 11.5 Hz, H23b), 2.73 (1H, dd, *J* = 13.5, 7.8 Hz, H12a), 2.44 (1H, dd, *J* = 13.5, 5.8 Hz, H12b), 2.38-2.30 (1H, m, H14a), 2.25 (1H, dd, *J* = 15.5 Hz, 7.0 Hz, H20a), 1.98-1.93 (1H, m, H20b), 1.88 (3H, d, *J* = 1.0 Hz, Me11), 1.76 (3H, s, Me19), 1.74-1.66 (1H, m, H14b), 1.49 (3H, s, $\underline{Me}_A Me_B CO(O))^A$, 1.42 (3H, s, $\underline{Me}_A Me_B CO(O))^A$, 1.42 (3H, s, $\underline{Me}_A Me_B CO(O))^B$, 1.37 (3H, s, $\underline{Me}_A Me_B CO(O))^B$, 1.03 (3H, s, Me22a), 0.93 (3H, s, Me16), 0.74 (3H, s, Me22b).

^{13}C NMR (125 MHz, $CDCl_3$) δ_C 145.6, 140.2, 121.3, 98.5^B, 97.4^A, 78.8, 76.9, 75.3, 74.5, 72.3, 69.7, 46.8, 38.5, 36.9, 32.9, 30.0^A, 29.9^B, 24.4, 21.8, 20.6, 19.2^A, 19.0, 18.8^B, 18.1.

IR (thin film): ν_{max} 2928, 1464, 1377, 1261, 1129, 1098.

$[\alpha]_D^{20}$ +17.9 (*c* 0.08, $CHCl_3$).

HRMS (ESI^+) calculated for $C_{25}H_{41}O_5IH$ $[M+H]^+$ 549.2077, found 549.2078.

[A]Signals attributed to the C15, C17 acetonide

[B]Signals attributed to the C21, C23 acetonide

The 15,17-*syn* configuration in *syn*-**19b** was confirmed firstly by observing the ^{13}C chemical shifts for the acetonide Me (19.2 and 30.0 ppm) and acetal centre (97.4 ppm), both of which were strongly indicative for the 15,17-*syn* stereochemistry adopted as a result of the chair conformation of the acetonide, placing the two acetonide Me groups in different chemical environments (3-7).[10] This was corroborated by running a series of NOE experiments. Notably, strong NOE enhancements were shown between *one* of the acetonide Me with *all of* H15, Me16 and H17, signifying that all three substituents are sitting on the same side of the ring (the other acetonide Me does not show any NOE enhancements to H15, Me16 or H17). This observation places H15 and H17 *cis* to each other in the ring, and therefore a 15,17-*syn* relationship exists between them

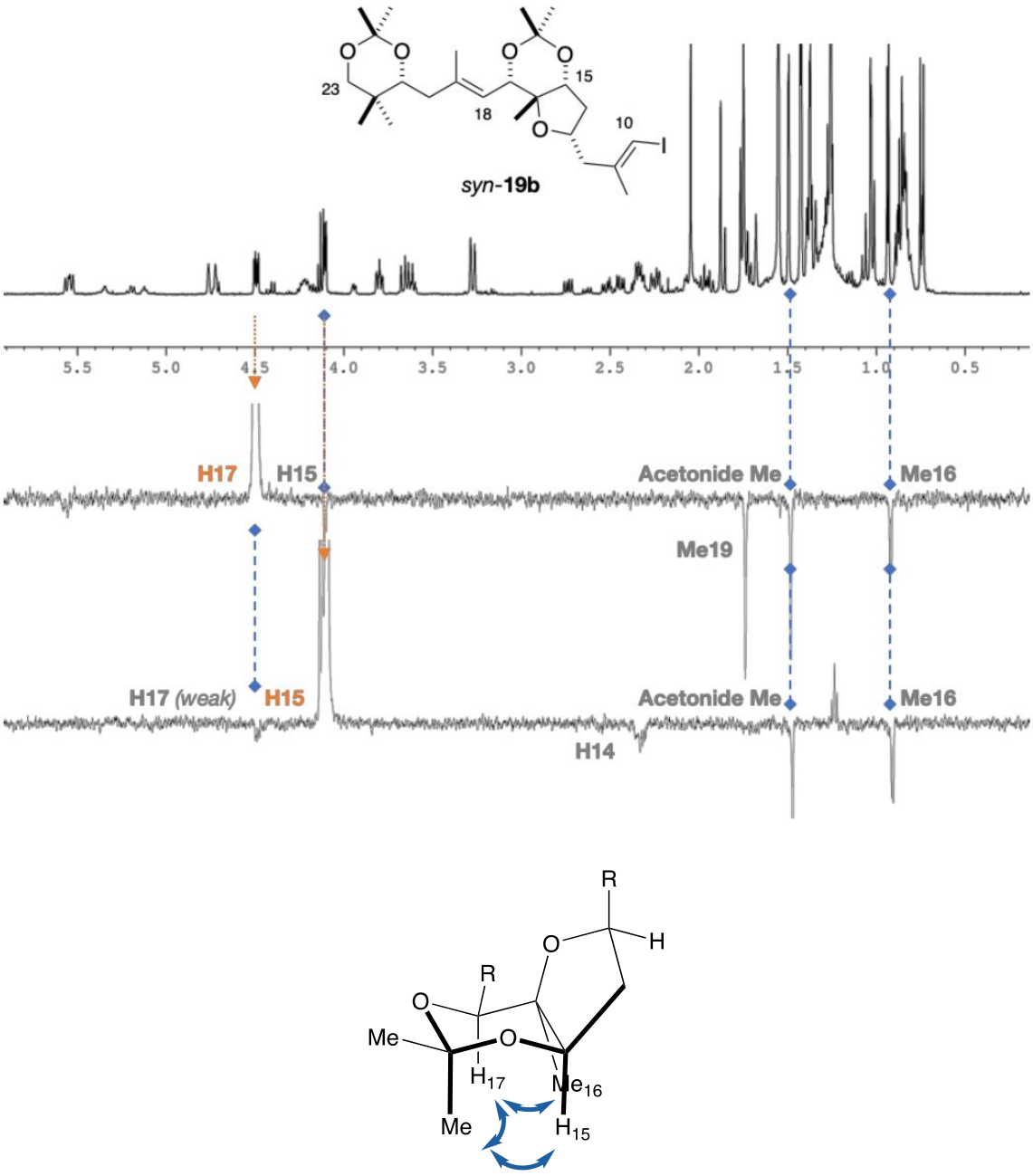

Figure 3-7. **Observed NOE correlations for syn-19b. Irradiated signals are denoted in orange, while observed NOE correlations from the irradiated signals are denoted in grey.**

Proof of 17*S* configuration in 17*b*

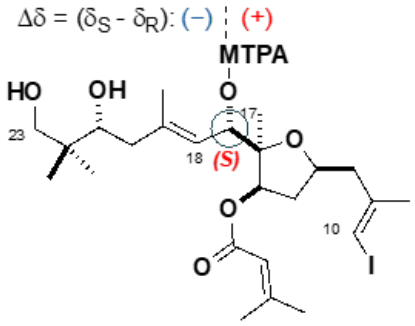

The assigned configuration at C17 was confirmed by forming the diastereomeric MTPA esters of alcohol **17b** described below: DCC (15 μL, 14.9 μmol, 1 M in dichloromethane) was added dropwise to a stirred solution of alcohol **17b** (2.75 mg, 3.73 μmol), (*R*) or (*S*)-MTPA (3.5 mg, 14.9 μmol) and DMAP (one crystal) in dichloromethane (50 μL). The reaction mixture was stirred at r.t. for 16 h before filtering through a pad of silica[1] The crude product was dissolved in MeOH (25 μL) and dichloromethane (25 μL) and PPTS (one crystal) was added. The solution was stirred at r.t. for 24 h before quenching with $NaHCO_3$ (one drop), dried ($MgSO_4$), filtered and the solvent removed under reduced pressure to afford the (*S*)-MTPA ester diols [(*S*)-MTPA-**17b**, 1.0 mg, 1.30 mmol, 46% over two steps] or (*R*)-MTPA ester diols [(*R*)-MTPA-**17b**, 1.0 mg, 1.30 mmol, 46% over two steps] as a colourless oil.

(*S*)-MTPA-17b

R_f (EtOAc/PE 40-60: 20%) = 0.25

^{1}H NMR (500 MHz, $CDCl_3$) δ_H 5.81 (1H, d, *J* = 10.0 Hz, H17), 5.79 (1H, s, H10), 5.66 (1H, s, =CH), 5.14 (1H, d, *J* = 10.0 Hz, H18), 5.04 (1H, dd, *J* = 7.0, 5.8 Hz, H15), 4.40 (1H, d, *J* = 10.8 Hz, H23a), 4.18 (1H, m, H13), 4.01 (1H, d, *J* = 10.8 Hz, H23b), 3.48 (1H, m, H21), 2.43 (1H, m, H14a), 2.41 (1H, m, H12a), 2.26 (1H, m, H12b), 2.19 (3H, s, =C$\underline{Me}_a$Me$_b$), 2.11 (1H, m, H20a), 1.94 (1H, m, H20b), 1.93 (3H, s, =CMe$_a$$\underline{Me}_b$), 1.82 (3H, s, Me11), 1.75 (3H, s, Me19), 1.65 (1H, m, H14b), 1.17 (3H, s, Me16), 0.92 (3H, s, Me22a), 0.88 (3H, s, Me22b).

(*R*)-MTPA-17b

R_f (EtOAc/PE 40-60: 20%) = 0.22

^{1}H NMR (500 MHz, $CDCl_3$) δ_H 5.88 (1H, s, H10), 5.73 (2H, m, =CH, H17), 5.33 (1H, s, H18), 4.95 (1H, dd, *J* = 7.8, 7.0 Hz, H15), 4.29 (1H, d, *J* = 10.4 Hz, H23a), 4.09 (1H, d, *J* = 10.4 Hz, H23b), 4.09 (1H, m, H13), 2.52 (1H, m, H12a), 3.50 (1H, m, H21), 2.51 (1H, m, H20a), 2.32 (1H, m, H12b), 2.25 (1H, m, H20b), 2.21 (3H, s, =C$\underline{Me}_a$Me$_b$), 2.13 (1H, m, H14a), 1.98 (3H, s, =CMe$_a$$\underline{Me}_b$), 1.81 (3H, s, Me11), 1.76 (3H, s, Me19), 1.14 (3H, s, Me16), 1.10 (1H, m, H14b), 0.92 (3H, s, Me22a), 0.88 (3H, s, Me22b).

Following the advanced Mosher model described by Hoye *et al.*,[22] the C17 stereocentre was assigned as *S* as anticipated from the polar Felkin-Anh controlled addition of the vinyl lithium to aldehyde **3** *via* TS-III in Figure S6.

Table 3-4 Diagnostic ^{1}H NMR signals for the configurational assignment of 17*S*

Proton	δ_H (*S*)-MTPA-**17b**	δ_H (*R*)-MTPA-**17b**	$\Delta\delta = \delta_S - \delta_R$
H13	4.18	4.09	+0.09
H14A	2.43	2.13	+0.30
H14B	1.65	1.10	+0.55
H15	5.04	4.95	+0.09
Me16	1.17	1.14	+0.03
H17	5.81	5.73	+0.08
H18	5.14	5.33	-0.19
Me19	1.75	1.76	-0.01
H20A	2.11	2.51	-0.40
H20B	1.94	2.25	-0.31
H21	3.48	3.50	-0.02

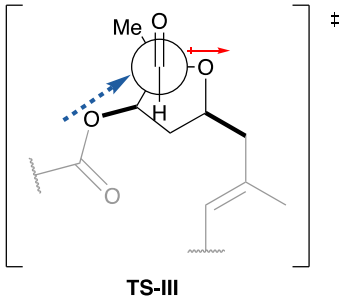

TS-III

Figure 3-8. Stereochemical rationalisation of adduct 17b via the Polar Felkin-Anh model.

Alcohol 17c and 21-epi-*anti* acetonide 21-epi-*anti*-19c

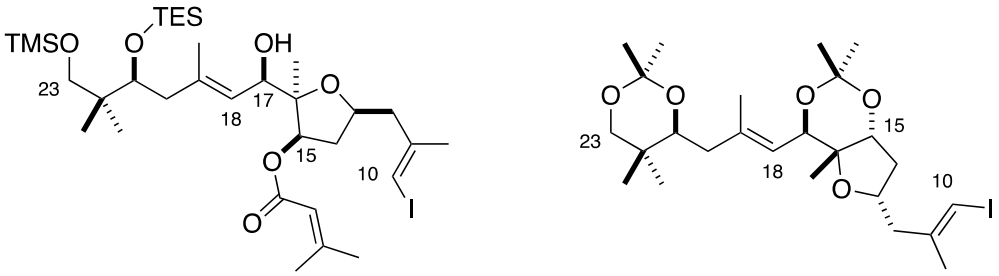

The addition reaction was performed according to the general procedure described above, using vinyl iodide ***ent*-2** (42.0 mg, 88.9 μmol), *t*BuLi (97 μL, 185 μmol, 1.9 M in pentane), $MgBr_2 \cdot OEt_2$ (381 μL, 229 μmol, 0.6 M solution in Et_2O), and aldehyde **3** (4.9 mg, 12.7 μmol) to afford the crude product **17c** (5.0 mg, 6.78 μmol, 53%), a colourless oil as an inseparable 5 : 1 mixture of diastereomers at C17, alongside with the C10 protodeiodinated material.

The crude product was transformed to the corresponding acetonide 21-*epi*-*anti*-**19c** according to the general procedure described above to afford the pure diacetonide 21-*epi*-*anti*-**19c** as a colourless oil (1.8 mg, 3.28 mmol, 48% over three steps)

R_f (EtOAc/PE 40-60: 20%) = 0.83

^{1}H NMR (500 MHz, $CDCl_3$) δ_H 5.98 (1H, q, *J* = 0.8 Hz, H10), 5.19 (1H, dq, *J* = 8.6, 1.2 Hz, H18), 4.42 (1H, d, *J* = 8.6 Hz, H17), 4.22-4.16 (1H, m, H13), 3.95 (1H, dd, *J* = 6.9, 1.9 Hz, H15), 3.77 (1H, dd, *J* = 9.2, 2.4 Hz, H21), 3.62 (1H, d, *J* = 11.4 Hz, H23a), 3.27 (1H, d, *J* = 11.4 Hz, H23b), 2.64 (1H, dd, *J* = 13.8, 7.8 Hz, H12a), 2.49 (1H, dd, *J* = 13.9, 6.2 Hz, H12b), 2.33 (1H, app dt, *J* = 14.0, 6.2 Hz, H14a), 2.21-2.18 (1H, m, H20a), 2.03-1.97 (1H, m, H20b), 1.86 (3H, d, *J* = 0.9 Hz, Me11), 1.76 (3H, d, *J* = 1.0 Hz, Me19), 1.75-1.68 (1H, m, H14b), 1.42 (3H, s, $\underline{Me}_A Me_B CO(O))^B$, 1.39 (3H, s, $\underline{Me}_A Me_B CO(O))^A$, 1.38 (3H, s, $Me_A \underline{Me}_B CO(O))^B$, 1.35 (3H, s, $Me_A \underline{Me}_B CO(O))^A$, 1.07 (3H, s, Me16), 1.02 (3H, s, Me22a), 0.73 (3H, s, Me22b).

^{13}C NMR (125 MHz, $CDCl_3$) δ_C 145.3, 138.9, 120.7, 100.4^A, 98.5^B, 86.9, 78.2, 76.7, 76.1, 71.9, 71.0, 46.5, 39.4, 36.6, 32.9, 30.9, 29.8^B, 25.3^A, 24.2, 23.6^A, 18.8^B, 18.7, 18.3, 18.1 ; **IR** (thin film): ν_{max} 2928, 2857, 1465, 1377, 1222, 1090, 1021.

$[\alpha]_D^{20}$ –22.9 (*c* 0.05, $CHCl_3$).

HRMS (ESI$^+$) calculated for $C_{25}H_{41}O_5INa$ $[M+Na]^+$ 571.1891, found 571.1885.

[A]Signals attributed to the C15, C17 acetonide

[B]Signals attributed to the C21, C23 acetonide

The 15,17-*anti* configuration in *21-epi-anti*-**19c** was confirmed firstly by observing the ^{13}C chemical shifts for the acetonide Me (25.6 and 23.8 ppm) and acetal centre (100.4 ppm), both of which were strongly indicative for the 15,17-*anti* stereochemistry adopted as a result of the twist-boat conformation of the acetonide, placing the two acetonide Me groups in a *pseudo* equivalent chemical environment (Figure 3-9).[10] This was corroborated by running a series of NOE experiments. Notably:

3) No NOE correlation was observed between Me16 and H17, indicating a *trans* relationship between Me16 and H17

4) H15 show strong NOE enhancements to Me16 and *one* of the acetonide Me, while H17 shows a strong NOE enhancement to the other acetonide Me, indicating that H15 and Me16 sit on one side of the acetonide, while H17 sits on the other. This places H15 and H17 *trans* to each other in this ring, and therefore a 15,17-*anti* relationship exists between them

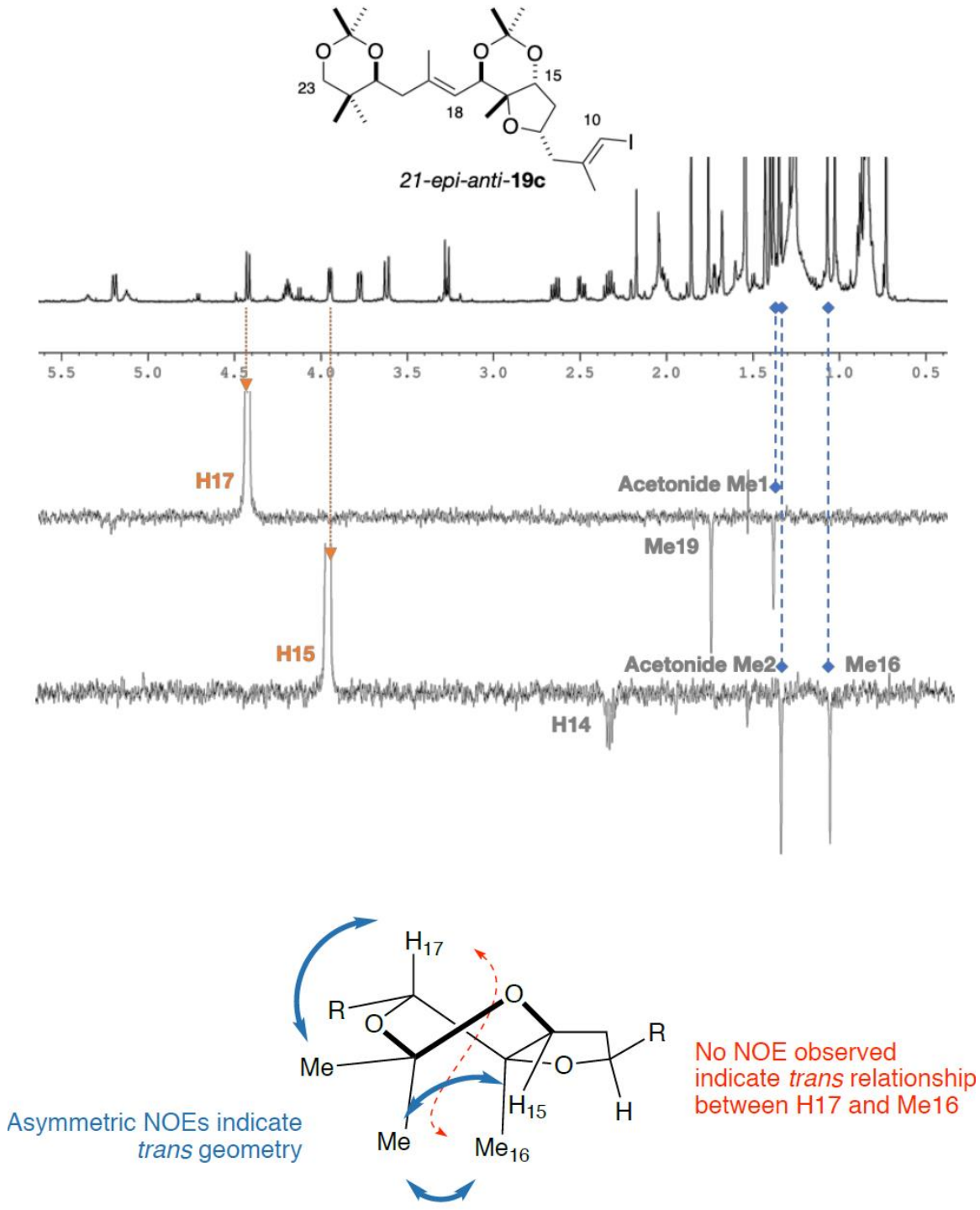

Figure 3-9. **Observed NOE correlations for 21-epi-anti-19c. Irradiated signals are denoted in orange, while observed NOE correlations from the irradiated signals are denoted in grey.**

3.6. Discussion on NMR data, Comparisons and Biogenetic data

3.6.1. Analysis of *J* Values and NOE Data for the Assignment of H17

With contradicting information from our foregoing analysis of the diastereomeric acetonides *vis-à-vis* the data reported for phormidolide A triacetonide, we turned to the reported NOE, $^{3}J_{CH}$ and $^{3}J_{HH}$ to further ascertain the configuration at C17.[2] Reanalysis of the reported NOE enhancements by taking into account all *J* values allowed us to conclude that C17 was misassigned. In particular, the reported conformer, while giving a geometry that takes into account all *J* values, places H18 and Me16 (C37 in isolation paper) too far away to observe a NOE enhancement (Table 3-5 and Figure 3-10). The alternative C17 epimer that takes into account all the reported *J* values positions H18 in a proximal geometry to Me16 (C37 in isolation paper), which accounts for the strong NOE correlation observed in the isolation paper. These observations, alongside with the interpretation of the data obtained from comparing *anti*-**19a** and *syn*-**19b** relative to phormidolide triacetonide **18** reinforce the proposed reassignment of C17 from *S* (reported) to *R*.

Table 3-5 Excerpt of the NOE and ^{3}J data used for the assignment of C17 from the original isolation paper. The key strong NOE enhancement between Me16 (C37 in the original isolation paper) and H18 is highlighted in orange.

Atom #	^{13}C (ppm)	^{1}H (ppm)	ROESY	COSY (Hz)	HSQMBC (Hz)
13	76.7	4.48	12b, 14b, Me11, Me16	14a (0.0), 14b (ovlp), 12a (14.0), 12b (5.0)	11 (<0.5), 16 (10.6)
14	34.8	1.57	15	15 (0.0), 13 (0.0)	13 (<0.5), 12 (4.1)
		2.33	13, 15, 2	15 (4.8), 13 (ovlp)	13 (<0.5), 12 (4.5)
15	79.6	5.15	12a, 14a, 17 (st), Me16 (wk), 18 (wk)	14a (0.0), 14b (4.8)	17 (<0.5), Me16 (5.5)
16	86.9	-			
17	69.7	4.70	Me19, 15 (st), Me16 (wk)	18 (9.0)	19 (3.7), 16 (5.6), 15 (5.5), Me16 (5.0)
18	127.0	5.40	Me16 (st), 20a, 15 (wk)	17 (9.0)	20 (6.0), 16 (0.8), Me19 (10.0)
19	137.4				
Me16	21.0	1.19	13, 17 (wk), 15, 18 (st)		

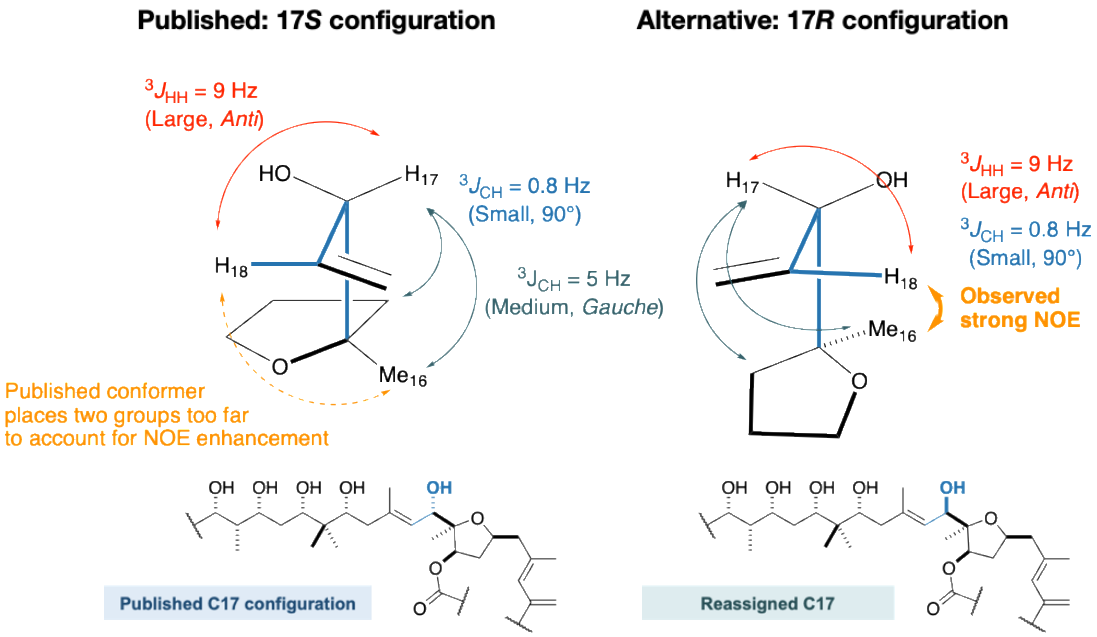

Figure 3-10: Diagramatic representation of the relevant conformer that enabled the assignment of C17, taking into account all ^{3}J and NOE data observed for phormidolide A. (Left) The conformer used in the isolation paper to give the orignally assigned 17*S* configuration. (Right) The conformer that gives the 17*R* configuration taking into account of the strong NOE observed.

3.6.2. Rationale for Necessitating the Re-Evaluation of C21 Relative to C17

In the isolation paper,[2] the stereochemical information at C17 was relayed across the planar sp^2 region (C18-C19) of the natural product. In the absence of a direct long-range correlation (e.g. NOE enhancement or multiple bond *J* values/correlations) between H/C17 and a diastereomeric proton on a sp^3 centre (e.g. H20a or H20b), one cannot definitively conclude that the natural product sits in a particular conformer, as in this instance, rotating the conformer by 180° would have all the *J* values conform but result in the opposite relative configuration of H/C17 relative to H/C21

There were two instances where this occurred in the assignment of phormidolide A. The first instance relates to the assignment of the THF core relative to H/C7 on the macrolactone. Here, the stereogenic information on H/C7 (absolute configuration at H/C7 definitively confirmed by Mosher ester analysis) was relayed across the planar sp^2 C9-C11 diene unit, and onwards onto the H/C13-H/C16 THF moiety. Fortuitously, the

alternative conformer (where the entire diene unit is rotated by 180°) would result in a geometry for C1-C7 protruding *away* from the THF that would be unacceptable for ring closure onto H/C15, leaving only one possible conformer for this planar sp^2 region and therefore allowing a conclusive assignment of the THF moiety relative to H/C7 (Table 3-6 and Figure 3-11).

Table 3-6 Excerpt of the NOE and ^3J data used for the assignment of C7 and C13 from the original isolation paper. Note that atom number 35 is the exocyclic methylene proton (=CH_2 at C9), and atom 36 is the allylic methyl group appended to C11.

Atom #	^{13}C (ppm)	^1H (ppm)	ROESY	COSY (Hz)	HSQMBC (Hz)
7	73.1	4.05	6b, 8b, 5, =CH_2 9b	8a (11.5), 8b (2.3), 6a (10.5), 6b (4.0)	9 (<0.5), 9 (<0.5)
8	43.8	2.46	10	7 (11.5)	10 (2.0), =CH_2 9 (3.5), 7 (ovlp), 6 (4.0)
		1.81	7	7 (2.3)	10 (1.4), =CH_2 9 (5.0), 7 (5.9), 6 (4.8)
9	141.5				
10	132.4	5.28	14b, 8a, 4, 2		36 (8.1), 12 (7.1), =CH_2 9 (6.5), 8 (4.7)
11	133.4				
12	48.3	2.33		13 (14.0)	14 (<0.5), 10 (4.8), Me11 (5.5)
		2.58	13, Me11	13 (5.0)	14 (<0.5), 10 (3.0), Me11 (2.8)
13	76.7	4.48	12b, 14b, Me11, Me16	14a (0.0), 14b (ovlp), 12a (14.0), 12b (5.0)	11 (<0.5), 16 (10.6)
=CH_2 9	133.8	4.76	Me3, Me11		10 (5.9), 8 (10.0)
		4.98	7		10 (11.2), 8 (5.9)
Me11	16.8	1.58	13, =CH_2 9a		9, 10, 12

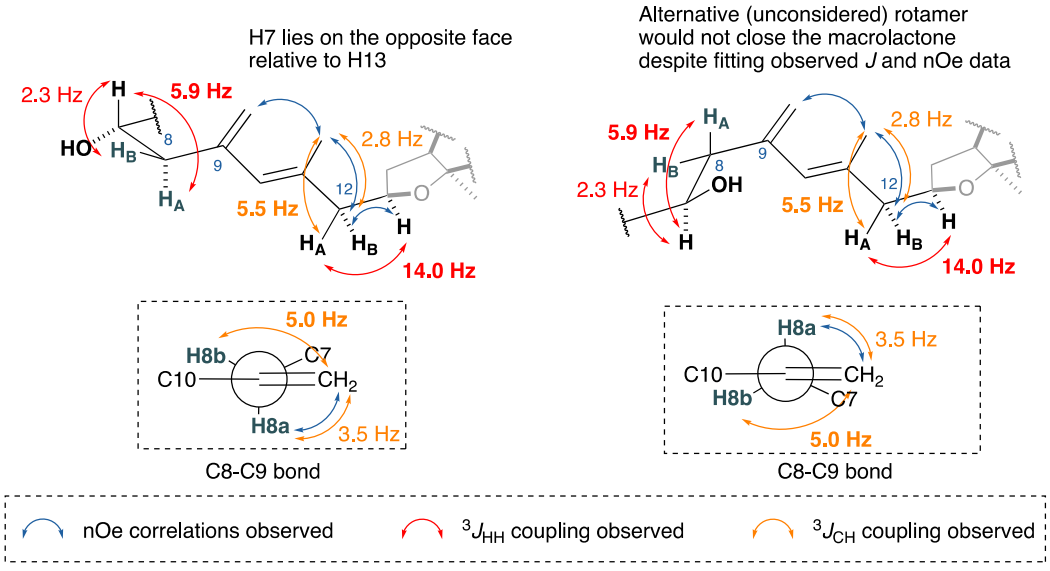

Figure 3-11 Analysis of the two candidate conformers between H/C7 and H/C13 highlight the alternative (unconsidered) conformer would place the remainder of the chain too far away to enable ring closure, despite fitting all J value and NOE data.

The same conclusion cannot be obtained by relaying the stereochemical relationship from H/C17 across the planar sp^2 region (C18-C19) onto H/C21. In this case, the side chain is linear and not constrained geometrically (compared to H/C7 where the macrocycle must close onto H/C15), and so two possible conformers can exist that fits all the observed *J* and NOE values (Table 3-7, Figure 3-12). As such, further investigation into the relative configuration between H/C17 and H/C21 was warranted. We optimistically hoped that despite the distal 1,5 nature between the two stereocentres, the conformational constraints imposed by the acetonides would allow for the facile NMR determination of the correct diastereomer between *anti*-**19a** (possessing the reassigned 17*R* configuration but the reported 21*R* configuration) and 21-*epi*-*anti*-**19c** (possessing the reassigned 17*R* configuration as well as the epimeric 21*S* configuration) (Figure 3-13).

Table 3-7 **Excerpt of the NOE and ^{3}J data used for the assignment of C17 and C21 from the original isolation paper. Note that atom number 38 is Me19 in our assignment of phormidolide A.**

Atom #	^{13}C (ppm)	^{1}H (ppm)	ROESY	COSY (Hz)	HSQMBC (Hz)
17	69.7	4.70	Me19 (st), 15 (st), Me16 (wk)	18 (9.0)	19 (3.7), 16 (5.6), 15 (5.5), Me16 (5.0)
18	127.0	5.40	Me16 (st), 20a, 15 (wk)	17 (9.0)	20 (6.0), 16 (0.8), Me19 (10.0)
19	137.4				
20	42.3	2.06	18, Me22a	21 (10.6)	22 (0.4), Me19 (6.3), 18 (6.5), 21 (2.0)
		2.34	21, Me22b, Me19	21 (2.3)	18, 19
21	77.5	3.65	20b, Me19, Me22b, 23	10a (10.6), 20b (2.4)	23 (2.0), Me22a, Me22b, 19 (3.5)
Me19	17.3	1.80	21, 17 (st), 20b		18, 19, 20

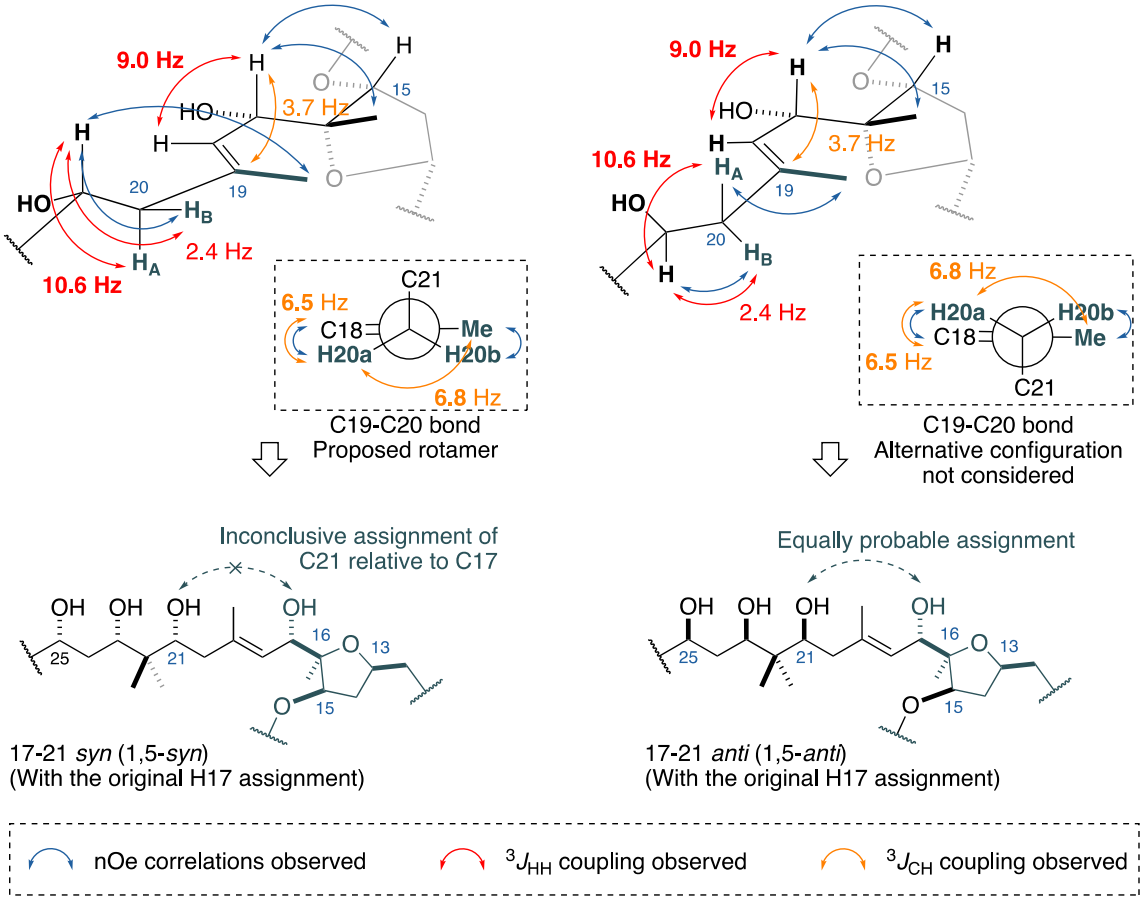

Figure 3-12 **Analysis of the two candidate conformers between H/C17 and H/C21 highlight the equally probable (unconsidered) conformer that conforms to all the J values and NOE correlations observed for phormidolide A.**

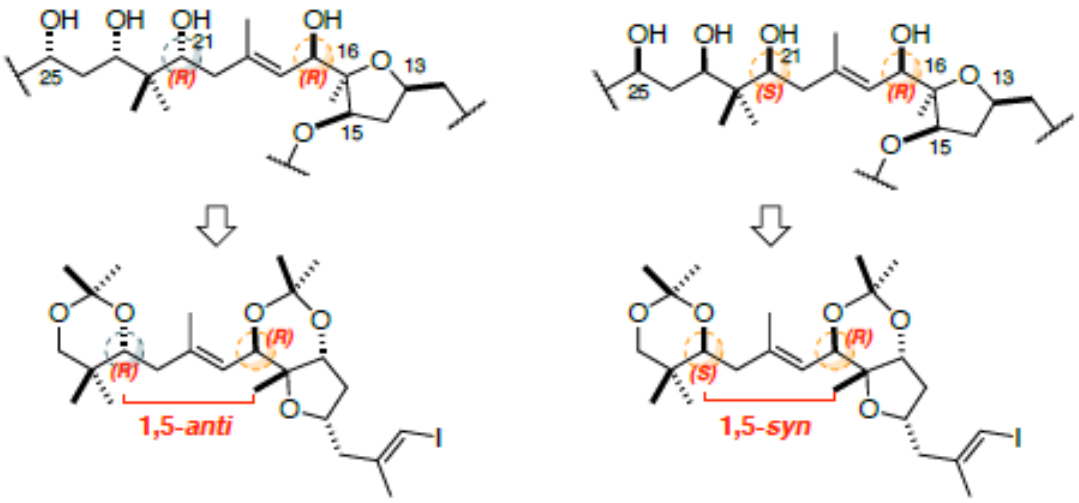

Figure 3-13 Candidate diastereomers to evaluate the distal 1,5-related stereocentres in the natural product.

The remaining *J* based analysis for the side chain from H/C21 to H/C33 was conclusive, especially taking into account the reported preparation of the phormidolide A diacetonide derivative (with the acetonide bridging between OH21 and OH23, and a second acetonide bridging OH25 and OH27). As there exists unambiguous NOE data and *J* values from both the natural product as well as the acetonide derivative to corroborate the all *syn* substitution on the polyol side chain, a reassignment of H/C21 will by extension, result in the analogous reassignment of all remaining stereocentres present on the side chain.

(For a detailed discussion of the assignment of the phormidolide A side chain, please refer to Williamson, R. T.; Boulanger, A.; Vulpanovici, A.; Roberts, M. A.; Gerwick, W. H. *J. Org. Chem.* **2002**, *67*, 7927–7936)

3.6.3. NMR Comparisions Between *anti*-19a, *syn*-19b and 21-*epi*-*anti*-19c with 18

Table 3-8 Table of 1H NMR data of phormidolide A triacetonide 18 and diacetonides *anti*-19a, *syn*-19b and 21-*epi*-*anti*-19c.

	Phm A triacetonide	*anti*-**19a**			*syn*-**19b**			21-*epi*-*anti*-**19c**		
	^{1}H (ppm)	**^{1}H**	**Δ**	**|Δ|**	**^{1}H**	**Δ**	**|Δ|**	**^{1}H**	**Δ**	**|Δ|**
Ac1	1.34	1.34	0.00	0.00	1.49	0.15	0.15	1.35	0.01	0.01
Ac2	1.38	1.39	0.01	0.01	1.38	0.00	0.00	1.39	0.01	0.01
H13*	4.16	4.17	0.01	0.01	4.11	-0.05	0.05	4.19	0.03	0.03
H14A	2.32	2.32	0.00	0.00	2.34	0.02	0.02	2.33	0.01	0.01
H14B	1.75	1.70	-0.05	0.05	1.72	-0.03	0.03	1.71	-0.04	0.04
H15*	3.94	3.94	0.00	0.00	4.21	0.27	0.27	3.95	0.01	0.01
Me16	1.07	1.06	-0.01	0.01	0.93	-0.14	0.14	1.07	0.00	0.00
H17	4.42	4.40	-0.02	0.02	4.50	0.08	0.08	4.42	0.00	0.00
H18	5.18	5.19	0.01	0.01	5.55	0.37	0.37	5.19	0.01	0.01
Me19	1.74	1.72	-0.02	0.02	1.76	0.02	0.02	1.76	0.02	0.02
H20A	2.20	2.09	-0.11	0.11	2.25	0.05	0.05	2.18	-0.02	0.02
H20B	2.03	2.05	0.02	0.02	1.98	-0.05	0.05	2.03	0.00	0.00
H21	3.70	3.64	-0.06	0.06	3.81	0.11	0.11	3.78	0.08	0.08
H23	3.44	3.28	-0.16	0.16	3.63	0.19	0.19	3.6	0.16	0.16

Table 3-9 Table of ^{13}C NMR data of phormidolide A triacetonide 18 and diacetonides *anti*-19a, *syn*-19b and 21-*epi*-*anti*-19c.

	Phm A triacetonide	*anti*-**19a**			*syn*-**19b**			21-*epi*-*anti*-***19c***		
	^{13}C (ppm)	**^{13}C**	**Δ**	**|Δ|**	**^{13}C**	**Δ**	**|Δ|**	**^{13}C**	**Δ**	**|Δ|**
Ac1	23.7	23.8	0.10	0.10	20.5	-3.2	3.2	23.6	0.1	0.1
Ac2	25.3	25.4	0.10	0.10	30.0	4.7	4.7	25.3	0.0	0.0
C13	76.8	76.6	-0.20	0.20	74.5	-2.3	2.3	76.7	-0.1	0.1
C14	36.7	36.7	0.00	0.00	36.9	0.2	0.2	36.6	-0.1	0.1
C15	78.2	77.7	-0.50	0.50	75.3	-2.9	2.9	78.2	0.0	0.0
C16	87.0	87.0	0.00	0.00	78.8	-8.2	8.2	86.9	-0.1	0.1
Me16	18.4	18.9	0.50	0.50	19.2	0.8	0.8	18.7	0.3	0.3
C17	71.8	73.0	1.20	1.20	70.0	-1.8	1.8	71.9	0.1	0.1
C18	120.3	123.0	2.70	2.70	121.5	1.2	1.2	120.7	0.4	0.4
Me19	18.2	17.8	-0.40	0.40	19.0	0.8	0.8	18.3	0.1	0.1
C20	39.0	40.0	1.00	1.00	38.5	-0.5	0.5	39.4	0.4	0.4
C21	77.6	76.1	-1.50	1.50	76.9	-0.7	0.7	76.1	-1.5	1.5
C23	73.5	72.4	-1.10	1.10	72.0	-1.5	1.5	72.3	-1.2	1.2

*In the paper that describes the formation of the phormidolide triacetonide derivative, the ^{1}H values for H13 and H15 were erroneously swapped. A reexamination of their 2D ^{1}H-^{1}H COSY data as well as our NMR data supports this conclusion. Specifically, the signal attributed to δ_H 4.1x ppm couples to δ_H 2.50 and 2.34 ppm (signals that are attributed to H12). This means the signal attributed to 4.1x ppm arises from H13, rather than H15.

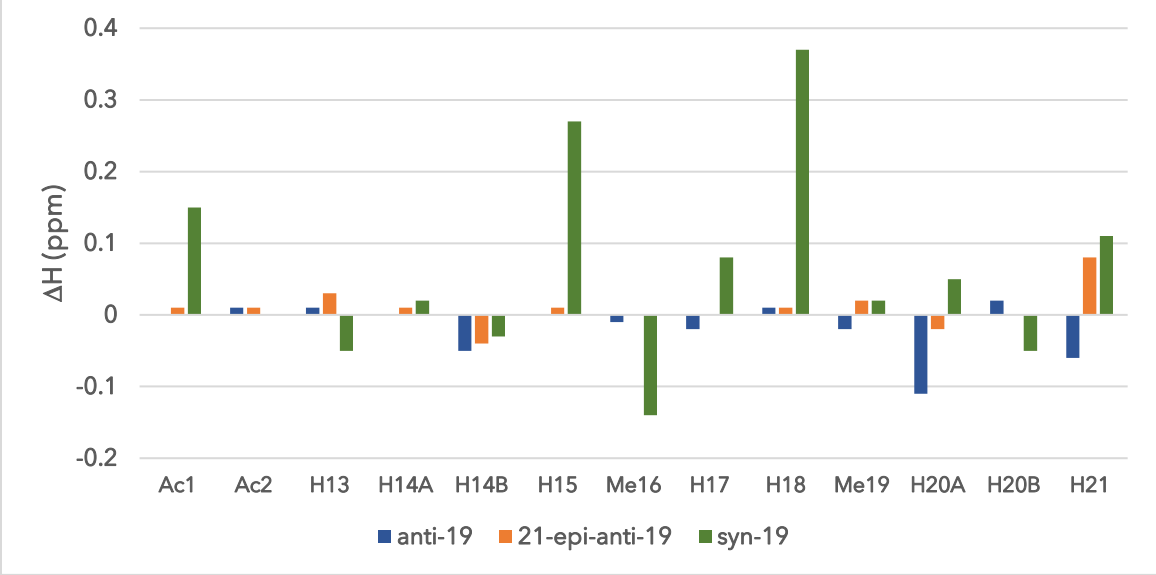

Figure 3-14 Bar chart showing ^{1}H NMR shift differences of diacetonides *anti*-19a, *syn*-19b and 21-*epi*-*anti*-19c between H13-H21 inclusive of acetonide protons.

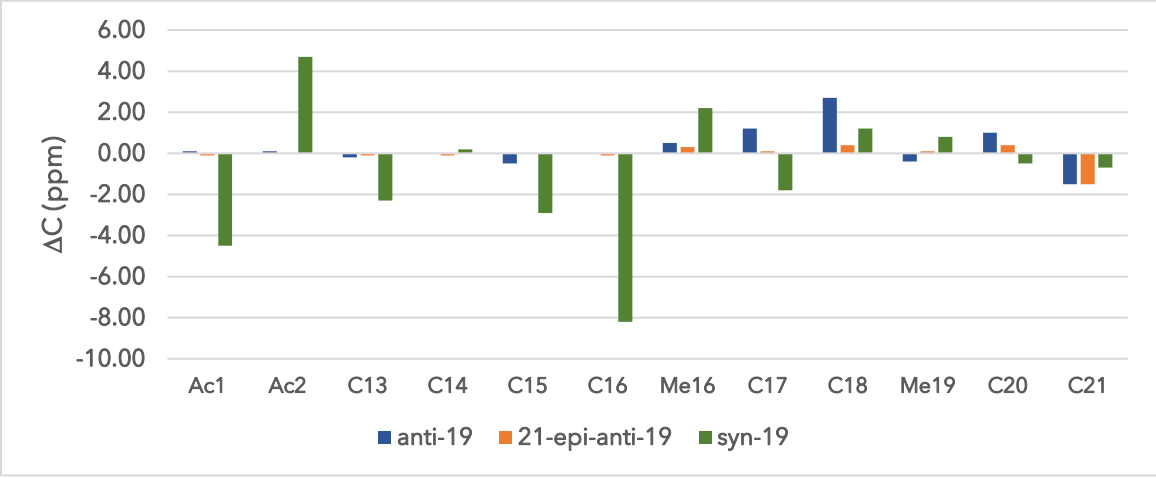

Figure 3-15 Bar chart showing ^{13}C NMR shift differences of diacetonides *anti*-19a, *syn*-19b and 21-*epi*-*anti*-19c between C13-C21 inclusive of acetonide carbons.

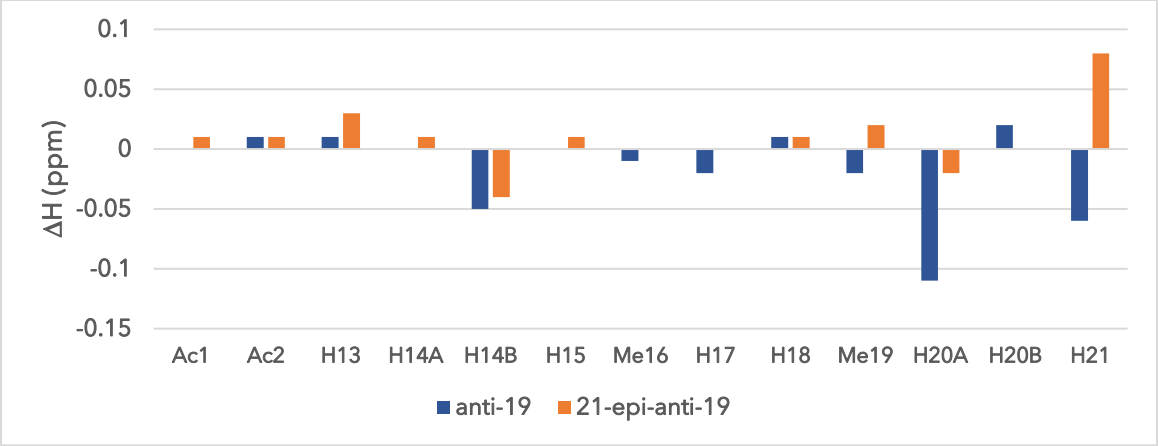

Figure 3-16: **Bar chart showing ^{1}H NMR shift differences of *anti*-19a and 21-*epi*-*anti*-19c between H13-H21 inclusive of acetonide protons. The omission of *syn*-19 allows a better comparison between which of the two diastereomers is likely to be correct.**

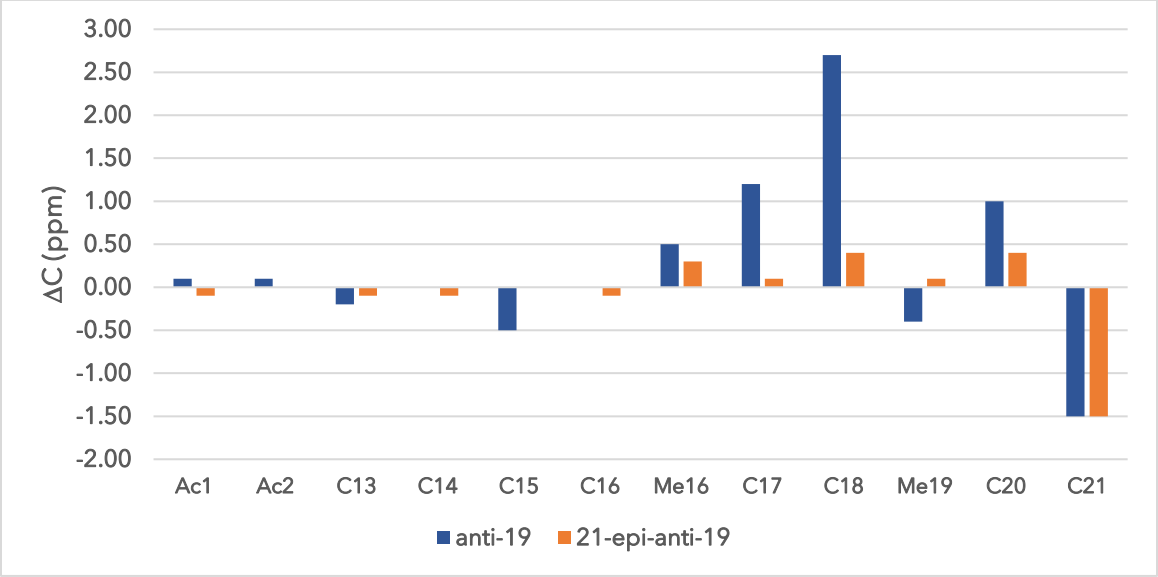

Figure 3-17 **Bar chart showing ^{13}C NMR shift differences of *anti*-19a and 21-*epi*-*anti*-19c between C13-C21 inclusive of acetonide protons. The omission of *syn*-19b allows a better comparison between which of the two diastereomers is likely to be correct.**

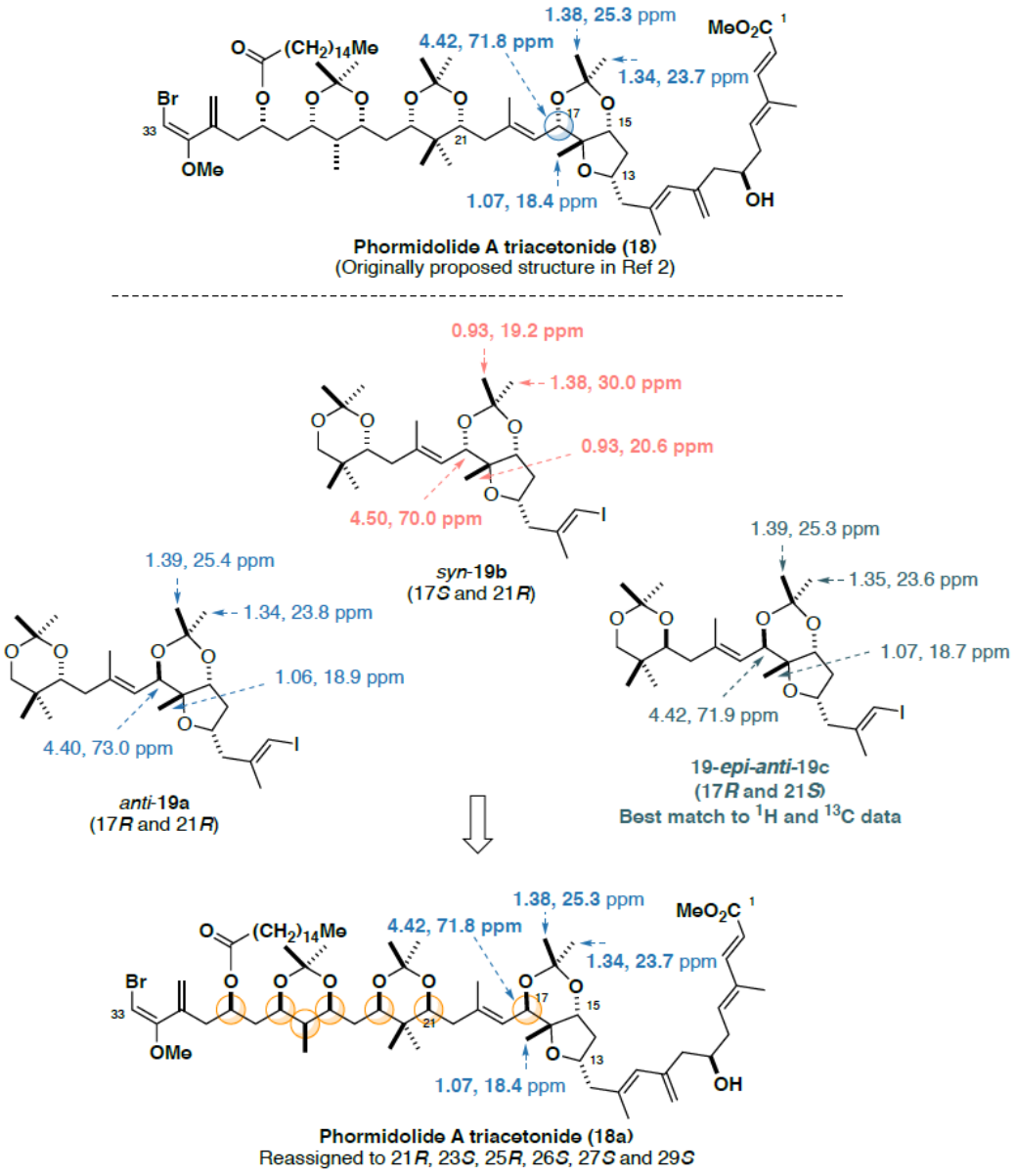

Figure 3-18 Summary of diagnostic chemical shifts between phormidolide A triacetonide 18 and diacetonides anti-19a, syn-19b and 21-*epi-anti*-19c.

On comparing NMR shift errors with phormidolide A triacetonide **18**, *syn*-**19b** was immediately eliminated as a possible diastereomer due to the large deviations in the 15,17-acetonide region of the molecule, leaving *anti*-**19a** and 19-*epi-anti* **19c** as the remaining candidates (see Figure 3-14, Figure 3-15). Of the two remaining diastereomers, ^{13}C NMR correlations were particularly diagnostic for the 17,21-*syn*

relationship (leading to the 21*R* configuration), in particular with the large deviations observed in Me16, C17 and C18 (Figure 3-17). This allowed us to eliminate *anti*-**19a** as a candidate diastereomer, leaving 19-*epi*-*anti*-**19c** as the candidate with the best match for the triacetonide **18**, which is reassigned as **18a** as shown above in Figure 3-18

3.7. Commentary on Ketoreductase Domains in the Biosynthesis of Phormidolide A

In a subsequent account, a comprehensive study[2] on the biosynthesis of phormidolide A was reported. Within the polyketide synthase for phormidolide A, there exists 10 ketoreductase enzymes responsible for catalysing the formation of secondary OH groups from carbonyls, and therefore set the absolute stereochemistry of each carbinol centre OH group present in phormidolide A. Ketoreductases in polyketide synthases are often categorised into one of two types; Type A ketoreductases and type B ketoreductases.[14,15] Type A ketoreductases often contain a W residue near the active site and generally catalyse the formation of L-configured OH groups. Type B ketoreductases often contain a LDD_{1758} motif at the active site and will generally catalyse the formation of D-configured OH groups. In particular, the D_{1758} residue is particularly diagnostic for the generation of D-configured OH groups.

The authors performed a sequence alignment of the 10 ketoreductases present in the phormidolide A polyketide synthase and highlighted that nine of the 10 ketoreductases present contain the D_{1758} motif (but not the LDD triad) (Figure 3-19a). As all the OHs present in phormidolide A are L configured (rather than the expected D configuration that arises from a type B-like ketoreductase), this prompted in a reevaluation of the absolute configuration of C7 by forming the diastereomeric MTPA esters of the phormidolide A triacetonide derivative, which confirmed the L configuration at C7 (Figure 3-19b). As the remaining OHs were all L configured, yet the ketoreductase responsible for the L-OH configuration contained the D_{1758} residue (predictive of a D-OH), they concluded that the presence of the D_{1758} residue was not predictive of D-OH formation and, by extension, reasoned that the remaining D_{1758} containing ketoreductases would also catalyse L-OHs present in phormidolide A.

In light of the ambiguous stereochemical assignment of C21 relative to C17 (See section 3.6.2) we did not see the analysis of the ketoreductase domains as a conclusive

proof for the stereochemistry of phormidolide A, despite several published examples where ketoreductases possessing the D_{1758} residue can go on to catalyse the formation of L-OHs. Our reassignment of the hydroxyl-bearing stereocentres (C17, C21, C23, C25 and C29) leads to reassigning these L-OH configured stereocentres to the corresponding D-OH epimer. Notably, this reassignment is more concordant with the observation that D_{1758} containing/type B-like ketoreductases catalyse the formation of D-OHs (Figure 3-20), leaving OH7 as the apparent singly anomalous L-OH formed by a D_{1758} containing ketoreductase (rather than *all* the ketoreductases being anomalous).

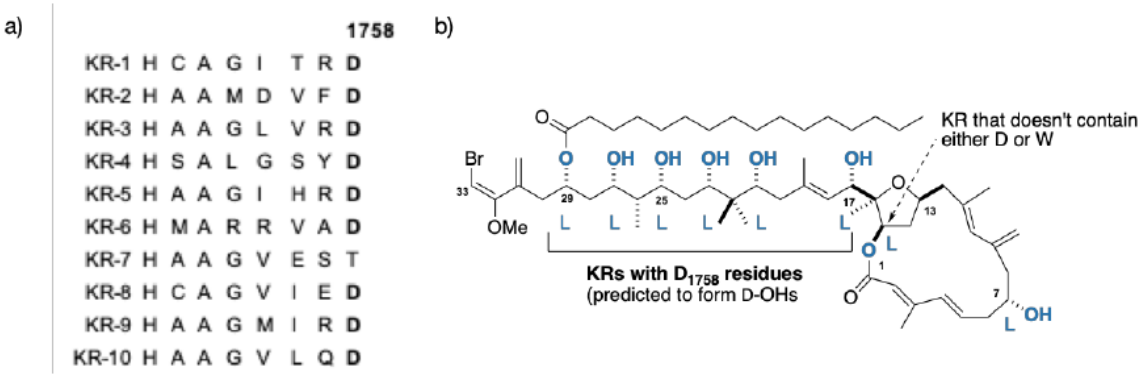

Figure 3-19 **A) Excerpt of sequence alignment data from ref 2, highlighting the conserved D1758 residue that is nominally indicative for D-OH formation B) Structure of phormidolide A highlighting that all OHs in the natural product are L configured. This apparent contradiction was resolved by confirming the absolute stereochemistry at C7 (confirmed L) and extending the logic that the remaining stereocentres could also be L configured.**

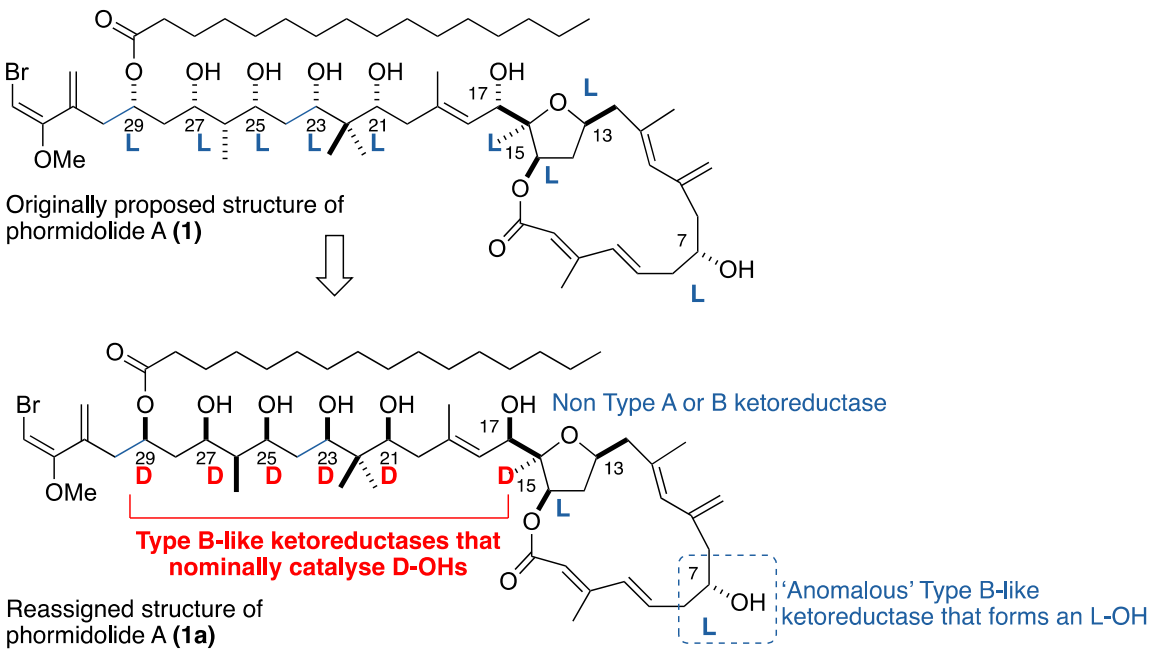

Figure 3-20 Reassignment of C17-C29 of phormidolide A from 1 to 1a allows for greater alignment of the observed stereochemistry of the natural product to the proposed biosynthesis.

In light of our spectroscopic data from the model acetonides, reanalysis of the *J*- and NOE-based configurational analysis as well as the reported genetic data on the biosynthesis of phormidolide A, we believe that this configurational reassignment is fully supported. However, conclusive proof must await the completion of the total synthesis of structure **1a** and comparison with natural phormidolide A.

(For a detailed discussion on the biosynthesis of phormidolide A, please refer to Bertin, M. J.; Vulpanovici, A.; Monroe, E. A.; Korobeynikov, A.; Sherman, D. H.; Gerwick, L.; Gerwick, W. H. *ChemBioChem* **2016**, *17*, 164–173)

References

(1) R. T. Williamson, A. Boulanger, A. Vulpanovici, M. A. Roberts and W. H. Gerwick, *J. Org. Chem*. **2002**, *67*, 7927.

(2) M. J. Bertin, A. Vulpanovici, E. A. Monroe, A. Korobeynikov, D. H. Sherman, L. Gerwick and W. H. Gerwick, *ChemBioChem* **2016**, *17*, 164.

(3) For related congeners to phormidolide A, see: (a) A. Lorente, A. Gil, R. Fernández, C. Cuevas, F. Albericio and M. Álvarez, M. *Chem. Eur. J.* **2015**, *21***,** 150 and (b) M. Murakami, H. Matsuda, K. Makabe and K. Yamaguchi, *Tetrahedron Lett.* **1991**, *32,* 2391.

(4) N. Matsumori, D. Kaneno, M. Murata, H. Nakamura and K. Tachibana, *J. Org. Chem.* **1999**, *64*, 866.

(5) For recent synthetic work directed towards the phormidolides, see: A. Gil, M. Giarrusso, J. Lamariano-Merketegi, A. Lorente, F. Albericio and M. Álvarez, *ACS Omega* **2018**, *3*, 2351.

(6) D. A. Evans, D. M. Fitch, T. E. Smith and V. J. Cee, *J. Am. Chem. Soc.* **2000**, *122*, 10033.

(7) E. Negishi, D. E. Van Horn and T. Yoshida, *J. Am. Chem. Soc.* **1985**, *107*, 6639.

(8) S. B. J. Kan, K. K.-H. Ng and I. Paterson, *Angew. Chem. Int. Ed.* **2013**, ***52***, 9097.

(9) S. Kiyooka and M. A. Hena *J. Org. Chem.* **1999**, *64*, 5511.

(10) M. Bergeron-Brlek, T. Teoh and R. Britton, *Org. Lett.* **2013**, *15*, 3554.

(11) E. P. Boden and G. E. Keck, *J. Org. Chem.* **1985**, *50*, 2394.

(12) Attempts to invert C15 through a Mitsunobu process failed to give any reactivity, presumably owing to steric constraints imposed by the proximal quaternary centre.

(13) S. D. Rychnovsky, B. Rogers and G. Yang, *J. Org. Chem.* **1993**, *58*, 3511. For a similar 1,3-*anti* acetonide on a THF-containing diol, see: A. R. Chamberlin, M. Dezube, S. H. Reich, D. J. Sall, *J. Am. Chem. Soc*. **1989**, *111*, 6247.

(14) The chelated structure is likely to be more complex, where further chelation from the C15 acyloxy group could contribute to the observed selectivity, see: J. Mowat, B. Kang, B. Fonovic, T. Dudding and R. Britton, *Org. Lett.* **2009**, *11*, 2057.

(15) (a) S. A. Bonnett, J. R. Whicher, K. Papireddy, G. Florova, J. L. Smith and K. A. Reynolds, *Chem. Biol.* **2013**, *20*, 772; (b) R. Reid, M. Piagentini, E. Rodriguez, G. Ashley, N. Viswanathan, J. Carney, D. V. Santi, C. R. Hutchinson and R. McDaniel, *Biochemistry* **2003**, *42*, 77.

(16) For recent work in our group, see: a) I. Paterson and N. Y. S Lam, *J. Antibiot.* 2017, **71**, 215; b) C. I. MacGregor, B. Y. Han, J. M. Goodman and I. Paterson, *Chem. Commun.* **2016**, *52*, 4632; c) B. Y. Han, N. Y. S. Lam, C. I. MacGregor, J. M. Goodman and I. Paterson, *Chem. Commun.* **2018**, *54*, 3247. For reviews on stereochemical reassignment, see: d) K. C. Nicolaou and S. A. Snyder, *Angew. Chem. Int. Ed*. **2005**, *44*, 1012 and e) T. L. Suyama, W. H. Gerwick and K. L. McPhail, *Bioorg. Med. Chem.* **2011**, *19*, 6675–6701.

(17) Penner, M.; Rauniyar, V.; Kaspar, L. T.; Hall, D. G. *J. Am. Chem. Soc.* **2009**, *131*, 14216.

(18) Berry, M. B.; Craig, D. *Synlett* **1992**, *1992* (01), 41.

(19) Inamoto, Y.; Kaga, Y.; Nishimoto, Y.; Yasuda, M.; Baba, A. *Chem. Eur. J.* **2014**, *20*, 11664.

(20) Kiyooka, S.; Hena, M. A. *J. Org. Chem.* **1999**, *64*, 5511.

(21) Corey, E. J.; Barnes-Seeman, D.; Lee, T. W. *Tetrahedron Lett.* **1997**, *38* (25), 4351.

(22) Hoye, T. R.; Jeffrey, C. S.; Shao, F. *Nat. Protoc.* **2007**, *2*, 2451.

Chapter 4.

Studies Towards the Synthesis of the Chimeric Glycopeptide Corresponding to the *Shigella Flexneri* Y O-polysaccharide and its Peptide Mimic MDWNMHAA

4.1. Introduction

Despite the tremendous progress achieved by modern medicine, infectious diseases continue to be a major threat to humans, accounting for the largest source of premature deaths and suffering worldwide.[1] Treatment of bacterial infections with antibiotics has saved millions of lives and cured many diseases. However, indiscriminate use of antibiotics has led to multidrug resistance in microbes, raising a major concern across the globe.[2] Vaccination offers an alternative to antibiotics and is considered to be one of the most efficient and cost-effective ways of controlling infectious diseases, as it confers long-term immunity among individuals.[3]

4.1.1. *Shigella* - The Pathogen

Shigella flexneri Y is one of the 15 serotypes of group B *Shigella*, a species of Gram-negative bacteria. It can cause shigellosis, a major form of bacillary dysentery by invading the large intestinal epithelium.[4] Most of those infected by this bacterium normally develop bloody diarrhoea, fever, and stomach cramps that usually resolve within one week. But other patients such as young children, the elderly, and the immunocompromised, could develop severe medical conditions, including septic shock that is often fatal. This disease is infectious and can be spread easily through food or person-to-person contact. *Shigella*-caused dysentery is endemic in poor countries without proper hygiene, causing an estimated 163 million illness episodes annually, and more than one million deaths worldwide.[5]

4.1.2. Development of Vaccine against *Shigella*

Antibiotics are commonly used to treat shigellosis however, antimicrobial resistance in its treatment was found years ago, and the resistance rates of *Shigella* isolates against various antibiotics are still increasing.[6] In addition, new multi-drug resistant *Shigella flexneri* species are emerging in developing countries such as China.[7] Hence, it would be worthwhile to develop vaccines against *Shigella* bacteria. There are several types of *Shigella* vaccines being developed, including live attenuated strains, proteasome vaccines, ribosomal vaccines, and conjugate vaccines.[8] Our research group has been working on developing conjugate vaccines against *Shigella flexneri* Y.[9,10]

As gram-negative bacteria, the cell wall of *Shigella flexneri* Y is coated by lipopolysaccharide (LPS), which is virulent and may be acquired from *Escherichia coli* via horizontal gene transmission.[11] The outer portion of LPS is the O-antigen polysaccharide (PS), a linear heteropolymer with a tetrasaccharide repeating unit ABCD [→2)-α-L-Rhap-(1→2)-α-L-Rhap-(1→3)-α-L-Rhap-(1→3)-β-D-GlcpNAc-(1→2)-α-L-Rhap-(1→][12] (Figure 4-1a), which could induce host humoral immune responses that are dominated by LPS-specific antibodies. A murine immunoglobulin G3 monoclonal antibody SYA/J6 was developed against *Shigella flexneri* Y LPS, and it can recognize the O-antigen polysaccharide[13]. A pentasaccharide portion ABCDA' **1** (Figure 4-1b) of this polysaccharide antigen can be recognized by antibody SYA/J6 as well with a binding constant K_A of 2.5 x 10^5 M^{-1}, and their interactions were studied in detail by crystallographic analysis.[14-16]

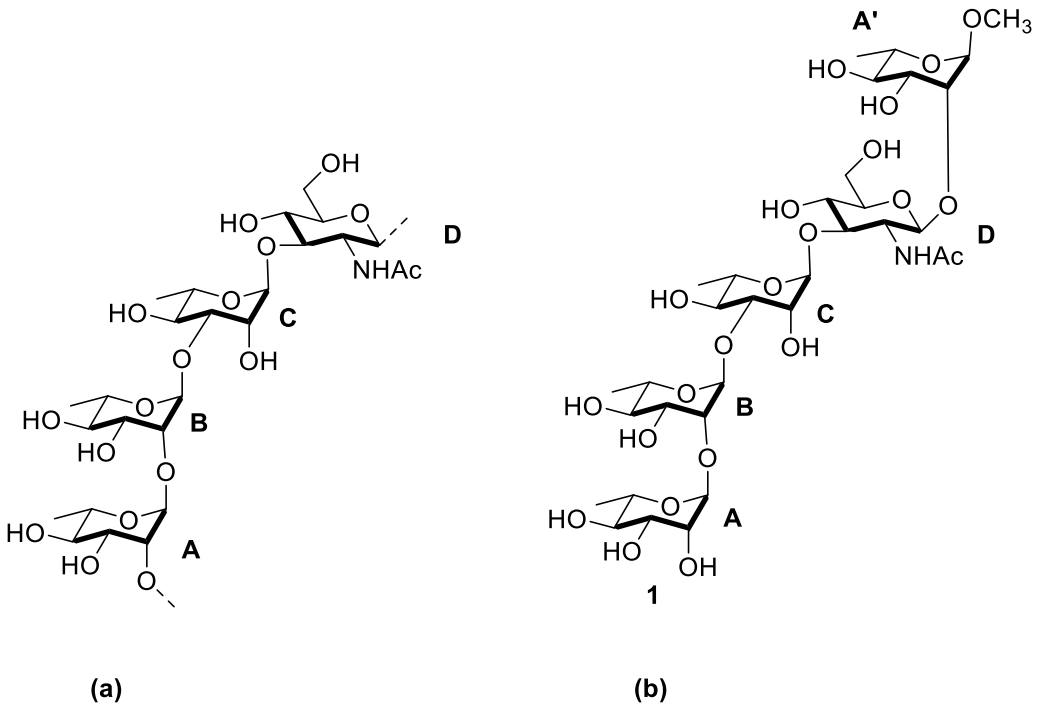

Figure 4-1 (a) Tetrasaccharide repeating unit on Shigella flexneri Y LPS. (b) Corresponding pentasaccharide hapten with an additional rhamnose unit from the next repeating unit.

In order to develop effective conjugate vaccines against bacteria, a poor antigen or hapten can be linked with an immunologic carrier protein such as bovine serum albumin or tetanus toxoid to form a conjugate.[17-21] For some bacteria, this poor antigen or hapten could be the corresponding O-antigen polysaccharide.[22] Upon immunization with this polysaccharide-protein conjugate vaccine, a T-cell-dependent immune response will be elicited in the host body (Figure 4-2) and protect the host from subsequent infection. Some antibodies on the surface of B cells would recognize the antigenic epitopes of the polysaccharide and bind to the conjugate. The conjugate is then internalized and processed by B cells and certain peptide fragments from the carrier protein are presented to T cells, which will excrete cytokines that help the B cell to differentiate and proliferate. Some B cells develop into plasma cells and produce plenty of antibodies that would specifically bind to polysaccharide on the pathogen and neutralize it. Other B cells differentiate into memory B cells, establishing immunological memory and immunity against the pathogen.

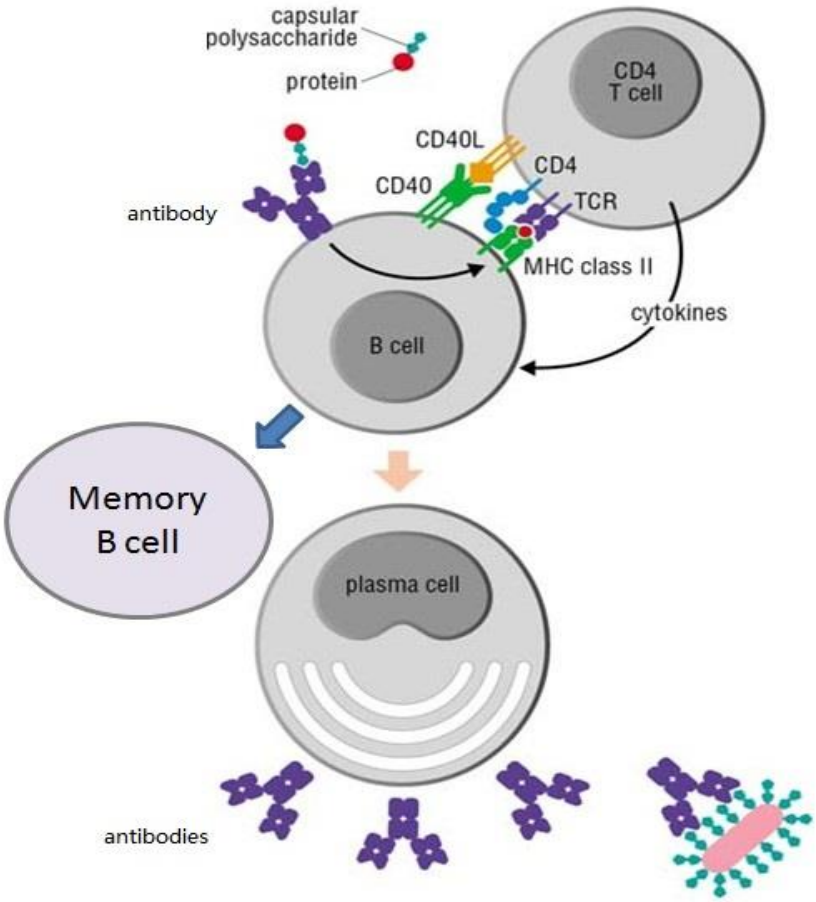

Figure 4-2 **Processing of polysaccahride-protein conjugate vaccine by the immune system.** ***(Figure originated from that published by Garland, http://www.ncbi.nlm.nih.gov/books/bv.fcgi?rid=imm.figgrp.1123).***

4.1.3. Carbohydrate-Peptide Mimicry

The interaction between proteins (antibodies) and carbohydrates is generally characterized by weak affinity,[23] which may result in an ineffective immune response. In addition, polysaccharides are usually difficult to synthesize by conventional organic chemical techniques. Molecular mimics of carbohydrates present an alternative approach to the development of conjugate vaccines. Some mimics such as peptides are easier to synthesize than carbohydrates. More importantly, those mimics could have higher binding affinity and selectivity toward corresponding antibodies, which may lead to stronger immunogenicity and immune responses.[24-26]

Screening of phage-displayed libraries with the monoclonal antibody SYA/J6 yielded an octapeptide **2** with sequence Met-Asp-Trp-Asn-Met-His-Ala-Ala (Figure 4-3), which served as a potential mimic of the O-polysaccharide of the *Shigella flexneri* Y.[14] The structure of the complex between the octapeptide and the Fab fragment of SYA/J6 was determined by X-Ray crystallography and it was found that the binding modes of the two ligands differ considerably (Figure 4-4).[15]

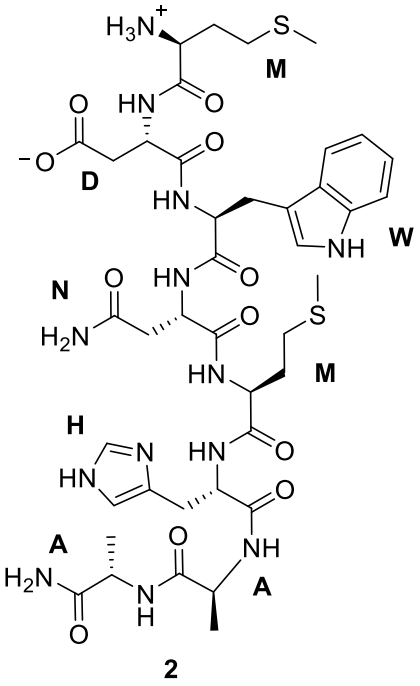

Figure 4-3 Structure of the octapeptide MDWNMHAA

First, octapeptide **2** binding complements the shape of the combining site groove much better than the pentasaccharide **1** binding, with more direct contacts [126 of ≤ 4Å in total] than that of pentasaccharide **1** [74 of ≤ 4Å in total]. Second, the indole ring of the Trp moiety, near the N-terminal end of the octapeptide **2**, enters a shallow hydrophobic cavity on the antibody. But the pentasaccharide **1** does not enter this pocket. Third, the octapeptide **2** shows no direct contacts with the central and deepest part of the binding groove, which is filled by ring C in the pentasaccharide **1**. This deep pocket is instead occupied by three hydrogen-bonded water molecules (Figure 4-4) in the octapeptide bound structure. Fourth, the last four residues in the octapeptide **2** NMHAA forms one turn of an α-helix, and this ordered structure is not significantly populated in its free conformations. The binding affinity of the octapeptide **2** (K_A=5.7×10^5 M^{-1}) is moderate and

only two-fold higher than that of the pentasaccharide **1**. Microcalorimetry data also revealed that the octapeptide **2** exhibits favorable enthalpy of binding (ΔH = -16.9 kcal mol^{-1}) was offset by an unfavorable entropy of binding ($-T\Delta S$ = 9.1 kcal mol^{-1}) and this entropic penalty can be attributed to the introduction of the α-helical turn and the immobilization of three water molecules in the deepest part of the combining groove.[15-16] As a functional mimic of the *Shigella flexneri* Y PS, the octapeptide **2** has been used in prime/boost immune strategies by forming a conjugate vaccine with the carrier protein tetanus toxoid (TT).[21] MDWNMHAA-TT indeed generated antibodies that cross-react with *Shigella flexneri* Y LPS, although the kinetics of the immune response in mice were slow, as several immunizations were found to be necessary.[9]

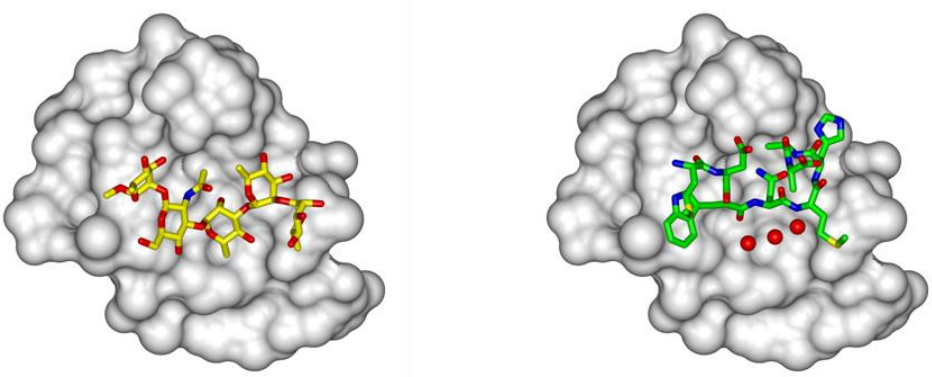

(a) (b)

Figure 4-4 **(a) Fab fragment of SYA/J6 antibody with bound pentasaccharide, (b) Fab fragment of SYA/J6 antibody with bound octapeptide MDWNMHAA; the red spheres represent three immobilized water molecules.**

4.1.4. Design of a Chimeric Glycopeptide as a Carbohydrate Mimic

In order to develop better haptens that can induce robust immune responses by mimicking the natural antigen, two chimeric glycopeptides (α-glycopeptide **3** and β-glycopeptide **4**) (Figure 4-5) were designed by combination of the certain structural elements of both the pentasaccharide **1** and the octapeptide **2**. The rhamnosyl trisaccharide motif (A-B-C) of the pentasaccharide **1** was retained, which presumably serves to reduce the entropic penalty by imposition of an α-helical turn within the NMHAA region of the octapeptide, and the Rha C should be able to establish direct contacts with the deepest cavity of the binding groove. Additionally, the Met, Asp, and Trp residues of

the octapeptide **2** were retained as they made favorable hydrophobic interactions within the binding site[10]. The thioglycosidic linkage was incorporated to increase the chemical stability of both the glycopeptides when compared to those of the corresponding *O*-glycosides.[27] Docking studies by AUTODOCK 3.022 showed that both glycopeptides could fit into the binding groove on the SYA/J6 antibody without spatial clashes (Figure 4-6).

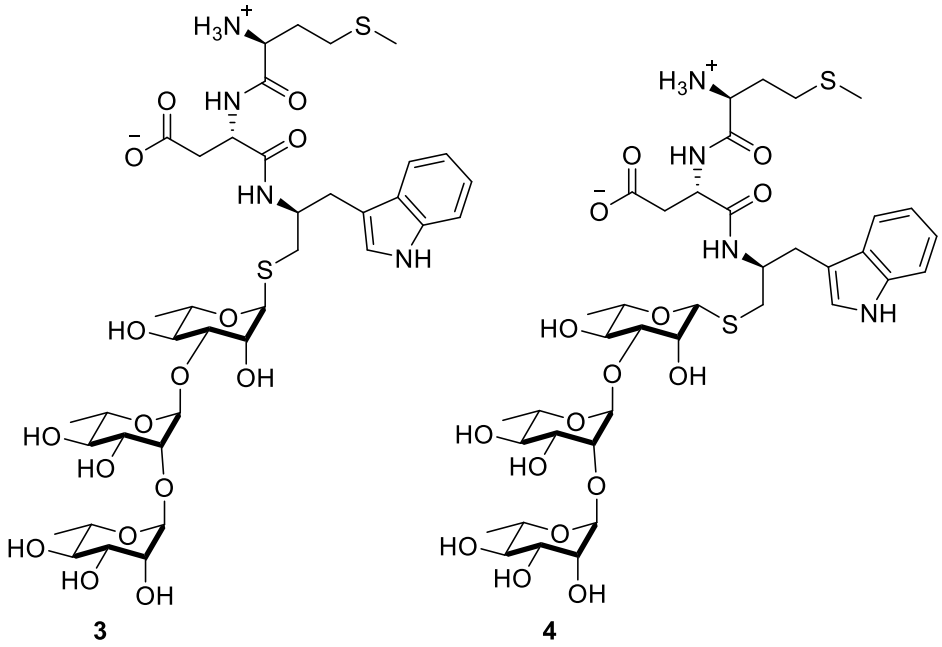

Figure 4-5 Structures of the α-glycopeptide 3 and the β-glycopeptide 4.

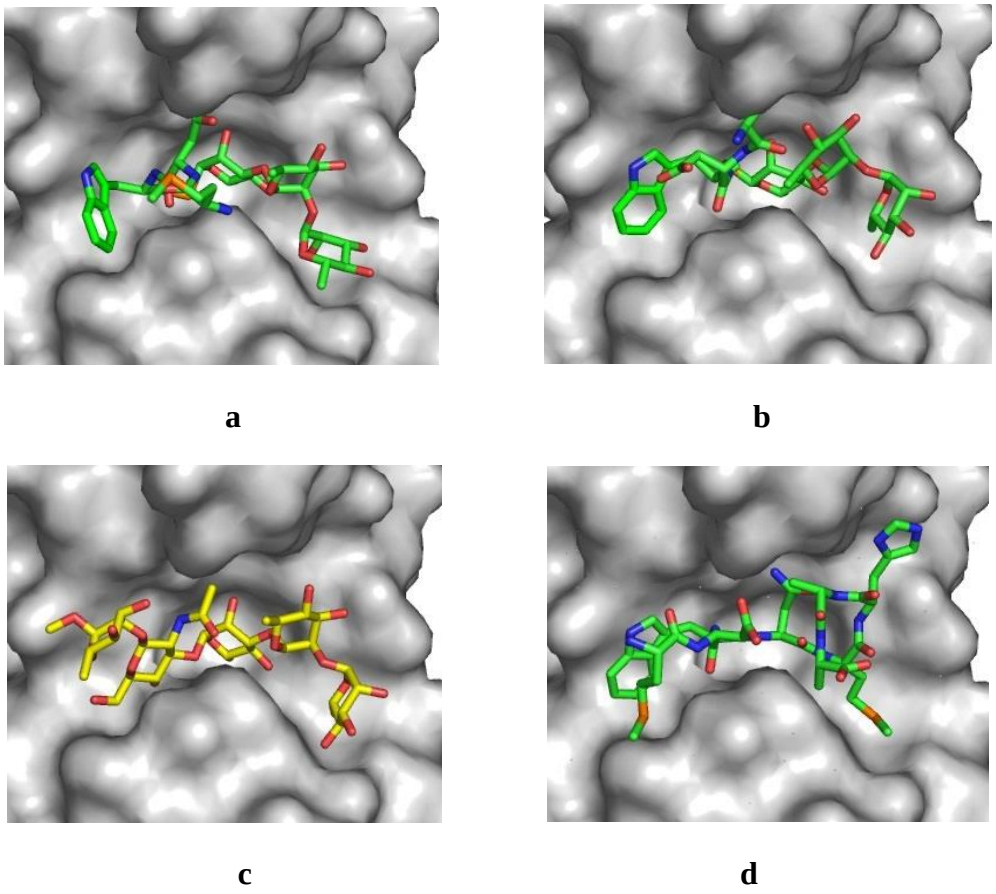

Figure 4-6 Docked structures of (a) α-glycopeptide, (b) β-glycopeptide, (c) pentasaccharide, (d) octapeptide.

The binding modes of the two glycopeptides to SYA/J6 antibody are different (Figure 4-7). At the sugar ring end, the orientation of Rha A in the α-glycopeptide **3** is almost perpendicular to that of the pentasaccharide **1**, while Rha A in the β-glycopeptide **4** assumes similar orientation as the pentasaccharide **1**, although the position is slightly different. At the amino acid end, the orientation of the indole ring in the α-glycopeptide **3** is considerably different from that of the octapeptide **2**, whereas the indole ring in the β-glycopeptide **4** almost completely superimposes on that of octapeptide **2**. Therefore, the β-glycopeptide **4** may bind tighter to the antibody than the α-glycopeptide **3.**

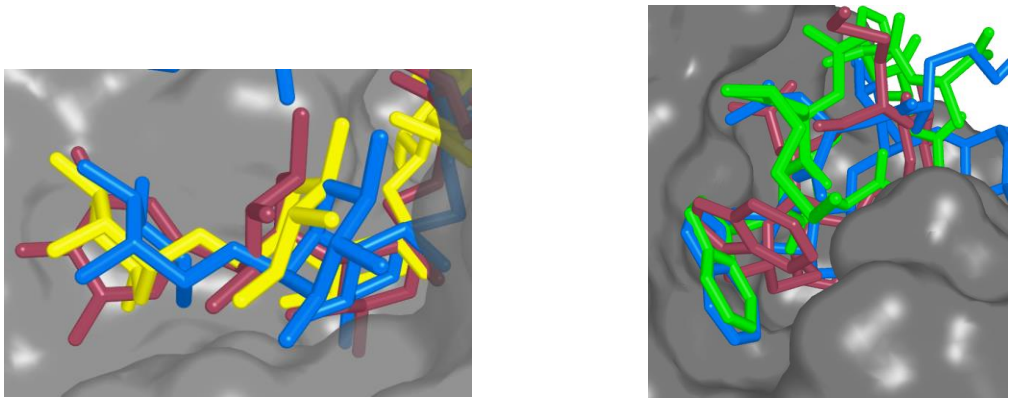

(a) (b)

Figure 4-7 Superpositions of (a) the sugar ring end of α-glycopeptide (red) and β-glycopeptide (blue) on the parent pentasaccharide; (b) the amino acid end of α-glycopeptide and β-glycopeptide on the parent octapeptide (green).[28]

The synthesis of the α-glycopeptide **3** was successfully completed in our research group, but it showed no inhibitory activity.[10] One possible reason could be that the α-glycopeptide **3** did not superimpose well with either pentasaccharide **1** or octapeptide **2**, as indicated by results from the docking study. Furthermore, the design of the two glycopeptides was partially based on docking results from AUTODOCK 3.0, which assumes the Fab domain of SYA/J6 to be completely rigid. However, the binding of ligands to antibody should be a dynamic process, and the conformation of the SYA/J6 antibody could change when interacting with glycopeptides. The better fit of the docked β-glycopeptide prompted us to question whether the latter compound would be a better binder. We therefore embarked on the chemical synthesis of the chimeric β-glycopeptide **4** in order to generate sufficient quantities of pure sample for immunochemical studies and further development. Our approach uses a highly convergent strategy for this complex molecule.

4.2. Results and Discussion

4.2.1. Proposed Retrosynthesis

Our retrosynthetic approach for the β-glycopetide **4** is outlined in Scheme 4-1. we envisaged that the target molecule **4** could potentially be obtained by global deprotection of the glycopeptide **5** which could be assembled by a coupling reaction of activated dipeptide **6** and the amine **7**. The amine **7** could, in turn, be obtained by the removal of the Fmoc protecting group from the intermediate **8**.

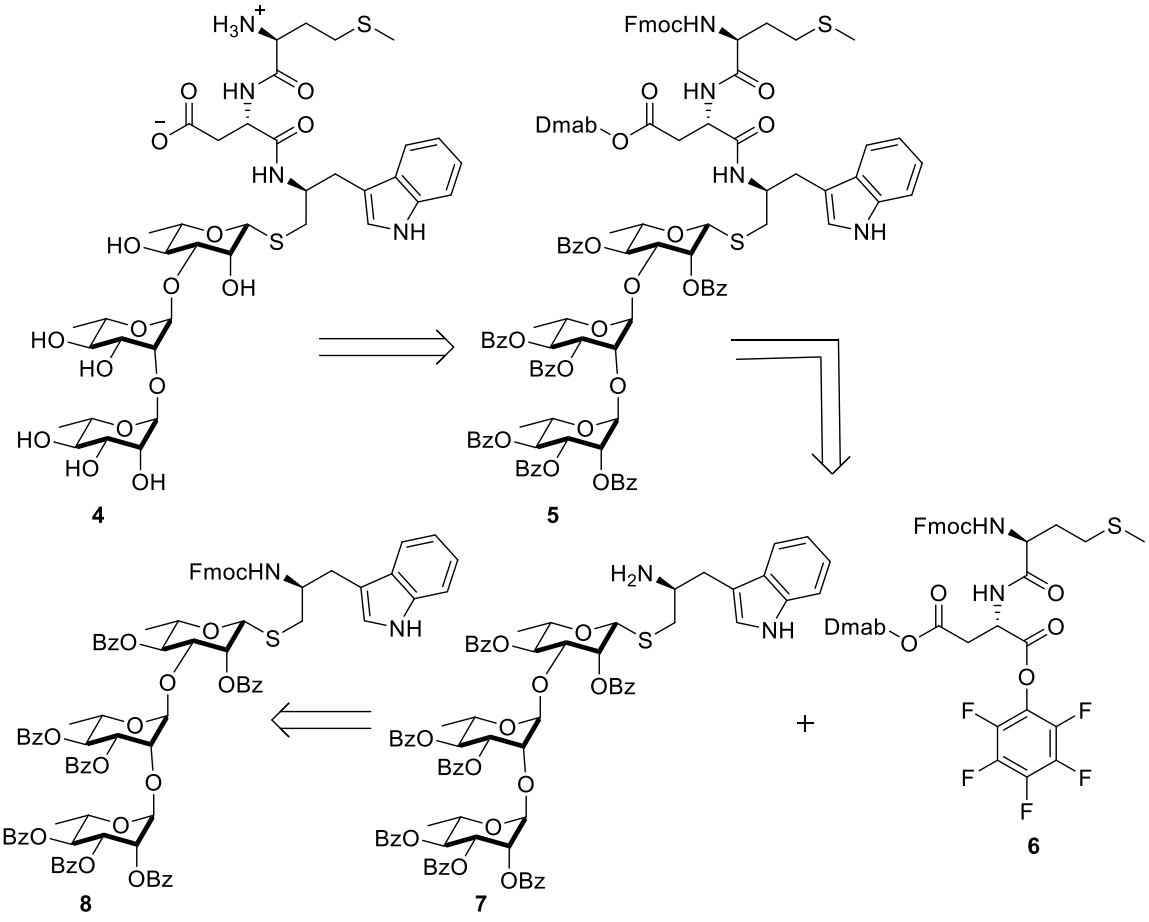

Scheme 4-1 Retrosynthetic analysis of the β-glycopeptide 4.

The retrosynthetic analysis of the trisaccharide intermediate **8** reveals that this could be obtained by following a [2+1] approach, utilizing the Schmidt[29] glycosylation procedure between the disaccharide donor **9** and the acceptor **10** (Scheme 4-2). In designing the retrosynthesis, attention was given to the fact that the construction of the

thio-Fmoc tryptophan derivative **10**, which involves a 1,2-*cis* glycosidic linkage, was the most demanding. We envisioned that the thio-Fmoc tryptophan derivative **10** could be synthesized by using a stereoselective β-rhamnopyranosylation[30] reaction between the ulosyl bromide **12** and the thiol **11**. On the other hand, glycosylation between the acceptor **13** and the donor **14** with a participating group at C2 would furnish the disaccharide **9**. The acceptor **13** and the ulosyl bromide **12** can be obtained from the common diol intermediate **15**.

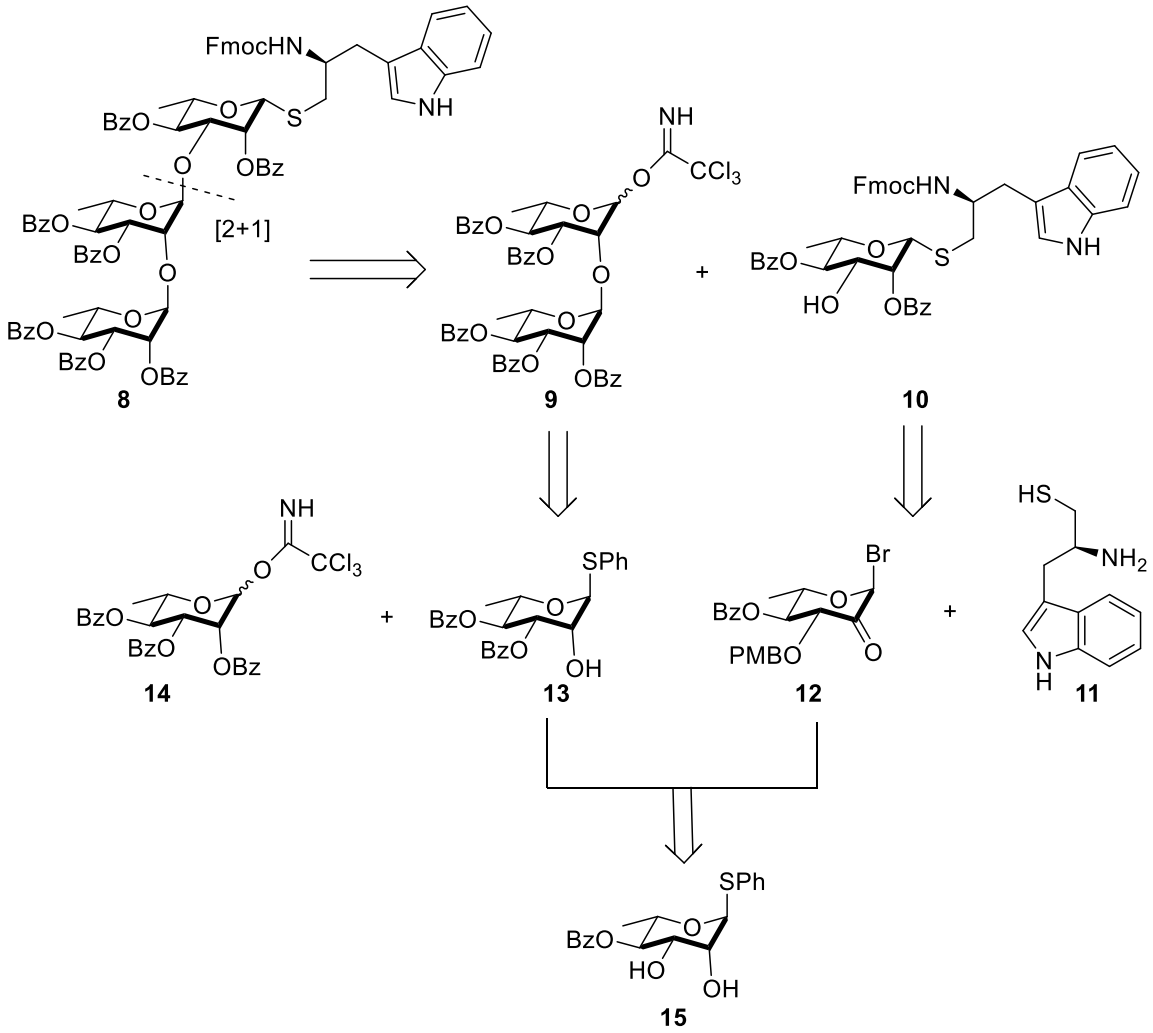

Scheme 4-2 Retrosynthesis of trisaccharide derivative 8

4.2.2. Synthesis of Disaccharide 7

Our synthesis began by accessing the known diol[31] **15** in gram quantities from the commercially available L-rhamnose which was peracetylated and linked to benzenethiol in the presence of boron trifluoride etherate (Scheme 4-3). The anomeric mixture obtained was purified by column chromatography to afford the pure α-anomer **17** in 65% yield. Deacetylation using Zemplen[32] conditions, followed by isopropylidene introduction yielded compound **19** in 94% yield over two steps. Next, benzoylation at the C4-alcohol under conventional conditions (BzCl/pyridine), followed by isopropylidene cleavage under acidic conditions, afforded the diol **15** in 82% yield over two steps.

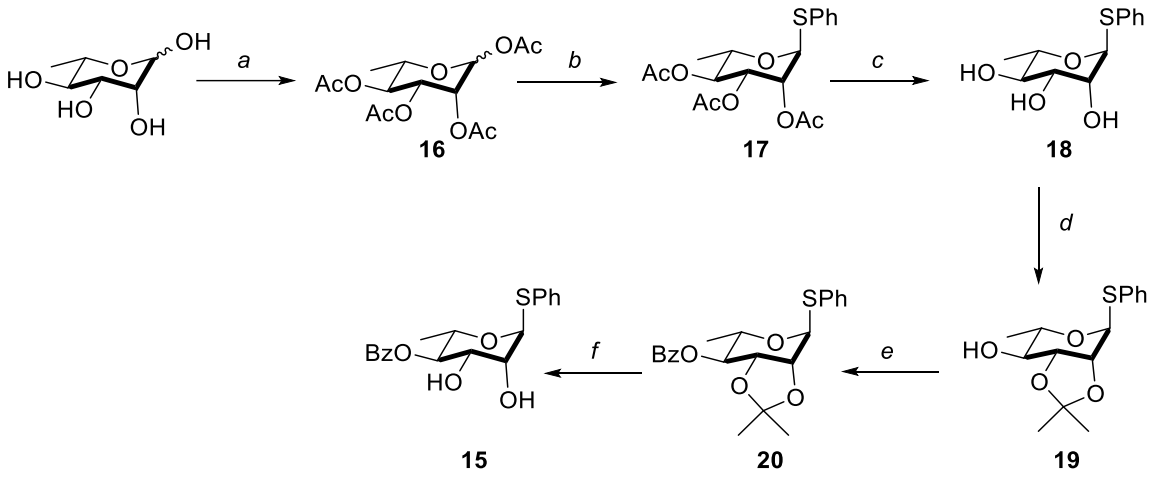

Scheme 4-3 Synthesis of the common diol intermediate

Reagents and conditions: (a) Ac_2O, CH_2Cl_2, cat. DMAP, TEA, (b) $BF_3.Et_2O$, thiophenol, 65%; (c) 1M NaOMe/MeOH, (d) 2,2-dimethoxypropane, PTSA (94% over two steps), (e) BzCl, py, CH_2Cl_2, (f) 80% AcOH, 80 °C, 82% over two steps.

The acceptor **13** was synthesized from the intermediate diol **15** in four steps (Scheme 4-4). Treatment of compound **15** with trimethyl orthoacetate in the presence of a catalytic amount of PTSA gave the corresponding ortho ester **21** in quantitative yield. Cleavage of the ortho ester **21** under acidic conditions yielded the C3-alcohol derivative **22** in 85% yield over two steps. Benzoylation of compound **22** yielded the C3-benzoate derivative **23.** Subsequently, selective hydrolysis of the C2-acetate group was carried out by treating compound **23** with acetyl chloride in methanol. After consumption of staring material, as monitored by TLC, the reaction mixture was quenched with triethyl amine. After work-up and purification, the major product obtained was the undesired compound

24 resulting from a 3-*O* to 2-*O* benzoyl ester migration in 40% yield and the minor desired **13** C2-alcohol in 10% yield (Scheme 4-4). Optimization of reaction conditions by reducing the equivalents of acetyl chloride and careful quenching of the reaction mixture with slow addition of aqueous saturated $NaHCO_3$ solution up to pH-7.0 avoided the benzoyl group migration to the vicinal hydroxyl group to a great extent. These optimized conditions yielded the acceptor **13** in 70% yield over two steps.

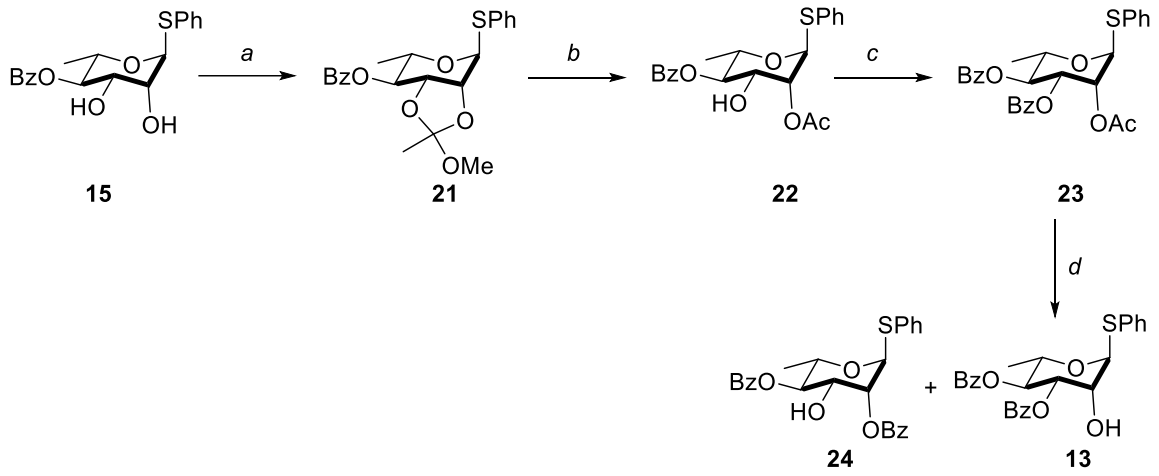

Scheme 4-4 Synthesis of the aceptor 24

Reagents and conditions: (a) Trimethylorthoaceate, PTSA, CH_3CN, (b) 80% AcOH, 85% over two steps, (c) BzCl, py, 0 °C→r.t., (d) MeOH, AcCl, 40 °C, 70% over two steps.

The glycosyl donor **14** was synthesized in 3 steps as shown in Scheme 4-5. L-rhamnose was subjected to benzoylation under standard conditions using benzoyl chloride and pyridine and gave the tetrabenzoyl derivative **25** in quantitative yield. The compound **25** was subjected to selective anomeric debenzoylation using hydrazine acetate in DMF to give the hemiacetal **26**. Activation of the anomeric centre in compound **26** by reaction with trichloroacetonitrile in presence of DBU as a base afforded the corresponding trichloroacetimidate **14** in 70% yield over three steps. Subsequently, glycosylation of the acceptor **13** with the trichloroacetimidate donor **14** in the presence of a catalytic amount of trimethylsilyl trifluorometahnesulfonate (TMSOTf) as a promoter at -35 ^{o}C gave exclusively the corresponding α-linked disaccharide **27** in 85% yield as a single isomer. The selectivity can be attributed to the neighboring group participation of the C2 benzoyl group of compound **14**.

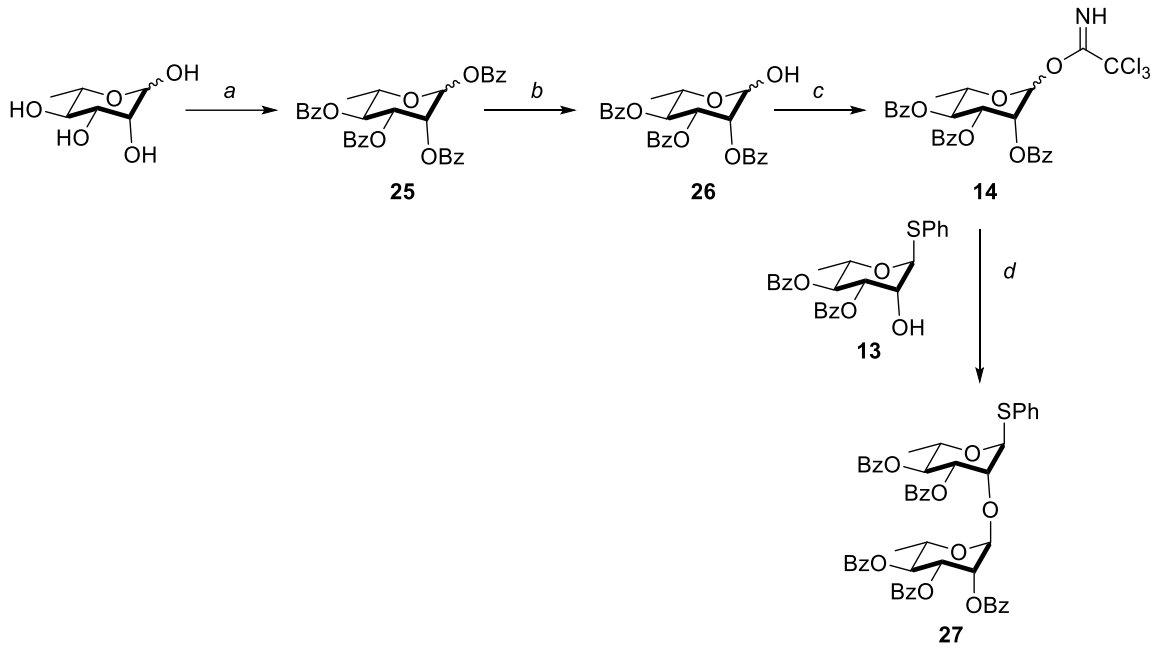

Scheme 4-5 Synthesis of the disaccharide 27.

Reagents and conditions: (a) BzCl, py, 0 °C→r.t., (b) NH_2NH_2.OAc, DMF, (c) Trichloroacetonitrile, DBU, CH_2Cl_2, 70% (over three steps), (d) TMSOTf, CH_2Cl_2, -30 °C, 85%.

4.2.3. Synthesis of 1- Thio-β-Rhamnose-Linked Fmoc-Tryptophan Derivative 10

Stereoselective synthesis of β-L-rhamnosides is challenging due to the unfavorable α-favored anomeric effect and the steric hindrance of the axial substituent at the C2 position as well as the non-availability of neighboring group participation.[33,34] Of the few methods available in the literature[35-41] for the synthesis of β-L-rhamnosides, we chose to adopt the Lichtentahler[30] method of glycosylation with an ulosyl bromide, known to give β-anomers with *O*-glycosides. However, to the best of our knowledge, glycosylation of ulosyl bromides with thiol acceptors to form S-β-L-ulosides is unprecedented.

The ulosyl bromide **12** was synthesized in six steps starting from the diol intermediate **15** as outlined in Scheme 4-6. The C3-alcohol of diol **15** was subjected to 2,3-*O* stannyl-activated regioselective alkylation, followed by acetylation at C2-alcohol to afford compound **28** in 70% yield over three steps. A different protecting group, 4-methoxybenzyl ether, was chosen at C3 in compound **28**, so that it could be removed

selectively in the presence of a benzoyl ester later in the synthesis. Oxidation of **28** with meta-chloroperoxybenzoic acid gave the sulfoxide **29**, which on subsequent elimination in the presence of base afforded the desired 2-acetoxy-L-rhamnal **30** in 70% yield over two steps. Next, the rhamnal **30** was treated with NBS/ethanol in CH_2Cl_2 at 0 °C to furnish the desired ulosyl bromide **12** in 85% yield.

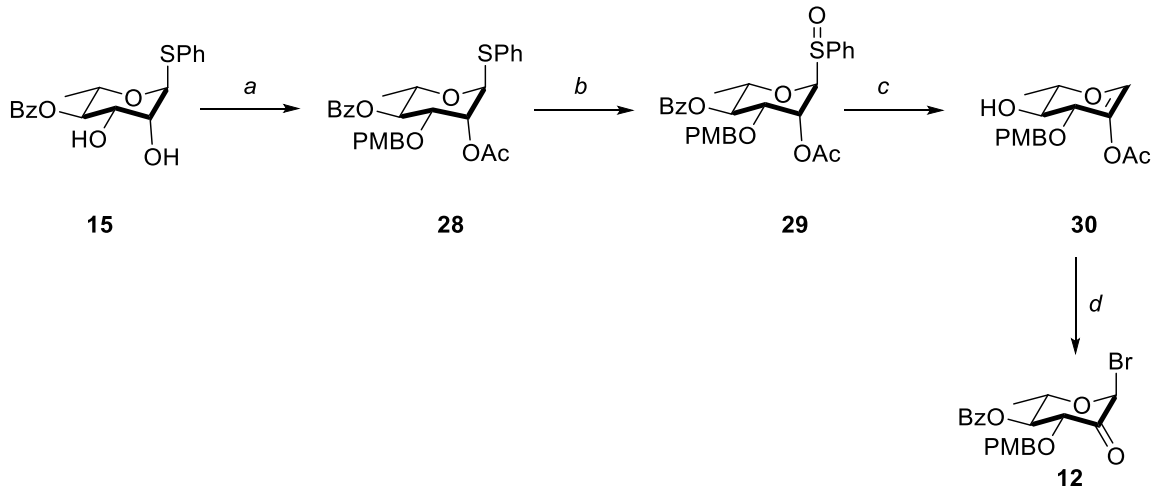

Scheme 4-6 Synthesis of the ulosyl bromide 33.

Reagents and conditions: (a) 1) Bu_2SnO, toluene, reflux with a Dean-Stark trap, 2) Bu_4NI, PMBBr, toluene, 3) Ac_2O, py, 86% over 3 steps, (b) KF/m-CPBA, 4:1 CH_3CN: H_2O, 0 °C, (c) toluene, py, reflux, 70% (over three steps), (d) NBS, EtOH, 0 °C, 85%.

With compound **12** in hand, we next proceeded to the synthesis of the Fmoc-thiotryptophanol derivative **11**. The known bromide **34**[10] (Scheme 4-7) was obtained from commercially available L-tryptophan in six steps. Accordingly, L-tryptophan was first subjected to esterification followed by reduction to give the corresponding L-tryptophanol (**32**),[42] which was then treated with Fmoc-succinimide to yield Fmoc-tryptophanol (**33**) in excellent yield (90%). Mesylation of compound **33**, followed by displacement with lithium bromide afforded the bromide **34** in 90% yield over two steps. Subsequently, the bromide **34**, was then refluxed with thiourea in acetonitrile, to give isothiouronium salt **35**, which was then treated with 15% sodium metabisulphite to afford the required thiol **11** in 80% yield over two steps.

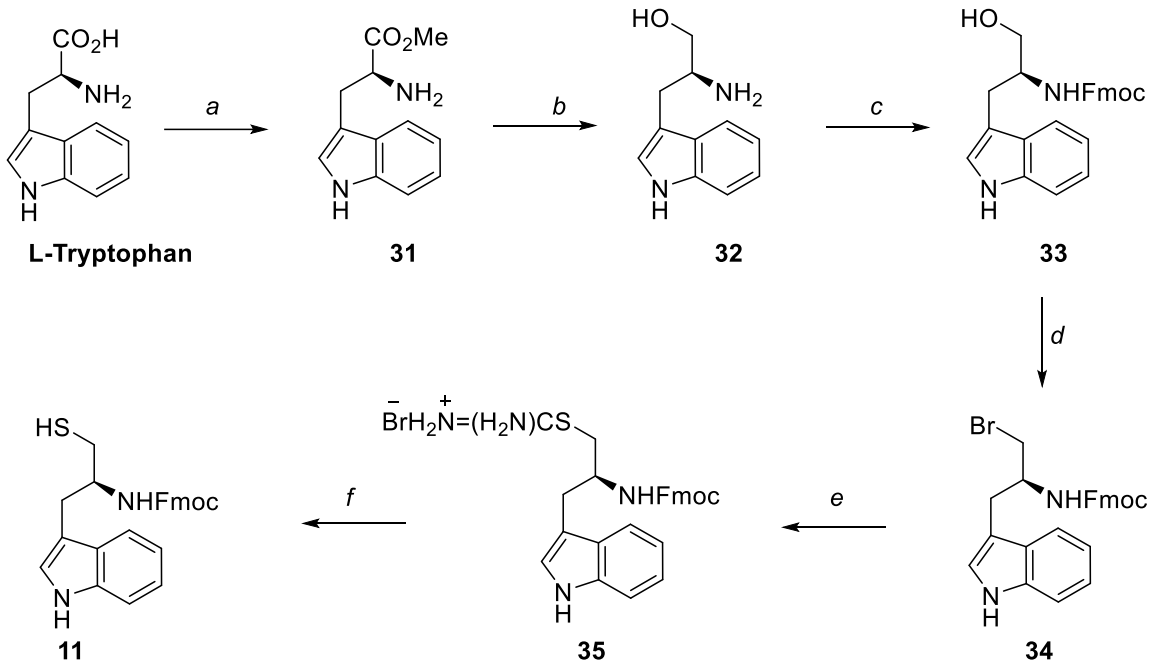

Scheme 4-7 Synthesis of thi-Fmoc tryptophanol derivative 11

Reagents and Conditions: (a) $SOCl_2$, MeOH, reflux, (b) $NaBH_4$, EtOH/H_2O, reflux 70% (over two steps), (c) Fmoc-OSu, $NaHCO_3$, acetone, 90%, (d) 1) MsCl, py 2) LiBr, reflux, 90% (over two steps), (e) thiourea, acetonitrile, reflux, (f) 15% $Na_2S_2O_5$, 80% (over two steps).

Having the ulosyl bromide **12** and thiol acceptor **11** in hand, we next turned our attention towards the stereoselective β-rhamnosylation reaction. Our initial attempts of glycosylation using the standard Koenigs-Knorr[43] conditions (Ag_2CO_3 in CH_2Cl_2) were unsuccessful. In an effort to effect this transformation, the solvent, temperature and the reaction time were varied, and the results are summarized in Table 4-1. All the reactions were continuously monitored using MALDI-TOF (Matrix-assisted laser desorption/ionization – Time of flight) mass spectrometry, as TLC analysis was not conclusive. Finally, when the reaction was carried out in acetone in the presence of Ag_2CO_3 (Table 4-1, entry 6) at -78 °C for 4 h and the temperature was slowly raised to -25 °C and maintained at this temperature for 6 h the crude compound **36** was obtained in quantitative yield. The ^{1}H NMR and HRMS spectral analysis of the crude **36** confirmed the presence of product along with other unknown impurities. The ratio of α/β anomers could not be inferred from the ^{1}H NMR spectrum due to the presence of overlapping proton resonances in the anomeric region around δ 4.5 to 6. Attempts to purify compound **36** by

column chromatography led to the decomposition of product. Owing to its limited stability, this material was partially purified by triturating with 50% ethyl acetate:hexane and was then carried to the next step as a mixture of α/β anomers.

Table 4-1 Efforts to access the β- thiorhamnoside 36.

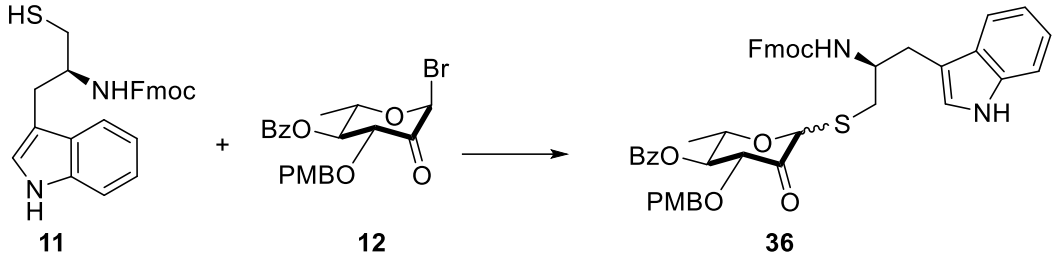

11 **12** **36**

Entry	Substrate	Conditions	Outcome
1	**11** (1.0 equiv) and **12** (1.0 equiv)	Acetone, Ag_2CO_3 20 °C	Decomposition
2	**11** (1.0 equiv) and **12** (1.0 equiv)	Acetone, Ag_2CO_3 10 to 5 °C	Decomposition
3	**11** (1.0 equiv) and **12** (1.0 equiv)	Acetone, Ag_2CO_3 -20 to -15 °C	Decomposition
4	**11** (1.0 equiv) and **12** (1.0 equiv)	Acetone, K_2CO_3 0 to 5 °C	No reaction
5	**11** (1.0 equiv) and **12** (1.0 equiv)	DMF, DIPEA 0 to 5 °C	No reaction
6	**11** (1.0 equiv) and **12** (1.0 equiv)	Acetone, Ag_2CO_3 -78 °C, 4h, -25 °C, 6h	Product formed **36**

The carbonyl group of the crude **36** was reduced with sodium borohydride to give the corresponding C2-alcohol **37**. This was purified by column chromatography to afford an inseparable mixture of diastereomers in a 3:1 ratio. This mixture was subjected to benzoylation using benzoyl chloride and pyridine, to give the crude C2-benzoate in a 3:1 ratio. The latter material was purified by column chromatography and we were pleased to obtain the two isomers **38** and **39** in pure form. The structures of the pure compound were elucidated by ^{1}H, ^{13}C, and HRMS spectral analysis.

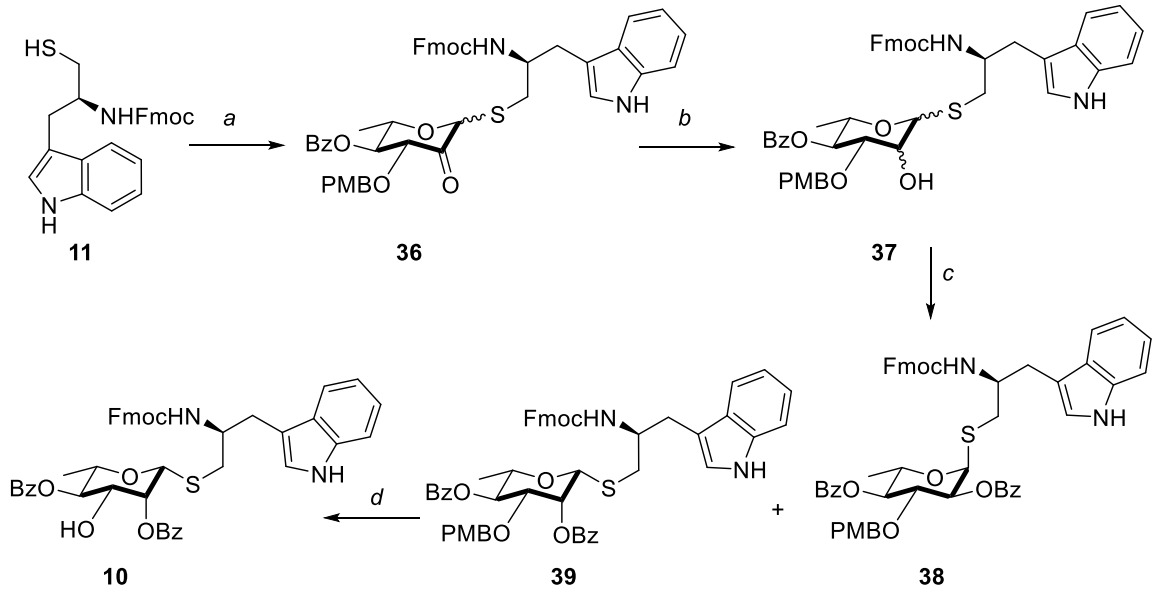

Scheme 4-8 Synthesis of the 1-thio-β-rhamnoside derivative 10

Reagents and conditions: (a) **12**, Ag_2CO_3, Acetone, -78 ^{0}C→ -25 ^{0}C (b) $NaBH_4$, CH_2Cl_2:MeOH (1:1) (c) BzCl, py (d) $SnCl_4$/PhSh, -78 ^{0}C, 70%

In Figure 4-8 the ^{1}H NMR spectrum of compound **39** is displayed. The resonance at δ 4.80 corresponds to the anomeric proton and the resonances at δ 5.95 and 3.72 correspond to the H2 and H3 protons, respectively. The small coupling constant $J_{2,3}$ = 2.7 Hz indicates an axial-equatorial coupling. The lower chemical shift value of the anomeric proton is indicative of the β-thioglycosidic linkage and the coupling constants reveal the orientation of C2-alcohol to be in an axial position. These results are further corroborated by observing the NOE enhancements between H5, H3 and H1. Thus, compound **39** was confirmed to be the desired major isomer with the β-configuration at the anomeric centre.

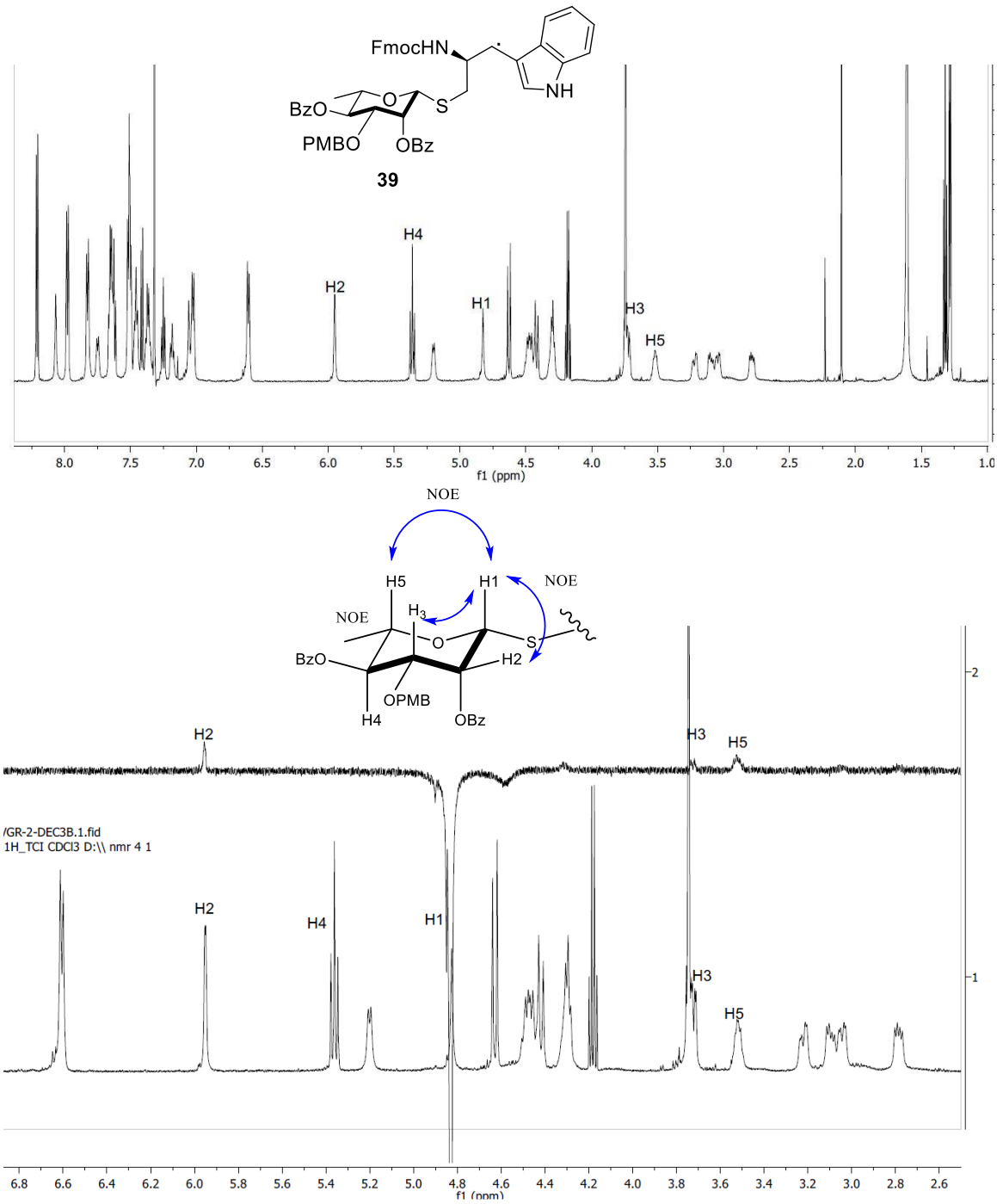

Figure 4-8 ^{1}H NMR and 1D NOE spectra of the β-anomer 39

The resonance at δ 5.75 in the ^{1}H NMR spectrum of compound **38** (Figure 4-9) corresponds to the anomeric proton and the resonances at δ 5.40 and 4.15 corresponds to H2 and H3 protons respectively. The large coupling constant $J_{2,3}$ = 9.4 Hz indicates an axial-axial coupling and $J_{2,1}$ = 5.4 Hz suggests an axial-equatorial coupling. The higher chemical shift value of anomeric proton is indicative of the α-thioglycosidic linkage and the

coupling constants reveal the orientation of C2-alcohol in the equatorial position. This evidence is further corroborated by observing the NOE enhancements between H2 and H1 and the absence of an observable NOE between H1 and H5. Compound **38** is the undesired minor isomer with the α-configuration at the anomeric centre. Thus, it is concluded that the β-anomer underwent a stereospecific reduction to give the axial 2-alcohol, whereas the α-anomer gave the equatorial C2-alcohol exclusively. Next, the β-anomer **39** was subjected to selective PMB cleavage using Tin (IV) chloride in the presence of thiophenol, to afford the free C3-alcohol **10** in good yield.

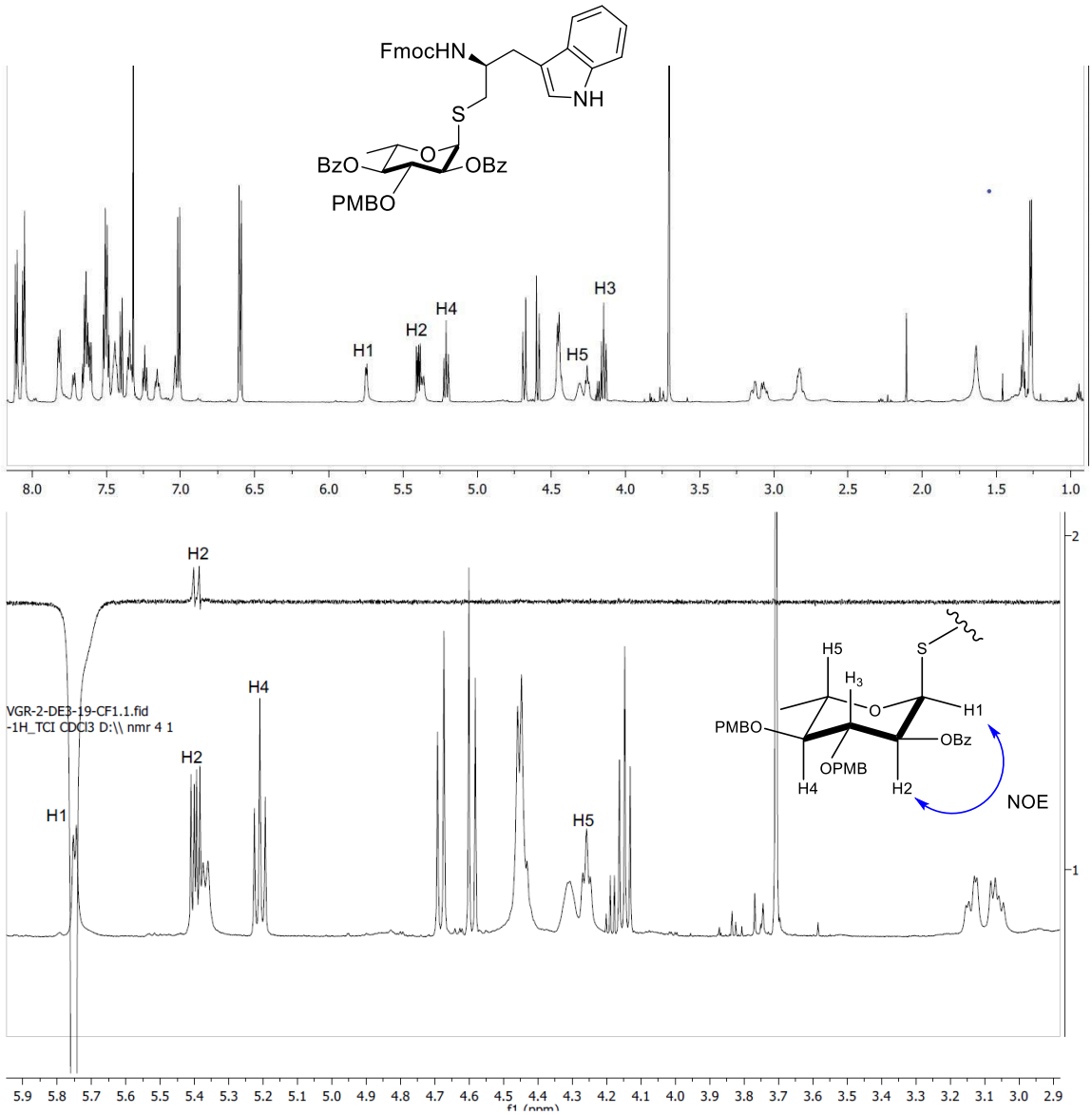

Figure 4-9 **^{1}H and 1D NOE spectra of the α anomer 38.**

4.2.4. Attempted Synthesis of the β-glycopeptide 4

After successful synthesis of the β-thiorhamnoside **10** we next turned our attention towards the synthesis of the known dipeptide **6**.[10] A solid phase synthesis using Fmoc chemistry and an HBTU-HOBt/DIPEA coupling strategy was employed to access the dipeptide **6** as shown in Scheme 4-9. The synthesis began with the introduction of the protecting group *N*-[1-(4,4-dimethyl-2,6-dioxocylcohexylidene)-3-methylbutyl]aminobenzyl ester (Dmab)[44] on the side chain of Fmoc-Asp-OtBu (**40**) as an orthogonal protecting group required for modification of the peptide on the resin at a later stage of the synthesis. The Dmab esters are stable to piperidine in DMF but can be removed by treatment with 2% hydrazine in DMF. Compound **40** was coupled with Dmab-OH in the presence of DTBMP, HOBt and DIC to afford the Fmoc-Asp (Dmab)-OtBu (**41**) in 70% yield. The hydrolysis of the *t*-butyl ester of compound (**41**) with 50% TFA in CH_2Cl_2 afforded Fmoc-Asp (ODmab)-OH (**42**) in 90% yield. The C-terminus of compound (**42**) was immobilized on 2-chlorotrityl resin[45] in the presence of DIPEA in DMF, then the on-resin peptide **44** was treated with with 25% piperidine in DMF to afford the free amine, which was subsequently coupled with Fmoc-Met-OH using HBTU, HOBt/DIPEA. Next, the coupled dipeptide was treated with 5% TFA in CH_2Cl_2 to cleave the C-terminus from the resin, which was further purified by column chromatography to afford the desired dipeptide **45** in 50% yield over three steps. Finally, in order to increase the coupling efficiency between the precursors **6** and **7** *en route* to the synthesis of the protected glycopeptide **8**, the carboxylic end of **45** was converted to the more active pentafluorophenyl ester **6** by treating **45** with pentafluorophenol and DIC in CH_2Cl_2.

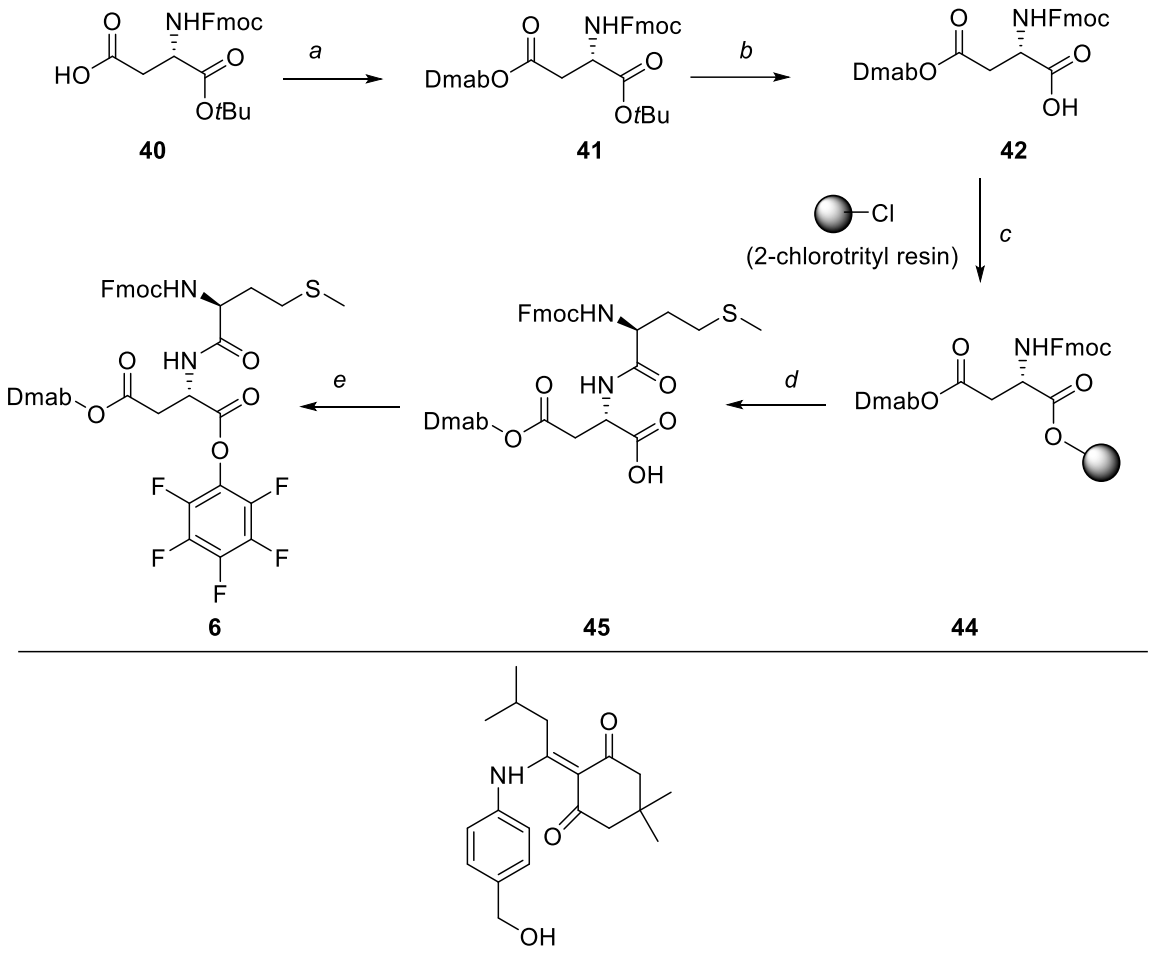

Dmab:-*N*-[1-(4,4-dimethyl-2,6-dioxocylcohexylidene)-3-methylbutyl]-amino benzyl alcohol

Scheme 4-9 Synthesis of the activated dipeptide 6

Reagents and conditions: (a) Dmab-OH, DTBMP, HOBt, DIC, 70% (b) 50% TFA in CH_2Cl_2, 90% (c) DIPEA, DMF (d) 1) 25% Piperidine/DMF 2) Fmoc-Met-OH, HBTU,HOBt/DIPEA, DMF 3) 5% TFA in CH_2Cl_2, 50% yield over three steps (e) Pentafluorophenol, DIC, CH_2Cl_2

With the β-thio-Fmoc derivative **10** and the disaccharide **27** in hand, the stage was set for the synthesis of the trisaccharide derivative **8** (Scheme 4-10). The disaccharide **27** was treated with NBS in a mixture of acetone water (9:1), to give the hemiacetal **46**, which upon reaction with trichloroacetonitrile in the presence of base DBU afforded the corresponding trichloroacetimidate **9** with 90% yield over two steps. Coupling of the glycosyl donor **9** with acceptor **10** was performed in CH_2Cl_2 in the presence of TMSOTf. MALDI-spectrometry and TLC analysis of the crude material indicated the presence of the

acceptor **10** and other unknown impurities, along with a trace amount of product that had the same Rf as the acceptor **10**.

Table 4-2 Optimization of the glycosylation reaction to access the trisaccharide derivative 8.

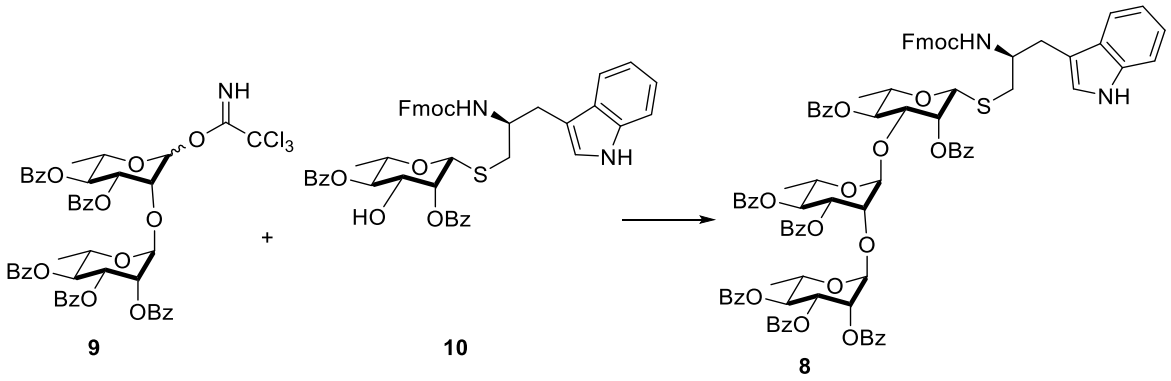

Entry	Substrate	Conditions	Outcome
1	**10** (1.0 equiv) and **9** (1.5 equiv)	0.1 equiv $BF_3.Et_2O$ -78 °C	Decomposition
2	**10** (1.0 equiv) and **9** (1.5 equiv)	0.1 equiv TBDMSOTf, -45 to -40 °C	Decomposition
3	**10** (1 equiv) and **9** (1.5 equiv)	0.1equiv TMSOTf -45 to -40 °C	Decomposition
4	**10** (1 equiv) and **9** (1.5 equiv)	0.3 equiv TMSOTf -35 to -30 °C	Traces of product mass peak observed from MALDI mass spectrum
5	**10** (1 equiv) and **9** (1.5 equiv)	0.2 equiv TMSOTf -35 to -30 °C Reverse addition	Product formed 40% yield

To optimize this glycosylation reaction, we probed the scope of reaction parameters, varying the number of equivalents of donor, promoter, and temperature (Table 4-2). Initial attempts (Table 4-2, entries 1-3) were not successful. Either decomposition of the donor **9** or tetrasaccharide side products arising from the self-condensation of the corresponding hemiacetal formed *in situ*, were observed. The side products were tentatively assigned as tetrasaccharide impurities based on the MALDI-

mass spectrum. These results suggest that the acceptor **10** is quite deactivated and sterically hindered to react with the donor **9**, thus leading to the formation of unwanted side products. To circumvent this issue, we applied an inverse procedure that involved, first dissolving the acceptor and catalytic amounts of TMSOTf and then adding a solution of the donor **9** dropwise. With these optimized conditions and the reverse addition procedure (Table 4-2, entry 5) the trisaccharide derivative **8** was obtained in 40% yield after HPLC purification. Unfortunately, the required compound **8** co-eluted with a 15% unknown carbohydrate impurity as indicated by HPLC analysis. Attempts to purify compound **8** were not successful and we decided to take this material to the next step and anticipated to separate the impurity after global deprotection of the glycopeptide. Next, compound **8** was subjected to Fmoc deprotection using DBU/octanethiol[46] to give the amine **7**, which was coupled with the activated dipeptide **6**, to give the protected glycopeptide **5** after column purification (Scheme 4-11). The ^{1}H NMR spectral analysis of compound **5** showed the presence of the unknown carbohydrate impurity (2:1) carried forward from the previous glycosylation stage.

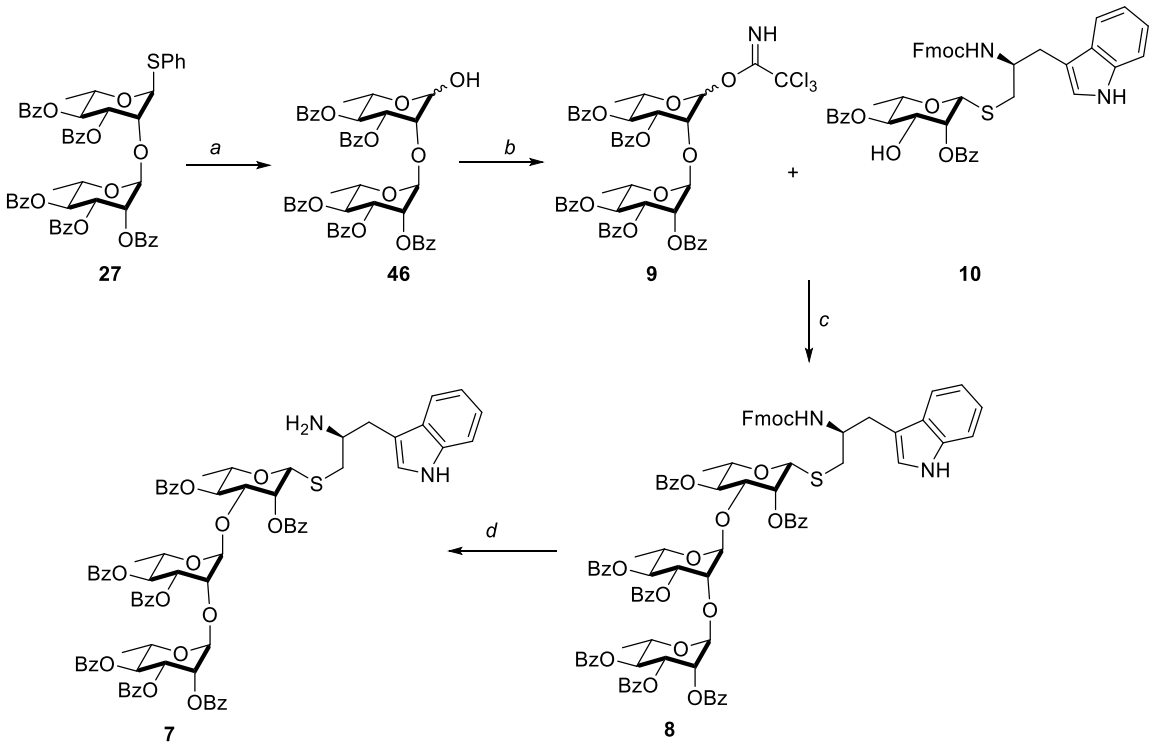

Scheme 4-10 Synthesis of the trisaccharide thio-Fmoc tryptophan derivative 7

Reagents and conditions: (a) NBS, Acetone:H_2O (9:1), (b) CCl_3CN, DBU, CH_2Cl_2, 80% (over two steps), (c) TMSOTf, CH_2Cl_2, -35 °C, 40%, (d) DBU, octanethiol, THF.

Finally, the glycopeptide **5** was subjected to sequential global deprotection as with the synthesis of the α-glycopeptide **3** (Scheme 4-11). [10] The glycopeptide **5** was treated with DBU in the presence of octanethiol, in THF gave an intractable mixture of compounds. Unfortunately, the MALDI mass spectrum of the partially purified compound showed a single, major mass corresponding to loss of 18 mass units from the expected glycopeptide **46** (Calcd for $C_{87}H_{87}N_4O_{23}S_2$ $[M+H]^+$is 1619.52, Found $C_{87}H_{85}N_4O_{22}S_2$ $[M+H]^+$is 1601.51). The quantity of material obtained was too low to continue with further purification. This material was analyzed using 1D-NMR, 2D-NMR, and HR-Q-TOF-MS, confirming the presence of the aspartimide (Asi) side product **47**. The signal assignment started from the ^1H-^{13}C HSQC spectrum, which showed a correlation peak of $\delta_H/\ \delta_C$ = 2.03/13.8 ppm which was assigned to Met-S-C*H*$_3$. The HMBC spectrum revealed the correlation of Met-S-*C*H_3 δ 13.8 ppm with Met-γ-C*H*$_2$ at 2.58 ppm, which in turn indicated a unidirectional correlation with Met-β-C*H*$_2$ δ 2.10 ppm. The signal at δ 3.96 ppm was attributed to Met-α-C*H,* which showed a correlation with Met-β-C*H*$_2$ in COSY spectrum. (Figure 4-10b). From the ^1H-^{13}C HSQC spectrum the resonances at $\delta_{H'}/\ \delta_{C'}$ = 5.24/99.7 ppm, $\delta_H/\ \delta_C$ = 4.85/81.5 ppm, and $\delta_{H''}/\ \delta_{C''}$ = 4.43/98.8 ppm were assigned to the anomeric protons and to their corresponding carbons of the rhamnose residues. (Figure 4-11b). The HMBC spectrum indicated the connectivity of β-thio rhamoside residue with the tryptophan motif. The Trp-β'-C*H*$_2$ signal at δ 2.94 and 2.54 ppm were confirmed by a cross peak with the anomeric carbon at δ 81.5 ppm in HMBC spectrum. The signal at δ 4.5 ppm was attributed to Trp-α-C*H,* which showed a correlation with Trp-β-C*H*$_2$ (δ 2.92 and 3.02 ppm) and Trp-β'-C*H*$_2$ (δ 2.94 and 3.02 ppm) in the COSY spectrum (Figure 4-11a). The COSY spectrum confirmed the coupling of Asi-β-C*H*$_2$ (δ 2.81 and 2.64 ppm) with the Asi-α-C*H* at δ 4.35 ppm (Figure 4-12a), which also showed a HMBC correlation with Asi-carbonyl carbons at δ 168.2 and 170.2 ppm respectively (Figure 4-12b). Thus, we unambiguously confirmed the peptide portion of the compound **47** (Table 4-3). Due to overlapping of signals from the other unknown carbohydrate impurity, it was difficult to assign the ring protons of the trisaccharide to its specific residues.

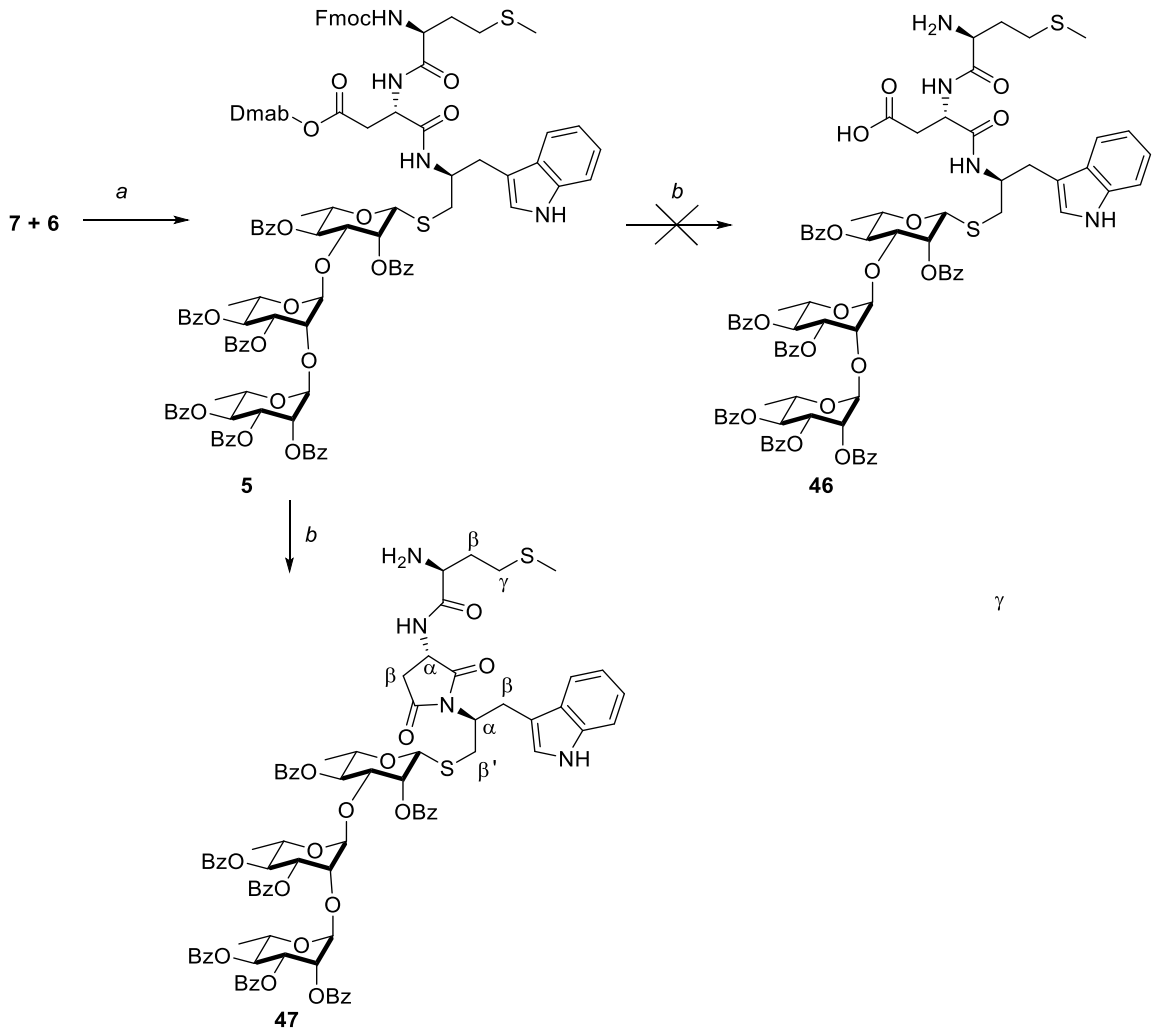

Scheme 4-11 Formation of aspartimide side product 47

Reagents and conditions: (a) DIPEA, THF, (b) DBU, octanethiol, THF.

(a)

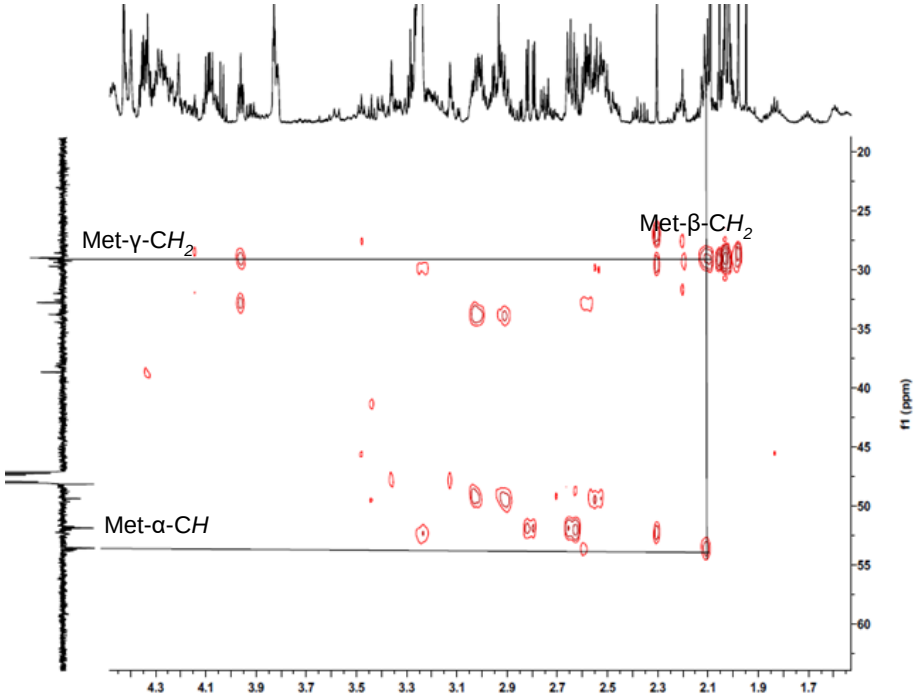

(b)

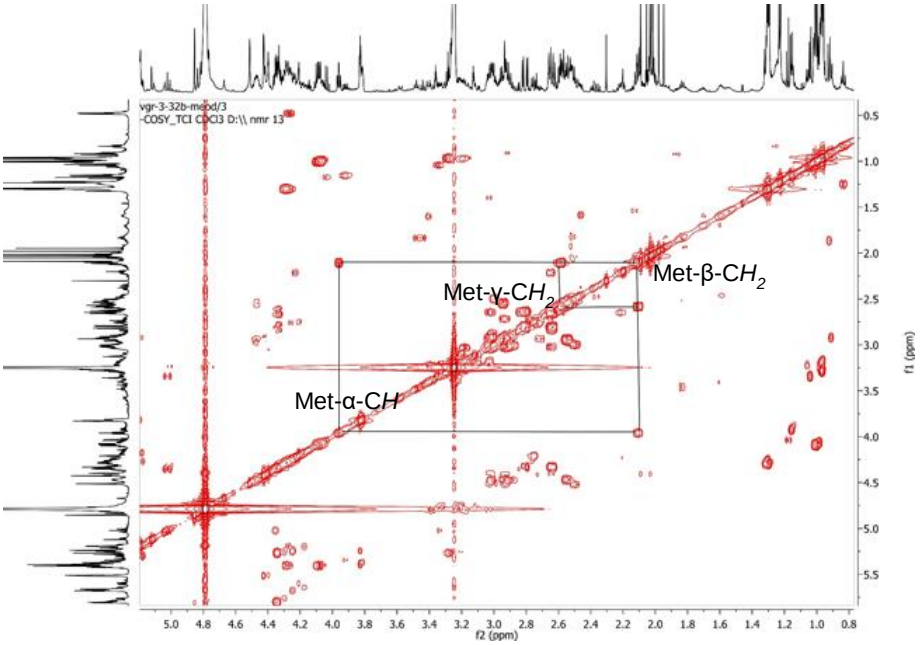

Figure 4-10 **Partial 2D NMR spectra of 47** (a) Indicated are the observed interresidue connections of Met-β-CH_2 from ^{1}H-^{13}C HMBC spectrum, (b) Observed coupled correlation of Met-α-CH from ^{1}H -^{1}H COSY spectrum.

(a)

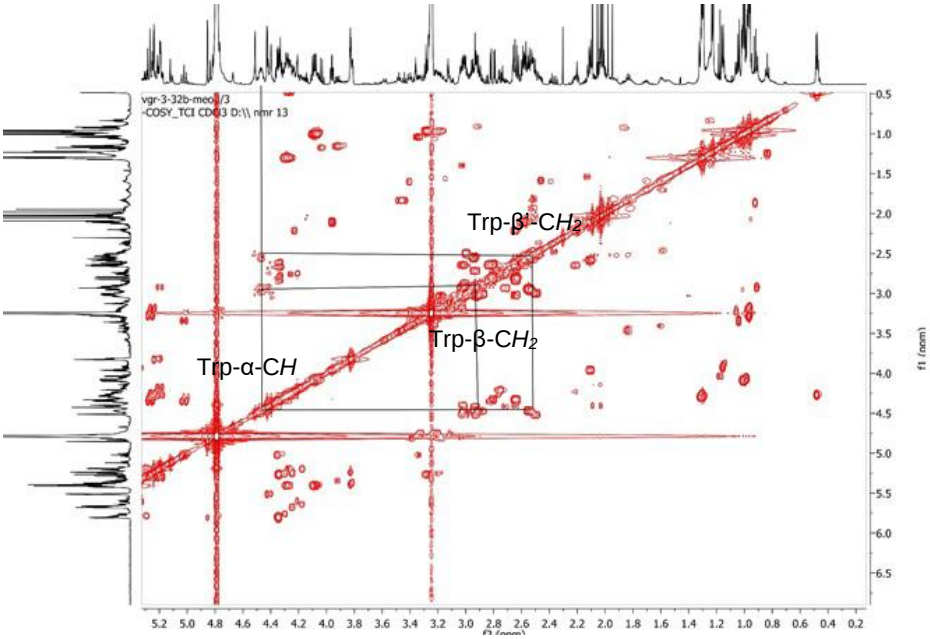

(b)

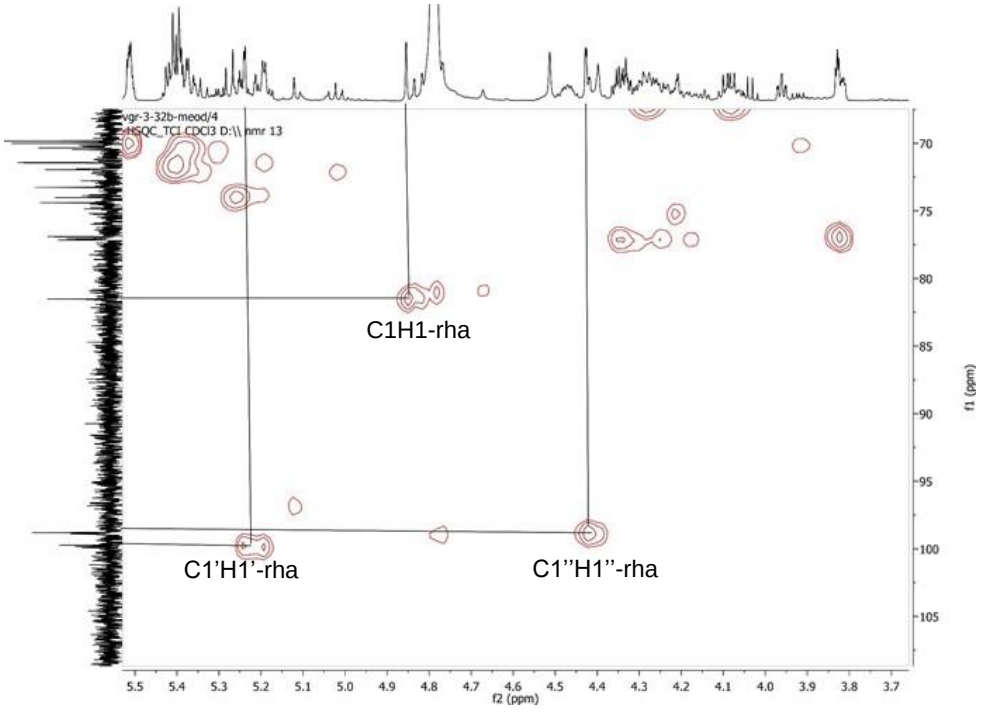

Figure 4-11 **Partial 2D NMR spectra of 47** (a) ^{1}H-^{1}H COSY spectrum, which shows the coupling of Trp-α-C*H* proton, (b) Indicated are the anomeric ^{1}H-^{13}C correlation of rhamnose residues from the HSQC spectrum.

(a)

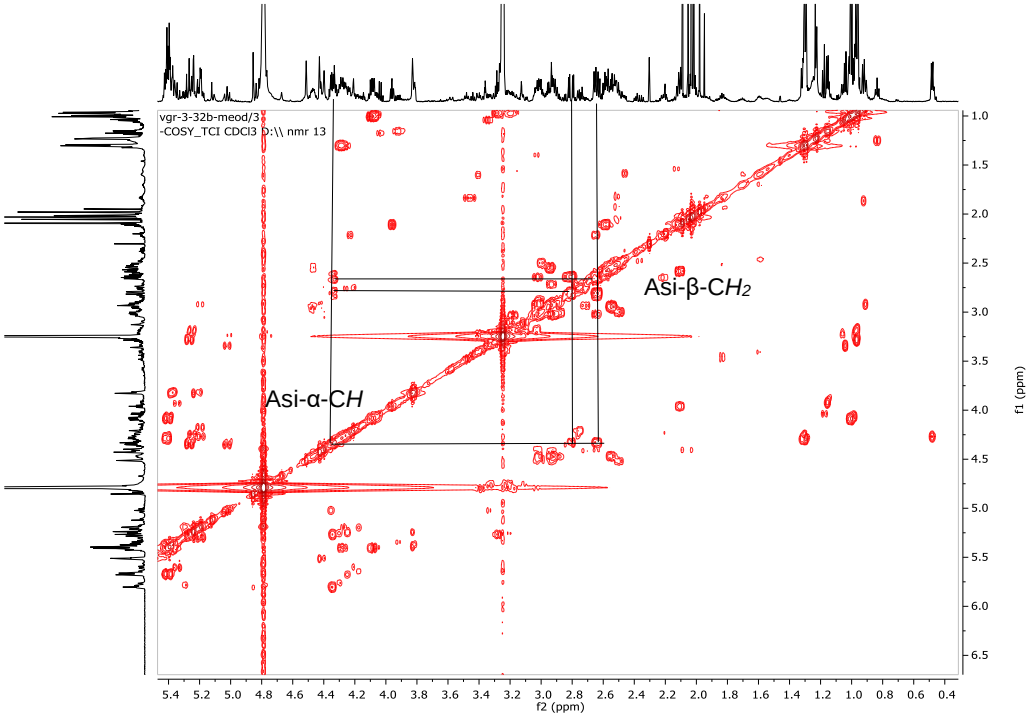

(b)

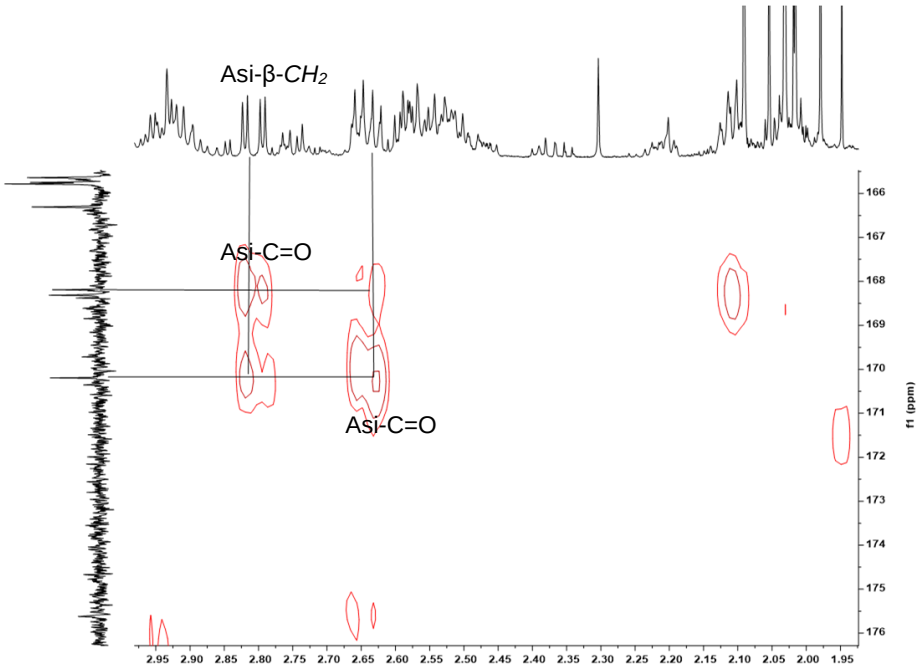

Figure 4-12 **Partial 2D NMR spectra of 47** (a) Observed coupled correlation of Asi-α-C*H* from ^{1}H -^{1}H COSY spectrum, (b) Indicated are the observed interresidue connections of Asi-β-C*H*$_2$ from ^{1}H-^{13}C HMBC spectrum.

Table 4-3 NMR signal assignments for the peptide portion of 47, as inferred through the ^{1}H and ^{13}C NMR spectra.

Assignment	^{1}H (ppm)	^{13}C (ppm)
Met-S-CH_3	2.03	13.8
Met –γ-CH_2	2.58	29.0
Met –β-CH_2	2.10	32.8
Met-α-CH	3.97	53.6
C(O)-Met		168.3
Trp-β'-CH_{2a}	2.94	33.8
Trp-β'-CH_{2b}	2.54	
Trp-β-CH_{2a}	3.02	29.7
Trp-β-CH_{2b}	2.92	
Trp –α-CH	4.47	49.4
Asi-β-CH_{2a}	2.81	38.7
Asi-β-CH_{2b}	2.64	
C(O)-Asp		170.2, 168.2

4.3. Conclusion

In summary, we have developed an efficient synthetic strategy to assemble the complex trirhamnan building block in a [2+1] manner linked to a tripeptide moiety through a 1-thio-β-rhamnosidic linkage. Unfortunately, the final global deprotection step of the β-glycopeptide **5** led to the formation of the unwanted aspartimide side product **47**. The result was disappointing, as a similar strategy was successfully employed in the synthesis of the α-glycopeptide[10] without formation of the aspartimide side product. This warrants further investigation of Fmoc and Dmab removal under basic conditions. However, owing to time constraints and the availability of only milligram amounts of material, a decision was made to stop the project at this point, with gratification that at least a viable synthetic route to the advanced glycopeptide intermediate **5** had been achieved.

4.4. Experimental

4.4.1. General Considerations

All reactions described were performed under an atmosphere of dry nitrogen using oven dried glassware unless otherwise specified. Analytical thin layer chromatography (TLC) was performed on aluminum plates precoated with Silica Gel 60F-254 as the adsorbent. The developed plates were air-dried, exposed to UV light and/or sprayed with a solution containing 1% $Ce(SO_4)_2$ and 1.5% molybdic acid in 10% aqueous H_2SO_4, and heated. Column chromatography was performed with Silica Gel 60 (230-400 mesh). All reagents and starting materials were purchased from Alfa Aesar, Sigma Aldrich, TCI America, Novabiochem, AK Scientific and were used without further purification. All solvents were purchased from Sigma Aldrich, EMD, Anachemia, Caledon, Fisher or ACP and used without further purification unless otherwise specified. DMF was freed of amines by concentrating under high vacuum and was then distilled and stored over molecular sieves whereas the other solvents were distilled according to standard procedures.[32]

Nuclear magnetic resonance (NMR) spectra were recorded using chloroform-d ($CDCl_3$), methanol-d_4 (CD_3OD), DMSO-d_6 or acetone-d_6. Signal positions (δ) are given in parts per million from tetramethylsilane (δ 0) and were measured relative to the signal of the solvent (^{1}H NMR: $CDCl_3$: δ 7.26, CD_3OD: δ 3.31; $(CD_3)_2SO$: δ 2.50; $(CD_3)_2CO$: δ 2.05. ^{13}C NMR: $CDCl_3$: δ 77.16, CD_3OD: δ 49.0; $(CD_3)_2SO$: δ 39.52; $(CD_3)_2CO$: δ 29.84.). Coupling constants (*J* values) are given in Hertz (Hz) and are reported to the nearest 0.1 Hz. ^{1}H NMR spectral data are tabulated in the order: number of protons, multiplicity (s, singlet; d, doublet; t, triplet; q, quartet; quint, quintet; m, multiplet; br, broad), and coupling constants. NMR spectra were recorded on a Bruker Avance 600 equipped with a QNP or TCI cryoprobe (600 MHz), Bruker 500 (500 MHz), or Bruker 400 (400 MHz). Diastereomeric ratios (d.r) are based on analyses of crude ^{1}H-NMR spectra. All assignments were confirmed with the aid of two-dimensional ^{1}H, ^{1}H (COSY) and/or ^{1}H, ^{13}C (HSQC) experiments using standard pulse programs. High resolution mass spectra were obtained by the electrospray ionization method, using an Agilent 6210 TOF LC/MS high resolution magnetic sector mass spectrometer. High performance liquid chromatography (HPLC) were performed on an Agilent 1200 HPLC, equipped with a variable wavelength UV-Vis detector.

4.4.2. Synthesis of 1-deoxy-1-phenylthio-α-L-rhamnopyranoside 17

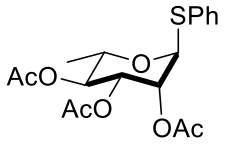

L-rhamnose monohydrate (10.0 g, 54.80 mmol) suspended in dichloromethane (40 mL) was treated at 0 °C with triethylamine (20.0 mL), DMAP (0.50 g, 4.20 mmol) and acetic anhydride (30.0 mL, 328.0 mmol). The reaction mixture was allowed to warm to rt, stirred for 12 h and then treated with methanol (5 mL). After concentration of the reaction mixture, the residue was dissolved in ethyl acetate (100 mL) and washed with brine (2 x 25 mL). The aqueous phase was extracted with ethyl acetate (3 x 20 mL) and the combined organic extracts were washed (0.5 N HCl 20 mL, sat. aq $NaHCO_3$ 20 mL, and brine 20 mL), dried (Na_2SO_4), and concentrated to afford the crude tetra acetate **16**.

To a solution of compound **16** (18.0 g, 54.1 mmol) and thiophenol (6.50 ml, 62.3 mmol) in dichloromethane (100 mL), $BF_3.Et_2O$ (8.0 mL, 62.3 mmol) was added at 0 °C. The reaction mixture was stirred for 1.5 h at rt, diluted with dichloromethane (100 mL), washed with water (2 x 100 mL), sat. aq $NaHCO_3$ (100 mL), dried (Na_2SO_4), and concentrated. The residue was recrystallized from anhydrous ethanol (50 mL) to give the pure α-phenyl-thioglycoside **17** (14.0 g, 65%) as white solid

^{1}H NMR (500 MHz, $CDCl_3$) δ 7.48 – 7.28 (5H, m, Ar), 5.50 (1H, dd, $J_{2,1}$ = 1.6 Hz, $J_{2,3}$ = 3.4 Hz, H2), 5.41 (1H, br d, $J_{1,2}$ = 1.6 Hz, H1), 5.29 (1H, dd, $J_{3,2}$ = 3.3 Hz, $J_{3,4}$ = 9.9 Hz, H3), 5.14 (1H, t, $J_{4,3}$ = $J_{4,5}$ = 9.9 Hz, H4), 4.36 (1H, dq, H5), 2.14, 2.08, 2.01 (each 3H, 3 s, 3 x CH_3-OAc), 1.25 (3H, d, $J_{6,5}$ = 6.2 Hz, H6).

^{13}C NMR (126 MHz, $CDCl_3$) δ 170.2, 170.1 (3C, 3 x OAc), 133.4 – 128.0 (6C, C_{Ar}), 85.8 (C1), 71.5 (C2), 71.3 (C4), 69.5 (C3), 67.9 (C5), 21.0 – 20.8 (3C, 3 x CH_3-OAc), 17.5 (C6).

HRMS (ESI$^+$) calculated for $C_{18}H_{26}NO_7S$ $[M+NH_4]^+$ 400.1424, found 400.1429.

4.4.3. Synthesis of the isopropylidene ketal 19

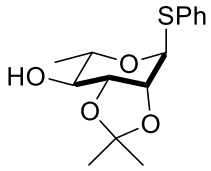

A solution of NaOMe-MeOH (1M, 5.0 mL) was added to a suspension of compound **17** (14.0 g, 36.6 mmol) in anhydrous methanol (75.0 mL), and the reaction mixture was stirred at room temperature for 12 h and was then neutralized by stirring with Rexyn 101 H^+ ion-exchange resin. The resin was removed by filtration, and the filtrate was concentrated to give a syrupy liquid. The residue was extracted by triturating with hexanes (2 x 50 mL) to remove MeOBz. The insoluble triol **18** was suspended in 2,2-dimethoxypropane (30 mL) and PTSA (0.20 g, 1.0 mmol) was added. The mixture was stirred for 2h at rt. Et_3N (1 mL) was added and concentrated by rotary evaporation to a syrup. Purification by column chromatography (EtOAc/hexanes: 30% → 50%) gave the isopropylidene ketal **19** (9.7 g, 94%) as a colorless solid.

^{1}H NMR (500 MHz, DMSO-d_6) δ 5.76 (1H, br s, H1), 5.35 (1H, d, $J_{OH,4}$ = 5.7 Hz, OH-C4), 4.29 (1H, d, $J_{2,3}$ = 5.6 Hz, H2), 3.96 (1H, dd, $J_{3,2}$ = 5.6 Hz, $J_{3,4}$ = 7.5 Hz, H3), 3.85 (1H, dq, $J_{5,6}$ = 6.2 Hz, $J_{5,4}$ = 9.8 Hz, H5), 3.19 – 3.15 (1H, m, H4), 1.42 and 1.29 (6H, 2 s, -O-C(C*H*$_3$)$_2$-O-), 1.06 (3H, d, $J_{6,5}$ = 6.2 Hz, H6).

^{13}C NMR (125 MHz, DMSO) δ 132.9-127.6 (6C, C_{Ar}), 108.5 (-O-*C*$(CH_3)_2$-O-) 82.8 (C1), 77.8 (C3), 75.7 (C2), 73.6 (C4), 67.4 (C5), 28.0 and 26.4 (2C, -O-C(*C*H_3)$_2$-O-), 17.2.(C6)

HRMS (ESI$^+$) calculated for $C_{15}H_{21}O_4S$ $[M+H]^+$ 297.1155, found 297.1149

4.4.4. Synthesis of the benzoylated intermediate 20

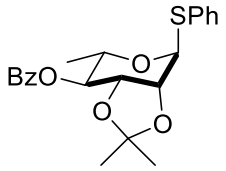

To a solution of **19** (10.0 g, 33.7 mmol) in dichloromethane (50.0 mL) was added pyridine (14.0 mL). The reaction mixture was cooled to 0 °C, then a solution of benzoyl chloride (6 mL, 50.6 mmol) was added dropwise. After complete consumption of starting material, the reaction was quenched with ice water and extracted with dichloromethane (2 x 25 mL). The combined organic layers were washed with aq $NaHCO_3$ and brine, dried over Na_2SO_4, and concentrated *in vacuo,* to afford **20** as a colorless foam, which was used directly in the next step without further purification.

4.4.5. Synthesis of the diol 15

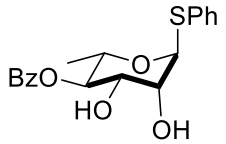

The compound **20** (13.0 g, 32.4 mmol) was dissolved in 80% aq. acetic acid (100 mL) and stirred at 80 °C for 3 h. The reaction mixture was cooled to rt and concentrated *in vacuo*. Toluene (30 mL) was added to remove any remaining water in the reaction mixture by azeotrpic evaporation at reduced pressure and this process was repeated 3 times. Subsequently, the residue was purified by flash column chromatography on silica gel ($CHCl_3$/MeOH: 0% → 10%) to obtain **15** (10.0 g, 82% over 2 steps) as a colorless solid.

^{1}H NMR (400 MHz, $CDCl_3$) δ 8.09 – 7.27 (10 H, m, Ar) 5.59 (1H, d, $J_{1,2}$ = 1.5 Hz, H1), 5.12 (1H, t, $J_{4,3}$ = $J_{4,5}$ = 9.5 Hz, H4), 4.48 (1H, dq, $J_{5,6}$ = 6.2 Hz, $J_{5,4}$ = 9.6 Hz, H5), 4.27 (1H, dt, $J_{2,1}$ = 1.6 Hz, $J_{2,OH}$ = $J_{2,3}$ = 3.6, H2), 4.07 (1H, ddd, $J_{3,2}$ = 3.5 Hz, $J_{3,OH}$ = 5.7 Hz, $J_{3,4}$ = 9.5 Hz, H3), 3.38 (1H, d, $J_{OH,3}$ = 5.7 Hz, OH-C3), 2.94 (1H, d, $J_{OH,2}$ = 3.7 Hz, OH-C2), 1.31 (3H, d, $J_{6,5}$ = 6.3 Hz, H6).

^{13}C NMR (100 MHz, $CDCl_3$) δ 167.8 [*C*(O)-OBz], 133.9 – 127.7 (12C, C_{Ar}) 87.3 (C1), 76.6 (C4), 72.5 (C2), 71.1 (C3), 67.2 (C5), 17.6 (C6).

HRMS (ESI$^+$) calculated for $C_{19}H_{21}O_5S$ $[M+H]^+$ 361.1104, found 361.1108.

4.4.6. Synthesis of the intermediate 22

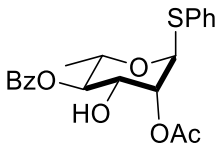

To a stirred solution of diol **15** (3.5 g, 9.2 mmol) in anhydrous acetonitrile (15 mL), trimethyl orthoacetate (3.5 mL, 27.3 mmol) and PTSA (35 mg, 0.2 mmol) were added and the mixture was stirred under vacum (30 psi) at 45 °C for 3 h. After complete consumption of starting material (as judged by TLC), Et_3N (1 mL) was added and the solvent was removed under reduced pressure to afford the crude ortho ester **21** as a viscous liquid. The crude **21** was dissolved in 80% aq. acetic acid (10 mL) and stirred at 80 °C for 3 h at which time TLC showed complete disappearance of **21.** The reaction mixture was cooled to rt , concentrated *in vacuo* and co-evaporated with toluene to give a colorless syrupy residue. The residue was purified by flash column chromatography on silica gel (EtOAc/hexanes: 10% → 30%) to obtain **22** (3.3 g, 85%) as a crystalline solid.

^{1}H NMR (400 MHz, $CDCl_3$) δ 8.12 – 7.28 (10H, m, ArH), 5.56 (1H, br d, $J_{1,2}$ = 1.4 Hz, H1), 5.43 (1H, dd, $J_{2,1}$ = 1.4, $J_{2,3}$ = 3.5 Hz, H2), 5.23 (1H, t, $J_{4,3}$ = $J_{4,5}$ = 9.8 Hz, H4), 4.51 (1H, dq, $J_{5,6}$ = 6.2 Hz, $J_{5,4}$ = 9.8 Hz, H5), 4.22 (1H, dd, $J_{3,2}$ = 3.5 Hz, $J_{3,4}$ = 9.8 Hz, H3), 1.33 (3H, d, $J_{6,5}$ = 6.2 Hz, H6).

^{13}C NMR (100 MHz, $CDCl_3$) δ 170.5 [*C*(O)-OAc], 167.0 [*C*(O)-OBz], 133.6 – 127.8 (12C, C_{Ar}), 85.8 (C1), 75.5 (C4), 74.4 (C2), 69.3 (C3), 67.5 (C5), 21.0 (*C*H3-OAc), 17.7 (1C, C6)

HRMS (ESI$^+$) calculated for $C_{21}H_{26}NaO_6S$ $[M+Na]^+$ 425.1029, found 425.1022

4.4.7. Synthesis of the acceptor 13

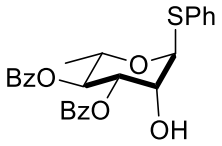

To a solution of **22** (5.0 g, 12.4 mmol) in dichloromethane (25.0 mL) was added pyridine (5.0 mL). The reaction mixture was cooled to 0 °C, then a solution of benzoyl chloride (3 mL, 25.0 mmol) was added dropwise. After complete consumption of starting material, the reaction was quenched with ice water and extracted with dichloromethane (2 x 10 mL). The combined organic layers were washed with aq $NaHCO_3$, and brine solution, dried over Na_2SO_4, and concentrated *in vacuo,* to afford **23** (6.5 g, quantitative) as a hard foam. The benzoylated compound **23** was dissolved in a mixture of methanol (90.0 ml) and dichloromethane (25.0 ml), acetyl chloride (1.5 ml, 21.0 mmol) was added dropwise. The reaction mixture was stirred at 45 °C for 12h and cooled to rt. The contents were poured dropwise into an ice-cooled mixture of water/dichloromethane (60 ml, 1:1), and then neutralized with sat. aq $NaHCO_3$ until pH -7.0 (Note: Increase in pH >7.0 leads to 3-*O* to 2-*O* benzoyl ester migration).The organic layer was separated, washed (brine 20 mL), dried (Na_2SO_4), and concentrated. Purification by column chromatography gave **13** (4.0 g, 70%) as colorless crystalline solid.

^{1}H NMR (400 MHz, $CDCl_3$) δ 8.00 – 7.28 (15H, m, ArH), 5.68 – 5.58 (3H, m, H1, H3, H4), 4.63 – 4.56 (2H, m, H5, H2), 2.45 (1H, br s, OH-C2), 1.34 (3H, d, $J_{6,5}$ = 6.3 Hz, H6).

^{13}C NMR (100 MHz, $CDCl_3$) δ 165.9 and 165.8 [2C, *C*(O)-Obz] 133.9 –127.8 (18C, $C_{Ar)}$, 87.8 (C1), 73.0 (C4), 71.8 (C3), 71.3 (C2), 68.3 (C5), 17.6 (C6).

HRMS (ESI$^+$) calculated for $C_{26}H_{28}NO_6S$ $[M+NH_4]^+$ 482.1632, found 482.1631

Data for the minor –OBz- migrated intermediate 24

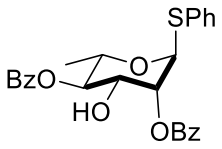

^{1}H NMR (400 MHz, $CDCl_3$) δ 8.12 – 7.29 (15H, m, ArH), 5.68 – 5.66 (2H, m, H1, H2), 5.34 (1H, t, $J_{4,3}$ = $J_{4,5}$ = 9.7 Hz, H4), 4.57 (1H, dq, $J_{5,6}$ = 6.2 Hz, $J_{5,4}$ = 9.7, H5), 4.31 (1H, ddd, $J_{3,2}$ = 3.3 Hz, $J_{3,OH}$ = 7.8 Hz, $J_{3,4}$ = 9.8 Hz, H3), 2.56 (1H, d, $J_{OH,3}$ = 7.8 Hz, OH-C3), 1.36 (3H, d, $J_{6,5}$= 6.3 Hz, H6).

^{13}C NMR (100 MHz, $CDCl_3$) δ 167.3 [2C, *C*(O)-OBz), 133.7-128.0 (18C, C_{Ar}), 86.1 (C1), 76.0 (C4), 75.1 (C2), 70.0 (C3), 67.8 (C5), 17.7 (C6).

HRMS (ESI$^+$) calculated for $C_{26}H_{28}NO_6S$ $[M+NH_4]^+$ 482.1632, found 482.1634.

4.4.8. Synthesis of the benzoylated rhamnose 25

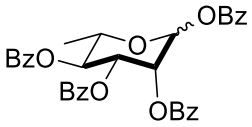

To a suspension of L-rhamnose monohydrate (5.0 g, 27.5 mmol) in pyridine (20.0 mL, 275 mmol) at 0 °C , was added benzoyl chloride (16.0 mL, 137.5 mmol). The reaction mixture was allowed to warm to rt, and then stirred for 6 h. After complete consumption of starting material, the reaction mixture was cooled to 0 °C and ice (10 g) was added. The solvent was removed under high vacuum and the residue was dissolved in dichloromethane (50 mL) was washed successively with water (50 mL), 1N HCl (50 mL), sat. aq $NaHCO_3$ (50 mL), and brine (50 mL), dried over Na_2SO_4 and concentrated under reduced pressure to give **25** as a colorless solid, that was essentially pure by NMR analysis and was used in the next reaction without purification.

4.4.9. Synthesis of the hemiacetal 26

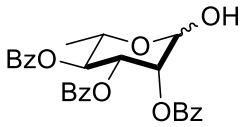

To a solution of the crude **25** in DMF (50 ml), was added hydrazine acetate (7.0 g, 77.5 mmol) and then stirred for 12 h at rt. The reaction mixture was diluted with EtOAc (200 mL), washed with water (2 x 100 mL), brine (100 mL), dried over Na_2SO_4 and concentrated *in vacuo* to obtain **26** as a pale yellow oil, which was used in the next step without any purification.

4.4.10. Synthesis of the trichloroacetimidate donor 14

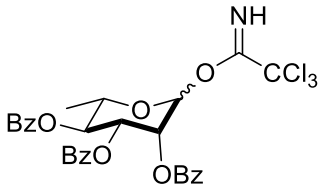

A solution of the above crude **26** in dichloromethane (100 mL) was cooled in an ice bath. Trichloroacetonitrile (10.5 mL, 103.3 mmol) and DBU (1.5 mL, 10.0 mmol) were added, and the mixture was stirred for 0.5 h. The cooling bath was removed, and the reaction mixture was allowed to warm to rt over 20 min. The solvent was removed under reduced pressure and the residue was purified by flash column chromatography on silica gel (EtOAc/hexanes: 10% → 30%) to give **14** as a pale-yellow foam (12.0 g, 70% over 3 steps). Prolonged storage at rt resulted in partial hydrolysis.

^{1}H NMR (400 MHz, Chloroform-*d*) δ 8.82 (1H, s, NH-trichloroacetimidate), 8.11 – 7.25 (15H, m, ArH-Bz), 6.49 (1H, d, $J_{1,2}$ = 1.6 Hz, H1), 5.91 – 5.87 (2H, m, H3), 5.78 (1H, t, $J_{4,3}$ = $J_{4,5}$ = 10.2 Hz H4), 4.44 – 4.37 (1H, m, H5), 1.42 (3H, d, $J_{6,5}$ = 6.2 Hz, H6).

^{13}C NMR (100 MHz, $CDCl_3$) δ 165.9 -165.5 [3C, *C*(O)-OBz], 160.3 (*C*=NH-trichloroacetimidate), 133.8 – 128.5 (18C, C_{Ar}-OBz), 95.0 (C1), 91.0 (*C*Cl3-trichloroacetimidate), 71.3 (C4), 69.9 (2C, C2, C3), 69.4 (C5), 17.9 (C6).

4.4.11. Synthesis of the disaccharide 27

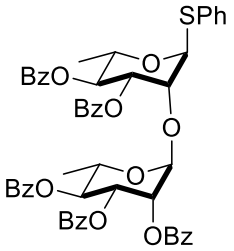

A solution of the trichloroacetimidate donor **14** (5.0 g, 8.0 mmol) and the acceptor **13** (3.4 g, 7.2 mmol) in anhydrous dichloromethane (30.0 mL) was stirred with freshly activated crushed 4 Å molecular sieves (4.0 g) at rt for 20 min. The mixture was then cooled to -30 °C and TMSOTf (70 µL, 0.4 mmol) was added. The temperature of the reaction mixture was allowed to raise to rt over 1 h and then stirred at rt for 30 min. Triethyl amine (0.5 ml) was added and the resulting mixture was filtered through a pad of Celite with the additional quantity of dichloromethane (50 mL). The filtrate was washed (sat. aq. $NaHCO_3$ 20 mL, brine 20 mL), dried (Na_2SO_4), concentrated and purified by flash column chromatography (EtOAc/hexanes: 5% → 25%) to afford the disaccharide **27** (8.5 g, 85%) as a colorless solid foam.

^{1}H NMR (600 MHz, $CDCl_3$) δ 8.03-7.24 (30 H, m, ArH), 5.94 (1H, dd, $J_{3',2'}$ = 3.4, $J_{3',4'}$ = 10.1 Hz, H3'), 5.81 – 5.63 (5H, m, H1, H2', H3, H4, H4'), 5.16 (1H, br s, H1'), 4.62-4.58 (2H, m, H2, H5), 4.32 (1H, dq, $J_{5',6'}$ = 6.3 Hz, $J_{5',4'}$ = 12.4 Hz, H5'), 1.43 (3H, d, $J_{6,5}$ = 6.3 Hz, H6), 1.27 (3H, d, $J_{6',5'}$ = 6.3 Hz, H6').

^{13}C NMR (150 MHz, $CDCl_3$) δ 166.0 – 165.2 [5C, 5 × *C*(O)-OBz], 133.9 – 128.1 (30C, Ar), 99.7 (C1'), 87.4 (C1), 78.5 (C2), 72.0 (C3), 71.8 (C4), 71.3 (C4'), 70.6 (C2'), 69.7 (C3'), 68.6 (C5), 67.9 (C5'), 17.8 (C6), 17.7 (C6').

HRMS (ESI$^+$) calculated for $C_{53}H_{46}NaO_{13}S$ $[M+Na]^+$ 945.2551, found 945.2554.

4.4.12. Synthesis of the disaccharide trichloroacetimidate donor 9

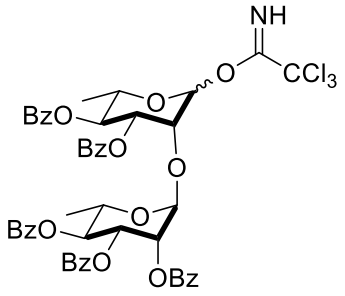

To a solution of the disaccharide **27** (2.0 g, 2.1 mmol) in acetone/water (10 mL; v/v 9:1), NBS (1.2 g, 6.5 mmol) was added and then stirred at rt for 4 h. After consumption of **27** (as indiacted by TLC), the reaction mixture was concentrated until turbidity arose. The mixture was diluted with EtOAc (10 mL), washed (sat.aq.$NaHCO_3$, brine), dried (Na_2SO_4), concentrated and purified by column chromatography (EtOAc/hexanes: 10% → 40%) to give the hemiacetal **46** (1.6 g, 90% yield)

To a solution of the hemiacetal **46** (1.5 g, 1.8 mmol) in dichloromethane (5.0 mL) at 0 °C, was added trichloroacetonitrile (550 µL, 5.4 mmol) followed by DBU (134 µL, 0.9 mmol) and stirred for 1h, at which time TLC showed complete disappearance of **46**. The reaction mixture was concentrated, and the residue was purified by flash column chromatography (EtOAc/hexanes: 10% → 30%) to afford the trichloroacetimidate donor **9** (1.6 g, 90%) as a colorless solid foam.

^{1}H NMR (500 MHz, $CDCl_3$) δ 8.75 (1H, s, NH-trichloroacetimidate), 8.03 – 7.26 (25H, m, ArH), 6.50 (1H, br d, $J_{1,2}$ = 1.9 Hz, H1), 5.96 (1H, dd, $J_{3',2'}$ = 3.5 Hz, $J_{3',4'}$ = 10.1 Hz, H3'), 5.87 – 5.83 (2H, m, H2', H3), 5.77 (1H, t, $J_{4,3}$ = $J_{4,5}$ = 9.9 Hz, H4), 5.69 (1H, t, $J_{4',3'}$ = $J_{4',5'}$ = 10 Hz, H4'), 5.22 (1H, br d, $J_{1',2'}$ = 1.7 Hz, H1'), 4.59 – 4.54 (1H, dd, $J_{2,1}$ = 2.0 Hz, $J_{2,3}$ = 3.3 Hz, H2), 4.42 – 4.35 (2H, m, H5, H5'), 1.46 (3H, d, $J_{6,5}$ = 6.2 Hz,H6), 1.39 (3H, d, $J_{6',5'}$ = 6.3 Hz,H6').

^{13}C NMR (150 MHz, $CDCl_3$): δ (ppm) 166.0-165.2 [5C, 5 × C(O)-OBz], 160.6 (1C, *C*=NH-trichloroacetimidate), 133.5-128.4 (30C, C_{Ar}), 99.6 (C1'), 96.6 (C1), 93.7 (*C*Cl_3-trichloroacetimidate), 74.31 (C2), 71.8 (C4'), 71.3 (C4), 70.8 (C2'), 70.6 (C3), 70.2 (C3'), 69.8 (C5'), 68.0 (C5), 18.0 –17.7 (2C, C6, C6').

4.4.13. Synthesis of the intermediate 28.

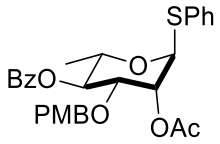

A suspension of **15** (10.0 g, 27.7 mmol) and dibutyltin oxide (8.3 g, 33.2 mmol) in benzene (100 mL) was heated to reflux in a Dean-Stark apparatus for 12 h, after which most of the solvent was removed under reduced pressure to give a gummy solid, which was then dissolved in toluene (90 mL). PMB-Cl (12.5 mL, 91.6 mmol) and tetrabutylammonium iodide (10.5 g, 28.3 mmol) were added and the mixture was stirred at 50 °C overnight.The brown solution was then concentrated, and the residue was stirred with EtOAc (100 mL). The solids were filtered off through a pad of Celite and the filtrate was concentrated to a syrup that was dissolved in pyridine (60 mL). The reaction mixture was cooled in an ice bath and then acetic anhydride (6 mL) was added dropwise. The cooling bath was removed, and the mixture was allowed to warm to rt over 30 min and continued to stir for 12 h, at which time TLC analysis indicated the consumption of stating material. The solvent was concentrated, and the resulting residue was purified by flash column chromatography on silica gel (EtOAc/hexanes: 5% → 25%) to yield **28** (12.5 g, 86%) as a colorless solid.

^{1}H NMR (500 MHz, $CDCl_3$) δ 8.07 – 6.60 (14H, m, ArH), 5.64 (1H, br s, H2), 5.48 (1H, br s, H1), 5.35 (1H, t, $J_{4,3}$ = $J_{4,5}$ = 9.9 Hz, H4), 4.58 (1H, d, $J_{a,b}$ = 12.1 Hz, OCH_{2a}-PMB), 4.42-4.36 (1H, m, H5, OCH_{2b}-PMB), 3.88 (1H, dd, $J_{3,2}$ = 3.1, $J_{3,4}$ = 9.9 Hz, H3), 3.77 (3H, s, OCH_3-PMB), 2.19 (3H, s, CH_3-OAc), 1.27 (3H, d, $J_{6,5}$ = 6.4 Hz, H6).

^{13}C NMR (126 MHz, $CDCl_3$) δ 170.6 [*C*(O)-OAc), 165.8 [*C*(O)-OBz), 159.5 (C_{Ar}OMe-PMB), 133.9-114.1 (17C, C_{Ar}), 86.5 (C1), 74.0 (C3), 73.2 (C4), 70.9 (OCH_2-PMB), 70.2 (C2), 69.3 (C5), 55.4 (OCH_3-PMB), 21.3 (*C*H_3-OAc), 17.7 (C6).

HRMS (ESI$^+$) calculated for $C_{29}H_{30}NaO_7S$ $[M+Na]^+$ 545.1604, found 545.1607.

4.4.14. Synthesis of the sulfoxide 29.

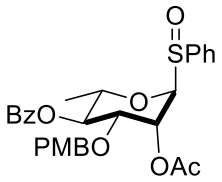

To a solution of KF (0.53 g, 9.1 mmol) in acetonitrile/water (10 mL; v/v 5:1), 70% *m*-CPBA (1.40 g, 8.3 mmol) was added and the reaction mixture was stirred at 0 ^{o}C for 30 min. To the ice-cooled reaction mixture was added **28** (4 g, 7.6 mmol) and the mixture was stirred for 15 min. TLC analysis indicated the disappearance of **28** and the reaction mixture was quenched with aq $FeSO_4$ solution (10 mL) and extracted with dichloromethane (2 x 15 mL), washed (sat. aq. $NaHCO_3$, brine), dried (Na_2SO_4), concentrated and purified by column chromatography on silica gel (EtOAc/hexanes: 0% → 30%) to afford the sulfoxide **29** (3.5g, 85%) as a pale yellow glassy solid .

^{1}H NMR (600 MHz, $CDCl_3$) δ7.98 – 6.68 (14H, m, ArH),5.82 (1H, dd, $J_{2,1}$ = 1.7 Hz, $J_{2,3}$ = 3.6 Hz, H2), 5.35 (1H, t, $J_{4,3}$ = $J_{4,5}$ = 9.7 Hz, H4), 4.60 (d, $J_{1,2}$ = 1.7 Hz, H1), 4.55 (1H, d, $J_{a,b}$ = 12.1 Hz, OCH_{2a}-PMB), 4.43 (1H, d, $J_{b,a}$ = 12.1 Hz, OCH_{2b}-PMB), 4.37 (1H, dq, dq, $J_{5,6}$ = 6.2 Hz, $J_{5,4}$ = 9.8, H5), 4.31 (1H, dd, $J_{3,2}$ = 3.5 Hz, $J_{3,4}$ = 9.7 Hz, H3), 3.76 (3H, s, OCH_3-PMB), 2.07 (3H, s, CH_3-OAc), 1.29 (3H, d, $J_{6,5}$ = 6.2 Hz, H6)

^{13}C NMR (150 MHz, $CDCl_3$) δ 169.9 [*C*(O)-OAc), 165.8 [*C*(O)-OBz), 159.4 (C_{Ar}OMe-PMB), 141.4 – 113.8 (17C, C_{Ar}), 96.6 (C1), 74.2 (C3), 73.3 (C5), 72.2 (C4), 71.4 (OCH_2-PMB), 65.6 (C2), 55.4 (OCH_3-PMB), 21.3 (CH_3-OAc), 17.7 (C6)

HRMS (ESI$^+$) calculated for $C_{29}H_{31}O_8S$ $[M+H]^+$ 539.1734, found 539.1729

4.4.15. Synthesis of the rhamnal 30

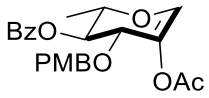

To a solution of sulfoxide **29** (3.0 g, 5.6 mmol) in toluene (15.0 mL), pyridine (0.9 mL) was added and heated to reflux temperature for 12 hours. The solvent was removed *in vacuo* and the residue was purified by flash column chromatography on silica gel (EtOAc:hexanes; 0% → 20%) to furnish the rhamnal **30** (1.90 g, 83%) as a white powder.

^{1}H NMR (500 MHz, $CDCl_3$) δ 8.05-7.43 (5H, m, ArH-OBz), 7.22 (2H, d, $J_{o,m}$ = 8.6 Hz, *ortho*ArH-PMB), 6.80 (2H, d, *meta* ArH-PMB), 6.62 (1H, d, $J_{1,3}$ = 0.8 Hz H1), 5.38 (1H, t, $J_{4,3}$ = $J_{4,5}$ = 4.9 Hz, H4), 4.59 (2H, s, OCH_2-PMB), 4.40 – 4.34 (2H, m, H3, H5), 3.76 (3H, s, OCH_3-PMB), 2.06 (3H, s, CH_3-OAc), 1.43 (3H, d, $J_{6,5}$ = 6.6 Hz, H6).

^{13}C NMR (125 MHz, $CDCl_3$): δ 169.8 [*C*(O)-OAc], 165.7 [*C*(O)-OBz], 159.4 (1C, C_{Ar}OMe-PMB), 138.1 (C1), 133.5 –113.9 (12C, C_{Ar}, C2), 73.0 (C3), 72.2 (C5), 72.1 (C4), 71.1 (OCH_2-PMB), 55.4 (OCH_3-PMB), 20.9 (CH_3-OAc), 16.3 (C6).

HRMS (ESI$^+$) calculated for $C_{23}H_{25}O_7$ $[M+H]^+$ 413.1595, found 413.1591.

4.4.16. Synthesis of the ulosyl bromide 12.

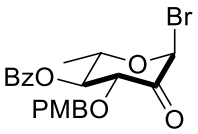

To a solution of rhamnal **30** (1.5 g, 3.6 mmol) in dichloromethane (10 mL), absolute ethanol (260 µL, 4.3 mmol) and freshly activated crushed 4 Å molecular sieves (2.0 g) were added and then stirred for 15 min. The reaction mixture was cooled to 0 ^{o}C, NBS (0.76 g, 4.3 mmol) was added and stirred for 15 min followed by immediate workup by dilution with cold dichloromethane (10 mL), filtered through a pad of celite, washed with 10% $Na_2S_2O_5$ and ice cooled water. The organic layer was separated, dried (Na_2SO_4), concentrated and purified by column chromatography (EtOAc:hexanes; 0% → 30%) to

give a colorless foam. Due to limited stability, this material was used immediately in next step.

^{1}H NMR (500 MHz, $CDCl_3$) δ 7.96 – 7.46 (5H, m, ArH-OBz), 7.08 (2H, d, $J_{o,m}$ = 8.3 Hz, *ortho*ArH-PMB), 6.65 (2H, d, *meta*ArH-PMB), 6.36 (1H, br s, H1), 5.31 (1H, t, $J_{4,3}$ = $J_{4,5}$ = 10.1 Hz, H4), 4.86 (1H, d, $J_{a,b}$ = 12.1 Hz, OCH_{2a}-PMB), 4.82 (1H, d, $J_{3,4}$ = 10.1 Hz, H3), 4.52 (1H, d, $J_{b,a}$ = 12.1 Hz, OCH_{2b}-PMB), 4.39(1H, dq, $J_{5,6}$ = 6.3 Hz, $J_{5,4}$ = 10.2 Hz, H5), 3.74 (3H, s, CH_3-OAc), 1.33 (3H, d, $J_{6,5}$ = 6.3 Hz, H6).

^{13}C NMR (125 MHz, $CDCl_3$) δ 194.4 (C2), 164.9 [*C*(O)-OBz], 159.6 (1C, C_{Ar}OMe-PMB), 133.7 – 113.9 (11C, C_{Ar}), 85.2 (C1), 76.7 (C3), 76.8, 74.1 (H4), 73.1 (OCH_2-PMB), 71.7 (C5), 55.3 (OCH_3-PMB), 17.0 (C6).

HRMS (ESI$^+$) calculated for $C_{21}H_{21}NaO_7$ $[M+NH_4]^+$ 471.0414, found 471.0410

4.4.17. Synthesis of the thiol 11

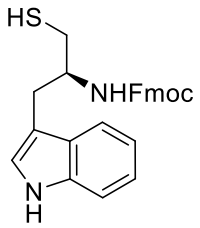

To a solution of the known bromide **35**[21] (5.0 g, 10.5 mmol) in acetonitrile (75 mL), thiourea (1.6 g, 21.0 mmol) was added and heated to reflux temperature for 12 h. The solvent was removed under reduced pressure and the crude isothiouronium salt **35** was passed through a pad of silica gel with 30% EtOAc/hexane (100 mL) to remove the nonpolar impurities and then washed with 90% EtOAC/MeOH (150 mL) to completely elute the product. The solvents were removed under reduced pressure to give a yellow solid. This material was suspended in EtOAc (50 mL), 15% $Na_2S_2O_5$ (25 mL) was added and heated to reflux temperature for 5 h. After completion of the reaction, the mixture was cooled to rt, and the organic layer was separated. The aqueous layer was extracted with EtOAc (2 x 25 mL) and the combined organic layers was washed with brine, dried over $Na_2S_2O_4$ and concentrated to pale yellow solid which was recrystallized from acetone to give the thiol **11** (3.6 g, 80%) as a white powder.

^{1}H NMR (500 MHz, Acetone-d_6) δ 10.14 (1H, br s, NH ring-Trp), 7.88 – 7.05 (13H, m, ArH), 6.57 (1H, d, $J_{NH,\alpha}$ = 8.3 Hz, NH-Trp), 4.35 (2H, d, $J_{9,10}$ = 7.0 Hz, CH_2-Fmoc), 4.23 (1H, t, J = 7.2 Hz, H9-Fmoc), 4.09 – 4.02 (1H, m, αH-Trp), 3.14 – 3.06 (2H, m, CH_2SH-Trp), 2.81 – 2.69 (2H, m, βCH_2-Trp).

^{13}C NMR (150 MHz, Acetone) δ 156.9 (*C*=O-urethane), 145.2 – 112.2 (20C, C_{Ar}), 66.7 (*C*H_2-Fmoc), 55.2 (*C*α-Trp), 48.2 (C9-Fmoc), 30.1 (*C*H_2SH), 29.0 (β*C*H_2-Trp).

HRMS (ESI$^+$) calculated for $C_{26}H_{24}N_2NaO_2S$ $[M+NH_4]^+$ 451.1451, found 451.1448.

4.4.18. Synthesis of the intermediate 36

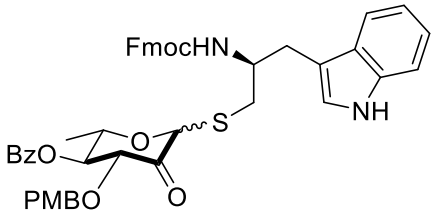

The thiol **11** (0.95 g, 2.23 mmol) was first dissolved in acetone (20 mL) with warming. Ulosyl bromide **12** (1 g, 2.23 mmol) and freshly activated crushed 4 Å molecular sieves were added and the mixture stirred for 30 min at rt. The reaction mixture was cooled to -78 °C and silver carbonate (0.92 g, 3.3 mmol) was added and stirred at -78 ^{o}C for 4 h. The temperature of the reaction mixture was slowly allowed to warm to -25 ^{o}C and maintained at this temperature for 6 h. The mixture was then filtered through a pad of Celite and concentrated to give a dark brown residue **36** as an inseparable mixture of anomers. Purification by flash column chromatography could not separate the anomers and led to the decomposition of the product.

4.4.19. Synthesis of the intermediate 37

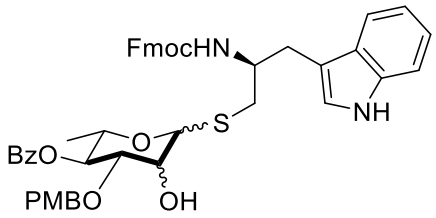

To a solution of the crude **36** in a mixture of dichloromethane/MeOH (5 mL; v/v 8:2) at 0 °C, $NaBH_4$ (0.30 g, 8.0 mmol) was added and then the reaction mixture was stirred at 0 °C for 2 h. MALDI TOF MS indicated the disappearance of **36** and the reaction mixture was diluted with dichloromethane (5 mL), washed with water (5 mL), aq 1% citric acid (5 mL) and brine (5 mL) successively. The organic layer was separated, dried over $Na_2S_2O_4$, concentrated and purified by flash column chromatography (EtOAc:hexanes; 10% → 40%) to give **37** (0.88 g) as an inseparable mixture of isomers in 3:1 ratio.

4.4.20. Synthesis of the 1-thio-β-rhamnoside derivative 39

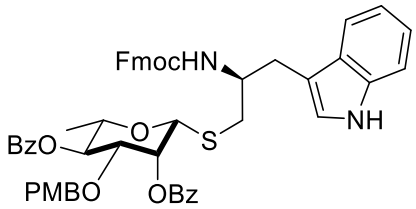

To a solution of the isomeric mixture of **37** (0.87 g) in dichloromethane (5 mL), pyridine (2 mL) was added. The temperature of the reaction mixture was cooled to 0 ^oC, benzoyl chloride (310 µL, 2.2 mmol) was added dropwise and then the reaction mixture was allowed to warm to rt over 30 min. The mixture was stirred at rt for 4 h at which time the TLC analysis indicated the disappearance of **37**. Ice (5 g) was added to the reaction mixture and the organic layer was separated. The aqueous layer is extracted with dichloromethane (2 x 5 mL). The combined organic layers were washed (aq. sat. $NaHCO_3$, brine), dried ($Na_2S_2O_4$), concentrated and purified by flash column chromatography to afford the pure β-anomer **39** (0.80 g, 40% over 3 steps) as a crystalline solid.

^1H NMR (500 MHz, $CDCl_3$) δ 8.16 – 6.55 (29H, m, NH ring-Trp, ArH), 5.89 (1H, br d, $J_{2,3}$ = 3.4 Hz, H2-rha), 5.30 (1H, t, $J_{4,3} = J_{4,5}$ = 9.7 Hz, H4-rha), 5.14 (1H, d, $J_{NH,\alpha}$ = 7.9 Hz, NH-Trp),

4.77 (1H, br s, H1-rha), 4.57 (1H, d, $J_{a,b}$ = 12.6 Hz, OCH_{2a}-PMB), 4.45 – 4.40 (2H, m, CH_{2a}-, H9-Fmoc), 4.36 (1H, d, $J_{b,a}$ = 12.6 Hz OCH_{2b}-PMB), 4.25 – 4.22 (2H, m, αH-Trp, CH_{2b}-Fmoc), 3.69 (3H, s, OCH_3-PMB), 3.68 – 3.65 (1H, m, H3-rha), 3.49 – 3.43 (1H, m, H5-rha), 3.16 (1H, dd, $J_{a,b}$ = 14.6 Hz, $J_{a,\alpha}$ = 4.0 Hz, βCH_{2a}-Trp), 3.05 – 2.97 (2H, m, βCH_{2b}-Trp, CH_{2a}S), 2.72 (1H, dd, $J_{b,a}$ = 14.8 Hz, $J_{b,\alpha}$ = 7.3 Hz, CH_{2b}S), 1.22 (3H, d, $J_{6,5}$ = 6.0 Hz, H6-rha).

^{13}C NMR (150 MHz, $CDCl_3$) δ 166.2 [*C*(O)-OBz], 165.6 [*C*(O)-OBz), 159.3 (1C, C_{Ar}OMe-PMB), 156.3 (C=O-urethane), 144.2 – 144.0 (2C, C8a-, C9a-Fmoc), 141.6 (2C, C4a-, C4b-Fmoc), 136.4 (C3a-Trp), 133.4-111.3 (31C, C_{Ar}), 82.9 (C1-rha), 76.5 (C3-rha), 75.3 (C4-rha), 74.6 (OCH_2-PMB), 73.9 (C2-rha), 67.1(C5-rha), 66.6 (CH_2-Fmoc), 55.2 (OCH_3-PMB), 51.2 (Cα-Trp), 47.4 (C9-Fmoc), 35.6 (CH_2S), 29.5 (βCH_2-Trp), 18.0 (C6-rha)

HRMS (ESI$^+$) calculated for $C_{54}H_{51}N_2aO_9S$ $[M+H]^+$ 903.3310, found 903.3307

Data for the minor isomer 1-thio-α-rhamnoside derivative 38

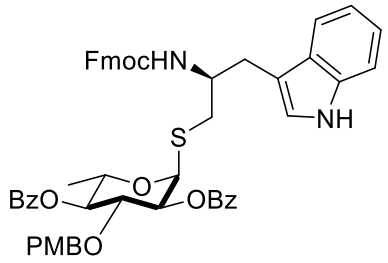

^{1}H NMR (600 MHz, $CDCl_3$) δ 8.06 – 6.54 (29H, m, NH ring-Trp, ArH), 5.70 (1H, d, H1-rha), 5.36 – 5.33 (2H, m, H2-rha, NH-Trp), 5.16 (1H, t, $J_{4,3}$ = $J_{4,5}$ = 9.4 Hz, H4-rha), 4.63 (1H, d, $J_{a,b}$ = 11.2 Hz, OCH_{2a}-PMB), 4.54 (1H, d, $J_{b,a}$ = 12.6 Hz, OCH_{2b}-PMB), 4.41 – 4.39 (3H, m, H5-rha, CH_2-Fmoc), 4.29 – 4.24 (1H, m, αH-Trp), 4.21 (1H, t *J* = 7.1 Hz, H9-Fmoc), 3.65 (3H, s, OCH_3-PMB), 3.08 (1H, dd, $J_{a,b}$ = 14.5, $J_{a,\alpha}$ = 5.4 Hz, βCH_{2a}-Trp), 3.01 (1H, dd, $J_{b,a}$ = 14.5, $J_{b,\alpha}$ = 7.9 Hz, βCH_{2b}-Trp), 2.81 – 2.74 (2H, m, CH_2S), 1.22 (3H, d, $J_{6,5}$ = 6.2 Hz, H6-rha).

^{13}C NMR (150 MHz, $CDCl_3$) δ 165.5 [2C, 2 x *C*(O)-OBz], 159.2 (1C, C_{Ar}OMe-PMB), 156.0 (C=O-urethane), 144.1 – 144.0 (2C, C8a-, C9a-Fmoc), 141.4 (2C, C4a-, C4b-Fmoc), 136.3 (C3a-Trp), 133.6-111.3 (31C, C_{Ar}), 84.3 (C1-rha), 77.1 (C3-rha), 75.3 (C5-rha), 72.7 (C4-

rha), 70.3 (O*C*H_2-PMB), 70.1 (C2-rha), 66.9 (*C*H_2-Fmoc), 55.3 (O*C*H_3-PMB), 51.2 (Cα-Trp), 47.4 (C9-Fmoc), 36.1 (*C*H_2S), 29.5 (β*C*H_2-Trp), 17.4 (C6-rha).

HRMS (ESI$^+$) calculated for $C_{54}H_{51}N_2aO_9S$ $[M+H]^+$ 903.3310, found 903.3282.

4.4.21. Synthesis of the 1-thio-β-rhamnoside acceptor 10

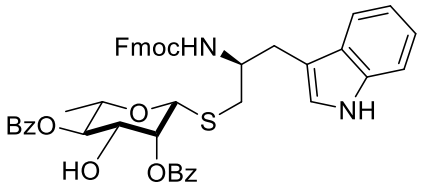

To a solution of **39** (0.7 g, 0.7 mmol) in anhydrous dichloromethane (5.0 mL) at -78 °C, thiophenol (95.0 µL, 0.93 mmol) and tin (IV) chloride (116.0 µL, 1.0 mmol) were added and the resulting pink solution was stirred at -78 ^oC for 1 h. After complete consumption of **39** as indicated by TLC, sat. aq. $NaHCO_3$ (3 mL) was added to the reaction mixture and was allowed to warm to rt over 30 min. The organic layer was separated, and the aqueous layer was extracted with dichloromethane (2 x 3 mL). The combined organic extracts were washed (brine), dried ($Na_2S_2O_4$), concentrated and purified by flash column chromatography to afford the acceptor **10** (0.4 g, 70%) as a colorless crystalline solid.

^{1}H NMR (600 MHz, $CDCl_3$) δ 8.16 – 7.0 (24H, m, NH ring-Trp, ArH), 5.74 (1H, d, $J_{1,2}$ = 3.5 Hz, H2-rha), 5.17 – 5.13 (2H, m, H4-rha, NH-Trp), 4.73 (1H, br s, H1-rha), 4.44-4.38 (2H, m, C*H*$_2$-Fmoc), 4.29 – 4.25(1H, m, αH-Trp), 4.22 (1H, t, *J* = 7.1 Hz, H9-Fmoc), 4.02 (1H, dd, $J_{3,2}$ = 3.4 Hz, $J_{3.4}$ = 10.13 Hz, H3), 3.60 – 3.53 (1H, m, H5), 3.15 (1H, dd, $J_{a,b}$ = 14.8, $J_{a,\alpha}$ = 5.5 Hz, βC*H*$_{2a}$-Trp), 3.03 (1H, dd, $J_{b,a}$ = 14.8, $J_{b,\alpha}$ = 6.8 Hz, βC*H*$_{2b}$-Trp), 2.98 (1H, dd, $J_{a,b}$ = 14.0 Hz, $J_{a,\alpha}$ = 5.4 Hz, C*H*$_{2a}$S), 2.73 (1H, dd, $J_{b,a}$ = 14.0 Hz, $J_{b,\alpha}$ = 6.8 Hz, C*H*$_{2b}$S), 1.26 (3H, d, $J_{6,5}$ = 6.5 Hz, H6-rha).

^{13}C NMR (150 MHz, $CDCl_3$) δ 167.1 [*C*(O)-OBz], 166.7 [*C*(O)-OBz], 156.3 (C=O-urethane), 144.1 (2C, C8a-, C9a-Fmoc), 141.5 (2C, C4a-, C4b-Fmoc), 136.4 (C3a-Trp), 133.7-111.4 (25C, C_{Ar}), 83.0 (C1-rha), 75.2 (C5-rha), 75.0 (C4-rha), 74.0 (C2-rha), 72.9 (C3-rha), 66.8 (*C*H_2-Fmoc), 50.9 (Cα-Trp), 47.4 (C9-Fmoc), 35.7 (CH_2S), 29.4 (βCH_2-Trp), 18.0 (C6-rha).

4.4.22. Synthesis of the trisaccharide derivative 8

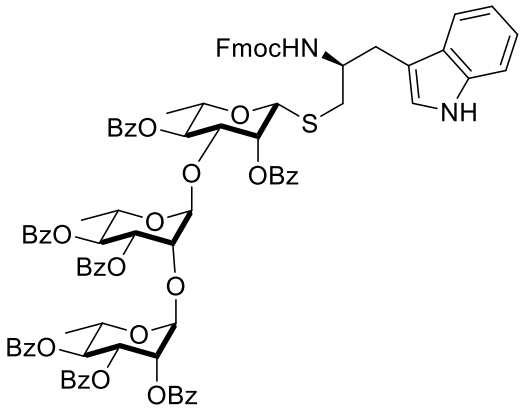

To a solution of the acceptor **10** (60 mg, 76.6 µmol) in anhydrous dichloromethane (5 mL), freshly activated and crushed 4 Å molecular sieves (100 mg) were added and stirred for 15 min at rt. The mixture was cooled to -40 °C, TMSOTf (6 µL, 22.2 µmol) was added followed by dropwise addition of the donor **9** (112 mg, 115 µmol) in dry dichloromethane (0.5 mL) over 15 min. The reaction mixture was stirred at -40 ^{o}C for 1 h. MALDI TOF MS indicated the disappearance of the acceptor **10**. Triethyl amine (100 µL) was added and the resulting mixture was filtered through a pad of Celite. The filtrate was washed with cold sat aq. $NaHCO_3$, dried over Na_2SO_4 and concentrated to give a thick syrup. Purification by HPLC gave **8** (48 mg, 40%) along with an inseparable unknown carbohydrate impurity (< 15%).

^{1}H NMR (600 MHz, Chloroform-*d*) δ 8.28 – 7.01(48H, m, ArH), 5.89 (1H, br s, NH-Trp), 5.78 (1H, dd, $J_{3'',2''}$ = 3.4 Hz, $J_{3'',4''}$ = 10.1 Hz, H3''-rha), 5.56 – 5.45 (6H, m, H4-, H4'-, H4''-,H3'-,H3'-',H2''-rha), 5.22 (1H, d, $J_{1',2'}$ = 1.8 Hz, H1'-rha), 4.93 (1H, br s, H1-rha), 4.53 (1H, d, $J_{1'',2''}$ = 1.9 Hz, H1''-rha), 4.45 – 4.02 (2H, m, CH_2-Fmoc), 4.38 – 4.33 (1H, m, H5''-rha), 4.3 – 4.23 (2H, m, αH-Trp, H2''-rha), 4.20 (1H, t, $J_{9,10}$ = 7.0 Hz, H9-Fmoc), 4.03 – 3.99 (1H, m,H5'-rha), 3.93 (1H, dd, $J_{2',1'}$ = 1,8 Hz, $J_{2',3'}$ = 3.1 Hz, H2'-rha), 3.60 – 3.54 (1H, m, H5-rha), 3.19 – 3.15 (1H, m, βCH_{2a}-Trp), 3.06 (1H,dd, $J_{b,a}$ = 13.5 Hz, $J_{b,\alpha}$ = 6.5 Hz, βCH_{2b}-Trp), 3.0 (1H, dd, $J_{a,b}$ = 14.5 Hz, $J_{a,\alpha}$ = 6.3 Hz, CH_{2a}S), 2.75 (1H, dd, $J_{b,a}$ = 14.5 Hz, $J_{b,\alpha}$ = 7.1 Hz, CH_{2b}S), 1.37 (3H, d, $J_{6,5}$= 6.2 Hz, H6-rha), 1.25 (3H, d, $J_{6,5}$= 6.1 Hz, H6'-rha), 0.98 (3H, d, $J_{6,5}$= 6.1 Hz, H6''-rha).

^{13}C NMR (150 MHz, $CDCl_3$) δ 166.5 – 164.9 [7C, *C*(O)-OBz] 156.3 (*C*=O urethane), 144.1 (2C, C8a-, C9a-Fmoc), 141.5 (2C, C4a-,C4b-Fmoc), 136.4 (C3a-Trp), 133.5 – 111.4 (

57C, C_{Ar}), 100.3 (C1'-rha), 99.0 (C1''-rha), 83.2 (C1-rha), 76.9 (2C, C2, C2'-rha), 75.5 (C5-rha), 73.9 (C4-rha), 73.0 (C3-rha), 71.9 (C4'-rha), 71.8 (C4''-rha), 70.5 (C3'-rha), 70.3 (C2''-rha), 69.7 (C3''-rha), 67.8 – 67.6(2c, C5', C5''-rha), 66.8 (*C*H_2Fmoc), 51.0 (α*C*-Trp), 47.4 (*C*9-Fmoc), 35.7 (CH_2S), 29.9 (β*C*H_2-Trp), 18.0 (2C, C6, C6'-rha), 17.6 (C6''-rha).

HRMS (ESI$^+$) calculated for $C_{93}H_{83}N_2O_{21}S$ $[M+H]^+$ 1595.5204, found 1595.5250.

4.4.23. Synthesis of the protected glycopeptide 5

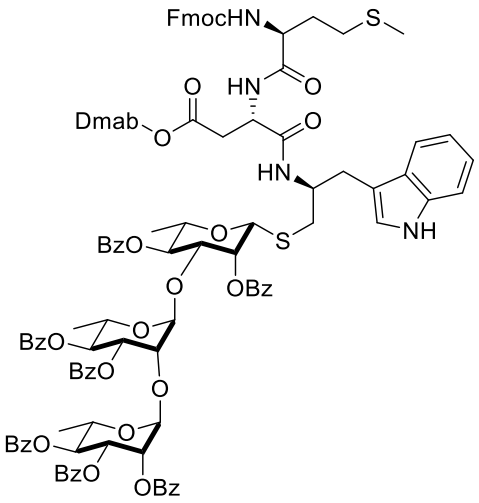

To a stirred solution of **8** (15.0 mg, 9.5 µmol) in THF (1 mL), octanethiol (16.3 µL, 95.0 µmol) and DBU (1.0 µL, 0.19 µmol) were added and stirred for 1 h at rt. The mixture was concentrated under reduced pressure to dryness and the residue was washed several times with warm ether to remove excess octanethiol and dibenzofulvene thiol adduct. The residue was dried over high vacumm for 2 h and carried to the next step without purification. To a solution of the crude amine **7** in THF (1 mL), Fmoc-Met-Asp(ODmab)-Opfp[21] (**6**) (10 mg,12 µmol) , HOBt (20.5 mg, 16 µmol) were added and stirred at rt for 4 h. MALDI TOF MS indicated the disappearance of peptide **6**. The solvent was removed under reduced pressure, purified by column chromatography over silica gel afforded **5 (**8 mg, 40% over 2 steps) along with an inseparable carbohydrate impurity.

^{1}H NMR (600 MHz, $CDCl_3$) δ 8.30 – 7.04 (53 H, m, ArH), 6.77 (1H, br s, NH-Trp), 5.79 (1H, dd, $J_{3'',2''}$ = 3.1 Hz, $J_{3'',4''}$ = 10.1 Hz, H3''-rham), 5.57 – 5.41 (6H, m, H4-, H4'-, H4''-,H3'-,H3'-',H2''-rha), 5.29 (1H, d, $J_{1',2'}$ = 1.8 Hz, H1'-rha), 4.98 (1H, br s, H1-rha), 4.55 (1H, br d, $J_{1'',2''}$ = 1.9 Hz, H1''-rha), 4.53 – 4.08 (11H, m, αH-Asp, αH-Met, αH-Trp, CH_2-Fmoc,

H9-Fmoc, H5'-,H5'', H2''-rha), 3.96 – 3.94 (1H, m, H2'-rha), 3.60 – 3.57 (1H, m, H5-rha), 3.10 – 2.97 (6H, m, βC*H*$_{2a}$-Trp, β'C*H*$_{2a}$-Trp, βC*H*$_{2a}$-Asp, C*H*$_2$CH-Dmab), 2.76 – 2.69 (2H, m,), 2.62 – 2.60 (1H, m, βC*H*$_{2b}$-Asp), 2.55 – 2.50 (2H, m, β'C*H*$_{2b}$-Trp), 2.47 (4H, br s, C*H*$_2$-ring Dmab), 2.09 (3H, s, SC*H*$_3$-Met), 1.85 – 1.80 (1H, m, CH$_2$C*H*-Dmab), 1.10 (6H, s, 2 x C*H*$_3$ ring-Dmab), 1.41 (3H, d, $J_{6,5}$= 6.2 Hz, H6-rha), 1.24 (3H, d, $J_{6,5}$= 6.1 Hz, H6'-rha), 0.77 (3H, d, $J_{6,5}$= 6.1 Hz, H6''-rha).

HRMS (ESI$^+$) calculated for $C_{122}H_{122}N_5O_{27}S_2$ $[M+H]^+$ 2152.7763, found 2152.7819.

4.4.24. Attempted deprotection of glycopeptide 5

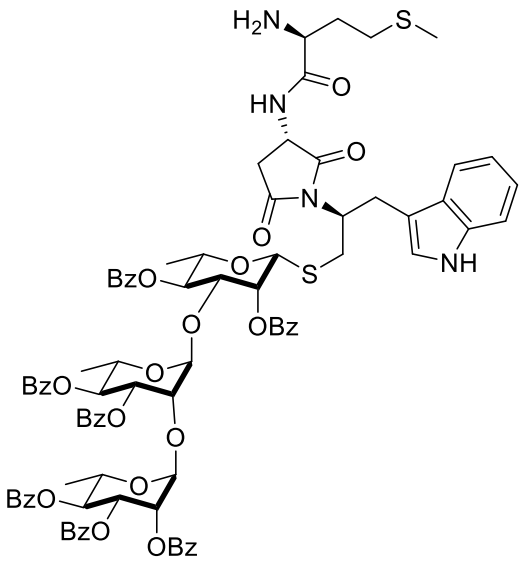

47

To a stirred mixture of compound **5** (5.0 mg**,** 2.3 µmol) in THF (0.1 mL), octanethiol (5 µL, 23 µmol) and DBU were added and the reaction mixture was stirred for 1 h at rt. MALDI TOF MS indicated the disappearance of **5** and showed a single major mass corresponding to loss of 18 mass units from the expected glycopeptide **46**. The solvent was evaporated to dryness. Purification by flash column chromatography on silica gel, followed by HPLC, showed the major aspartimide side product **47** (3 mg) had coeluted with an unknown carbohydrate impurity.

^{1}H NMR (600 MHz, MeOD) δ 8.10 – 7.02 (40 H, m, ArH), 5.81 – 5.80 (1H, m, H3'-rha), 5.68 – 5.61 (1H, m), 5.5 – 5.3 (7H, m, 3 x H4-, 2 x H3-, H2-, H5- rha), 5.24 (1H, d, $J_{1',2;'}$ = 1.8 Hz, H1'-rha), 4.85 (1H, br s, H1-rha), 4.42 (1H, d, $J_{1'',2''}$ = 1.9 Hz, H1''-rha), 4.47 (1H,

m, αH-Trp), 4.36 – 4.34 (1H, m, αH-Asi), 4.33 – 4.32 (1H, m, H2'-rha), 4.11 – 4.06 (1H, m, H5-rha), 3.97 (1H, m, αH-Met), 3.83 – 3.82 (1H, m, H5-rha), 3.04 – 3.01 (1H, m, βCH_{2a}-Trp), 2.96 – 2.93 (1H, m, β'CH_{2a}-Trp), 2.93 – 2.91 (1H, m, βCH_{2b}-Trp), 2.80 (1H, dd, J = 4.3, 15.5 Hz, βCH_{2a}-Asi), 2.64 (1H, dd, J = 7.2, 15.5 Hz, βCH_{2b}-Asi), 2.60 – 2.57 (2H, m, γCH_2-Met), 2.55 – 2.51 (1H, m, β'CH_{2b}-Trp), 2.12 – 2.09 (2H, m, βCH_2-Met), 2.03 (3H, s, SCH_3-Met), 1.30 (3H, d, $J_{6,5}$= 6.3 Hz, H6-rha), 1.01 (3H, d, $J_{6,5}$= 6.1 Hz, H6'-rha), 0.96 (3H, d, $J_{6,5}$= 6.1 Hz, H6''-rha).

^{13}C NMR (151 MHz, MeOD) δ 170.20 [*C*(O)-Asi], 168.3 [*C*(O)-Met], 168.2 [*C*(O)-Asi] , 166.3, 165.8, 165.7, 165.6, 165.2, 165.0, 164.9 [7C, *C*(O)-OBz] ,136.9 –110.74 (50C, C_{Ar}), 99.8 (C1'-rha), 98.80 (C1''-rha), 81.5 (C1-rha), 77.2 – 67.2 (12 C, 3 x C2-rha, 3 x C3-rha, 3 x C4-rha, 3 x C5-rha), 53.6 (Cα-Met), 51.9 (Cα-Asi), 49.4 (Cα-Trp), 38.7 (β*C*H_2-Asi), 33.8 (β'*C*H_2-Trp), 32.8 (β*C*H_2-Met), 29.7 (β*C*H_2-Trp) , 29.0 (γ*C*H_2-Met), 16.8 – 16.5 (3C, 3 x C6-rha), 13.8 (S*C*H_3-Met).

HRMS (ESI$^+$) calculated for $C_{87}H_{85}N_4O_{22}S_2$ $[M+H]^+$ 1601.5091, found 1601.5072.

References

(1) WHO, in *World Health Organisation*; Geneva, 2004.

(2) Montefiore, D.; Rotimi, V. O.; Adeyemi-doro, F. A. B. *J. Antimicrob. Chemother.* **1989**, *23*, 641–651.

(3) Baker, S. J.; Payne, D. J.; Rappuoli, R.; De Gregorio, E. *Proc. Natl. Acad. Sci. U.S.A.*, **2018**, *51*, 12887–12895.

(4) Hale, T. L. In Topley and Wilson's Microbiology and Microbial Infections; Hansler, W. J., Shumman, M., Eds.; Arnold: London, 1998; pp 479–493.

(5) (a) Kweon, M. N. *Curr Opin Infect Dis* **2008**, *21*, 313; (b) Niyogi, S. K. *J. Microbiol, **2005**, 43,* 133–143.

(6) Sivapalasingam, S.; Nelson, J. M.; Joyce, K.; Hoekstra, M.; Angulo, F. J.; Mintz, E. D. *Antimicrob. Agents Chemother*. **2006**, *50*, 49–54.

(7) Ye, C.; Lan, R.; Xia, S.; Zhang, J.; Sun, Q.; Zhang, S.; Jing, H.; Wang, Z.; Li, Z.; Zhou, Z.; Zhao, A.; Cui, Z.; Cao, J.; Jin, D.; Huang, L.; Wang, Y.; Luo, X.; Bai, X. ;Wang, P.; Xu, Q.; Xu, J. *J. Clin. Microbiol.* **2010**, *48*, 419.

(8) Mani, S.; Wierzba, T.; Walker, R. I. *Vaccine* **2016**, *34*, 2887–2894.

(9) Borrelli, S.; Hossany, R. B.; Pinto, B. M. *Clin. Vaccine. Immunol.* **2008**, *15*, 1106–1114.

(10) B. R. Hossany, B. D. Johnston, X. Wen, S. Borrelli, Y. Yuan, M. A. Johnson, B. M. Pinto, *Carbohydr. Res.* **2009**, *344*, 1412–1427.

(11) Kaper, J. B., Nataro, J. P., Mobley, H. L. T. *Nat. Rev. Microbiol.* **2004**, *2*, 123-140.

(12) Carlin, N. I.; Lindberg, A. A.; Bock, K.; Bundle, D. R. *Eur. J. Biochem*. **1984**, *139*, 189–194.

(13) Bundle, D. R. *Pure Appl. Chem*. **1989**, *61*, 1171–1180.

(14) Harris, S. L.; Craig, L.; Mehroke, J. S.; Rashed, M.; Zwick, M. B.; Kenar, K.; Toone, E. J.; Greenspan, N.; Auzanneau, F. I.; Marino-Albernas, J. R.; Pinto, B. M.; Scott, J. E. J.; Greenspan, N.; Auzanneau, F. I.; Marino-Albernas, J. R.; Pinto, B. M.; Scott, J. K. *Proc. Natl. Acad. Sci. U.S.A.* **1997**, *94*, 2454–2459.

(15) Vyas, N. K.; Vyas, M. N.; Chervenak, M. C.; Johnson, M. A.; Pinto, B. M.; Bundle, D. R.; Quiocho, F. A. *Biochemistry* **2002**, *41*, 13575–13586.

(16) Vyas, N. K.; Vyas, M. N.; Chervenak, M. C.; Bundle, D. R.; Pinto, B. M.; Quiocho, F. A. *Proc. Natl. Acad. Sci. U.S.A.* **2003***, 100*, 15023–15028.

(17) Janeway, C. A., Travers, P. In *Immunobiology: The Immune System in Health and Disease*; 3rd ed.; Garland: New York, 1997.

(18) Jennings, H. J. *Adv. Exp. Med. Biol.* **1988**, *228*, 495–550.

(19) Jennings, H. J. *Curr. Top. Microbiol. Immunol.* **1990**, *150*, 97–127.

(20) McCool, T. L., Harding, C. V., Greenspan, N. S., Schreiber, J. R. *Infect. Immun.* **1999**, *67*, 4862-4866.

(21) Weintraub, A. *Carbohydr. Res.* **2003**, *338*, 2539–2547.

(22) Lindberg, A. A. *Vaccine* **1999**, *17 Suppl. 2*, 28–36.

(23) Sears, P.; Wong, C.-H. *Angew. Chem. Int. Ed.* **1999**, *38*, 2300–2324.

(24) Johnson, M. A., Pinto, B. M. *Topics Curr. Chem.* **2008**, *160*, 1001–1011.

(25) Johnson, M. A.; Pinto, B. M. *Aust. J. Chem.* **2002**, *55*, 13–25.

(26) Johnson, M. A.; Pinto, B. M. *Carbohydr. Res.* **2004**, *339*, 907–928.

(27) Horton, D.; Wander, J. D. In The Carbohydrates; Pigman, W. W., Horton, D., Eds.; Academic: New York, 1980; Vol. 1A, p 799.

(28) Shi, Y.; Pinto, B. M. *Carbohydr. Res.* **2012**, *358*, 89–95.

(29) Schmidt, R. R.; Michel. J. *Angew. Chem. Int. Ed.* **1980**, *19*, 731–732.

(30) Lichtenthaler, F. W.; Metz, T. *Eur. J. Org. Chem.* **2003**, 3081–3093.

(31) Pozgay, V. *Carbohyd. Res*. **1992**, *235*, 295–302.

(32) Zemplén, G.; Pacsu, E. *Ber. Dtsch. Chem. Ges*. **1929**, *62*, 613 – 1614.

(33) Paulsen, H. *Angew. Chem., Int. Ed.* **1982**, *21*, 155–173

(34) El Ashry, E.-S. H.; Rashed, N.; Ibrahim, E.-S. *Tetrahedron* **2008**, *64*, 10631–10648.

(35) Nigudkar, S. S.; Demchenko, A. V. *Chem. Sci.* **2015**, *6*, 2687–2704.

(36) Elferink, H.; Pedersen, C. M. *Eur. J. Org. Chem.* **2017**, 53–59.

(37) Lee, Y. J.; Ishiwata, A.; Ito, Y. *J. Am. Chem. Soc.* **2008**, *130*, 6330–6331.

(38) Crich, D.; Li, L. *J. Org. Chem*. **2009**, *74*, 773–781.

(39) Heuckendorff, M.; Pedersen, C. M. Bols, *J. Org. Chem*. **2012**, *77*, 5559–5568.

(40) Zhu, Y.; Shen, Z.; Li, W.; Yu, B. *Org. Biomol. Chem. **2016**, 14, 1536–1539.*

(41) Nishi, N.; Sueoka, K.; Iijima, K.; Sawa, R.; Takahashi, D.; Toshima, K. *Angew. Chem. Int. Ed.* **2018**, *57*, 13858–13862.

(42) Hvidt, T.; Szarek, W. A.; Maclean, D. B. *Can. J. Chem*. **1988**, *66*, 779–782.

(43) Koenigs W, Knorr. E. *Chem. Ber.* **1901**, *34*, 957–981.

(44) Chan, W. C.; Bycroft, B. W.; Evans, D. J.; White, P. D. *J. Chem. Soc*., *Chem. Commun.* **1995**, 2209–2210.

(45) Barlos, K.; Gatos, D. In *Fmoc Solid Phase Peptide Synthesis: A Practical Approach*; Chan, W. C., White, P. D., Eds.; Oxford University: Oxford, 2000; pp 215–228.

(46) Sheppeck, J. E.; Kar, H.; Hong, H. *Tetrahedron Lett.* **2000**, *41*, 5329–5333.

Chapter 5.

Conclusions and Future Work

In this thesis work, we demonstrate the application of our previously developed chlorohydrin based methodology to access the functionalized tetrahydrofuranol motif *en-route* towards the total synthesis of two tetrahydrofuran (THF) containing marine natural products. In Chapter 2 of this thesis, we have shown a concise convergent total synthesis of biselide A (**1**), a naturally occurring marine macrolide isolated from Okinawan ascidian *Didemnidae sp*.[1] Among the members of the biselide family, biselide A (**1**) was found to be cytotoxic towards various human cancer cell lines[2] and might serve as a lead compound in the development of a novel anticancer drug. Biselide A (**1**) is a 14-membered macrolide that contains a core trisubstituted THF ring, a *Z*-vinyl chloride functionality and five stereogenic centres. Our strategy to access this complex molecule involved a key stereoselective reduction and cyclization of β-ketochlorohydrin to generate the THF ring, a cross metathesis reaction and Reformatsky macrocyclization. We have successfully completed the total synthesis of biselide A (**1**) in 20 steps (LLS) as compared to Hayakawa's[3] first total synthesis in 32 steps (LLS).

Our efficient synthetic strategy should now allow us to explore the synthesis of other members of biselide family and unnatural analogues of biselide A to investigate their structure activity relationship studies (SAR). For instance, the structure of biselide B (**2**) differs from biselide A (**1**) in having a 2-methylene-3-oxobutyl ester at C19 instead of a free carboxylic acid. The biological properties of biselide B (**2**) were not evaluated due to lack of material available through initial isolation and no total synthesis currently exists. We propose the synthesis of biselide B starting from our advanced macrocycle aldehyde intermediate **3**. Our retrosynthetic approach is outlined in Scheme 5-1. We envisage that the target molecule (**2**) could potentially be obtained by Nozaki-Hiyama–Kishi coupling[4] (NHK) between the aldehyde **3** and the ester **4**. The ester could in turn be obtained by Steglich[5] esterification between the carboxylic acid **5** and the alcohol **6**.[6] As depicted in Scheme 5-2, the macrocycle aldehyde **3** can be used as a starting point for the synthesis of unnatural analogues of biselide A containing bio-isosteres of carboxylic acid as apart of the SAR studies.

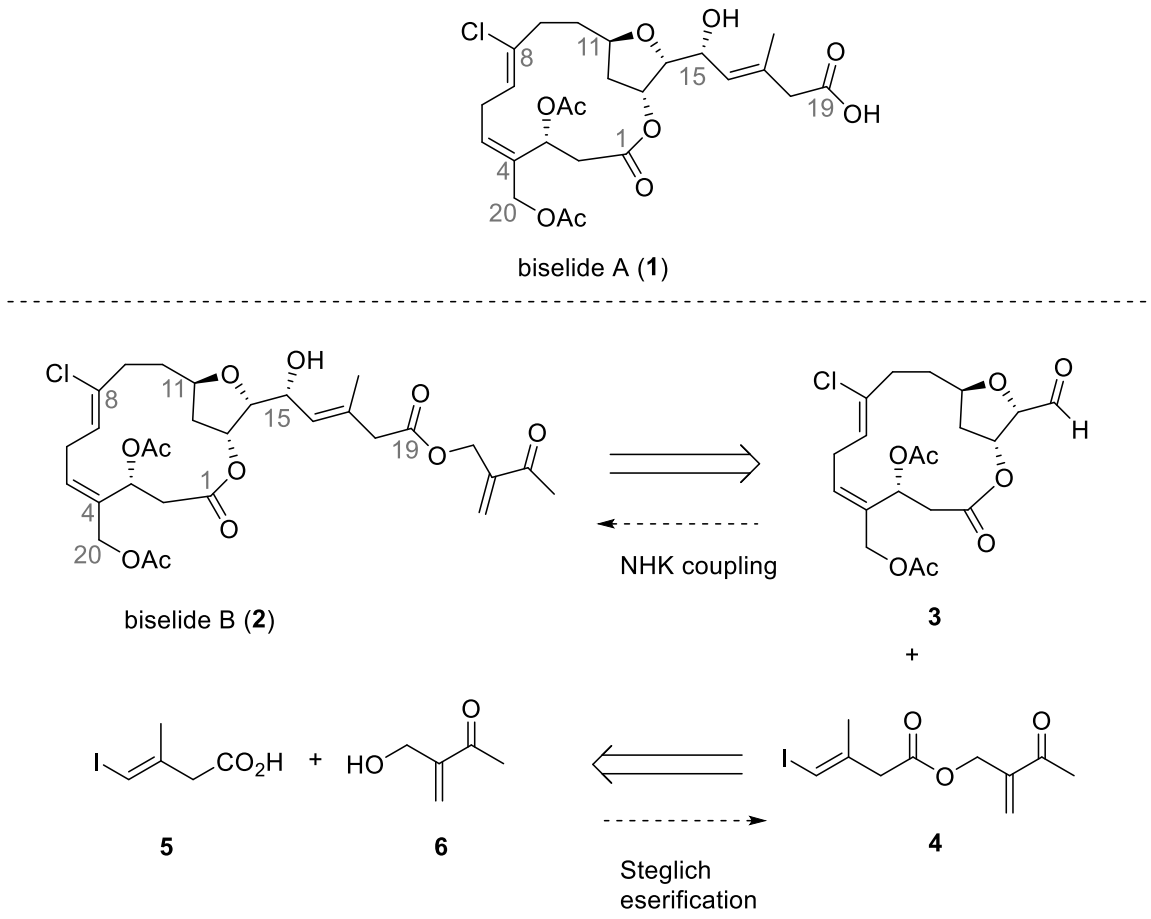

Scheme 5-1 Proposed retrosynthesis of biselide B (2)

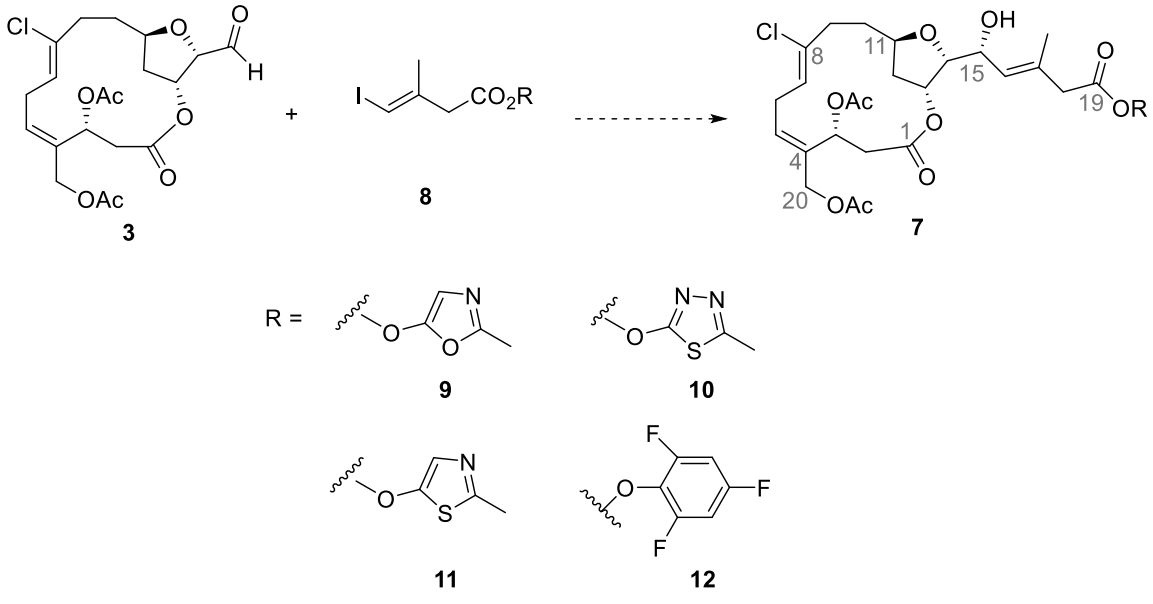

Scheme 5-2 Synthesis of analogues of biselide A (1).

Phormidolide A (**13**) is a member of the phormidolide family of THF containing marine macrolides that show potentially useful biological activity and complex structural features. In Chapter 3 of this thesis work, we described studies towards the synthesis and structural reassignment of the phormidolide A (**13**). This synthesis uses a key (*S*)-proline catalyzed α-chlorination and aldol reaction that proceeds through a dynamic kinetic resolution to give enatiomerically enriched β-keteochlorohydrin. A methylation and cyclization of this adduct gave the THF motif of the macrocyclic core. The synthesis of three model acetonide derivatives of the tetrahydrofuranol core and detailed spectroscopic comparisons to the triacetonide derivative of phormidolide A supports a reassignment of seven of the 11 stereogenic centres in phormidolide A.[7]

As future work, we propose to complete the total synthesis of phormidolide A, as shown in Scheme 5-3. The new strategy will begin with the addition of vinyl lithium derivative of compound **14** to the advanced aldehyde intermediate **15** to give the THF **16**. Next, we will use a selective Stille coupling reaction to couple vinyl stannane **17** to the THF **18** and anticipate that the enhanced reactivity of the vinyl iodide over vinyl bromide should favour the production of the desired diene **18**.[8] Subsequently, a Hodgoson-Takai olefination[9] of compound **18** would afford the vinyl stannane **19**. The intramolecular macro-Stille macrocyclization of the diene **19** should then afford the macrocycle **20**. The second half of the side chain can then be coupled to compound **20** and subsequent global deprotection should then afford the natural product (**13**).

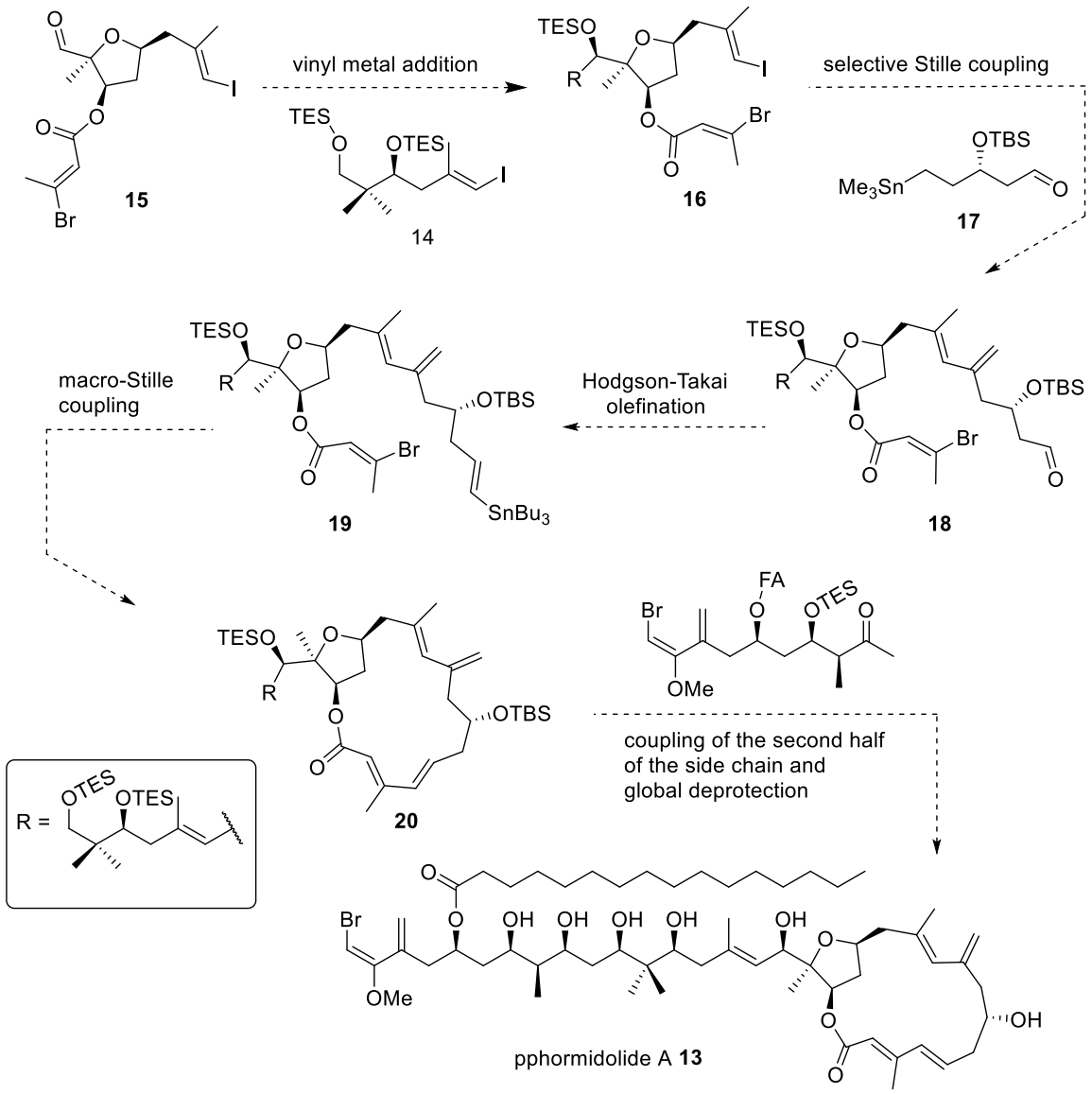

Scheme 5-3 Proposed completion of synthesis of phormidolide A (13)

The study presented in *Chapter 4*, describes our efforts towards the synthesis of the chimeric glycopeptide corresponding to the *Shigella flexneri* Y O-polysaccharide and its peptide mimic MDWNMHAA. The monoclonal antibody SYA/J6 is specific for the O-polysaccharide of the *Shigella flexneri* Y bacterium.[10] Two haptens, a pentasaccharide and a mimetic octapeptide bind to SYA/J6 with moderate binding affinities.[11] In search for a new class of compounds as mimics of the carbohydrate, two chimeric glycopeptides were designed in order to increase the binding affinity to SYA/J6 and retain all the favourable interactions made by the pentasaccharide and mimetic octapeptide within the combining site of the antibody SYA/J6.[12] The β-glycopeptide **21** contains a rhamnose

trisaccharide joined through a β-glycosidic linkage to the tripeptide motif. In this synthesis we have used an iterative glycosylation strategy for the assembly of trirhamnan building block in [2+1] manner. The synthesis of thermodynamically less favoured 1-thio-β-rhamnosidic linkage was achieved through an ulosyl bromide approach.[13] However, we were unsuccessful in completing the total synthesis of the β-glycopeptide. Unfortunately, the final global deprotection of the glycopeptide led to the formation of unwanted aspartimide (Asi) side product (**22**). It is well-known that the strong basic conditions lead to this unwanted side reaction [14]

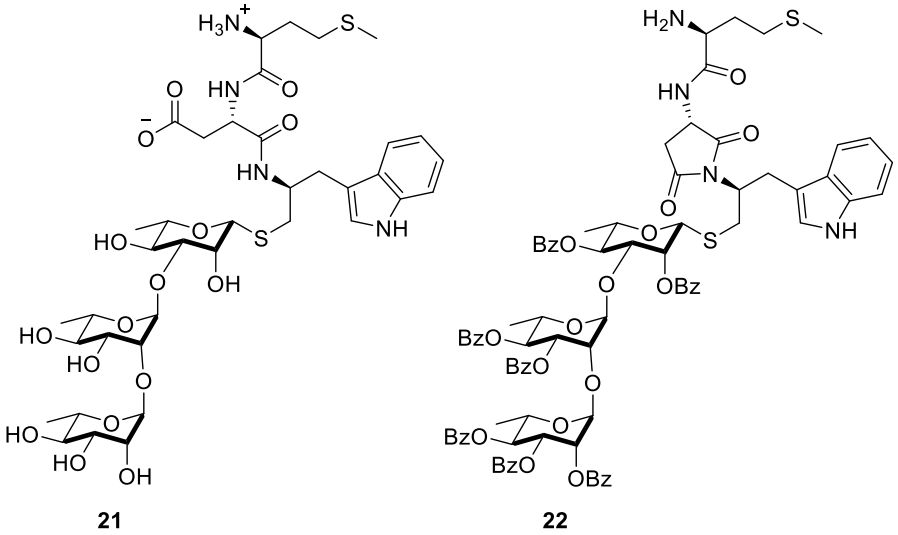

Scheme 5-4 Structures of β-glycopeptide 21 and aspartimide side product 22.

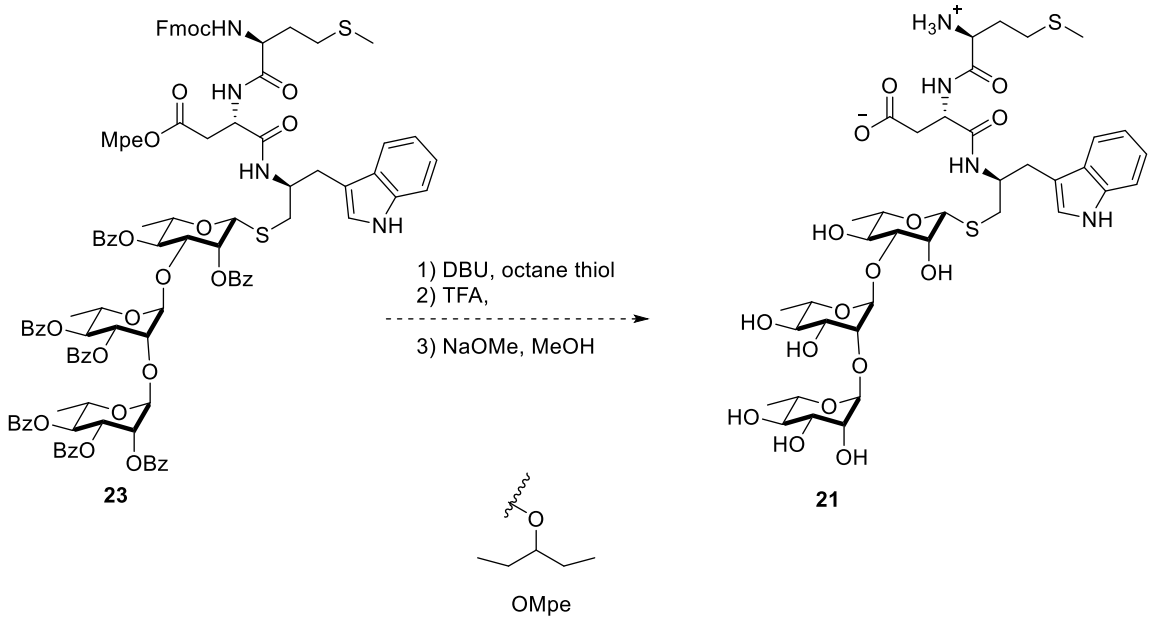

Scheme 5-5 Proposed synthesis to access the β-glycopeptide 21

As future work, to circumvent this issue of Asi formation, we propose to optimize the reaction conditions by lowering the equivalents of base and temperature, used to effect Fmoc deprotection. Alternatively, addition of acidic reagents such as 1-hydroxybenzotriazole, (HOBt, pKa of 4.60), 7-aza-1-hydroxy benzotriazole (HOAt, pKa of 4.60) and 2-cyano-2-(hydroximino) acetate (Oxyma) has been shown to be effective at suppressing the formation of Asi under basic reaction conditions.[15,16] Finally, a new class of 3-Methylpent-3-yl esters (OMpe), an acid labile carboxy-protecting group has been used for aspartic acid side chain protection. This sterically demanding analog of the *t*-butyl ester has been developed especially for reducing the base catalyzed Asi formation.[17] As depicted in Scheme 5-5, the Asi problem can be avoided by the synthesis of the glycopeptide **23** in which the Dmab ester will be replaced by OMpe ester and subsequent sequential deprotection will afford the required β-glycopeptide **21**. Then the binding of the β-glycopeptide to the monoclonal antibody SYA/J6 can be determined by competitive inhibition ELISA studies, using *S. flexneri* Y LPS as the coating antigen.[18] If binding is observed, then the binding affinity can be determined and protein conjugates of the glycopeptide will be prepared as potential immunogens.

References

(1) Teruya, T.; Shimogawa, H.; Suenaga, K.; Kigoshi, H. *Chemistry. lett.* **2004**, 33, 1184–1185.

(2) Teruya, T; Suenaga, K.; Maruyama, S.; Kurotaki, M.; Kigoshi, H. *Tetrahedron*, **2005**, *61*, 6561-6567.

(3) Hayakawa, I.; Okamura, M.; Suzuki, K.; Shimanuki, M.; Kimura, K.; Yamada, T.; Ohyoshi, T.; Kigoshi, H. *Synth.* **2017**, *49*, 2958–2970.

(4) (a) Takai, K.; Kimura, K.; Kuroda, T.; Hiyama, T.; Nozaki, H. *Tetrahedron Lett.* **1983**, *24*, 5281–5284; (b) Takai, K.; Tagashira, M.; Kuroda, T.; Oshima, K.; Utimoto, K.; Nozaki, H. *J. Am. Chem. Soc.* **1986**, *108*, 6048–6050.

(5) Neises, B.; Steglich, W. *Angew. Chem. Int. Ed.* **1978**, *17*, 522–524.

(6) Ueda, M.; Yamaura, M.; Ikeda, Y.; Suzuki, Y.; Yoshizato, K.; Hayakawa, I.; Kigoshi, H. *J. Org. Chem.* **2009**, *74*, 3370–3377.

(7) Lam, N. Y. S.; Muir, G.; Challa, V. R.; Britton, R.; Paterson, I. *Chem. Commun.* **2019**, *55*, 9717–9720.

(8) Williams, S.; Jin, J.; Kan, S. B. J.; Li, M.; Gibson, L. J.; Paterson, I. *Angew. Chem - Int. Ed.* **2017**, *56*, 645–649.

(9) Hodgson, D. M.; Boulton, L. T.; Maw, G. N. *Tetrahedron* **1995**, *51*, 3713–3724.

(10) Bundle, D. R. Pure Appl. Chem. **1989**, *61*, 1171–1180.

(11) Harris, S. L.; Craig, L.; Mehroke, J. S.; Rashed, M.; Zwick, M. B.; Kenar, K.; Toone, E. J.; Greenspan, N.; Auzanneau, F. I.; Marino-Albernas, J. R.; Pinto, B. M.; Scott, J. E. J.; Greenspan, N.; Auzanneau, F. I.; Marino-Albernas, J. R.; Pinto, B. M.; Scott, J. K. *Proc. Natl. Acad. Sci. U.S.A.* **1997**, *94*, 2454–2459.

(12) Vyas, N. K.; Vyas, M. N.; Chervenak, M. C.; Johnson, M. A.; Pinto, B. M.; Bundle, D. R.; Quiocho, F. A. *Biochemistry* **2002**, *41*, 13575–13586; (b) Vyas, N. K.; Vyas, M. N.; Chervenak, M. C.; Bundle, D. R.; Pinto, B. M.; Quiocho, F. A. *Proc. Natl. Acad. Sci. U.S.A.* **2003***, 100*, 15023–15028.

(13) Lichtenthaler, F. W.; Metz, T. *Eur. J. Org. Chem.* **2003**, 3081–3093.

(14) Mergler, M; Dick. F. *J. pept. Sci.***2005,** *11*, 650-657.

(15) Koing, W.; Geiger, R. *Chem Ber* **1970**, *103*, 788-798.

(16) Subiros-Funosas, R.; El-Faham, A.; Albericio, F. *Org Bimol chem* **2010**, 8, 3665-3673.

(17) Behrendt, R.; Huber, S.; White, P. *J. Pept. Sci.* **2016,** *22*, 92-97.